Particulate organic carbon mobilisation and export from temperate forested uplands

Joanne Caroline Smith

St John's College and Department of Earth Sciences

University of Cambridge

A thesis submitted for the degree of

Doctor of Philosophy

May 2013

Declaration

This thesis is the result of my own work and contains nothing which is the outcome of work done in collaboration with others, except as declared in the Acknowledgements and specified in the text. It is not substantially the same as any other work that has been or will be submitted for any other qualification at the University of Cambridge or any other university. This thesis does not exceed the total page limit of 275, nor the limit of 225 pages of text, illustrations, references and appendices, prescribed for the Department of Earth Sciences by the Degree Committee for the Faculty of Earth Sciences and Geography.

Joanne Caroline Smith
2 May 2013

Acknowledgements

Throughout this project, I have been grateful for support and collaboration of every kind from a great many people. I would like to take this opportunity to thank them all.

My supervisors, Albert Galy and Niels Hovius at Cambridge, and Andy Tye at the BGS, have been thoroughly excellent. Whether in person or by email, they have consistently offered sound advice, insightful discussion, unwavering encouragement and occasional flashes of brilliance, and are the foundation on which this research is built. All three have also been very welcome friends during long weeks of fieldwork abroad.

A large part of this project owes its success to a very productive collaboration with the Swiss Federal Institute for Forest, Snow and Landscape Research (WSL). In particular I would like to thank Jens Turowski for providing vital logistical help, responding to my never-ending data requests, putting me up in his flat in Zürich on several occasions, and never failing to provide black tea despite not drinking it himself—all tasks dispatched with typical German efficiency. Patrick Schleppi and Kim Krause deserve special mention for two years of filtering (not to mention storing) my samples, as well as plenty of helpful discussion. Manuel Nitsche provided the Alptal DEM and maps in both digital and paper form. Karl Steiner has my enduring gratitude for the most impressive piece of digging I've ever seen in some thoroughly miserable weather. He and Bruno Fritschi were also responsible for maintaining sampling equipment and collecting samples weekly; without their meticulous and continued efforts my life would have been much harder. Not least, I would like to thank all these people, and many besides, who made me welcome and helped in any way (however small) at WSL.

Still in Switzerland, Margrith Konrad and her staff at the Hotel Brunni made fieldwork in the Alptal a pleasure: it was great to come home to comfort and hearty Swiss food, to have my muddy wellies and bags of soil accepted without question, and to be sent off in the morning after a superb breakfast of fresh croissants and rolls, apricot and cherry jam, and gallons of café au lait.

The Oregon section of the project also owes a huge amount to others. Kathy Keable and Mark Schulze at H.J. Andrews, and Jeff McDonnell, Tina Garland, Sherri Johnson, Arne Skaugset and Amy Simmons at Oregon State University, were all extremely helpful in both logistic and scientific matters on the ground. Mark, Arne and Sherri, in addition to Phil Adams at Roseburg Forest Products Cooperative, are particularly thanked for giving me permission to sample in various Oregon watersheds, and to use suspended sediment samples already collected. In addition, Sherri, Don Henshaw, Fred Bierlmaier and Steve Wondzell responded admirably to my subsequent email requests for data and ideas. Cam Jones at CCAL deserves special mention for keeping a lot of apparently useless filters, and for the extra filtering of WS2 samples in winter–spring 2012. Chris Gabrielli obtained the Alsea bedrock cores and let me take sub-samples from them. Alex Irving provided the keys and truck (and dog?) required for a visit to Hinkle, and collected additional soil samples from Trask. Ben Pennington's field assisting was greatly appreciated, and doubled the amount of sampling I was able to do during the November storms. I must also thank Anna Coles for the chanterelles and company, and Ashley Bies for taking time out from trapping weasels to teach me how to distinguish western hemlock and douglas-fir.

In the Earth Science department at Cambridge, Rob Sparkes and Caroline Martin have been impeccable office-mates. For three years, Rob was the first port of call for all my questions, giving help and advice freely and generously, running the office coffee machine and creating the Raman spectroscopy figures used in Chapter 4. Caroline has always been an ally, and I must admit to benefiting from her encyclopaedic knowledge of Cambridge's restaurants. Together with Vicky Rennie and Gilad Antler, she also collected several additional samples from Oregon in December 2012, saving me a long flight for a single day's fieldwork.

James Rolfe at the Godwin Lab has always found time and space among other demands on the machine to analyse my samples, and been willing to discuss the finer details of the procedure when necessary. Jason Day allowed me free run of S415, kept chemical and other lab supplies well stocked, and gave advice on both chemical matters and the crushing and grinding machines in the basement. Jeannie and Simon in the Sed Lab deserve thanks for allowing me to use their equipment and impinge on a very busy marine sediment sieving operation, as does Linda, for lending me her 2 mm sieve. I must also thank Martin in the workshop for creating the bottle-holder that enabled sampling away from the stream banks, and Sarah in the library for finding various obscure maps. Countless other members of the department—staff and students alike—have contributed to making it a pleasant and stimulating place to spend four years. Finally, although our time at Cambridge never overlapped, I am very grateful to Bob Hilton—not only for laying the foundations for this work, but for being a friendly, helpful and enthusiastic voice at the end of the telephone and on occasional visits. His thesis became a permanent feature on my desk, with a bookmark in almost every page by the end.

Elsewhere in Cambridge, Chris Rolfe and Steve Boreham at the Department of Geography are thanked for letting me use their mill grinder for vegetation samples, and thus sparing me the need to buy a coffee grinder to do the job—amusing though that might have been for the rest of the office! I would also like to thank St John's College, for a series of excellent (free) dinners and other financial incentives.

On that subject, this project would not have been possible without the financial support of a NERC studentship and additional funds from the British Geological Survey's BUFI scheme. The latter in particular meant that fieldwork and labwork costs were never the limiting factor to the scope of the project. At the BGS, thanks are also due to Chris Vane and Simon Kemp for additional analyses, and especially to Mike Ellis for unofficial mentoring and stimulating discussion. Radiocarbon analysis was additionally funded by an NRCF grant (no. 1573.0911), and thanks are due to Charlotte Bryant, Callum Murray and all at the RCL, East Kilbride, not only for taking care and time with my samples, but for showing me round with patience and comprehensive explanations.

On a personal note, I would like to thank my family and friends for their support and for believing in me. Particularly the folk of Cambridge University Hillwalking Club: being able to escape to the hills every other weekend with the best company imaginable was a lifeline. Finally, all my thanks and love to Dave (not least, but not most, for help with MATLAB)—you've enriched my life immeasurably. Here's to the next great adventure.

Particulate organic carbon mobilisation and export from temperate forested uplands

Joanne Caroline Smith

The transfer of organic carbon stored in continental biomass to geological storage is an important pathway in the global carbon cycle, with the potential to sequester significant amounts of carbon dioxide. Despite an initial focus on active mountain belts as prime locations for such erosion, temperate forested uplands also have a significant role to play. This thesis investigates the origins, mobilisation and export of particulate organic carbon (POC) in the headwaters of two representative temperate areas, the Swiss Prealps and Western Oregon, and addresses the significance of the results in a global context.

Broadly, organic carbon concentration as a percentage of the suspended load is inversely correlated with clastic yield. Mean values in natural catchments range from 1.5% in Switzerland to 10% in Oregon. By chemically fingerprinting this POC and major organic carbon stores within each catchment, using carbon and nitrogen elemental and stable isotopic compositions, its provenance is determined. By monitoring its changing concentration and composition over a range of discharge, the processes by which it is mobilised are elucidated. In Switzerland, additional methods including radiocarbon analysis, Raman spectroscopy and biomarker geochemistry add further insights into sources and pathways.

Riverine POC in Switzerland derives from binary mixing between bedrock and modern biomass with a soil-like composition, with little direct input of plant matter. The hillslope and actively incising channel are strongly coupled, allowing overland flow to deliver biogenic material directly to the stream beyond a moderate discharge threshold. At this point, the broad trend is reversed; the proportion of organic carbon now increases with discharge and suspended sediment concentration. At higher flows, more biomass is mobilised and the fraction of modern organic carbon in

the suspended load reaches 0.70, increased from 0.30 during background conditions. In Oregon, little fossil organic carbon enters the suspended load even where it is present. Instead, riverine POC derives from mixing between soil-like material and foliage from a variety of plants. Overland flow rarely develops and hillslopes are isolated from channels. Material comes instead from the channel itself and immediately adjacent areas. There is no systematic switch to POC addition; instead, continued dilution by clastic material is observed as discharge increases.

Significant amounts of non-fossil organic carbon are thus mobilised in both areas without the need for extreme events such as landsliding. Precipitation is key: as soon as the rain stops, biomass supply ceases and fossil carbon again dominates in Switzerland, while Oregon streams run clear once more.

Relationships with discharge are used where possible to calculate long-term export fluxes of total and non-fossil POC. In the most active Swiss catchment, rating curves are integrated over 29-year discharge records, giving fluxes of 23 ± 6 t km^{-2} yr^{-1} and 14 ± 5 t km^{-2} yr^{-1} respectively. On the order of 6 t km^{-2} yr^{-1} of total POC are exported from the Oregon Cascades, of which $\sim$100% is non-fossil. These represent near-end members of POC export in temperate forested uplands, with the other catchments forming a continuum between them. One Oregon catchment subjected to intensive recent logging shows dramatically different behaviour, marked by high clastic yield and a much-reduced fraction of modern organic carbon. Ecosystem biology is shown to be the principal control on POC export style, with lithology having a lesser influence.

Yields of non-fossil POC from the temperate forested uplands studied are comparable to those from active mountain belts, yet the processes responsible for them are much more widely applicable. Their collective contribution to global land-ocean POC discharge may be greater than previously thought, and their role in the carbon cycle—including potential Earth–climate feedbacks—more significant.

Contents

List of Figures

List of Tables

Nomenclature

δ^{13}C	Stable isotopic composition of organic carbon, expressed as parts per thousand (‰)
Δ^{14}C	Radiocarbon concentration, equal to (F_{mod}–1) x 1000
δ^{15}N	Stable isotopic composition of nitrogen, expressed as parts per thousand (‰)
Λ	Sum of vanillyl, syringyl and cinnamyl compounds
(Ad/Al)v	Ratio of vanillic acid to vanillic aldehyde
ALS	Alsea headwaters
BGS	British Geological Survey
C_{org}	Organic carbon concentration, expressed as a percentage
C_{org}/N	Organic carbon to nitrogen ratio (used in Chapter 1)
C/N	Organic carbon to nitrogen ratio (used in subsequent chapters)
C/V	Ratio of cinnamyl to vanillyl compounds
CO_2	Carbon dioxide
DEM	Digital elevation model
DIC	Dissolved inorganic carbon
DOC	Dissolved organic carbon
F_{mod}	Fraction of modern carbon in a sample, represented by abundance of ^{14}C atoms compared to the year 1950
F_{nf}	Modelled fraction of non-fossil organic carbon in a sample
fPOC	Fossil particulate organic carbon
Gt	Gigatonne (=10^9 t or 10^{15} g)
HJA	H.J. Andrews Forest
LO	Lookout Creek in H.J. Andrews Forest

LTER Long-Term Ecological Research

N/C Nitrogen to organic carbon ratio

NFH North Fork of Hinkle Creek headwaters

nfPOC Non-fossil particulate organic carbon

NPP Net primary productivity

POC Particulate organic carbon

POM Particulate organic matter

Q Water discharge, in litres per second (l s^{-1}) unless otherwise stated

Q_e Effective discharge; the discharge that, on average, transports the largest proportion of a given constituent load

Q_{mean} Long-term mean water discharge for a particular catchment, in litres per second (l s^{-1}) unless otherwise stated

Q/Q_{mean} Water discharge expressed relative to long-term mean for a particular catchment

S/V Ratio of syringyl to vanillyl compounds

SS Suspended sediment

SSC Suspended sediment concentration, in milligrams per litre (mg l^{-1})

TOC Total organic carbon; comprises POC and DOC

tPOC Total particulate organic carbon

TR Trask headwaters (and surrounding area)

TSL Total suspended load, in grams per second (g s^{-1})

WS1 Watershed 1 in H.J. Andrews Forest

WS2 Watershed 2 in H.J. Andrews Forest

WSL Swiss Federal Institute for Forest, Snow and Landscape Research

Chapter 1

Introduction

1.1 Rationale

The erosion of continental biomass in the form of particulate organic carbon (POC) derived from plants and soils is an important pathway in the global carbon cycle, because it is one way in which carbon dioxide (CO_2) can be transferred from the atmosphere–biosphere system into geological storage. However, the flux is still under-constrained and the processes poorly understood.

There have been many estimates of the global flux of POC from continents to oceans, but all use a broad brush, require multiple assumptions and avoid delving into the mechanisms by which the transfer occurs. Conversely, there have been many small-scale studies on the carbon dynamics of individual catchments, but as a group they are geographically sparse and not always methodologically compatible, making it difficult to extrapolate the results more widely.

To evaluate the importance of continental biomass erosion on a global scale, we must quantify the long-term POC export from a range of representative settings. To grasp how this pathway may respond to climate change, and understand its influence on Earth–climate feedbacks, we must characterise the mechanisms of and controls on POC export from a range of representative settings.

In order to place this project within the framework of these broad goals, it is first necessary to review existing knowledge regarding the role of organic carbon in the global carbon cycle, and to identify the areas where more research is needed. The specific aims of this project, and the rationale behind them, are returned to later in the chapter, particularly in Sections 1.3.5 and 1.4.

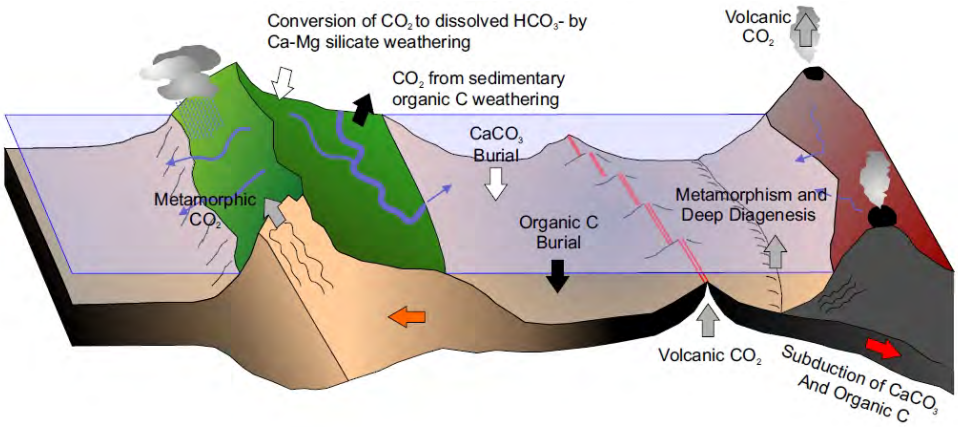

Figure 1.1: The Earth's carbon cycle. From Hilton (2008), after Berner (1999). Schematic showing the processes by which carbon is cycled between the solid earth (crust) and the atmosphere–biosphere–ocean system. More detailed diagrams, including quantitative reservoirs and fluxes, are given in Figures 1.1 and 1.3.

1.2 The global carbon cycle

Broadly, the parts of the Earth system involved in the global carbon cycle (Figure 1.1) can be divided into three: solid earth, deep ocean, and atmosphere–biosphere, including the surface ocean. The latter component is often regarded separately as the short-term carbon cycle, as it comprises multiple internal exchange pathways operating on much shorter timescales than the overall cycle.

From the solid earth, CO_2 is initially and continuously added to the atmosphere by degassing through volcanic activity and metamorphism. From the atmosphere, it can dissolve in water to form carbonic acid and then bicarbonate, a reversible process in constant flux:

$$CO_2 + H_2O \rightleftharpoons H_2CO_3 \rightleftharpoons HCO_3^- + H^+ \tag{1.1}$$

Bicarbonate ions are used in the formation of calcium carbonate, which releases one mole of CO_2, but locks another away in limestone and other carbonate rocks (equation 1.2). The reverse, carbonate dissolution, takes one mole of carbon each from the atmosphere and the solid earth and puts them ultimately in the ocean. Both the solid and dissolved forms of carbonate are inorganic.

$$Ca^{2+} + 2HCO_3^- \rightleftharpoons CaCO_3 + CO_2 + H_2O \tag{1.2}$$

Alternatively, carbon can be organic; that is, related to a living entity and existing in reduced form. In both aqueous and terrestrial environments, carbon is fixed by photosynthesis in primary organisms, a process summarised by the formation of

glucose:

$$6CO_2 + 6H_2O \rightleftharpoons C_6H_{12}O_6 + 6O_2 \tag{1.3}$$

In the short-term cycle, this carbon may be passed down the food chain, and is returned to the atmosphere or ocean by oxidation (the reverse of equation 1.3) on the death and decay of organisms.

Carbon is returned to long-term geological storage in significant amounts in two principal ways. The weathering of silicate rocks, which make up the majority of the Earth's crust, uses two moles of CO_2 to produce two moles of bicarbonate ions:

$$2CO_2 + 3H_2O + CaSiO_3 \rightarrow Ca^{2+} + 2HCO_3^- + Si(OH)_4 \tag{1.4}$$

which sequester one mole of carbon dioxide by forming carbonate rocks according to equation 1.2. The other pathway is the direct preservation of organic matter, both marine and terrestrial. For terrestrial organic matter to survive into the rock record, it must be transferred by rivers to areas of sediment deposition and lithification, commonly the ocean although inland waters and overfilled foreland basins are also viable sinks. In these regions, and in the marine realm, rapid burial rates and anoxic conditions aid organic matter preservation (Burdige, 2005; Galy *et al.* , 2007b; Hilton *et al.* , 2008b; Sparkes, 2012).

That fossil organic matter exists is demonstrated by coal and oil deposits in the geological record, as well as more subtly in the inclusion of organic particles in sedimentary rocks such as mudstones and sandstones (e.g. Copard *et al.* , 2007), and the existence of ancient organic matter in soil weathering profiles (Petsch *et al.* , 2000), but scepticism has persisted over the volumetric importance of this material. The prevailing view has been that nearly all organic matter is oxidised before it can be finally buried (Hedges, 1992; Hedges & Keil, 1995; Schlesinger, 1995; Schlünz & Schneider, 2000), but in recent decades evidence has increasingly begun to suggest otherwise (e.g. Hayes *et al.* , 1999; Smith *et al.* , 2001), i.e. that burial of organic carbon may be comparable to silicate weathering in terms of its ability to sequester CO_2 (Figure 1.2).

If re-exposed at the Earth's surface for a critical length of time under the right conditions, fossil organic matter in sedimentary rocks can be oxidised, representing a source of CO_2 to the atmosphere (Bouchez *et al.* , 2010; Hedges, 1992). Any fossil organic matter that is eroded, transported and re-buried before it can be oxidised has no effect on atmospheric CO_2 on the timescale of its burial and remineralisation (Blair *et al.* , 2003; Hilton *et al.* , 2011a).

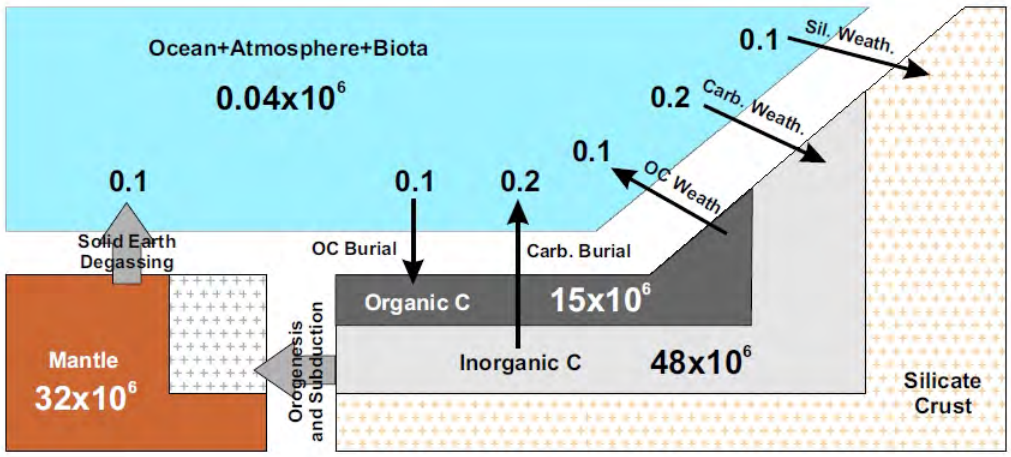

Figure 1.2: Reservoirs and fluxes of the long-term carbon cycle, illustrating the links between the short-term cycle and geological storage. From Hilton (2008), after Berner (1999). Major carbon reservoirs, with approximate amounts stored (Gt) and approximate fluxes between them (Gt C yr^{-1}). Data are from Gaillardet *et al.* (1999); Sigman & Boyle (2000); Sundquist (1993); Sundquist & Visser (2003). Sil.=silicate, Carb.=carbonate, Weath.=weathering, OC=organic carbon.

1.2.1 Magnitude of carbon stores and fluxes

By far the largest reservoirs of carbon are found in the solid earth (Figure 1.2), with ~$32x10^6$ Gt (1 Gt=10^{15} g) stored in the mantle, ~$48x10^6$ Gt in carbonate rocks and ~$15x10^6$ Gt as organic carbon in sedimentary rocks, with a further 3700 Gt as fossil fuels (Denman *et al.* , 2007). The deep ocean contains ~38000 Gt of carbon, almost all in the form of dissolved inorganic carbon (DIC) (Sigman & Boyle, 2000), while the surface ocean–atmosphere–biosphere system combined—illustrated in Figure 1.3—holds ~4200 Gt. In the surface ocean, there is ~800 Gt of carbon stored as DIC (Sigman & Boyle, 2000; Sundquist & Visser, 2003), and a further ~700 Gt as dissolved organic carbon (DOC) from marine biota (Siegenthaler & Sarmiento, 1993). Terrestrial organic carbon stores are split between soil, which holds ~1400–1600 Gt (Bianchi, 2011; Post *et al.* , 1982; Schlesinger, 1984), and vegetation, which holds ~500–600 Gt (Bianchi, 2011; Prentice *et al.* , 2001; Sundquist, 1993). The (pre-industrial) atmosphere is one of the smallest carbon pools with ~600 Gt (Denman *et al.* , 2007; Sigman & Boyle, 2000), but it plays an important role as a major exchange pathway.

Net primary productivity (NPP), the difference between the production of chemical energy via photosynthesis and its use via respiration, accounts for balanced fluxes of ~60 Gt C yr^{-1} and ~50 Gt C yr^{-1} between the atmosphere and the terrestrial and marine biospheres respectively (Figure 1.3) (Prentice *et al.* , 2001). There is also

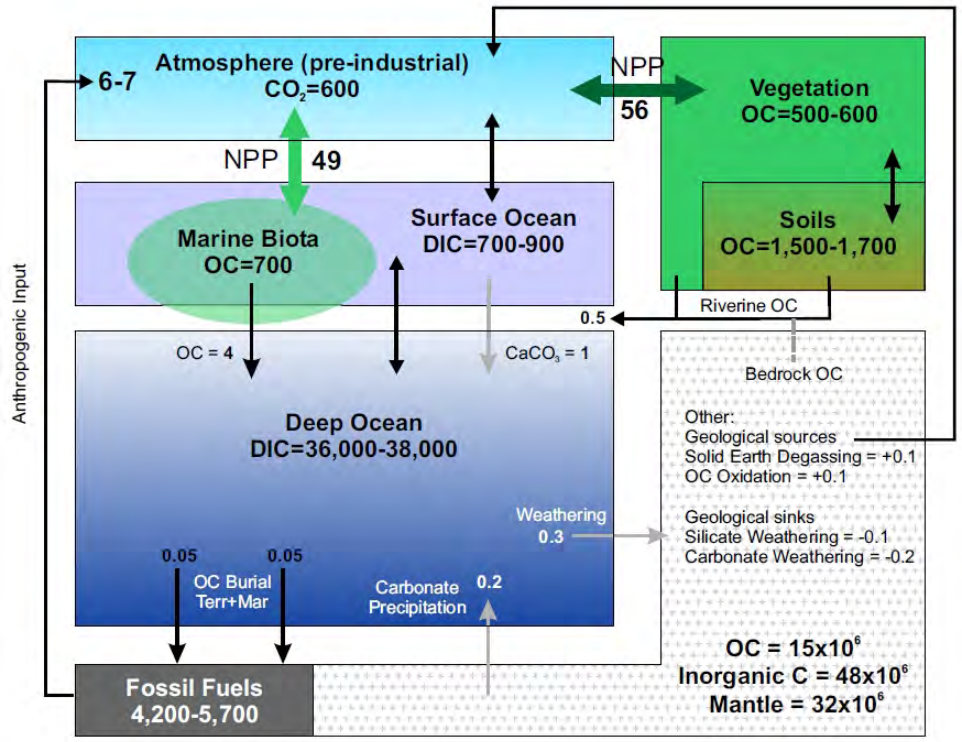

Figure 1.3: Reservoirs and fluxes of the short-term carbon cycle, illustrating the interactions between surface ocean, atmosphere and biosphere, and relevant geological processes. From Hilton (2008). Major carbon reservoirs, with approximate amounts stored (Gt) and approximate fluxes between them (Gt C yr^{-1}). Data are from Gaillardet *et al.* (1999); Prentice *et al.* (2001); Sarmiento & Sundquist (1992); Schlünz & Schneider (2000); Sigman & Boyle (2000); Sundquist (1993); Sundquist & Visser (2003). OC=organic carbon, DIC=dissolved inorganic carbon, Terr=terrestrial, Mar=marine.

constant exchange between vegetation and soil, atmosphere and surface ocean, and surface and deep ocean. Current estimates of the riverine flux of organic carbon to the ocean, from soil, vegetation and fossil sources, are on the order of 0.5 Gt C yr^{-1} (Schlünz & Schneider, 2000, and references therein). Net fluxes of ∼4 Gt yr^{-1} of organic carbon and ∼1 Gt yr^{-1} of inorganic carbon in the form of calcium carbonate are transferred from surface to deep ocean (Sigman & Boyle, 2000), and ∼0.05 Gt yr^{-1} each of terrestrial and marine organic carbon are buried in the deep ocean (Prentice *et al.* , 2001). This burial is balanced by solid earth degassing of ∼0.1 Gt C yr^{-1}; anthropogenic burning of fossil fuels is currently adding a further ∼7 Gt C yr^{-1} to the atmosphere (Denman *et al.* , 2007; Sundquist, 1993).

Rock weathering accounts for the transfer of ∼0.3 Gt C yr^{-1} to the solid earth, of which about one third is via silicate weathering (Gaillardet *et al.* , 1999). The rest is due to carbonate weathering, but this is balanced by the release of carbon during

carbonate precipitation (Sigman & Boyle, 2000).

Although many of the carbon reservoirs are very large relative to the fluxes between them, the carbon cycle system is so finely balanced that small perturbations, such as anthropogenic input of CO_2 to the atmosphere or changes in silicate weathering or the riverine organic carbon flux, may have large effects (Prentice *et al.* , 2001; Raymo & Ruddiman, 1992; Schlünz & Schneider, 2000; Sigman & Boyle, 2000). These are most important in the atmosphere–biosphere short-term cycle, as it is here that the fluxes are largest in proportion to the reservoirs.

1.3 Biomass export via the organic pathway

As outlined above, the burial of continental biomass exported by rivers can act as a CO_2 sink and thus influence atmospheric carbon dioxide and global climate. In reality, determining the magnitude and nature of the export flux is complex and ongoing. Existing knowledge and previous efforts towards this goal are detailed in the following sections.

1.3.1 Particulate and dissolved organic carbon

POC is defined as the carbon contained within particulate organic matter, i.e. the organic matter that is too large to pass through a filter with a certain pore size. The exact cut-off varies, but is generally between 0.2 and 1.2 μm. Material that can pass through such a filter is deemed to be dissolved organic matter.

Although DOC makes up around half the total organic carbon input to the ocean (Ludwig *et al.* , 1996; Meybeck, 1993; Stallard, 1998), it is extremely reactive in the marine environment and does not contribute significantly to the marine burial flux of organic carbon (e.g. Hedges *et al.* , 1997). In addition, while POC derives almost exclusively from continental biomass and consists of plant fragments and carbon associated with soil particles, DOC can result from in-stream algal growth and other biological activity (e.g. Dean & Gorham, 1998; Finlay *et al.* , 1999). POC is therefore the primary interest for an investigation focusing on continental biomass erosion as part of a pathway ultimately ending in marine burial.

Total organic carbon (TOC) comprises POC and DOC.

1.3.2 Sources of POC and differentiating between them

Elucidating the origin of POC exported by rivers (whether during transit or in depositional sites) not only provides valuable insights into transfer mechanisms, but is critical to interpreting that POC in the context of the carbon cycle. It is particularly important to distinguish between carbon from fossil and non-fossil sources, because only non-fossil carbon burial has an effect on contemporary CO_2 drawdown (e.g. Berner, 1982; France-Lanord & Derry, 1997).

1.3.2.1 Carbon and nitrogen elemental and stable isotopic ratios

Organic matter from particular sources can be identified by characteristic carbon and nitrogen stable isotopic compositions, and by the ratio of elemental organic carbon (C_{org}) to nitrogen (N). Isotopic compositions are reported in delta notation, which compares the isotopic ratio of a sample to a universal standard and gives a value in parts per thousand (‰). This is given by:

$$\delta^{13}C = 1000 \left[\frac{(^{13}C/^{12}C)_{sample}}{(^{13}C/^{12}C)_{standard}} - 1 \right] \tag{1.5}$$

and

$$\delta^{15}N = 1000 \left[\frac{(^{15}N/^{14}N)_{sample}}{(^{15}N/^{14}N)_{standard}} - 1 \right] \tag{1.6}$$

where the standards are the Pee Dee Belemnite (PDB) and air for carbon and nitrogen respectively (Coplen, 1994).

Primary producers convert inorganic carbon in the form of atmospheric CO_2 (terrestrial) or dissolved bicarbonate (marine) into carbohydrates via equation 1.3. Fractionation during these processes, largely kinetic in nature, results in a depletion of the heavy isotope of carbon (^{13}C) in organic matter relative to the light isotope (^{12}C). Incorporation of nitrogen into organic matter is similarly affected, with a resulting depletion of ^{15}N relative to ^{14}N, although expected values of δ^{15}N for different organic carbon pools are much less widely reported.

The degree of depletion depends on both the isotopic composition of the starting material and a fractionation factor (e.g. Hayes, 1993). Marine organic matter typically has C_{org}/N of ~7 and δ^{13}C of -18‰ to -20‰ (Holtvoeth *et al.* , 2005), while terrestrial plant matter formed by the C3 photosynthetic pathway tends to have C_{org}/N values greater than 20 and more negative isotopic compositions (Holtvoeth *et al.* , 2005). These can vary widely between species, with δ^{13}C values ranging from ~-24‰ up to ~-30‰ (e.g. Bowen, 2010; Guehl *et al.* , 1998). C4 plants have a lower fractionation

factor because they are more efficient, so have more positive $\delta^{13}C$ of around 4‰–5‰ (Bowen, 2010). In general, wood cellulose has higher $\delta^{13}C$ values than leaves of the same plant by ∼2‰–3‰ (Guehl *et al.* , 1998), and higher C_{org}/N (O'Leary, 1981). Nitrogen isotopes follow the same pattern, with marine organic matter having heavier N ($\delta^{15}N$ values of up to ∼9‰–10‰) (Middelburg & Nieuwenhuize, 1998; Thornton & McManus, 1994) and terrestrial plant matter exhibiting values ranging roughly from -8‰ to 4‰, though with no difference between C3 and C4 plants (Bowen, 2010; Hilton, 2008; Peterson & Fry, 1987). At least one study (Ometto *et al.* , 2006) found no significant difference in $\delta^{15}N$ between foliage and wood.

Subsequent processing of this organic matter during litter decomposition and soil formation also involves isotopic fractionation. The direction and magnitude of the fractionation is dependent on multiple factors. However, in general the action of microbial organisms on fresh plant material tends to enrich it in ^{13}C and ^{15}N (Coyle *et al.* , 2009; Dijkstra *et al.* , 2006; Melillo *et al.* , 1989; Natelhoffer & Fry, 1988), though there is evidence that on some substrates the opposite occurs (Macko & Estep, 1984). Soil $\delta^{13}C$ and $\delta^{15}N$ values are higher relative to plants by around 1‰–3‰ (Townsend-Small *et al.* , 2005) and 3‰–8‰ (Amundson *et al.* , 2003) respectively, giving an approximate range of -26‰ to -27‰ in $\delta^{13}C$ (Bird *et al.* , 2002), and 4‰ to -2‰ in $\delta^{15}N$ (Martinelli *et al.* , 1999) in forested terrain. C_{org}/N ratios are also affected by the decomposition process: microbial C_{org}/N is ∼7–9 in forests (Cenciani *et al.* , 2008; Cleveland & Liptzin, 2007), so soils generally have lower C_{org}/N values than the plants that grow in them.

Global latitudinal trends also exist in plant and soil stable isotopic ratios (Bowen, 2010; Körner *et al.* , 1991). For example, a study in Canada showed that soil $\delta^{13}C$ is higher in forest than tundra (Bird *et al.* , 2002), while plant ^{15}N is higher in tropical forests than temperate ones (Bowen, 2010; Martinelli *et al.* , 1999). The difference in $\delta^{15}N$ between plants and soils is greater in cold climates (Amundson *et al.* , 2003). The effect of altitude is also observed globally (Körner *et al.* , 1988), with Bird *et al.* (1994) reporting an increase in the $\delta^{13}C$ of both soil and C3 foliage over a height difference of ∼4000 m. It is therefore important to know the local values for plants and soils that may be sources for riverine organic matter.

Aged organic matter is a component of many sedimentary rocks (e.g. Copard *et al.* , 2007). Like soil formation, the processes involved in lithification fractionate C and N stable isotopes in highly variable ways (e.g. Ader *et al.* , 2006), and depend additionally on the starting material. Published values of bedrock $\delta^{13}C$ and $\delta^{15}N$ reflect this (e.g. Hilton *et al.* , 2008a, 2010; Komada *et al.* , 2005; Sparkes, 2012) and it is impossible to quote generalised values. Again, when considering different sources for

riverine organic matter, it is important to know the values for the rocks underlying the particular catchment in question.

Particulate organic matter (POM) in riverine suspended sediment exported from headwaters commonly contains a mixture of carbon from two or more end member sources, including bedrock, soil, vegetation, geomorphic features such as landslides and subdivisions of these categories (Blair *et al.* , 2003; Hilton *et al.* , 2008a,b; Komada *et al.* , 2004; Leithold *et al.* , 2006), all of which have distinctive C_{org}/N, $\delta^{13}C$ and $\delta^{15}N$ values because of the fractionation processes described above. In less turbulent downstream reaches and in lakes, autochthonous algal organic material can be incorporated (Dean & Gorham, 1998; Finlay *et al.* , 1999), while ocean sediments have the additional input of marine organic matter.

Mixing between these different sources can be primarily elucidated in N/C_{org}–$\delta^{13}C$ and C_{org}/N–$\delta^{15}N$ space, where sources plot in distinct areas and mixing relationships appear as straight lines or zones between them (e.g. Hilton, 2008; Hilton *et al.* , 2010; Sparkes, 2012). This is the principal method utilised in this project. However, there may be ambiguities which these parameters cannot resolve, and two other geochemical methods that can be of use in adding further detail to organic matter source determination are described below.

1.3.2.2 Radiocarbon and biomarker analysis

Radiocarbon (^{14}C) provides an additional constraint on the input of fossil carbon (e.g. Blair *et al.* , 2003; Hilton *et al.* , 2008b; Komada *et al.* , 2005). ^{14}C is a naturally-occurring isotope of carbon that decays to ^{14}N with a half-life of 5730 years. It is continuously produced in the stratosphere and incorporated in trace amounts into the carbon cycle. As long as there is exchange with the atmosphere via photosynthesis and respiration, the ^{14}C content of a particular carbon pool stays constant as atoms decay but are replaced by others from the atmosphere. However, as soon as this exchange ceases, the ^{14}C content decreases until, after seven half-lives or ~40000 years, the amount left (~0.8%) is below detection limits. By measuring the ^{14}C content of any organic sample, its age and "fraction modern" (F_{mod}), the proportion of ^{14}C atoms in the sample compared to that present in the atmosphere in the year 1950, can be found by calculation and calibration. Owing to the incorporation of additional ^{14}C from nuclear weapons testing during the second half of the twentieth century (Levin & Hesshaimer, 2006), modern biogenic material has F_{mod} of 1–1.1, while fossil petrogenic material has F_{mod} of 0. Directly determining or otherwise modelling the F_{mod} of riverine suspended sediment enables fossil and non-fossil carbon to be considered as

separate components. This is important because, as discussed in Section 1.2, only the erosion of non-fossil carbon has the potential to draw down CO_2.

Biomarker analysis is a broad group of techniques that involve identifying and measuring the abundance of compounds at the molecular level, allowing the identification and quantification of more specific plant sources. Some of the first such analyses were performed by Hedges & Mann (1979a) and Hedges & Mann (1979b), who measured the concentrations of vanillyl, syringyl and cinnamyl phenols, all products of lignin oxidation, in a variety of plants, soils and sediments. Combinations of these parameters allowed them to distinguish five types of plant matter: nonvascular plants, gymnosperm woods, non-woody gymnosperm tissues, angiosperm woods and non-woody angiosperm tissues. Similar techniques have since been developed to measure a wide range of other compounds derived from non-lignin precursors, including benzoic acids, *n*-alkanes, *n*-alkanoic acids and terpenoids (e.g. Eglinton & Eglinton, 2008; Gordon & Goñi, 2003; Hastings *et al.* , 2012; Karlsson *et al.* , 2011; Medeiros & Simoneit, 2008; Meyers, 1997; Prahl *et al.* , 1994). Biomarker analysis is commonly used to determine the contributions of different terrestrial sources to organic matter in marine sediments, and more detail on this is given in Section 1.3.4.1. It can also distinguish between allochthonous and autochthonous material (Bianchi *et al.* , 2007).

1.3.3 Global estimates of riverine organic carbon export

Previously published estimates of riverine organic carbon discharge to the ocean have, if at all, variably distinguished between DOC and POC, and modern and fossil organic carbon. One of the first attempts to quantify riverine export of TOC was by Schlesinger & Melack (1981), who also noted that lack of data and inadequate sampling presented a barrier to understanding. They estimated a flux of $370\text{x}10^{12}$ g yr^{-1} based on loss of carbon per unit volume of river discharge from twelve large rivers, or $410\text{x}10^{12}$ g yr^{-1} based on fluvial loss of carbon per unit area of land in different ecosystems. Ittekkot (1988) was one of the first to consider different types of organic matter delivered to the ocean by major rivers, estimating that 35% of a total flux of $231\text{x}10^{12}$ g yr^{-1} belonged to a labile fraction that would likely be oxidised before burial. Sarmiento & Sundquist (1992) emphasised the importance of the riverine transfer of organic carbon to the ocean in balancing global carbon budgets.

Meybeck (1993) considered the "total atmospheric carbon" export flux, including POC, DOC and DIC from silicate weathering reactions, to be $542\text{x}10^{12}$ g yr^{-1}, with a further $80\text{x}10^{12}$ g yr^{-1} POC and $137\text{x}10^{12}$ g yr^{-1} DIC from rock erosion. He estimated that 18% of the total atmospheric carbon flux, or $98\text{x}10^{12}$ g yr^{-1}, was in the form of

soil-derived POC, with 37% as DOC and 45% as DIC. Meybeck (1993) also distinguished between export from different biomes, reporting that most total atmospheric carbon comes from rivers draining humid tropics (46%), followed by temperate forest and grassland (31%).

Ludwig *et al.* (1996) did not distinguish between modern and fossil carbon, but used an empirical approach to establish relationships between organic carbon flux and climatic, biologic and geomorphic characteristics of river basins. Extrapolating the model to the entire globe, they obtained a value for TOC flux to the ocean of 380x10^{12} g yr^{-1}, of which around 170x10^{12} g yr^{-1} was particulate. On average, higher fluxes (∼6–8 mg l^{-1}) of POC entered the Pacific and Indian Oceans, while lower fluxes (∼2–3 mg l^{-1}) entered the polar and Atlantic Oceans. They found that drainage intensity (discharge normalised to basin area) and specific sediment flux were the main controls on TOC export, although there was no clear correlation with any one parameter for POC.

These early estimates focused almost exclusively on the world's major rivers, which ignored the input from high-standing oceanic islands. Schlünz & Schneider (2000) incorporated new data from New Guinea, the Philippines, Java, New Zealand and Taiwan (Bird *et al.* , 1995) suggesting that the amount of total organic carbon supplied to the ocean from these locations was greater than for North America, South America and Africa combined. Their revised estimate for the global riverine TOC flux was 430x10^{12} g yr^{-1}. More recently, the global Nutrient Export from Watersheds (NEWS) model, based on natural and anthropogenic biogeophysical properties of basins, predicts global fluxes of 197x10^{12} g yr^{-1} POC and 170x10^{12} g yr^{-1} DOC (Seitzinger *et al.* , 2005), again making no distinction between modern and fossil carbon.

Considering these estimates as a group, the current consensus is that approximately 400x10^{12} g yr^{-1} of TOC is exported to the global ocean by the world's rivers, of which about half, or 200x10^{12} g yr^{-1}, is in the form of POC; the remainder as DOC. The figure of 98x10^{12} g yr^{-1} (Meybeck, 1993) remains the only global estimate of specifically non-fossil POC export. In the rest of this thesis, these values will be used as extant estimates of global fluxes whenever comparisons are made.

1.3.4 Organic carbon burial

1.3.4.1 Burial in marine sediments

Although it is generally accepted that rivers deliver organic carbon to the ocean in both dissolved and particulate forms, there is considerable debate over what happens to it there: whether it is mostly preserved, or mostly oxidised before it can be finally

buried (Blair & Aller, 2012). Berner (1982) collated the organic carbon content of deltaic shelf sediments from some of the world's major rivers and concluded that $126x10^{12}$ g yr^{-1} of organic carbon is buried globally such that it enters the geological record: far less than is delivered to the ocean by rivers, particularly if the contribution of marine organic matter is taken out. Similarly, Schlünz & Schneider (2000) assert that only around 10% of their calculated riverine organic carbon flux is buried in marine sediments, while Hedges & Keil (1995) suggest that overall organic matter preservation in the marine realm is less than 0.5% efficient.

The question is complicated by the need to distinguish between marine and terrestrial organic matter in marine sediments. Burdige (2005) showed that terrestrial organic matter is less efficiently remineralised than more reactive marine organic matter in the oceans, and that despite the much greater volume produced by marine photosynthesis than delivered by rivers, around a third of all organic matter buried in marine sediments is of terrestrial origin. Recently, biomarkers (Section 1.3.2.2) have been particularly useful in demonstrating the presence of terrestrial organic matter in marine sediments. In the Gulf of Mexico, terrestrial soil and plant material accounts for ~79% and ~66% of the organic matter content of inshore and outshore sediments respectively (Gordon & Goñi, 2003). There is also evidence for a predominantly terrestrial origin of organic matter in sediments of the Fly River delta in Papua New Guinea (Goñi *et al.* , 2008), on the Mississippi Delta and Eel River (California) margin (Wakeham *et al.* , 2009) and on the Washington margin shelf, decreasing from 60% to 30% on the slope and to ≤15% in basin sediments (Prahl *et al.* , 1994). Even on the Hauraki Gulf, New Zealand, a non-river dominated margin, the terrestrial contribution to organic matter in surface sediments is ~40–65% (Sikes *et al.* , 2009).

These studies indicate that marine preservation of terrestrial organic matter depends on many local factors. Indeed, it has been suggested that significant burial might only happen under, and is certainly encouraged by, specific conditions. These include high clastic sediment yields that form hyperpycnal flows (Burdige, 2005; Hilton *et al.* , 2008b), deposition in oxygen-poor waters (Aller, 1998; Burdige, 2005; Galy *et al.* , 2007b) or submarine canyons (Hilton *et al.* , 2008b; Lorenzoni *et al.* , 2012; Masson *et al.* , 2010), and extreme storm events (Lorenzoni *et al.* , 2012; West *et al.* , 2011).

Evidence of terrestrial organic carbon input to marine sediments is observed not only in modern deposits, but also in palaeo-systems. Using combined optical kerogen analysis and biomarker geochemistry, Meckler *et al.* (2008) tracked terrigenous input to the Gulf of Mexico over the last 25000 years, finding that while Holocene sediments contained mainly marine organic matter, terrigenous material was dominant during

deglaciation, likely because of large meltwater fluxes. Tyson & Follows (2000) and Sparkes (2012) have found evidence for substantial preservation of organic matter in the Cretaceous to Miocene turbidites of ancient sedimentary basins now exposed in the Pyrenees and Apennines, using palynological, geochemical and optical spectroscopic methods.

1.3.4.2 Terrestrial storage

While the focus has been on the burial of organic carbon in marine settings, consideration is also now being given to the fluvial deposition of organic carbon in terrestrial environments (e.g. Aufdenkampe *et al.* , 2011; Smith *et al.* , 2001), since input of organic carbon from land to inland waters is twice that from land to the ocean (Cole *et al.* , 2007). This is driven partly by the question of whether river basins are net sources or sinks of CO_2 (Ramos Scharrón *et al.* , 2012; Yue *et al.* , 2012). Terrestrial deposition may be temporary, and some of the organic material accumulating in lakes and elsewhere on flood plains is certainly remineralised by oxidation (Bouchez *et al.* , 2010; Gudasz *et al.* , 2010). However, storage may be long enough to remove material from the atmosphere–biosphere carbon cycle on a medium-term basis: Galy & Eglinton (2011) report evidence for a refractory component of biospheric carbon in the Ganges–Brahmaputra basin with an average age of 15000 years. Vascular plant material can spend several thousand years in intermediate reservoirs before transfer to the ocean, even in small river systems such as the Eel in California (Drenzek *et al.* , 2009). In total, roughly $100\text{x}10^{12}$ g yr^{-1} of organic carbon is buried in terrestrial sinks (Stallard, 1998), although much of this is autochthonous rather than soil- and plant-derived (Dean & Gorham, 1998).

It is evident that the downstream persistence of organic carbon mobilised by rivers is large and complex area of investigation, but it is largely outside the scope of this project, which concentrates on the mobilisation of POC in headwaters.

1.3.5 Headwater processes: landsliding versus runoff

Previous work on organic carbon export has focused on active mountain belts because of their importance in the physical erosion budget (Burbank *et al.* , 1996; Milliman & Syvitski, 1992), and the belief that riverine POC is strongly linked to clastic sediment (Stallard, 1998). Recent studies (Carey *et al.* , 2005; Hilton *et al.* , 2008a,b; Lyons *et al.* , 2002) suggest that storm-driven erosion of terrestrial biomass can effectively sequester carbon in tectonically and climatically extreme regimes, such as the active mountain belts of Taiwan and New Zealand. Deep-seated landslides and gully erosion

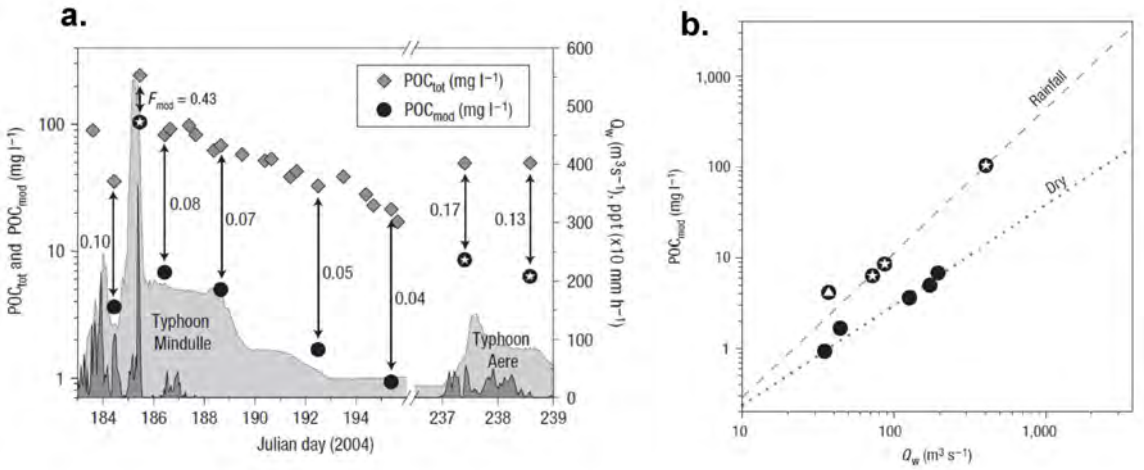

Figure 1.4: Effect of sustained rainfall on modern POC export in the LiWu River, Taiwan, from Hilton *et al.* (2008b). White stars indicate samples collected near the peaks of Typhoons Mindulle and Aere in July–August 2004; white triangle indicates sample collected in March 2004. (**a**) Total and modern POC concentrations in suspended sediment samples collected during the two typhoons, shown with hourly water discharge (Q_w) in light grey and hourly precipitation (ppt) in dark grey. The fraction of organic carbon coming from modern sources (F_{mod}) is given next to the arrows. (**b**) Separate rating curves for modern POC carried in suspended sediment in dry conditions and after sustained rainfall.

are important in mobilising particulate organic carbon (POC) in extreme events in these environments (Goldsmith *et al.* , 2008; Hilton *et al.* , 2008a; West *et al.* , 2011).

However, Hilton *et al.* (2008b) showed that, in Taiwan, there is a different relationship between river discharge and the amount of modern POC exported after sustained rainfall than at other times, and also that the proportion of modern organic carbon carried in the suspended load dramatically increases at flood peaks after heavy rain (Figure 1.4). This could be accounted for by runoff erosion via overland flow, which removes only the surface layer of soil and litter, while deep landslides and gully erosion also mobilise bedrock containing fossil organic carbon (Horton, 1945; Wheatcroft *et al.* , 2010). The suggestion that simply rain and runoff, rather than the deep-seated landslides induced by them, is important in mobilising modern organic carbon from steeplands even in areas dominated by bedrock and gully erosion, is supported by observations in New Zealand: Hilton *et al.* (2011b) compared the amount of modern organic carbon mobilised by deep-seated landslides in the western Southern Alps and that exported in the suspended load of its rivers, and concluded that there must be additional input from overland flow or shallow landsliding. Gomez *et al.* (2010) found that the modern component of POC in the Waipaoa River during a significant flood was 71%, mostly from alluvial stream bank collapses, although these may be closer to landslides than true runoff processes.

These observations raise the possibility that the harvest of organic matter recently fixed from the atmosphere and stored in plants and soils could happen anywhere, and potentially everywhere, where there is enough rain on soil organic carbon stores to generate overland flow or shallow landslides. As noted in Section 1.3.4.1, there is evidence that terrigenous biogenic material does reach marine sediments on less active margins (Gordon & Goñi, 2003; Hastings *et al.* , 2012; Prahl *et al.* , 1994; Wakeham *et al.* , 2009). Modern POC derived from plants and soils has also been observed in the suspended load of rivers entering the Pacific Ocean from the Oregon Coast Range (Goñi *et al.* , 2013; Hatten *et al.* , 2012). However, there is still insufficient understanding of the processes which may mobilise POC in temperate, forested headwaters around the globe.

If rain-driven runoff is important in eroding non-fossil POC from unremarkable upland landscapes, then there is potential for significant POC yield from a substantial area of the world's landmass, whereas the link with rapid mass wasting is much more restrictive. An understanding of the relative global significance of the two processes is critical to modelling carbon cycle processes, and ultimately climate change, on timescales from 100 years to glacial-interglacial cycles. It is, therefore, essential to observe and characterise POC mobilisation and transfer processes—and to determine their magnitude and extent—in headwaters with steep relief and high rainfall rates, but outside the domains of greatest tectonic activity.

1.4 Project aims and outcomes

This project investigates POC sources and initial pathways under changing hydrologic conditions in headwater catchments in temperate, forested uplands, where deep-seated landslides are not dominant and runoff processes can be studied unmasked.

In its simplest terms, the project aims to answer the following questions:

1. How much POC is exported in riverine suspended sediment from forested uplands in climatically and tectonically non-extreme settings?
2. What are the sources of this POC and how is it mobilised?
3. How does the amount and type of POC change with hydrologic conditions, and what are the potential feedback loops?

The investigation is focused in two temperate forested upland areas: the Swiss Prealps and the western Oregon Cascades and Coast Range, USA. Data and samples are collected from a number of headwater catchments of varying size and nature. For many of these, suspended sediment sampling was already in progress and long-term discharge records are available, meaning that relationships can be developed between

discharge and the suspended load of various components, and fluxes extrapolated to much longer timescales than can be directly observed. Though geographically distant, the two field areas have similar biologic, tectonic and climatic regimes, and are relatively unaffected by anthropogenic activity.

The principal outcomes of the project are:

1. A comprehensive dataset of organic carbon and nitrogen concentrations and isotopic ratios in suspended sediment from two representative Prealpine headwater catchments, over nearly the full range of observed discharges;
2. A comprehensive dataset of the same chemical parameters from the major organic carbon pools that form potential sources for riverine POC in these catchments, including soil, plants and bedrock;
3. Equivalent sediment and source datasets for one watershed in the Oregon Cascades, with additional, but less comprehensive, data from another Cascades watershed and two in the Oregon Coast Range
4. An understanding of (i) how compositionally distinct organic carbon pools are distributed within these settings and how they interact, (ii) the mechanisms by which these are mobilised, transferred to streams and exported, and (iii) the conditions under which this occurs;
5. Robust estimates (where possible) of the long-term flux out of these catchments of total, fossil and non-fossil POC and an understanding of how and why such fluxes vary between similar settings;
6. An indication of whether such fluxes could potentially lead to the sequestration of globally significant amounts of atmospheric CO_2;
7. An indication of how the erosion of organic carbon from such settings could change in response to local and global climate change, and how this might feed back into the Earth system.

1.5 Outline

Chapter 2 describes the field areas used as case studies in this project, including their geography, geologic and tectonic settings, climate, ecosystems and geomorphologic and hydrologic character. Chapter 3 outlines the methods used both in the field to collect samples and hydrologic and climatic data, and in the lab to obtain geochemical data. Sample preparation, subsequent processing and analysis, including error characterisation, are covered.

Following these initial chapters, results are presented and discussed in three chapters. First, Chapter 4 describes a comprehensive dataset from a single catchment in

Switzerland, including source materials and suspended sediment samples collected at high temporal resolution over a series of storm events, which is used to elucidate the processes operating there. Long-term fluxes of suspended sediment and total, fossil and non-fossil POC from this and similar settings are calculated. In Chapter 5, additional data from discharge-proportional compound sampling in the same and a second Swiss catchment are presented, giving insights into POC mobilisation under a slightly different geomorphologic regime. Chapter 6 presents geochemical data from source materials and suspended sediment collected in several watersheds in Oregon, including some from the Cascades collected at high temporal resolution during storms. Long-term POC export is discussed, and fluxes constrained as much as possible.

Chapter 7 draws all catchments studied in the two settings together. By comparing them to each other, controls on POC export style are elucidated, and their relative importance assessed. The chapter then describes how the combined findings may be used to scale up to global fluxes, compares these to extant estimates, and speculates on the global significance of runoff-driven POC erosion in temperate forested uplands on CO_2 sequestration and in Earth–climate feedbacks. Finally, in Chapter 8, the major conclusions of the thesis are summarised, and areas where future research will lead to a better understanding of the organic pathway are identified.

Chapter 2

Case study sites

2.1 Selection of sites

Chapter 1 explained the motivation for studying POC mobilisation and export mechanisms in headwater catchments that are subject to reasonably high levels of rainfall, but without the intense climate and tectonics of the world's most active mountain belts. Because of the focus on natural processes, it was also necessary to choose sites where anthropogenic disturbance has been minimal. Yet these requirements were coupled with logistical considerations: catchments had to be accessible, permission was needed to sample, and the project would be greatly enhanced if long-term discharge records already existed, as it would not be possible to collect these over the timescale of the project. The two areas described below fulfil these criteria, and additionally offer a degree of variability in environmental factors such as geology and ecology that allows the effect of these on POC export to be investigated. Between them, they are a representative model for temperate forested uplands across the globe.

For each case study area, physical characteristics are grouped into sections in the following order: location and geography; geology and tectonics; climate; geomorphology; biosphere (including anthropogenic activity); hydrology.

2.2 Alptal, Switzerland

2.2.1 Location

The Alptal is a valley in the northern foothills of the Swiss Alps, drained by the Alp river. It is located 40 km south of Zürich in Canton Schwyz, near the town of Einsiedeln. Within this valley, two small tributaries are of interest: the Erlenbach

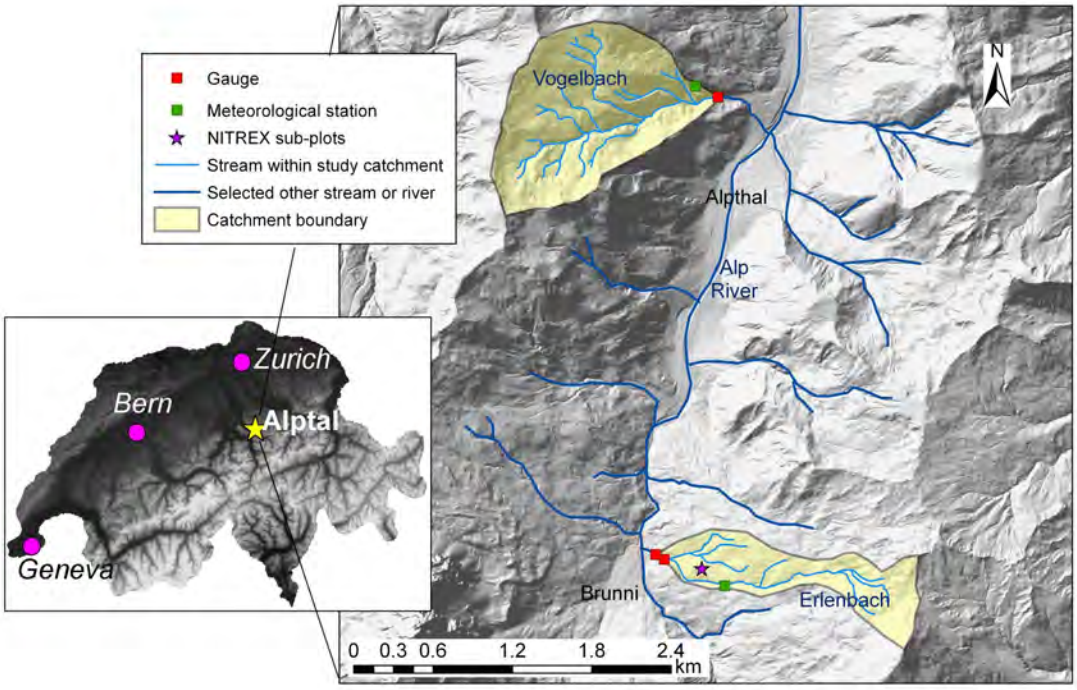

Figure 2.1: Location and geography of the Alptal, showing catchment boundaries and monitoring stations, including NITREX subplots (see Section 2.2.6). Switzerland DEM is from Sarmap (`http://www.sarmap.ch/page.php?page=topography`); Alptal hillshade is used courtesy of WSL.

(74 ha, 1110–1655 m above sea level), near the village of Brunni, and the Vogelbach (152 ha, 1050–1500 m above sea level), near the village of Alpthal (Figure 2.1).

2.2.2 Geology and tectonics

The Alptal is largely underlain by flysch deposits, composed of pelitic turbidites (Winkler *et al.* , 1985). The Vogelbach lies entirely on Cretaceous (Campanian–Maastrichtian) Wägital-Flysch bedrock; the Erlenbach lies mainly on Tertiary (Eocene) Wägital-Flysch (Figure 2.2). The latter catchment is developed on a large bedrock landslide complex (Hantke, 1967, discussed in Schuerch *et al.* (2006)). Towards the top of the Erlenbach, Helvetic nappe limestone is briefly exposed before a return to flysch—this time of the lower Schlieren Formation, again Eocene in age.

There are significant lithological differences between Cretaceous and Eocene Flysch which are manifested in contrasting geomorphologic regimes in the Erlenbach and Vogelbach (Section 2.2.4). The Eocene Flysch underlying the Erlenbach is, for its vast majority, uniformly fine-grained and prone to gravity movement with evidence of submarine slumps, although the Schlieren-Flysch also contains some arenites and con-

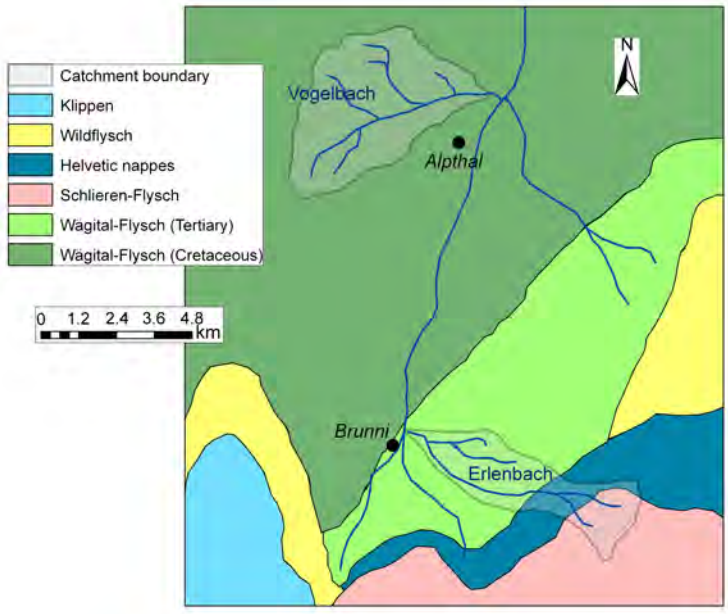

Figure 2.2: The geology of the Alptal, redrawn from Winkler *et al.* (1985).

glomerates (Winkler *et al.* , 1985). The Cretaceous Flysch underlying the Vogelbach has a sandier lithology, with abundant layers of arenites, microconglomerates and calcareous arenites (Winkler *et al.* , 1985) as well as some bentonite schists (Milzow *et al.* , 2006).

Overlying the solid geology in the upper parts of the Alptal are recent glacial till deposits. These clay-rich diamicts are very thick in places, particularly at lower elevations: they are up to several metres thick on the lower left bank of the Erlenbach.

The Alps were formed as a result of convergence between a subducting European plate and an overriding Adriatic plate, beginning in the Cretaceous and continuing to the present day (Bernet *et al.* , 2001; Frisch, 1979). In the Alpine foreland molasse basins, erosion rates are generally on the order of 0.15–0.3 mm yr^{-1} (Schlunegger & Hinderer, 2003; Wittmann *et al.* , 2007), but this varies locally. The published denudation rate in the Alptal is 0.64 mm yr^{-1} (Turowski *et al.* , 2009).

2.2.3 Climate

Mean air temperature in the Alptal is 6°C, and mean precipitation is 2300 mm per year at the Erlenbach weather station (Hagedorn *et al.* , 2001; Rickenmann, 1997) and 2100 mm per year in the Vogelbach (Kirsch *et al.* , 2007). Precipitation is relatively well spread over the year, with a mean annual number of rain days of 161 (Turowski *et al.* , 2009). The largest precipitation events typically occur as convective rainfall

Figure 2.3: General character of the Alptal study catchments. (**a**) Lower channel of the Erlenbach after rain, showing lack of riparian zone, creep landslides adjoining the channel and step-pool morphology. (**b**) Upper channel of the Erlenbach, with large boulders and representative vegetation. (**c**) Lower channel of the Vogelbach, also showing lack of riparian zone, and lack of creep landslides. (**d**) Vogelbach lower hillslope, showing steep slopes and beech forest with lack of understory.

during July and August. During the winter, snow is the main form of precipitation.

2.2.4 Geomorphology

Both streams lack a well-developed riparian zone and have a step-pool morphology, with logs and boulders forming the steps (Milzow *et al.* , 2006; Turowski *et al.* , 2009) (Figure 2.3). The average gradient of the Erlenbach channel is 18% (Turowski *et al.* , 2009); the Vogelbach's channel gradient has the same mean value and ranges from 10% to 30% (Kirsch *et al.* , 2007; Milzow *et al.* , 2006). While the two streams are similar, the character of the hillslopes differs significantly. Creep landslides are common in the Erlenbach, particularly in the lower reaches where steep channel sides cut into active complexes (Figure 2.4), devloped mainly in the till. These incrementally deliver substantial amounts of sediment to the stream channel during winter, which

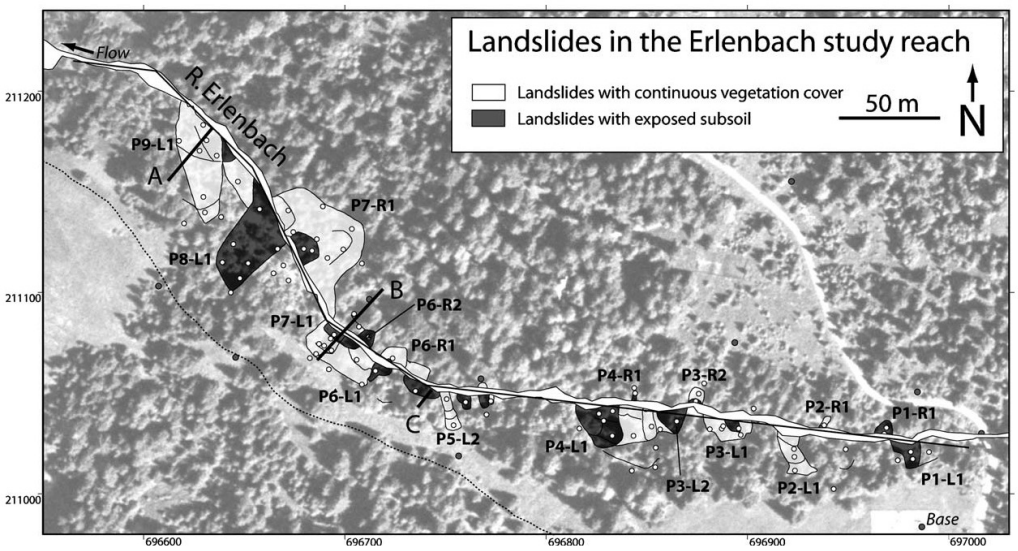

Figure 2.4: Location and nature of major creep landslides in the lower Erlenbach, from Schuerch *et al.* (2006).

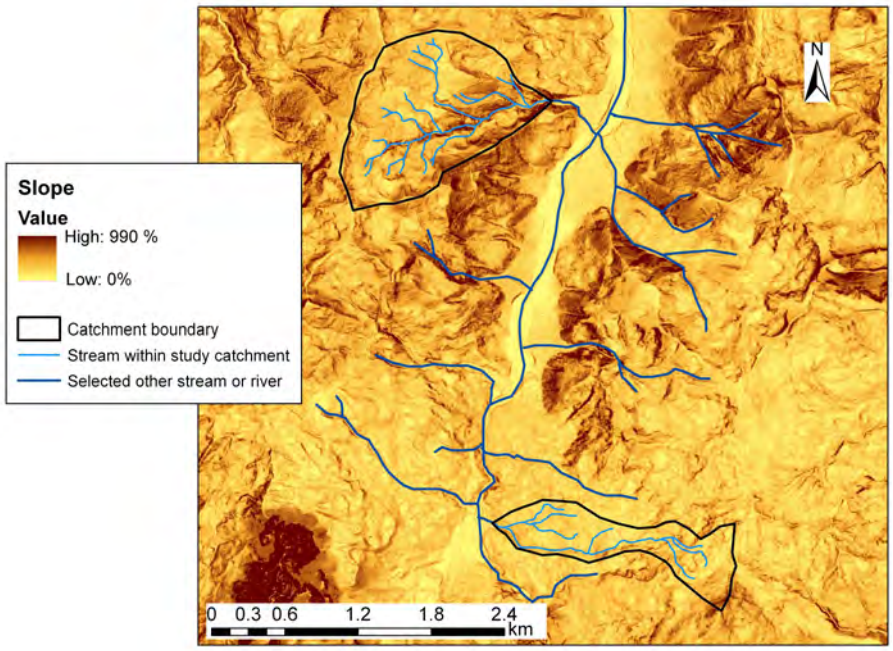

Figure 2.5: Hillslope angle in the Alptal, calculated from 5-metre digital terrain model and expressed as a percentage. Data from WSL.

is removed by summer storms (Schuerch *et al.* , 2006). Average hillslope steepness is ∼20% (Hagedorn *et al.* , 2000). The Vogelbach's better-draining and more competent lithology results in drier, higher and considerably steeper hillslopes—on average 37% (Kirsch *et al.* , 2007) (Figure 2.5)—with fewer (but larger) mass wasting events and little creep landsliding. This means that suspended sediment concentration (SSC) is generally lower in the Vogelbach than the Erlenbach, and the channel contains less debris. Further hydrological characteristics are described in Section 2.2.6.

Figure 2.5 also shows that, throughout the Alptal (but best seen in the Vogelbach), the steepest slopes occur along stream channels, an indication that the streams are actively incising.

2.2.5 Biosphere

Ground cover in the Erlenbach is ∼40% forest and ∼60% grassland and wetland, with a very minor fraction un-vegetated (Turowski *et al.* , 2009). The Vogelbach has a higher proportion of forest (∼65%), with the remainder covered by alpine meadow (Milzow *et al.* , 2006). Net primary productivity (NPP) in the Alptal is around 1000 g C m^{-2} yr^{-1} (Oak Ridge National Laboratory Distributed Active Archive Center, 2011; Schleppi, 2013). This is split between above-ground biomass and soils in a ratio of about 1:2 (Dixon *et al.* , 1994).

The soils found in each catchment partially reflect their geology. In the Erlenbach, both bedrock and drift deposits are fine-grained, clay-rich and impermeable, resulting in water-saturated, reduced gleysols with weakly-developed profiles (Hagedorn *et al.* , 2000; Zimmerman *et al.* , 2006). Average composition is 48% clay, 46% silt and 6% sand (Xu *et al.* , 2009). Soils in the Vogelbach also have high clay content and a low infiltration rate, and are mostly gleysols and regosols (Milzow *et al.* , 2006). Forested areas have a slightly higher infiltration rate, generally resulting in less waterlogging, but there are variations in soil and humus type following micro-topography and height of the water table: mor humus on the drier mounds and muck humus in the wetter depressions (Hagedorn *et al.* , 2000). Soils are relatively thin in the Vogelbach, with depths to bedrock of 30–40 cm (Burch, 1994, discussed in Milzow *et al.* (2006)). In the Erlenbach they are generally thicker, reaching at least 80 cm (Zimmerman *et al.* , 2006).

Major tree species in the Alptal are *Picea abies* (Norway spruce) and *Abies alba* (European silver fir), with smaller amounts of *Alnus viridis* (green alder) (Schleppi *et al.* , 1999). *Sorbus aucaparia* (rowan) and *Corylus avellana* (European hazel) also occur as minor species. In the Vogelbach, *Fagus sylvatica* (beech) is also abundant

at lower elevations, and in these areas there is little to no understory (Figure 2.3(d)). Beech trees create low light levels beneath the canopy and produce a large amount of leaf litter, meaning that other plants struggle to grow (von Wühlisch, 2008). In the Erlenbach and higher in the Vogelbach, shrubs and ground plants flourish. The understory on drier, forested slopes is mainly composed of *Vaccinium sp.*, particularly bilberries. Depressions in the Erlenbach are generally too waterlogged for trees to grow, and in the wet soil here two understory sub-communities are found: in shade under dense tree canopy, *Caltha palustris* (marsh marigold) and *Petasites alba* (white butterbur) dominate, while *Poa trivialis* (rough bluegrass) and *Carex ferruginea* (rusty sedge) grow in more open areas (Muller, 1997).

The study catchments are relatively free from human influence at present. The area is not frequented by foreign tourists, and many local visitors come only to hike up the Mythen at the head of the valley or to ski on the less-forested slopes west and south of Brunni (Figure 2.1). Minor footpaths run up the northern edge of the Erlenbach catchment and on both sides of the Vogelbach stream, and there is also a private access road, mainly used for research-related traffic, in the Erlenbach. There is some small-scale logging in the Vogelbach catchment. It is also important to consider land use history, as this has a lasting impact on vegetation age and patterns. Until the end of the nineteenth century, much of the valley was subjected to large-scale clear-cutting (Gimmi *et al.* , 2008). However, the Erlenbach stand is naturally regenerated, with trees up to 250 years old (Schleppi *et al.* , 1999).

2.2.6 Hydrology and research history

Hydrological monitoring was started by the Swiss Federal Institute for Forest, Snow and Landscape Research (WSL) in the mid-20th century (Hegg *et al.* , 2006). WSL operates two gauging stations in the Erlenbach, one either side of a large sediment retention basin, and one in the Vogelbach (Figure 2.1). There are climate stations in both catchments. Continuous discharge measurements at a frequency of 10 minutes exist back to 1983 for the Erlenbach and 1985 for the Vogelbach; this study uses data from then until the end of 2011 (further details are given in Chapter 3).

In common with other small mountain river systems (Wheatcroft *et al.* , 2010), discharge in both catchments rises quickly during storms and is highly episodic in response to rainfall (Schleppi *et al.* , 2006). Hence, the largest discharges—and most bedload transport events—generally occur during the summer months, although there are also higher flows during snow melt. The impermeable nature of the pelitic bedrock increases this flashy tendency, to a greater extent in the Erlenbach than the sandier,

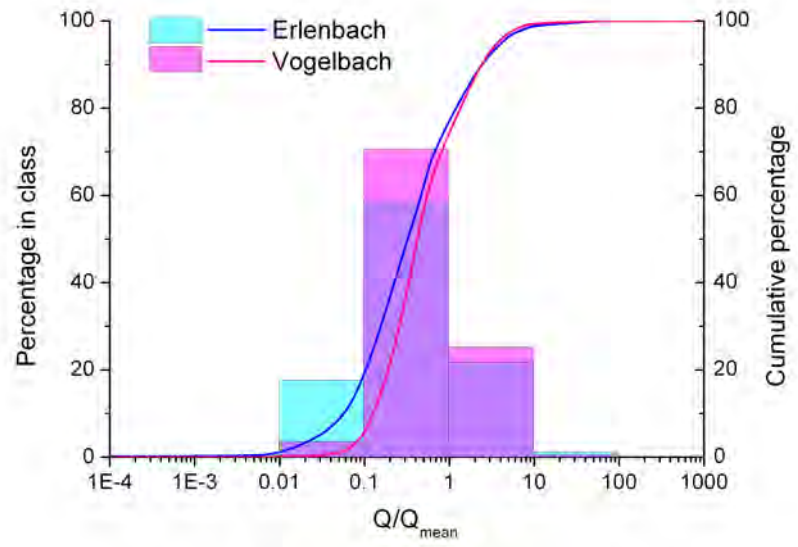

Figure 2.6: Discharge characteristics of the Erlenbach and Vogelbach, based on measurements taken every 10 minutes from 1983–2011 and 1985–2011 respectively. Bars indicate the percentage of measurements falling in each discharge class, expressed relative to mean discharge (as Q/Q_{mean}); lines indicate the cumulative percentage. Data from WSL.

better-draining Vogelbach.

Over the monitoring period, mean discharges for the Erlenbach and Vogelbach were 39 l s^{-1} and 77 l s^{-1} respectively, the difference reflecting the latter's twice-as-large catchment area. Hereafter, discharges are reported relative to the mean (as Q/Q_{mean}), as well as absolute values, to allow comparison between catchments. Peak 10-minute discharge in the Erlenbach was ∼12 m^3 s^{-1}, equivalent to Q/Q_{mean} of 310, in July 1984, although a discharge of 15 m^3 s^{-1} was recorded during higher-frequency measurements in June 2007. The Vogelbach 10-minute discharge record does not include the 1984 event, but a peak discharge of ∼6.4 m^3 s^{-1} (Q/Q_{mean}=80) occurred during the summer of 1995 (Milzow *et al.* , 2006), when the Erlenbach reached ∼10 m^3 s^{-1}(Q/Q_{mean}=260). Lower peak discharge in the Vogelbach reflects the catchment's greater infiltration capacity during high rainfall, which also translates into higher base flow rate (see next paragraph).

The long-term discharge behaviour of the Erlenbach and Vogelbach is summarised in Figure 2.6. The Erlenbach spends a higher proportion of its time in a very low-flow state (Q/Q_{mean}<0.1). Flows in both streams are between $0.1Q_{mean}$ and Q_{mean} for the majority of the time, but the median flow is higher, relative to Q_{mean}, in the Vogelbach. Flow was less than or equal to Q_{mean} for 77% and 74% of time for the Erlenbach and Vogelbach respectively. The Vogelbach has a greater proportion

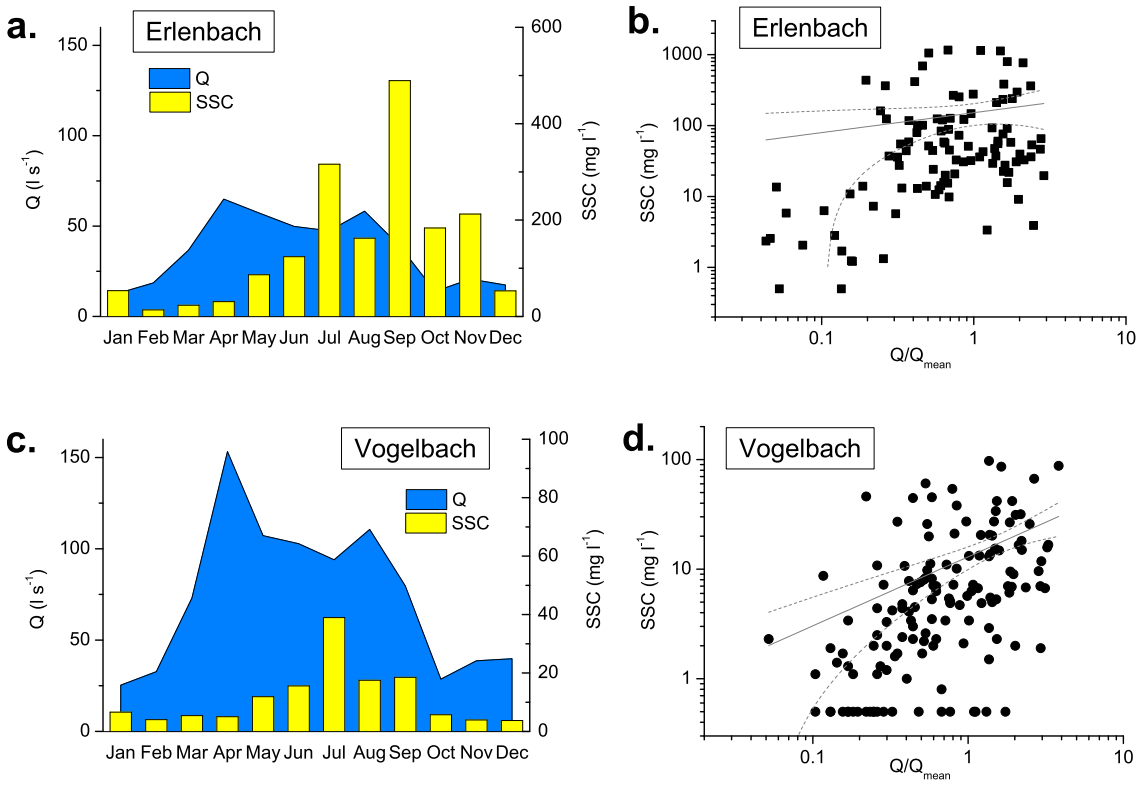

Figure 2.7: Bar and line graphs show mean monthly discharge and SSC for (**a**) the Erlenbach and (**c**) the Vogelbach. Data are derived from biweekly discharge proportional samples collected January 2005–December 2010. Samples were allocated to the month in which the majority of the period they relate to fell, then all values for each month were averaged. Cross-plots show relationship between discharge and SSC in the same samples from (**b**) the Erlenbach and (**d**) the Vogelbach. Solid lines show best-fit power law; dashed lines are 95% confidence intervals. Raw data from the Swiss Federal Institute of Aquatic Science and Technology (EAWAG; http://www.eawag.ch/forschung/wut/schwerpunkte/chemievonwasserresourcen/naduf/datendownload_EN; see Section 3.2.1.1 on page 51 for details of their involvement at the Alptal).

of flows between Q_{mean} and $10Q_{mean}$, but very high flows (Q/Q_{mean}>10) are more common in the Erlenbach. For the Erlenbach, less than 1% of discharges were above the threshold at which substantial bedload transport starts, which corresponds to a Q/Q_{mean} of ∼13 (Turowski *et al.* , 2011). Discharges less than or equal to Q/Q_{mean}, the state of both streams for over two thirds of the time, account for only ∼1% of suspended sediment transport.

Sediment sampling, mainly for water quality purposes, has been operating in both catchments since 2003; the protocol is described in Chapter 3. Additionally, the Erlenbach channel has a lower experimental reach that is equipped with geophone bedload sensors and event-triggered collector baskets for research on bedload transport

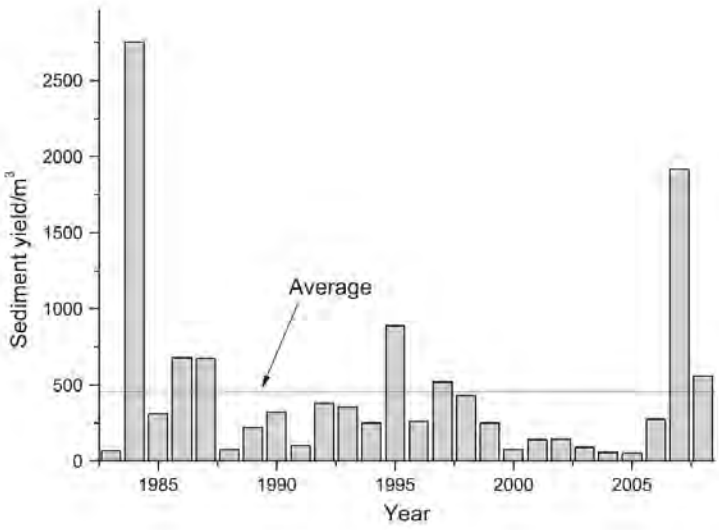

Figure 2.8: Annual sediment yield in cubic metres for the Erlenbach, as surveyed in the retention basin between 1983 and 2008. From Turowski *et al.* (2009).

and channel morphology (Rickenmann & McArdell, 2007; Rickenmann *et al.* , 2012). Figure 2.7 shows that SSC does not follow discharge very closely, with discharge peaking in April but SSC peaking in late summer. Similarly, the cross-plots (R^2=0.02 for the Erlenbach; 0.14 for the Vogelbach) show only a weak positive power law relationship in both catchments. The Vogelbach has a considerably lower sediment yield than the Erlenbach, due to its more stable channel and slopes, lack of creep landslides feeding into the channel, deeper soils and higher proportion of forest cover (Keller *et al.* , 1991).

On an inter-annual basis, sediment transport varies significantly, as shown by the yields surveyed in the Erlenbach retention basin (Figure 2.8). In general, years with large floods (e.g. 1984 and 2007) match those with substantial sediment transport. Bedload transport is relatively more important in the Erlenbach than in larger mountain rivers, constituting ∼50% of the total sediment flux (Rickenmann *et al.* , 2012).

The Erlenbach catchment is also a site for the NITREX project (NITRogen saturation EXperiments) (Wright & Rasmussen, 1998); as such, it has three <1 ha sub-plots also equipped with V-notch weirs in forest, meadow and an experimental forest plot where nitrogen is added (Schleppi *et al.* , 1998). Their location is indicated on Figure 2.1.

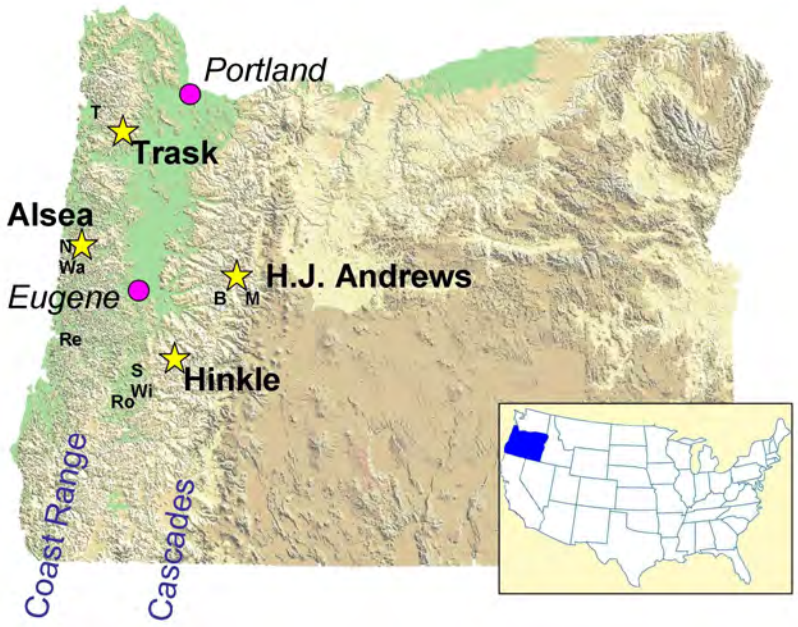

Figure 2.9: Location of study watersheds in Oregon in relation to major cities and mountain ranges. Small labels mark towns referred to in Section 2.3.1 and climate stations which are sources for the data in Figure 2.13: B=Blue River, M=McKenzie Bridge, N=Newport, Re=Reedsport, Ro=Roseburg, S=Sutherlin, T=Tillamook, Wa=Waldport, Wi=Winchester. Base relief map is from US Geological Survey (http://commons.wikimedia.org/wiki/File:Oregon_DEM_relief_map.png).

2.3 Western Oregon, USA

2.3.1 Location and geography of study sites

This study uses material from four watersheds in western Oregon: two in the Cascades and two in the Coast Range (Figure 2.9).

Hinkle Creek, located in the western Cascades foothills to the east of Sutherlin and 40 km north-east of Roseburg, is the most southerly study stream. It flows into Calapooya Creek, then the Umpqua River and into the Pacific Ocean at Reedsport. Hinkle Creek has two forks, of which only the North Fork (873 ha), covering elevations of approximately 440 m to 1220 m, is studied here. The North Fork has two major tributary streams, DeMersseman Creek (∼70 ha) and Meyers Creek (∼40 ha) (Figure 2.10(a)).

The H.J. Andrews Experimental Forest is located 80 km east of Eugene, near the town of Blue River in the Willamette National Forest. It is in the central Cascades and comprises the 6242 ha drainage basin of Lookout Creek, whose major tributaries include McRae Creek and Mack Creek (Figure 2.10(b)). Lookout Creek flows into

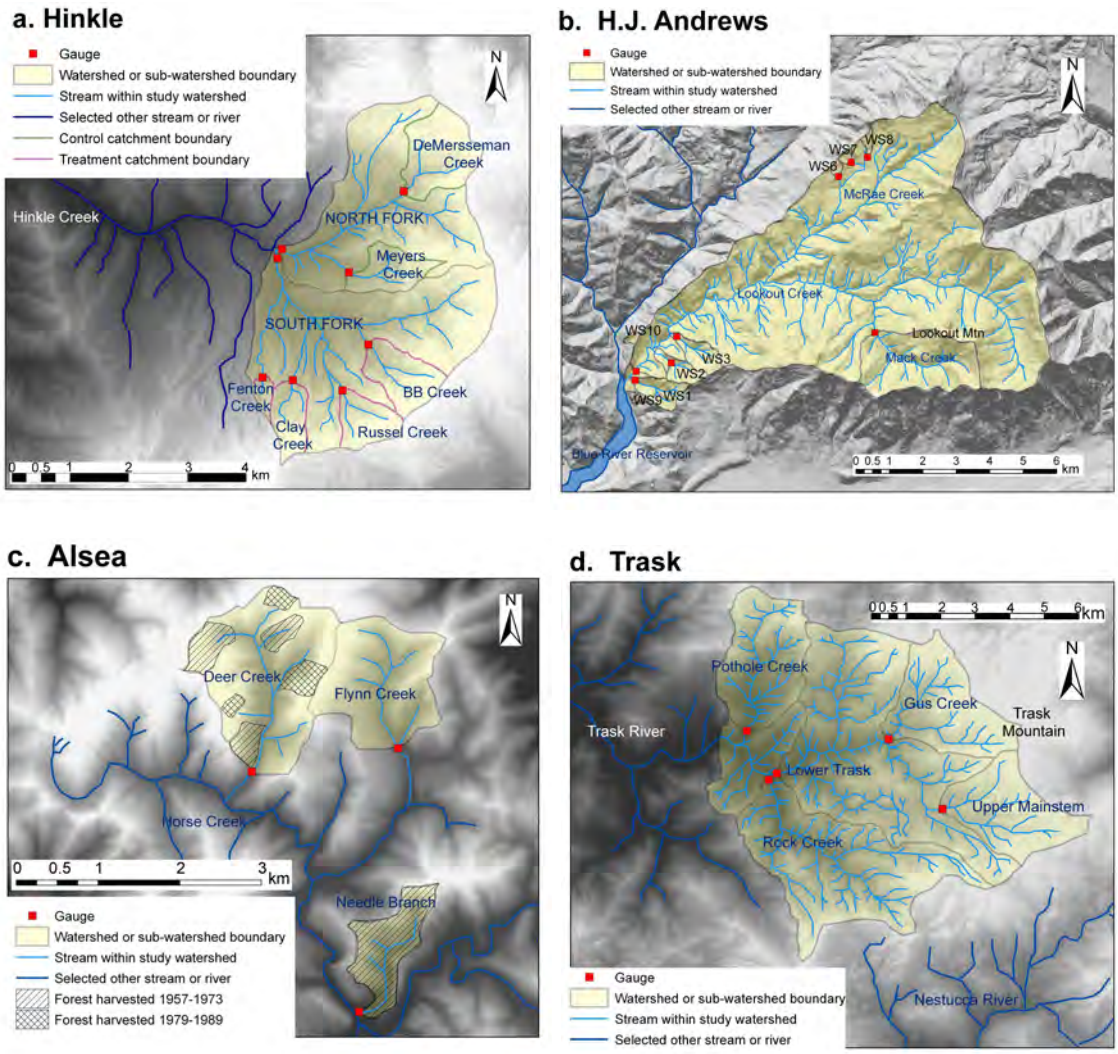

Figure 2.10: Geography of the Oregon study watersheds, including sub-watersheds and gauge locations. H.J. Andrews hillshade is from Valentine & Lienkaemper (2005); base DEM for other catchments is from US Geological Survey, available from University of Oregon Libraries (`http://library.uoregon.edu/map/gis_data/or_10mdemlist.htm`). (**a**) Hinkle, based on Skaugset *et al.* (2004). (**b**) H.J. Andrews, based on map available on Andrews Forest website (`http://andrewsforest.oregonstate.edu/lter/about/site/map.cfm?topnav=219`). More detailed geography is given in Figure 3.4 on page 61. (**c**) Alsea, based on Ice *et al.* (2005). (**d**) Trask, based on Watersheds Research Cooperative (2008).

Blue River Reservoir, then into the McKenzie River, and the Willamette River, which joins the Columbia and flows into the Pacific Ocean on Oregon's northern border. Elevation for the whole catchment ranges from 410 m to 1630 m at the top of Lookout Mountain. In addition to Lookout Creek, a smaller nested catchment, Watershed 1 (WS1; 95.9 ha), is studied as a separate entity. This stream flows into Lookout Creek near Blue River Reservoir, but still covers elevations of 425 m to 1000 m. Watershed 2 (WS2; 60.3 ha; 550 m to 1075 m) is also considered briefly.

Alsea and Trask are the two watersheds in the Coast Range. The Alsea headwaters are located 16 km from the Pacific Ocean in the Siuslaw National Forest, near Newport. Three catchments within the Alsea watershed are gauged, of which two are used in this study: Flynn Creek (203 ha, elevation 150 m to 350 m) and Deer Creek (303 ha, elevation 175 m to 375 m) (Figure 2.10(c)). Both flow into Horse Creek, then Drift Creek, joining the Alsea River just before flowing into the Pacific at Waldport.

Trask is the most northerly watershed, located west of Portland near Tillamook, in Tillamook State Forest. The basin covers an area of approximately 2800 ha, with elevations from 275 m to 1100 m. The Trask River flows directly into Tillamook Bay. The main gauged watershed is the eastern part of East Fork, and consists of many smaller creeks, including Rock Creek, Gus Creek and Pothole Creek (Figure 2.10(d)). Owing to the inaccessibility of the watershed, contextual material was collected from a representative neighbouring catchment to the south, draining into the Nestucca River.

2.3.2 Geology and tectonics

The Cascades are extensively underlain by Tertiary volcanics (Figure 2.11). The dominant rock type at H.J. Andrews is middle to upper Miocene andesite of the Sardine Formation, largely in the form of lava flows (Peck, 1961; Swanson & James, 1975). In the west of the catchment, the Little Butte Formation of the upper Oligocene to lower Miocene outcrops, consisting of intercalated tuffs and basaltic flows (Swanson & James, 1975). Basalt and rhyolite dykes occur in the far western corner (Swanson & James, 1975), between Lookout Creek and Blue River. Lookout Ridge, the watershed's southern boundary, is formed of Pliocene andesite and basalt flows (Peck, 1961; Swanson & James, 1975). Hinkle is underlain by basalt flows and pillow basalts of the Eocene Siletz Volcanics Formation (Skaugset *et al.* , 2004).

Coast Range geology consists of both volcanics and sediments (Walker & King, 1969) (Figure 2.11). A large part of the Trask headwaters is also underlain by Siletz Volcanics, but in the upper reaches there are significant outcrops of siltstones belonging to the Yamhill Formation, with bands of tuff, sandstone and calcareous con-

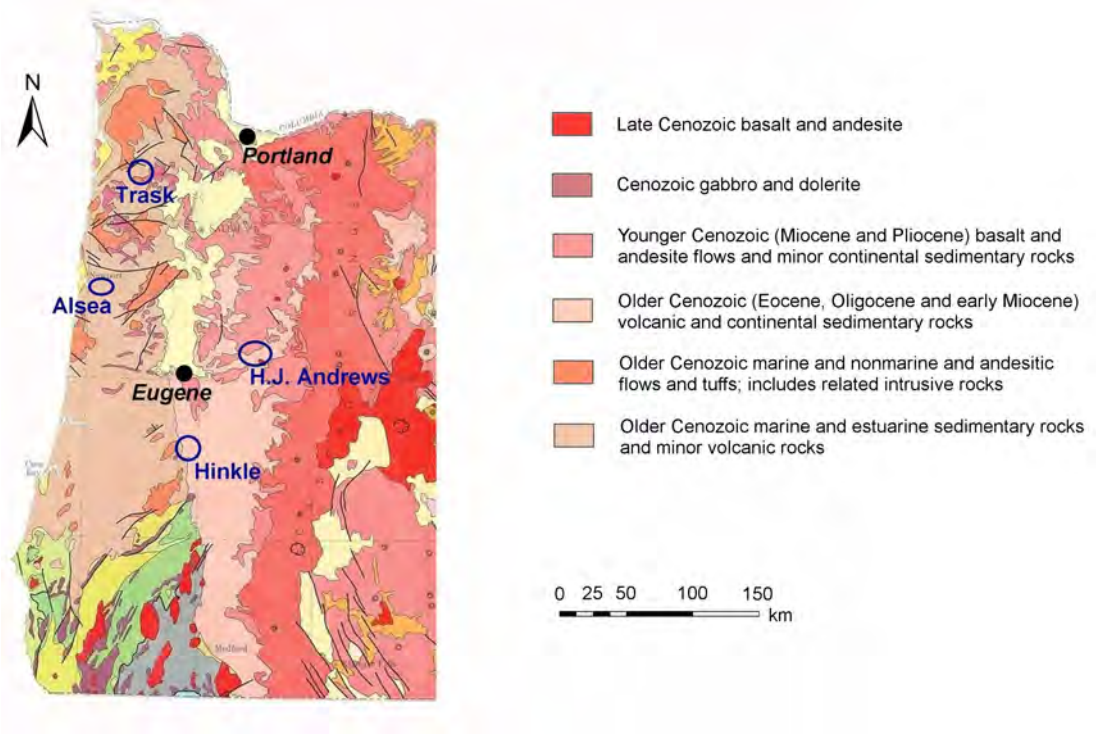

Figure 2.11: Geology of western Oregon, modified from Walker & King (1969). The locations of the study catchments are indicated; only the units relevant to these areas are described in the legend.

cretions, and of dolerite intrusives (Wells et al., 1994, discussed in Watersheds Research Cooperative (2008)). These three units extend into the Nestucca area to the south. In the north of the Trask watershed, there are minor amounts of Trask River sandstone, and submarine basalts and tuffs. In contrast, the Alsea is underlain exclusively by cyclic sedimentary rocks of the Middle Eocene Tyee and Burpee Formations. These are estuarine and marine in origin, consisting of graded medium- to fine-grained sandstone and micaceous siltstones, as well as carbonaceous fragments and diagnostic fossils (Beschta & Jackson, 2008; Peck, 1961).

The predominance of volcanic substrate at H.J. Andrews, Hinkle and Trask watersheds offers the advantage of working with suspended sediment where there is very little fossil organic carbon input, in contrast to the Alptal.

Situated on the western edge of the North American continent, where the Juan de Fuca plate is subducting, the Pacific Northwest region is tectonically active. In addition to the active volcanism in the Cascades, the entire area forms a large-scale dextral shear zone caused by the north-westerly motion of the Pacific plate relative to North America, at a rate of $\sim$50 mm yr^{-1} (Atwater, 1970; McCaffrey *et al.* , 2007), and oblique subduction along the margin (Heller & Ryberg, 1983). GPS velocity

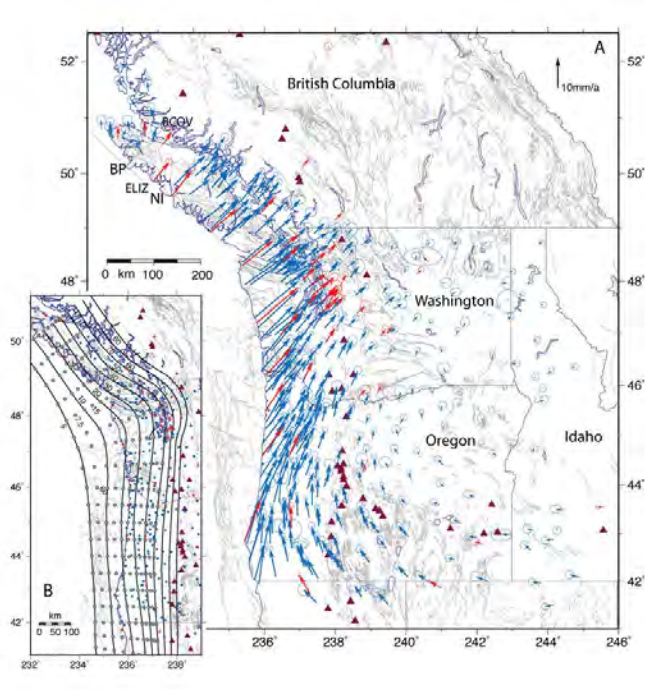

Figure 2.12: GPS velocity measurements (North American reference frame) in the Pacific Northwest, from McCaffrey *et al.* (2007). Inset shows depth to top of subducting Juan de Fuca plate; contours in kilometres.

measurements show that Oregon is rotating clockwise in several blocks, around an axis in eastern Oregon (McCaffrey *et al.* , 2007). This means that most of strain occurs along the coast, with minimal deformation in the interior (Figure 2.12).

Long-term rock exhumation rates based on apatite (U-Th)/He data have been calculated for the Skykomish river basin in the central Washington Cascades by Reiners *et al.* (2003) and Hren *et al.* (2007). These range from 0.05 to 0.33 mm yr^{-1} on the whole-landscape scale, but from 0.06 to 0.17 mm yr^{-1} for individual watersheds. The Washington and Oregon Cascades occupy a very similar tectonic setting, so exhumation rates on the order of a few tenths of a millimetre are also likely for the latter.

The Oregon Coast Range has been extensively studied and far more data is available for this area. Dating of wave-cut platforms along the southern and central Oregon coast suggests uplift on the order of 0.1–0.3 mm yr^{-1} (Kelsey *et al.* , 1996), and fluvial incision rates of 0.6–0.9 mm yr^{-1} were obtained by Personius (1995) for the Coast Range north of Newport by dating river terraces. Erosion rates are broadly consistent with these, with values of 0.05–3 mm yr^{-1} from sediment yield studies (Beschta, 1978; Heimsath *et al.* , 2001; Roering *et al.* , 2004).

Although appreciable, such rates are relatively low; exhumation rates in Taiwan

and New Zealand are known to reach 10 mm yr^{-1} (Dadson *et al.* , 2003; Tippett & Kamp, 1993). For further comparison, erosion rates in the Alptal (Section 2.2.2) are between those of the Oregon Cascades and Coast Range.

2.3.3 Climate

In common with the whole of western Oregon, the study watersheds share some climatic features. They are all close enough to the coast to have a maritime climate, with dry, relatively cool summers and wet, mild winters. Over half of the annual precipitation occurs between November and January as a result of frontal depressions moving eastwards from the north Pacific, and rainfall events tend to last several days, or longer if several storms occur sequentially. However, there are also climatic differences, related principally to latitude and distance from the ocean and reflected in the division of Oregon into nine climatic zones by the National Climatic Data Center. Trask and Alsea lie within Division 1 (Oregon Coast), H.J. Andrews is in Division 4 (Northern Cascade), and Hinkle is in Division 3 (Southwestern Interior). Figure 2.13 illustrates these geographic variations in mean monthly precipitation and temperature. Although most of the climate stations used here are in valleys and can be compared directly, the watersheds reach elevations significant enough to affect climate further, primarily causing an increase in orographic precipitation and in the proportion falling as snow. Table 2.1 shows mean annual precipitation in each watershed compared to that at the most relevant nearby climate station, and the disparity throughout the year in both precipitation and temperature is also illustrated in Figure 2.13(b) for H.J. Andrews. Within the H.J. Andrews itself, both precipitation and temperature vary with altitude: mean annual precipitation is ∼75% higher and mean annual temperature ∼20% lower on Lookout Ridge than at Blue River Reservoir (Rosentrater, 1997), and a seasonal snowpack develops above ∼1000 m (Swanson & Jones, 2002). Similar patterns are likely to occur at the other sites.

The area around Hinkle (Figure 2.13(a)), furthest south and somewhat inland, has the highest summer temperatures and significantly lower precipitation, especially in the summer, than the other regions. Rainfall in the mountains is higher (Table 2.1), but still only half as much as in the other study watersheds. Winter temperatures can still drop quite low, and snow occurs every winter. H.J. Andrews is further into the Cascades than Hinkle and slightly further north. These factors result in cooler temperatures, particularly in winter, and considerably higher rainfall (Figure 2.13(b)). Summer temperatures in the mountains are similar to those at Eugene in the Willamette Valley—July mean annual temperature at HJA CS2 meteorological

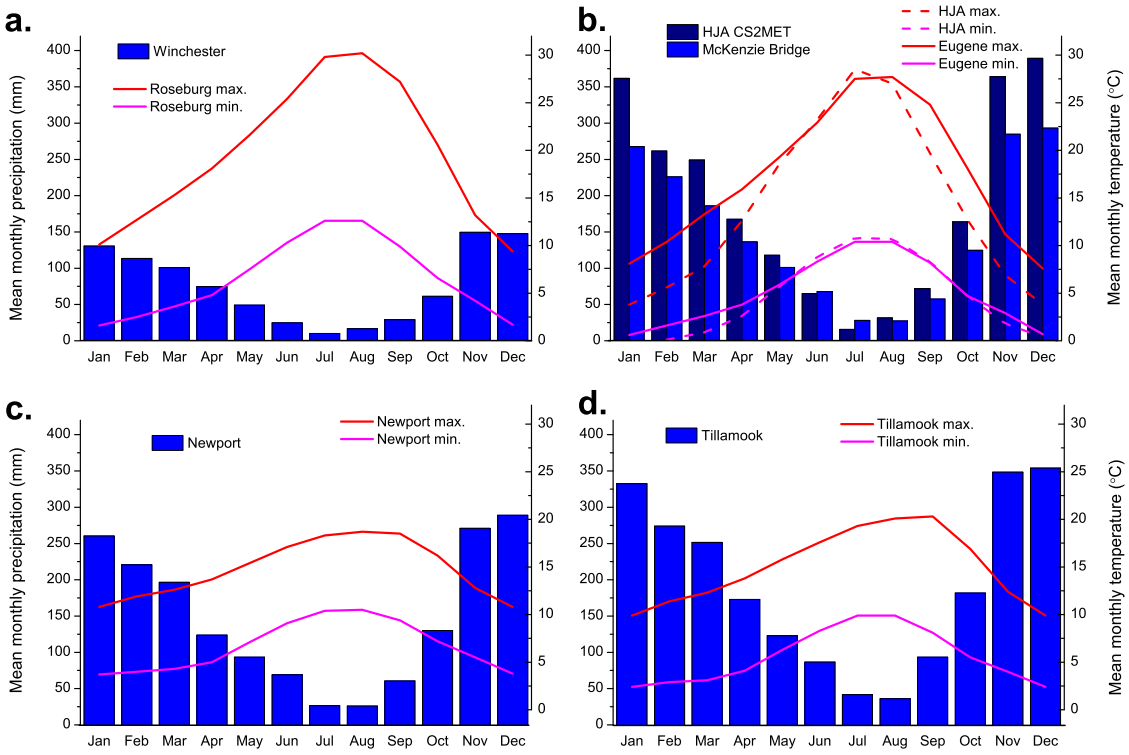

Figure 2.13: Mean monthly precipitation (blue bars), maximum temperature (red lines) and minimum temperature (pink lines) at various locations in western Oregon (see Figure 2.9), in the vicinity of (**a**) Hinkle, (**b**) H.J. Andrews, (**c**) Alsea and (**d**) Trask. Data are from the Oregon Climate Service at Oregon State University (`www.ocs.orst.edu/oregon-climate-data`), 1971–2000. Also included in (**b**) is mean monthly precipitation (dark blue bars) and maximum and minimum temperatures (dashed lines) as recorded between 1957 and 2009 at H.J. Andrews CS2 meteorological station (HJA), located near the bottom of the catchment and shown on Figure 3.4 on page 61 (data from Daly & McKee, 2012).

Watershed	**Precip. (mm)**	**Source**	**Nearest climate station**	**Precip. (mm)**
Hinkle	1400–1900	1	Winchester (27 km)	910
HJA	2300–3550	2	McKenzie Bridge (4 km)	1800
Alsea	2500	3	Newport (15 km)	1770
Trask	2100–6000	4	Tillamook (13 km)	2300

Table 2.1: Mean annual precipitation (Precip., in millimetres) at study watersheds and nearby climate stations in Oregon. Where a range is given, this represents low to high elevations. Sources: 1) Skaugset *et al.* (2004), 2) H.J. Andrews Experimental Forest Brochure, 3) Stednick (2008), 4) Watersheds Research Cooperative (2008); climate station data from Oregon Climate Service, Oregon State University (`www.ocs.orst.edu/oregon-climate-data`).

station is 19°C compared to 18°C—and winters are slightly cooler (1°C compared to 4°C).

The two Coast Range locations (Figure 2.13(c) and (d)) have similar climate patterns, with a smaller seasonal temperature differential—warmer winters, cooler summers—than the Cascades, reflecting the damping effect of the adjacent ocean. The lowland areas have a median amount of rainfall, slightly higher at Tillamook to the north where depression system tracks normally fall. This pattern is reflected in the mountain headwaters, with Trask seeing the highest rainfall rates of all the study catchments (Table 2.1).

Rain-on-snow events are common in the Oregon Cascades (McCabe *et al.* , 2007), and are typically responsible for very large floods at H.J. Andrews (Harr, 1981). Such conditions are rare in coastal areas, but may have a disproportionately large effect on hillslope erosion (Beschta & Jackson, 2008).

2.3.4 Geomorphology

Western Oregon headwaters have a very different physiognomy to those in the Alptal. Hillslopes are stable enough to allow the growth of large trees and abundant shrubs (Figure 2.14), despite an average gradient of 36% for H.J. Andrews (Uhlenbrook *et al.* , 2007)—considerably steeper than the Erlenbach's average 20%. Many streams have significant very low-gradient riparian zones developed on alluviated and colluviated valley floors (Figures 2.14 and 2.15), a feature that can be seen in Figure 2.16 in the wide yellow strips on at least one side of Lookout Creek and many of the smaller streams. This contrasts to the slope distribution in the Alptal (Figure 2.5), where the steepest slopes occur along the headwater channels, particularly in the Vogelbach, indicating active incision. Compared to the other small watersheds, Watershed 1 has a high proportion of steep slopes, but even here they are not concentrated along the channel. This indicates that the channel and hillslope are decoupled and that channel lowering is not significant—although there may be limited connectivity where channel sinuosity causes localised undercutting. The upper parts of Lookout Creek were glaciated during the Wisconsin glaciation (85–10 kyr), resulting in north and north-east facing cirques, U-shaped valleys and isolated till deposits above ∼1370 m (Swanson & James, 1975).

Although much of the forest is stable, shallow (<5 m) mass movements, particularly earth flows and debris flows, are observed at H.J. Andrews and elsewhere in western Oregon (Dyrness, 1967; Stock & Dietrich, 2006; Swanson & James, 1975; Swanson & Jones, 2002). These occur particularly during large rainfall events: over the 60-

Figure 2.14: General character of study catchments in the Cascades. (**a**) Watershed 1 hillslope, showing lush vegetation (trees and understory) on a steep slope with no soil exposed. (**b**) Watershed 1 channel and wide, vegetated riparian zone. (**c**) Lookout Creek, showing flat riparian zone where large trees flourish. (**d**) Hinkle Creek, also showing significant riparian zone, and thinner stand than Lookout Creek.

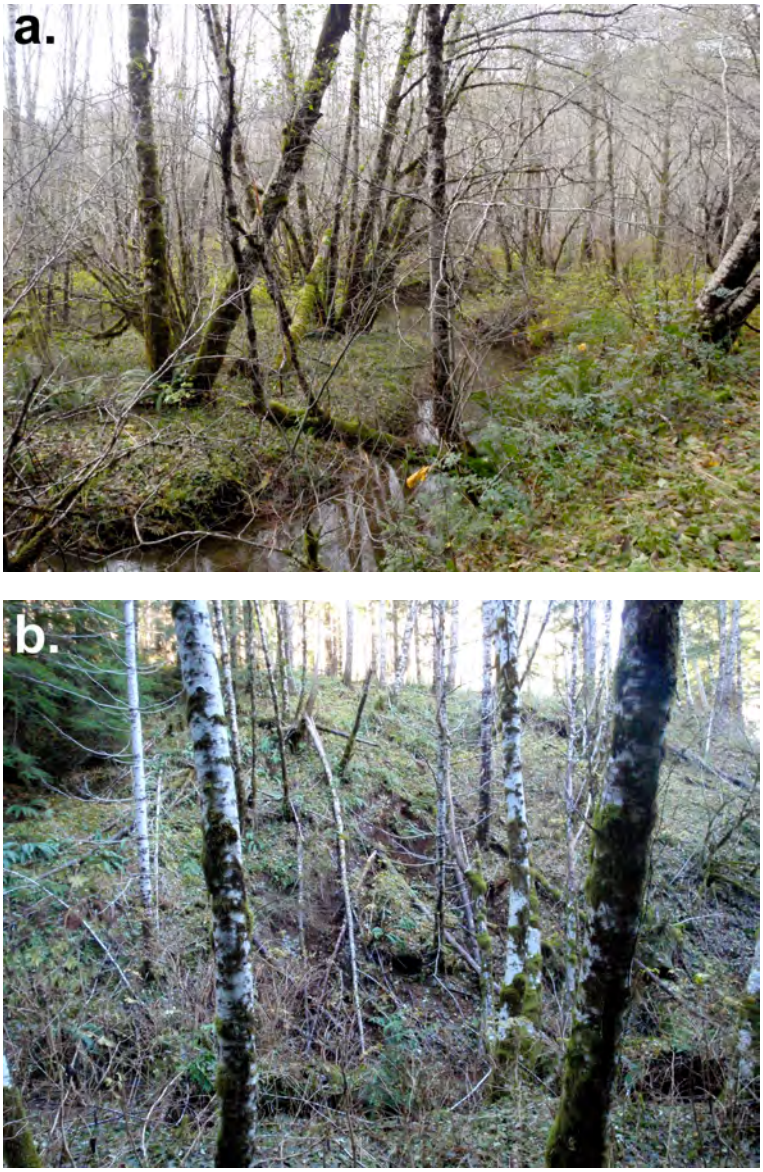

Figure 2.15: General character of study catchments in the Coast Range. (**a**) Flynn Creek in the Alsea watershed, showing flat channel gradient, large riparian wetland and abundance of red alder. (**b**) Stream near the Trask watershed, showing steep slopes adjacent to the channel (running through the bottom of the photograph) and a recent landslide scarp exposing fresh soil.

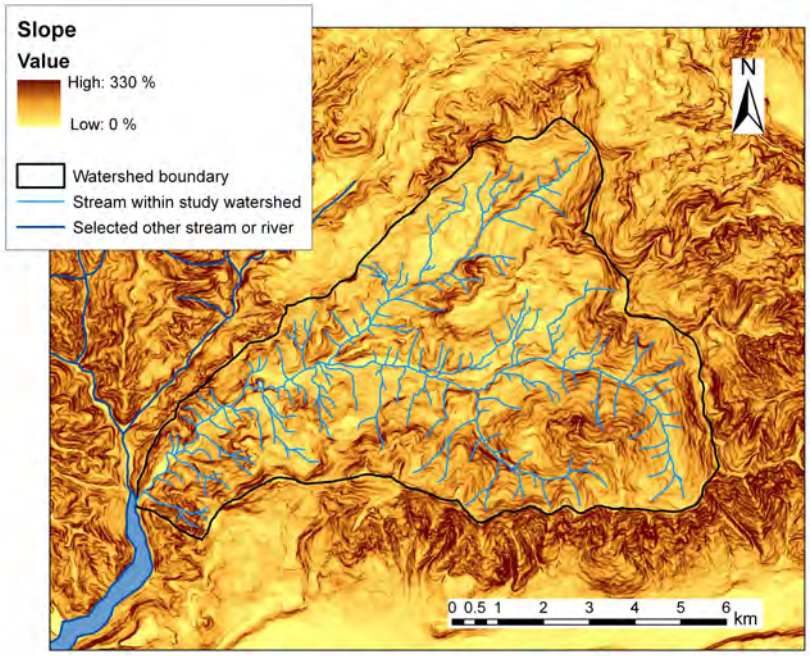

Figure 2.16: H.J. Andrews hillslope angle, expressed as a percentage. Data from Valentine & Lienkaemper (2005).

year record that exists at H.J. Andrews, ∼65% of debris flows occurred during the storms of winter 1964–1965 and winter 1995–1996 (Swanson & Jones, 2002). Forest removal and associated infrastructure has a significant effect on the frequency of debris flow initiation, with an increase of 3–7 times observed in clear-cut areas relative to forested areas (Snyder, 2000). Many debris flows originate from forest roads (initiation frequency increased 11–50 times compared to non-roads (Snyder, 2000)), although the geomorphological impact of roads depends on the road location and construction, geology and the storm characteristics (Wemple *et al.* , 2001). Depending on the location and other factors of each event, debris flows can fill channels with material eroded from further up the catchment, or clear channels by sweeping out previously accumulated sediment and woody debris.

Complex, unstable terrains formed by large, deep-seated (>5 m) slumps and earth flows are also observed at H.J. Andrews (Figure 2.17), and are inferred to have been important in forming the present-day landscape (Swanson & James, 1975; Swanson & Swanston, 1977). However, these are now largely inactive (Swanson & James, 1975), and are in any case prevented from yielding sediment to the channel system by wide intervening riparian zones. In contrast, large, deep-seated landslides as well as smaller mass movements are presently active in the Coast Range, and can affect up to 25% of land area where bedrock is silt-rich rather than sandy (Roering *et al.* , 2004). Shallow landslides tend to occur in areas of reduced root strength (Roering *et al.* ,

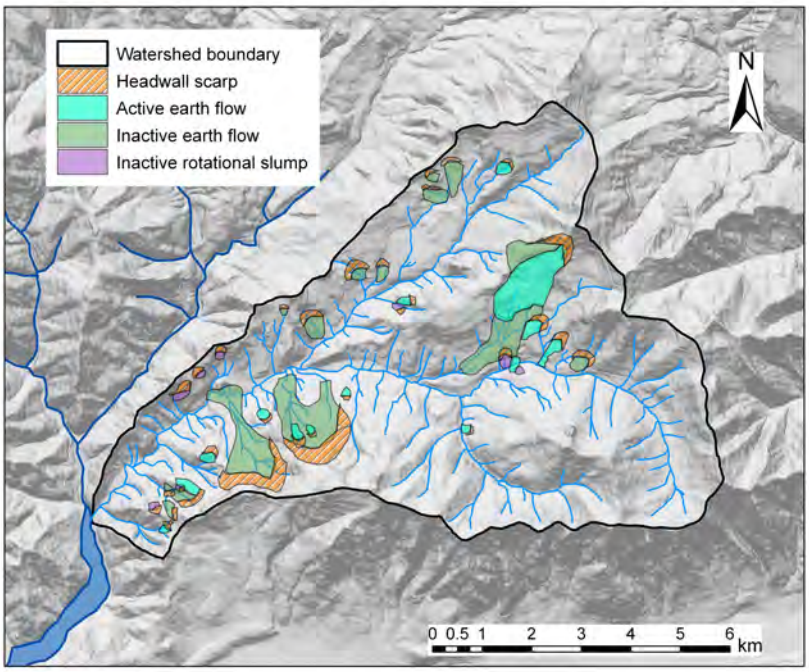

Figure 2.17: Deep-seated mass movements at H.J. Andrews Forest, redrawn from Swanson & James (1975).

2003). In the Alsea watershed, where the mean hillslope angle is 35%–40% but the streams are flat and have large riparian zones with common wetlands and beaver ponds (Beschta & Jackson, 2008), most landslides occur in unchannelled valleys (Beschta & Jackson, 2008). Over the last few decades, there have been many more landslides related to forestry than natural ones (Beschta & Jackson, 2008). In contrast, many streams in the Trask watershed flow through a steep (>60%), dissected landscape where shallow debris slides and flows originate (Figures 2.15 and 2.18). There are large mass movement complexes here, but as at H.J. Andrews, they are ancient, and inactive over the timescale of this study.

The Oregon headwaters studied here have much lower channel gradients than those in the Alptal, and consequently more varied morphology. The average channel gradient of Lookout Creek is 3.8%, and morphology consists of boulder-dominated pools, riffles, rapids, cascades and steps (Montgomery & Buffington, 1997), each with a characteristic gradient (Grant *et al.* , 1990). GIS data allowing measurement of hillslope and channel gradients does not yet exist for Hinkle Creek, but the landscape and stream character are very similar to H.J. Andrews (Figure 2.14). Alsea streams are relatively flat (Beschta & Jackson, 2008), while streams in the much larger Trask watershed range from wide, low-gradient reaches to short sections greater than 30% in very small first-order streams (Watersheds Research Cooperative, 2008) (Figure 2.18).

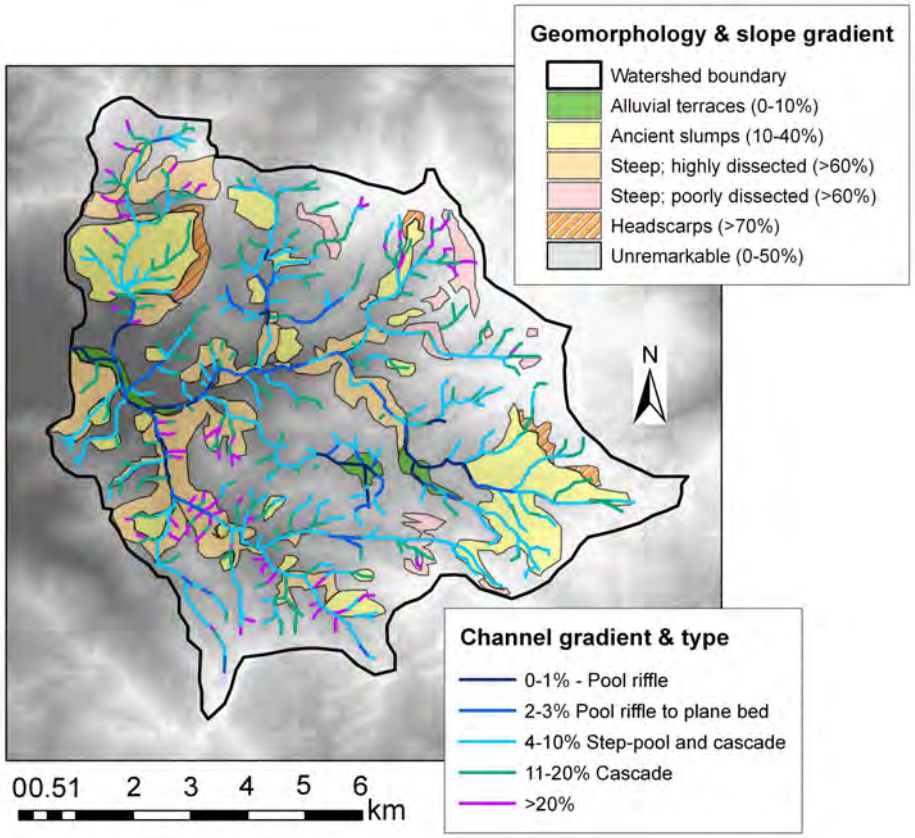

Figure 2.18: Channel gradients and geomorphologic units in the Trask watershed, redrawn from Watersheds Research Cooperative (2008).

As a general trend, Oregon headwaters transport very low levels of suspended sediment and run clear for a large proportion of the time. Coarse woody debris is an important component of the fluvial system in such settings, both in providing habitat and as an erosive force during floods (e.g. Fetherston *et al.* , 1995; Johnson *et al.* , 2000; Wohl, 2011).

2.3.5 Biosphere and forestry

Soils in all the Oregon study catchments are broadly similar, being well-drained and having a relatively coarse, open structure. In the actively eroding Coast Range, the soil mantle is thinnest (around 0.5 m or less) on side slopes and thickest (1–2 m) in unchannelled valleys (Anderson & Dietrich, 2001; Heimsath *et al.* , 2001; Roering *et al.* , 2004). It is generally rocky and produced largely by mechanical processes such as tree throw, animal burrowing and freeze-thaw cycles (Heimsath *et al.* , 2001), and rapid weathering (Beschta & Jackson, 2008). In the Trask watershed, surface soils

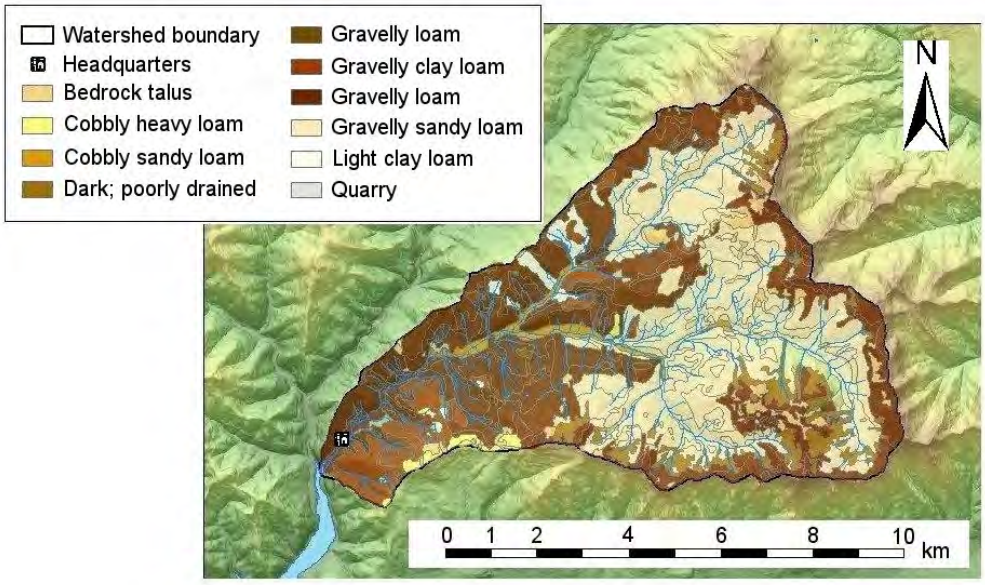

Figure 2.19: Distribution of soil types at H.J. Andrews Forest, based on 1964 survey and revised in 1994 (Dyrness *et al.* , 2005).

are loamy with a low clay content, varying from silty to extremely gravelly, while the subsoils of some units have a higher clay content (Watersheds Research Cooperative, 2008).

Hinkle soils are also loamy with a range of textures from silty clay to gravel. They are classified as typic palehumults and typic haplohumults (Skaugset *et al.* , 2004), in the broad group of ultisols. At H.J. Andrews, soils are classified as mostly inceptisols, with local alfisols and spodosols, but the overall texture is similar to elsewhere in western Oregon (Figure 2.19). Little information is available regarding soil thickness in the Oregon Cascades. If they are assumed to be similar to the Skykomish River in the Washington Cascades then shallow depths are expected—Hren *et al.* (2007) found a basin-wide mean depth-to-bedrock of 25–42 cm—but personal experience shows that soil thicknesses of greater than 80 cm do occur at least locally.

Like the Alptal, the Pacific Northwest coast has high NPP compared to much of the world (Bowman *et al.* , 2009), with forest plots giving values ranging from 120 g C m^{-2} yr^{-1} to 1300 g C m^{-2} yr^{-1}, depending on stand age and composition (Van Tuyl *et al.* , 2005; Waring *et al.* , 1998). NPP is highest in the Coast Range, and reaches its lowest values in Klamath Mountains in south-west Oregon (Van Tuyl *et al.* , 2005). Hatten *et al.* (2012) report NPP of 820–950 g C m^{-2} yr^{-1} for the Alsea River watershed, while Goñi *et al.* (2013) report 600 g C m^{-2} yr^{-1} for the Umpqua, into which Hinkle drains. Because of these high NPP values, low human population density and very widespread occurrence of forest, timber harvesting is a

major industry in western Oregon. As well as affecting ground stability and mass movement (Section 2.3.4), logging activities and infrastructure have an impact on hydrology, resulting in increased peak discharge due to reduced evapotranspiration and changes in snowpack dynamics and subsurface flow interception (Jones, 2000), and increased SSC, often related to road-induced failures (Beschta & Jackson, 2008). Increased SSC and bank erosion rates as a response to timber harvesting have also been reported elsewhere (e.g Stott *et al.* , 2001). An excellent review of the many dependencies and interactions between vegetation and hydrogeomorphic processes is provided by Stoffel & Wilford (2012). Harvest activity relating to the watersheds in this study is therefore briefly considered in the sections below.

Similar vegetation is found throughout western Oregon (Franklin & Dyrness, 1973; Rochelle *et al.* , 2005), with minor geographic differences in species abundance. Over 500 vascular plant species grow at H.J. Andrews, where the major coniferous trees are *Pseudotsuga menziesii* (douglas-fir) and *Tsuga heterophylla* (western hemlock). *Thuja plicata* (western redcedar) is also relatively abundant, and true firs (*Abies procera* (noble fir), *Abies amabilis* (Pacific silver fir)) are found at the highest elevations. Throughout, but especially at low elevations, several hardwood trees are also common, particularly *Alnus rubra* (red alder), *Acer macrophyllum* (bigleaf maple) and *Populus trichocarpa* (black cottonwood). The latter, though not one of the most abundant species in the watershed, grows preferentially alongside streams. Common shrubs and ground plants include *Polystichum munitum* (sword fern), *Acer circinatum* (vine maple), *Pteridium sp.* (bracken), *Berberis nervosa* (Oregon grape), and *Rubus sp.* (bramble).

Currently, about 40% of the Lookout Creek watershed is covered by old-growth forest (∼450 years old), with a further ∼20% covered by mature forest (100–150 years old) dating from mid-1800s to early-1900s wildfires. Most of the rest is covered by younger stands created as a result of replanting after harvests beginning in the 1950s, but there are also small areas of wet and dry meadow, rock cliffs and talus slopes. Figure 2.20 gives an indication of the distribution of forest types through the watershed. Regarding the small watersheds used in this study, Watershed 1 was clear-cut between 1962 and 1966, while Watershed 2 is a control catchment and has never been cut (Swanson & Jones, 2002). Excluding a single large debris flow, post-logging annual sediment export (1958–1988) in Watershed 1 was more than twice that in uncut paired catchment Watershed 3 (Grant & Wolff, 1991).

Hinkle overstory vegetation consists of 75% *Pseudotsuga menziesii* with the rest mainly *Tsuga heterophylla* (Skaugset *et al.* , 2004). The trees do not reach such heights as those at H.J. Andrews because of the drier climate and more intensive

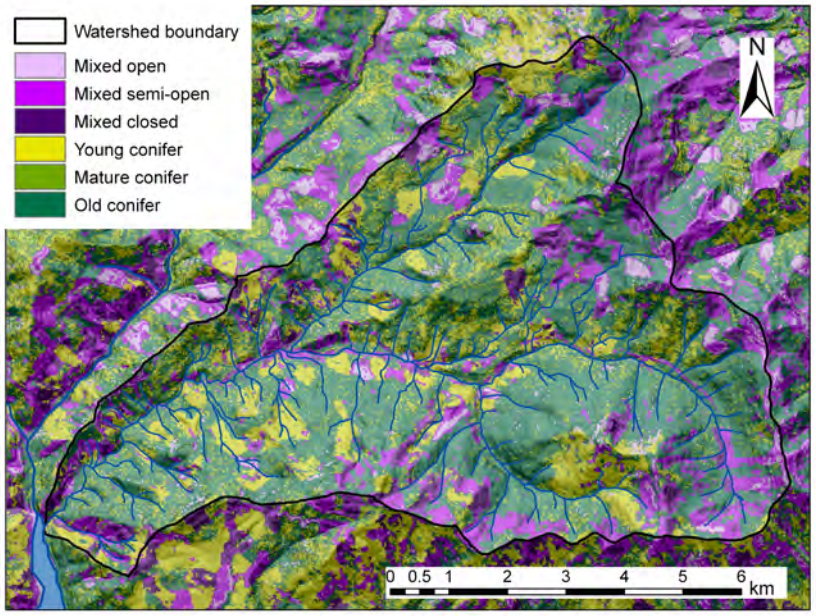

Figure 2.20: Age and type of forest stand at H.J. Andrews, classified from 1988 thematic mapper satellite image. Data from Schulze (2005).

management. Hinkle understory comprises *Polystichum munitum*, *Rhododendron sp.*, *Acer circinatum*, *Gaultheria sallon* (salal), *Berberis nervosa* and *Vaccinium parvifolium* (red huckleberry) (Skaugset *et al.* , 2004). The watershed is entirely owned by Roseburg Forest Products, and the current stand in non-harvest areas, including all of the North Fork control, is a 55 year-old regeneration (Skaugset *et al.* , 2004).

Trask is dominated by second-growth conifers, but hardwood species cluster along the stream channels, especially Gus Creek where *Alnus rubra* is dominant (Watersheds Research Cooperative, 2008). Most of the original stand in the study area was destroyed by the fires of the Tillamook Burn (1933–1951) and by harvesting during the mid twentieth century (Walstad *et al.*, 1990, discussed in Watersheds Research Cooperative, 2008). The majority of the forest is currently owned by Weyerhaeuser and the Oregon Department of Forestry; forestry activities are ongoing, but since 2006 when the Trask Watershed Study was initiated, there has been no harvest during a phase of baseline data collection. Gus Creek and Upper Mainstem (Figure 2.10(d)) are the sub-catchments least affected by recent harvesting, while Rock Creek and Pothole Creek underwent substantial thinning between 1980 and 2005. There is a network of private tracks through the study area, and there has been extensive use by all-terrain vehicles (Watersheds Research Cooperative, 2008).

Alsea, owned by the Plum Creek Timber Company and the U.S. Forest Service, is again dominated by *Pseudotsuga menziesii* and *Tsuga heterophylla*, with some *Abies*

procera at high elevations. *Alnus rubra* is more common here than in the other study watersheds (Figure 2.15(a)), and there is a dense understory. The original Alsea Watershed Study (1957–1973) was one of the first paired watershed studies to investigate the effects of forest management practices on hydrology and the stream environment (Beschta & Jackson, 2008). During that study, Flynn Creek acted as the control while Deer Creek was patch-cut to 25% and burned with a riparian buffer left intact (Ice *et al.* , 2005). Deer Creek was harvested again in the 1970s and 1980s; in total, 39% of its area has now been harvested (Beschta & Jackson, 2008). In the present study, which began in 2006, no harvests are taking place in Flynn Creek or Deer Creek, but Deer Creek still shows elevated discharge and suspended sediment concentrations compared to pre-logging conditions due to intensive prior harvesting.

In addition to the anthropogenic disturbances associated with timber harvest, wildfire is an important part of the natural system in western Oregon and can play a substantial role in shaping the landscape, most obviously through forest regeneration, but also by influencing climate, geomorphologic response and carbon dynamics (e.g. Bowman *et al.* , 2009; Hatten *et al.* , 2010; Jackson & Roering, 2009; Meigs *et al.* , 2009). Fire releases carbon stored in biomass and generally reduces aboveground carbon pools (Meigs *et al.* , 2009), but destruction of woody vegetation may be balanced by regeneration and increased uptake from surviving vegetation (Bowman *et al.* , 2009). Organic carbon that is not converted to CO_2 may change its form, and fire-related increases in charcoal and other pyrogenic-derived organic carbon have been observed in the suspended load of Oregon rivers (Hatten *et al.* , 2010). Fires may also generate hydrophobic soil layers, leading to increased runoff, although the principal way in which they cause erosion is by dry ravel (Gabet, 2003; Jackson & Roering, 2009). Observed carbon and landscape responses to fire are, however, highly variable.

2.3.6 Hydrology and research history

H.J. Andrews was established as an Experimental Forest in 1948, and is now part of the Long-Term Ecological Research (LTER) network of sites throughout the USA. The Lookout Creek gauge is maintained by the US Geological Survey (station number 14161500). In addition, there are eight small gauged watersheds, plus a gauge on a significant tributary, Mack Creek. The stream in Watershed 1 enters Lookout Creek just downstream of the gauge, and Watersheds 9 and 10 discharge directly into Blue River (Figure 2.10(b)). Continuous discharge monitoring began via trapezoidal flume-type weirs at different times in the various watersheds, with records available at high temporal resolution back to 1953 for Watershed 1 and 1987 for Lookout

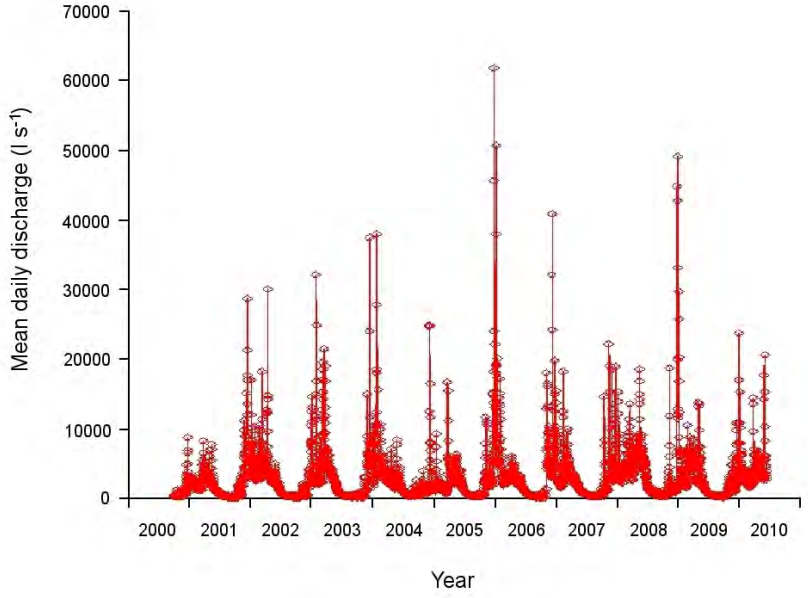

Figure 2.21: Daily discharge of Lookout Creek, 2000–2010, in l s^{-1}. Modified from an image generated by Andrews Forest website (data from Johnson & Rothacher, 2012).

Creek. Long-term programmes of regular sampling for suspended sediment load and water chemistry have been set up in many of the watersheds, with different start dates. These data are available from May 2003 for Watershed 1, and May 2005 for Lookout Creek. Discharge-proportional samples are taken automatically and collected for analysis every three weeks (more details are given in Chapter 3). Because of its long research history, far more hydrometric data is available for H.J. Andrews than any of the other study watersheds, and so this is used as the "type example" for Oregon headwaters, with additional details given for the other watersheds (where it exists and is accessible) at the end of the section.

Discharge at H.J. Andrews generally follows precipitation patterns, with the maximum flow of Lookout Creek in winter more than three orders of magnitude greater than the summer minimum (Figure 2.21). Rain-on-snow events trigger some of the highest discharges (Harr, 1981), and there is a slight peak in March–April relative to precipitation that likely represents snow melt. Over the sampling period (1987–2008 inclusive for Lookout Creek, and 1980–2009 inclusive for Watershed 1), mean discharge was 3250 l s^{-1} for Lookout Creek and 40 l s^{-1} for Watershed 1 respectively. Maximum flows in both catchments were reached on 7 February 1996, peaking at 310 m^3 s^{-1} in Lookout Creek and 2.4 m^3 s^{-1} in Watershed 1. Other major forest-wide historical floods occurred in December 1964–January 1965 (peak Lookout Creek discharge 190 m^3 s^{-1}), January 1972 (120 m^3 s^{-1}), and February 1986 (77 m^3 s^{-1}) (Swanson & Jones, 2002). General discharge behaviour for the two catchments is

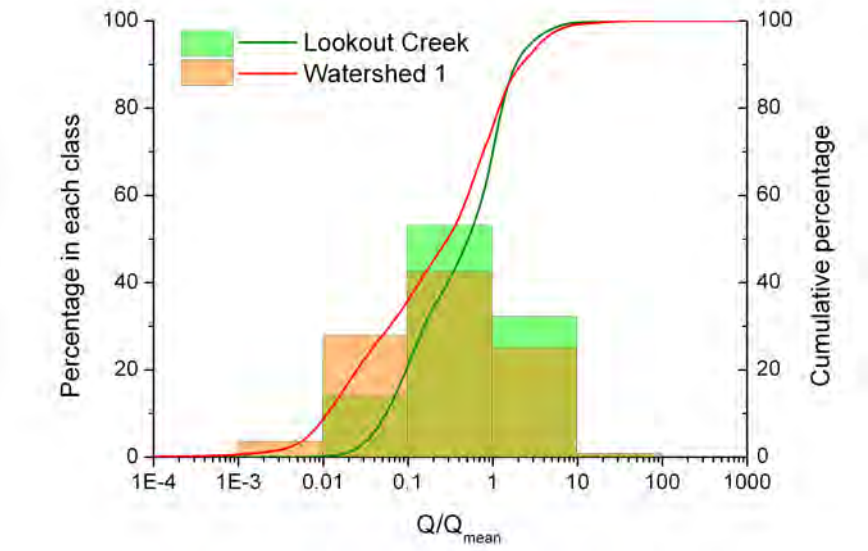

Figure 2.22: Discharge characteristics of Lookout Creek (based on instantaneous measurements taken every 30 minutes from 1987–2008) and Watershed 1 (based on mean measurements every 15 minutes from 1980–2009). Bars indicate the percentage of measurements falling in each discharge class, expressed relative to mean discharge (as Q/Q_{mean}); lines indicate the cumulative percentage. Data from Johnson & Rothacher (2012).

illustrated in Figure 2.22. Lookout Creek shows less variability in discharge than Watershed 1, with relatively more time spent in the modal class of Q/Q_{mean}=0.1–1, and relatively less at lower and higher discharges. Flow is less than or equal to Q/Q_{mean} for 67% of the time in Lookout Creek, and 74% in Watershed 1. The latter figure is directly comparable with the Alptal (Section 2.2.6), while the proportion for Lookout Creek is slightly lower.

Suspended sediment yield follows discharge relatively closely (Figure 2.23). Yields are low relative to discharge in February and March in Watershed 1, perhaps because channels have been "flushed out" during the preceding months. There is a positive power law relationship between discharge and SSC in both Lookout Creek and Watershed 1 (Figure 2.23), but this is not well-defined (R^2=0.55 and 0.01 respectively) and it is clear that many factors other than discharge also control SSC. Bedload transport is not measured, but Pelletier (2012) suggests that sediment transport at H.J. Andrews is bedload-dominated over timescales that include large landslides.

H.J. Andrews is the site of much research into water flow paths. The mean residence time for baseflow in the forest ranges from 0.8 to 3.3 years (McGuire *et al.* , 2005), but this pool makes a relatively small (<50%) contribution to stream water compared to other LTER sites, with quickflow from surface runoff or interflow making up the rest (Post & Jones, 2001). It is thought that the majority of quickflow comes from

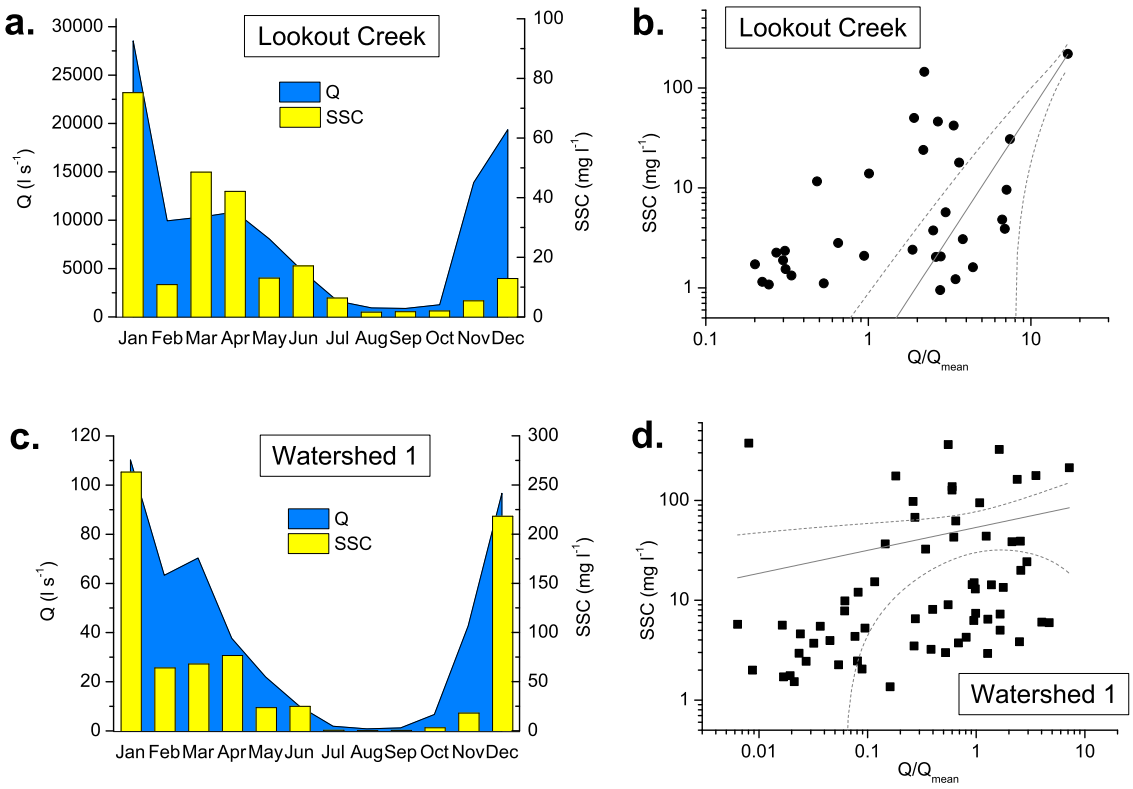

Figure 2.23: Bar and line graphs show mean monthly discharge and SSC for (**a**) Lookout Creek and (**c**) Watershed 1. For Watershed 1, data are actual monthly means June 2003–August 2009. For Lookout Creek, data are derived from three-week discharge proportional samples collected June 2005–March 2007. Samples were allocated to the month in which the majority of the period they relate to fell, then all values for each month were averaged. Cross-plots show relationship between discharge and SSC in three-week discharge proportional samples collected June 2005–March 2007 (Lookout Creek; (**b**)) and June 2003–March 2007 (Watershed 1; (**d**)). Solid lines show best-fit power law; dashed lines are 95% confidence intervals. Raw data from Johnson & Rothacher (2012) and Johnson & Frederiksen (2012).

the soil–bedrock interface, where a "fill and spill" mechanism in hollows ensures rapid conduct to the channel, while the baseflow runs deeper in the bedrock (Freer *et al.* , 2002; McDonnell, 2003). Tracers applied to the hillslope in Watershed 10 showed peak breakthrough to the stream at ∼40 hours after the rain started (McGuire *et al.* , 2007). The soil appears to contain two entirely separate pools of water: one tightly bound and taken up by trees, and a second that participates in translatory flow and enters the streams (Renée Brooks *et al.* , 2010). At fine temporal resolution, stream flow shows high spatial variability and is not closely related to precipitation, pointing to a strong hydrologic role for the forest canopy in terms of interception and transpiration (Post & Jones, 2001). Surface runoff is uncommon both at H.J. Andrews and in the Coast Range, where observations suggest that most precipitation reaches streams

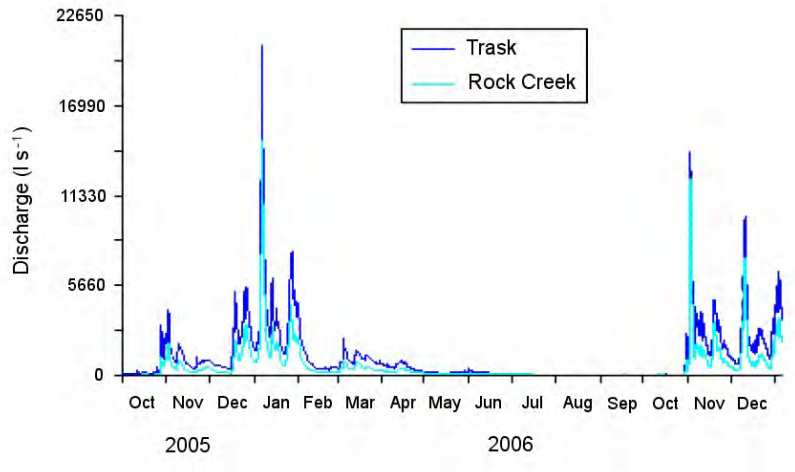

Figure 2.24: Discharge measured at Lower Trask and Rock Creek (30-minute means) between October 2005 and January 2007, in litres per second. Modified from Watersheds Research Cooperative (2008).

by flowing through colluvium and near-surface bedrock (Montgomery *et al.* , 1997). Smaller precipitation events frequently produce an insignificant response—or none at all—in stream discharge: a critical intensity-duration of rain is needed to overcome the storage capacity of the porous soils found in western Oregon (Montgomery *et al.* , 1997).

The other sites are paired watershed studies investigating the effects of various forest management practices, at different stages of their 10-year programmes. Starting from the study initiation date (2001 for Hinkle, and 2006 for Alsea and Trask), measurements of discharge, stream temperature, conductivity and turbidity are recorded every 10 minutes at a number of gauges (Figure 2.10). However, due to the involvement of commercial stakeholders and the ongoing nature of the projects, this data is not readily accessible. Suspended sediment is collected via threshold turbidity sampling (details in Chapter 3); several years' worth of these samples exist for each site.

As at H.J. Andrews, discharge at these sites is event-dominated, with events clustered in the winter when storms occur. In the Trask watershed, the peak discharge measured so far at the Lower Trask gauge occurred in January 2006, reaching $\sim$21 m^3 s^{-1} (Figure 2.24). The peak flow for the February 1996 event (a flood with a 50-year return period in this catchment) was reconstructed from the flood mark and slope–area calculations, and estimated to be $\sim$740 m^3 s^{-1} (Watersheds Research Cooperative, 2008). In the Alsea, the year 2006 saw discharges of 2–1530 l s^{-1} in Flynn Creek and 3–2430 l s^{-1} in Deer Creek. For Hinkle, the only available information is the discharges at which suspended sediment samples were taken over a short period.

The ranges were: 200–2290 l s^{-1} for the North Fork (November 2007–January 2009), 40–650 l s^{-1} for DeMersseman Creek (March 2008–May 2009) and 40–420 l s^{-1} for Meyers Creek (January 2009–June 2009).

Wheatcroft & Sommerfield (2005) give values for the mean sediment yield for various small rivers draining the Oregon Coast. Per unit area, the Alsea River delivers about half the sediment (75x10^3 kg km^2 yr^{-1}) to the ocean as does the Umpqua River (147x10^3 kg km^2 yr^{-1}), into which Hinkle Creek drains.

Chapter 3

Materials and methods

3.1 Introduction

This chapter provides detailed descriptions of the methods used in this project, from field sampling to analysis. The first section details the collection of suspended sediment, source materials and hydrometric data, with the Alptal and Oregon dealt with separately. Sampling localities are described, with reference to the general site information provided in the previous chapter. The second section covers sample preparation, including homogenisation and carbonate removal. The final section reviews the analytical methods used to obtain geochemical data—C and N concentrations and stable isotopes and radiocarbon—and the biomarker and Raman techniques that are used qualitatively. Consideration is given to analytical and other potential sources of error, and to the characterisation and correction of an internal blank.

3.2 Sample and data collection

3.2.1 Suspended sediment

Suspended sediment samples were collected in two ways: i) regular sampling programmes managed by in-country researchers and generally set up prior to this study (total of 295 samples), and ii) instantaneous, hand-grab samples collected in targeted campaigns during each area's storm season (total of 156 samples).

3.2.1.1 Alptal

As part of the long-term National River Monitoring and Survey Programme (NADUF), weekly discharge-proportional samples are collected at both the Erlenbach and Vogel-

bach from a portion of the stream diverted through a 1 mm mesh under the outflow gauges by WSL, and analysed for standard water quality parameters by the Swiss Federal Institute of Aquatic Science and Technology (EAWAG). Unlike other sampling protocols, the discharge-proportional method has been found to give unbiased flux estimates (Schleppi *et al.* , 2006). Impulses are triggered after a threshold volume of water has passed, equivalent to 1 mm of precipitation over the drainage area. Under normal flow conditions a 20 ml sample is taken after two impulses, adjusted to three during spring snow melt. This is transferred to a 15-litre glass collection bottle, refrigerated at 5°C, where each week's samples accumulate. Once a week, water collected over each 7-day period (if any) is homogenised by swirling the collection bottle, and a compound aliquot is poured into a one-litre wide-necked plastic bottle. For the period of this study, a second aliquot of up to one litre (two litres from March 2010) was taken for POC determination. For the Erlenbach, this dataset consists of samples collected between August 2009 and November 2010; because the Vogelbach transports less sediment, more time was needed to obtain a comparable range of data, so sampling was extended to September 2011 (Table 3.1).

A similar, smaller-scale set-up exists for the Erlenbach sub-plots. Water from these is analysed internally by WSL for chemical parameters and the sediment normally discarded, so for this study the sediment was retained and no additional aliquot required. A subset of these samples (August 2009–November 2010 for the forest control sub-plot; November 2010–August 2011 for the meadow sub-plot) was analysed to characterise the hillslope input signal. These are referred to in Chapter 4 and elsewhere as "runoff suspended sediment", and are not included in Table 3.1.

In the Erlenbach, instantaneous suspended sediment samples were collected directly from the stream at the upper gauging station (Figure 2.1, page 20) in 100 ml plastic bottles, every few minutes during five storms in July 2010 (Figure 3.1). The largest of these (12 July) had a characteristic return period of one year and a peak discharge of 2290 l s^{-1}. The remaining four events took place within 10 days and covered a range of peak discharges from 300 to 1580 l s^{-1} (Table 3.1). With the exception of 12 July, the storms were characterised by intermittent rain. Hydrographs for the events are shown in Figure 4.8 (page 92). Owing to the rarity of large floods in the Vogelbach, coupled with logistical constraints, no instantaneous sampling was done in this catchment. Auto-samplers were set up during the summer of 2011, but the season was relatively dry and no useful samples were obtained.

Watershed	Date	Local time[a]	Number of samples			Discharge range	
			collected[b]	*combined*[c]	*analysed*	l s^{-1}	Q/Q_{mean}[d]
Erlenbach	12 July 2010	19.00–20.30	37	-	37	46–2290	1.2–59
Erlenbach	22–23 July 2010	20.30–02.30	37 + 1	-	38	17–420	0.4–11
Erlenbach	26 July 2010	21.00–00.00	16 + 1	-	17	21–300	0.5–8
Erlenbach	29 July 2010	06.30–16.45	25	-	25	150–1190	3.9–31
Erlenbach	30 July 2010	08.45–16.00	9	-	9	125–1250	3.2–32
Lookout	16–17 Nov 2011	21.25–17.45	7	2 → 1	6	1730–7220	0.5–2.2
Lookout	21–22 Nov 2011	20.00–18.35	9	5 → 2	6	3890–11920	1.2–3.7
WS1	16–17 Nov 2011	17.00–09.30	16	10 → 3	9	13–90	0.3–2.3
WS1	21–22 Nov 2011	19.55–18.45	16	10 → 4	10	63–185	1.6–4.4

Watershed	Date range	Frequency	Number of samples			Discharge range	
			collected[e]	*combined*[c]	*analysed*[f]	l s^{-1}	Q/Q_{mean}[d]
Erlenbach	Aug-09–Nov-10	1 week	51	-	45	6.5–205	0.2–5.3
Vogelbach	Aug-09–Sep-10	1 week	93	10 → 4	32	22–409	0.3–5.2
Lookout	May-05–Jul-06	3 weeks	23	5 → 2	10	1720–51580	0.5–16
WS1	Oct-04–Aug-06	3 weeks	35	-	29	0.6–288	0.02–7.2
WS2	Nov-11–Apr-12	3 weeks	7	2 → 1	3	93–206	3.7–8.2

Table 3.1: Instantaneous (top) and discharge-proportional compound suspended sediment samples (bottom) from the Alptal and H.J. Andrews (Lookout Creek and Watersheds 1 (WS1) and 2 (WS2))used in this study. [a]Local time is Swiss summer time (UTC+2) for the Erlenbach; Pacific Standard Time (UTC–8) for H.J. Andrews. [b]Additional samples for 22 and 26 July in the Erlenbach were collected at preceding low flow. [c]Owing to small sample size, samples collected consecutively or at similar discharges were combined until there was enough material to analyse. This column describes the number of original samples that were combined, and how many samples they were combined into. [d]Q/Q_{mean} is the discharge relative to the average discharge as stated in Sections 2.2.6 (page 25) and 2.3.6 (page 45). [e]Weeks where there was insufficient water for a sample to be taken are not included. [f]Number of samples collected, less those combined and those too small to be analysed.

Initial stabilisation of samples, both instantaneous and compound, took place at WSL. Each turbid river water sample was passed through a Millipore Express Plus 0.2 μm nylon filter using a vacuum system within two weeks of collection, following interim storage and settling at 5°C. The majority of samples, including the entire compound dataset, were filtered within three days of collection; the exceptions occurring during some of the July 2010 storms when manpower was limited. Potential implications of protracted storage before filtration are discussed in Chapter 5. The filters with sediment were stored in glass petri dishes at -18 °C before lyophilisation and shipment to Cambridge for analysis (∼twice yearly).

3.2.1.2 Oregon

Stream water samples proportional to discharge have been collected at H.J. Andrews since 1968, with the present sampling system established in 2003 in Watershed 1 and 2005 in Lookout Creek. The system consists of a Sigma Model 900 portable sampler, with a Campbell Scientific CR-10X datalogger which records stage height at the gauging station (Creel & Henshaw, 2007). The Sigma sampler is set in flow-based composite mode, and the CR-10X controls the sampling rate based on the stage. Samples accumulate in a storage container in the insulated base housing of the Sigma, and are collected every three weeks. The purpose of sampling is to measure SSC and dissolved nutrients, which is done at the Cooperative Chemical Analytical Laboratory (CCAL) at Oregon State University. Suspended sediment is defined as the residue that will pass through a 1 mm mesh screen (Motter & Jones, 2010). Water samples are filtered through Whatman GF/C (1.2 μm) glass microfibre filters, and dried at 80°C for five days. The filters with sediment are folded and stored in small paper envelopes. The potential consequences of this filtration and storage method are discussed in Section 3.4.1.3. Samples used in this study were collected between May 2005 and September 2006 for Lookout Creek, and between October 2004 and September 2006 for Watershed 1 (Table 3.1). The existing Watershed 2 samples were unavailable for use in this project, but an extra aliquot was filtered between November 2011 and April 2012, yielding three data points (Table 3.1).

At Hinkle, Trask and Alsea watersheds, stream water is collected via turbidity threshold sampling at the flume gauges. In this system, turbidity is measured continuously by a turbidimeter, suspended in the middle of the stream by a boom along with an ISCO water sampler. At a threshold turbidity value, a sample is taken by the ISCO sampler. A probabilistic element exists to ensure that water samples are collected randomly above the threshold (Skaugset *et al.* , 2004). Instead of being

Figure 3.1: Suspended sediment sampling. (**a**) Sampling in the Erlenbach at peak flow of the 29 July event. (**b**) Sampling bottle and bottle holder used in Oregon to make sampling safer and ensure clearance of stream banks. (**c**) Watershed 1: falling limb of the 21–22 November event. (**d**) Lookout Creek: falling limb of the 16–17 November event.

compounded as in the discharge-proportional methods used in the Alptal and at H.J. Andrews, each sample is kept separately. A maximum of 24 samples can be stored at one time, and samples are collected as soon as possible after a storm. As at H.J. Andrews, SSC and water chemistry are obtained for each sample. This is coordinated by the Watersheds Research Cooperative, operating across several departments and laboratories at Oregon State University. Again, samples are filtered through glass fibre filters, which are stored with their sediment in plastic petri dishes. Sample sets used in this study are concentrated in just a few flood events between November 2007 and March 2010 (Table 3.2).

In Oregon, instantaneous samples were collected at Lookout Creek and Watershed 1, in November 2011 (Table 3.1). Two medium-sized events were sampled, peaking in the early mornings of 17 November and 22 November. Hydrographs for these events are shown in Figure 6.13 (page 163). Because stream discharge in Oregon responds more slowly to precipitation than in Switzerland, and because of limited equipment and the need to sample in two locations at once, samples were taken much less frequently: roughly every hour at Watershed 1 and every two hours at Lookout Creek over the peak, and less frequently at either end of the hydrograph. Samples were collected using a 1-litre plastic bottle held in a steel bottle-holder and connected

Watershed	**Date**	**Number of samples**		**Discharge range (l s^{-1})**
		obtained	***analysed***	
Hinkle	20-Nov-07	3	60 (3 of those obtained were too small)	39–2290
	12-Mar-08	2		
	25-Mar-08	8		
	7-Jan-09	32*		
	24-Feb-09	1		
	18-Mar-09	13*		
	6-May-09	2*		
	30-Apr-09	1		
	3-Jun-09	1		
Trask	11–13-Nov-08	34*	51 (4 of those obtained were too small)	240–11500
	15–16-Mar-09	9*		
	8-Apr-09	1		
	12-Apr-09	1		
	6-May-09	10*		
Alsea (Flynn)	5-Dec-07	9	44	unknown
	3-Oct-08	5		
	30-Dec-08	7		
	6-Jan-09	5		
	18-Nov-09	4		
	7-Jan-10	5		
	15-Mar-10	3		
	unknown	6		
Alsea (Deer)	30-Dec-08	18	20	unknown
	6-Jan-09	1		
	15-Mar-10	1		

Table 3.2: Oregon suspended samples collected by turbidity threshold sampling. "Samples obtained" in this table refers to a subset of the total number of samples actually collected. These were selected and brought to Cambridge on the basis of their high sediment content. Discharge ranges are not given in terms of Q/Q_{mean} because discharge records needed to calculate a robust Q_{mean} are unavailable for these watersheds. *Samples for these dates were collected at more than one gauge in the watershed.

to a long sturdy stick by two jubilee clips (Figure 3.1). Using this apparatus enabled samples to be collected away from stream banks. Water was immediately poured from the collector bottle into a one-litre or 500 ml plastic storage bottle, filling 1–4 per sample depending on the turbidity of the water. The collector was rinsed with stream water before each sample.

Samples were refrigerated at 5°C, and filtered within 12 hours of collection by passing through Millipore Express Plus 0.2 μm nylon filters with the aid of an electric pump. Filters with sediment were then oven-dried at 80°C and stored in glass petri dishes.

3.2.2 Source materials

As discussed in Chapter 1, material carried in a stream's suspended load, and hence its POC, can come from a variety of sources corresponding to carbon stores within the catchment. Samples of bedrock, surface soil, deep soil, foliage, wood, bedload, landslides and banks adjoining the channel were collected from the Erlenbach and H.J. Andrews, with less comprehensive sample sets collected in the Vogelbach, Hinkle and Alsea watersheds, and in a catchment adjacent to Trask (Table 3.3). All samples were stored in sealed plastic bags and oven-dried in covered foil dishes at <80 °C as soon as possible (1–12 days for the Alptal and 1–3 days for Oregon) after collection. General sample collection details are given below, with catchment-specific details and sampling maps in the following sections.

Bedrock was collected at exposed outcrops, either on hillslopes, in the stream bed, or in quarries: no drilling equipment was used. Weathered rock was cleaned from the surface before sampling. For the Alsea, drilled rock cores already existed (details below), and sub-samples of these were taken using a rock hammer.

Surface soil was collected from the top ∼10 cm with a clean trowel, after removal of overlying vegetation and litter. At each locality, samples as representative as possible of the immediate surroundings were taken. Although the timing of collection could potentially affect the isotopic composition of soil samples because more decomposed litter tends to be enriched in ^{13}C and ^{15}N (Coyle *et al.* , 2009; Dijkstra *et al.* , 2008), this collection method and subsequent processing should result in samples homogenised over a long enough period to negate any seasonal differences. These samples were generally some combination of O and A layers, but no attempt was made to distinguish between these or other layers: the objective was simply to collect the soil material most prone to mobilisation by distributed surface runoff.

Profiles through stable soil and landslides were taken at selected locations (details

	ER	VO	WS1	LO	NFH	TR	ALS
Bedrock	22	4	-	2	3	-	23
Bedload	11	8	3	3	3	3	2
Channel banks	8	-	2	-	1	2	-
Landslide[a]	22(2)	-	-	-	-	1	-
Deep soil (<10 cm)[a]	10(2)	-	15(5)	-	16(4)	9(3)	-
Surface soil (>10 cm)	17	12	16	11	1	11	6
Foliage	8	-	22	11	8	6	5
Standing wood	5	-	8	10	4	3	3
Woody debris	12	-	4	2	1	-	-
Charcoal	-	-	1	-	3	-	-
Other (see notes)	1[b]	-	4[c]	7[d]	-	-	-
Total	**116**	**24**	**75**	**46**	**40**	**35**	**39**

Table 3.3: Source material samples collected in all study watersheds; see text for more information about the different sample types. Watershed abbreviations: ER=Erlenbach, VO=Vogelbach, WS1=Watershed 1, LO=Lookout Creek, NFH=North Fork Hinkle (referred to in the text as Hinkle), ALS=Alsea, TR=Trask and adjacent watershed. [a]Numbers in parentheses refer to number of separate profiles from which the samples were collected. [b]From sediment retention basin. [c]One sample of litter; three samples of stream-conditioned plant matter. [d]Three samples of litter; four samples of stream-conditioned plant matter.

below). When grouping the results, the uppermost soil samples from each stable hillslope profile (<10 cm depth) are treated as "surface soils" and are excluded from the profile group ("deep soils", >10 cm depth). Soil is generally poorly developed on top of the landslides and so no such distinction is made for these.

Foliage, comprising needles, leaves and twigs, was collected from major tree and understory plant species growing in each catchment. "Standing wood" is the woody interior of twigs and branches from selected foliage samples. There was no formal weighting, but attempt was made to sample roughly in the proportions that plant types occur. However, in reporting the results and throughout the discussion, plant species are also considered individually because streams could sample preferentially. Samples of woody debris embedded in landslides and the channel bed were also collected. Throughout this thesis, "foliage" and "wood" are used as convenient terms for different types of biomass, and include all associated microbial organisms.

3.2.2.1 Alptal

116 source material samples from the Erlenbach (Figure 3.2) and 24 from the Vogelbach (Figure 3.3) were collected in October–November 2009 and July–August 2010 (Table 3.3).

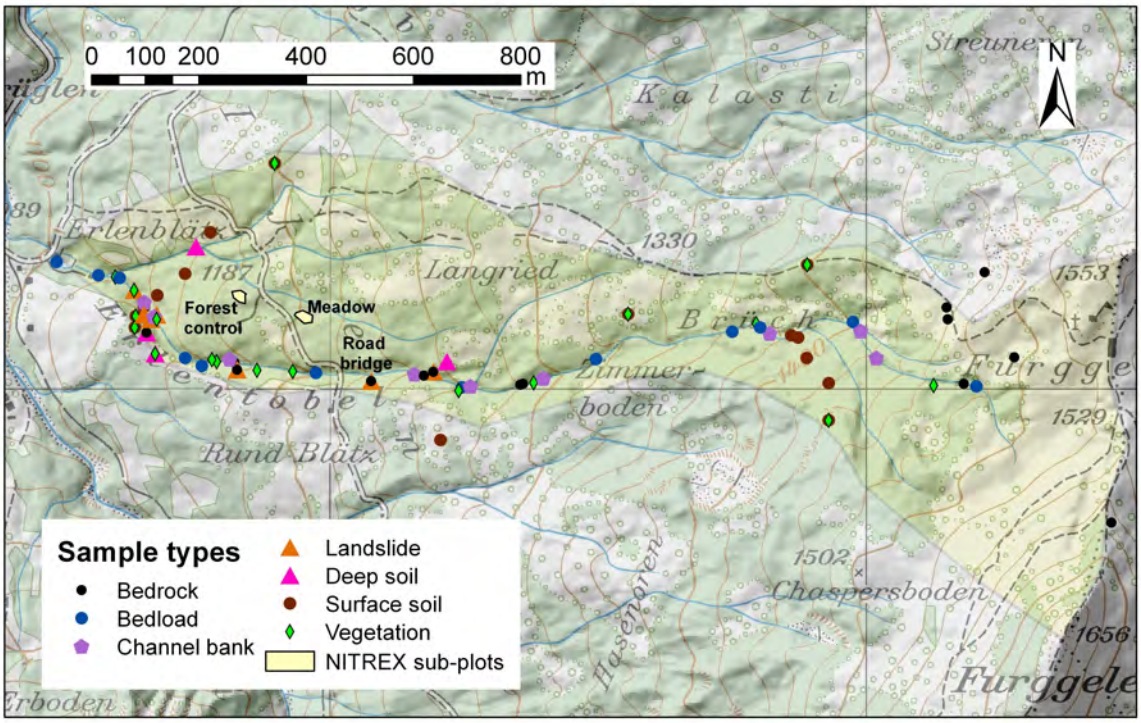

Figure 3.2: Sampling localities in the Erlenbach catchment. Symbols indicate the type of sample collected at each locality. Profiles with multiple samples were taken at deep soil and landslide localities. Locations of sub-plots for collection of discharge-proportional runoff suspended sediment are also indicated.

Bedrock samples were obtained from right across each catchment, from both hillslopes and stream bed. Bedload was collected at roughly equal intervals along the full length of both main channels, and channel bank material from the whole channel length of the Erlenbach. One sample was collected from the Erlenbach sediment retention basin a few days after a very large event in August 2010. It was taken from the edge of the basin, but clearly from a recent deposit that would have been well underwater during the event peak.

Surface soil and foliage were collected in transects across the catchment at a range of elevations, covering all major geomorphologic and ecologic conditions. Foliage included multiple samples of the three main tree types (*Picea abies*, *Abies alba*, and *Alnus viridis*) and representative understory. Collection of material in soil and landslide profiles was concentrated in the lower section of the Erlenbach, below the road bridge (Figure 3.2). Two profiles were taken through landslides (down to 80 cm and 170 cm, the latter with the aid of an auger), and two through stable hillslopes (to 60 cm and 160 cm); these were sampled at 10–60 cm intervals. Representative photographs are given in Figure 4.4 on page 85. No profiles were dug in the Vogelbach.

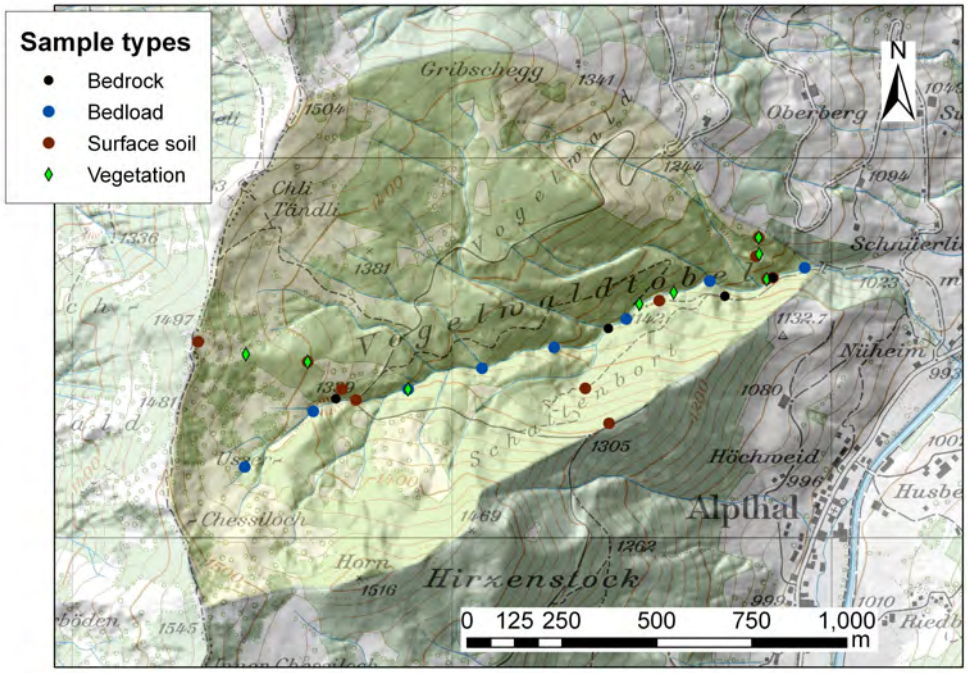

Figure 3.3: Sampling localities in the Vogelbach catchment. Symbols indicate the type of sample collected at each locality.

3.2.2.2 Oregon

201 samples from potential source materials were collected from Oregon in November–December 2011, plus a further 23 samples from existing Alsea bedrock cores. An additional 11 samples were collected from H.J. Andrews in December 2012 by Caroline Martin, Vicky Rennie and Gilad Antler, colleagues at the Department of Earth Sciences, University of Cambridge. Sample collection localities for H.J. Andrews are shown in Figure 3.4; localities for Hinkle and Alsea are described in relation to gauging stations and landscape features (refer to Figure 2.10, page 30). Sample collection sites in the Trask area are described in terms of their landscape setting.

At Hinkle and Lookout Creek, bedrock samples were obtained from road cuts and quarries; no bedrock was collected in Watershed 1 or in the Trask area. Bedrock cores for the Alsea had been previously drilled by Chris Gabrielli of Oregon State University in the Needle Branch catchment (Figure 2.10(c), page 30), which has the same geology as Flynn and Deer Creeks. Three of these were used in this study: UNB-5 (∼270 cm below soil base) and UNB-4 (∼580 cm), both from the upper catchment, and NBL-1 (∼200 cm) from the riparian zone. They were sampled at intervals of a few tens of centimetres. Bedload was collected at high, medium and low elevations in both Watershed 1 and Lookout Creek, at each of the three gauges at Hinkle (North Fork,

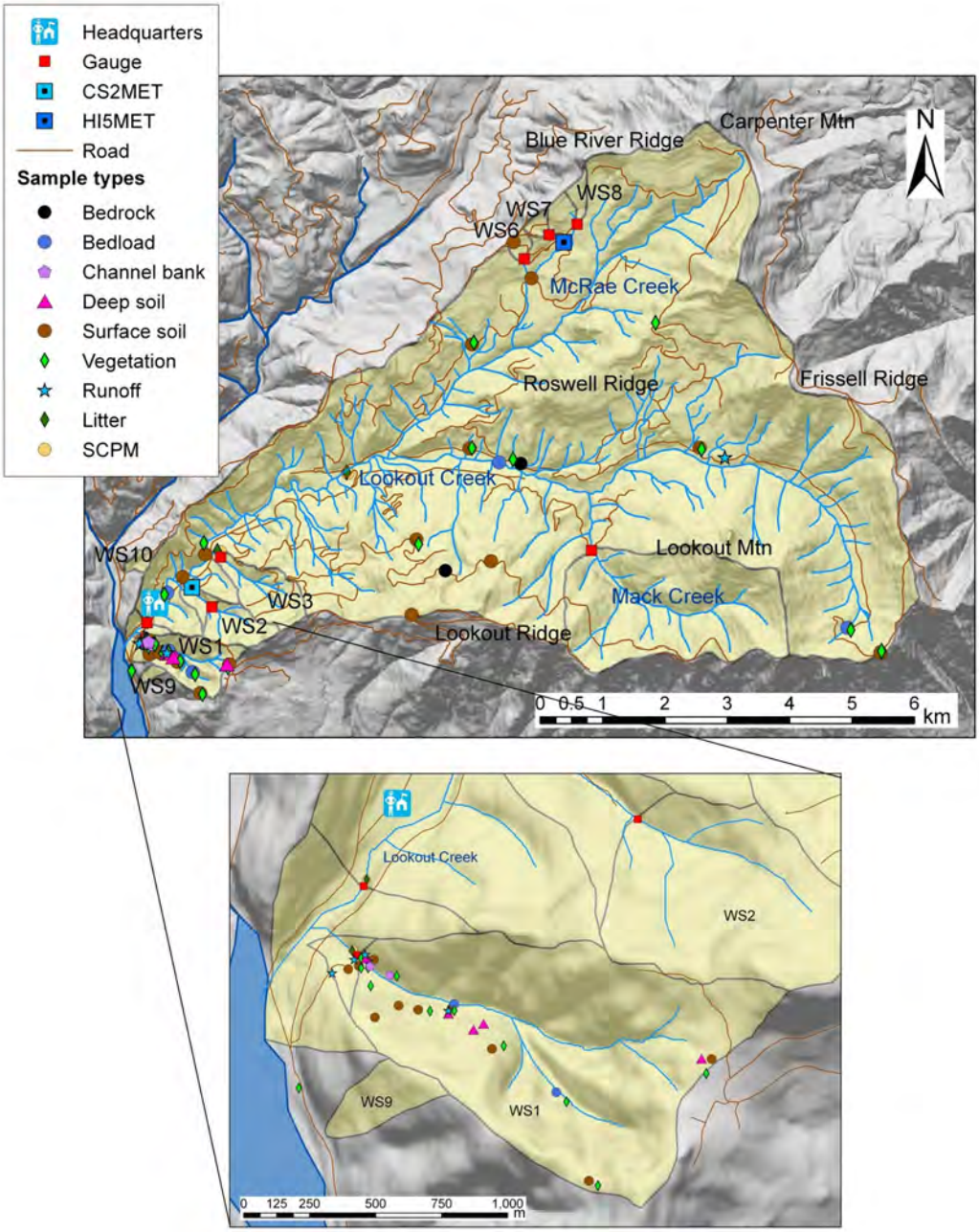

Figure 3.4: Sampling localities at H.J. Andrews Forest, with (inset) close-up of localities in Watershed 1 (WS1). Symbols indicate the type of sample collected at each locality (SCPM=stream-conditioned plant matter); profiles with multiple samples were taken at deep soil localities. Also shown are the smaller watersheds (WS) and gauges, the Forest headquarters, the meteorological stations where climate data used in Chapter 2 (CS2MET) and in Chapter 6 (HI5MET) were obtained, and notable geographic features. Base map data from Henshaw & Creel (2005); Johnson & Lienkaemper (2005a,b); Swanson & Lienkaemper (2005); Valentine & Lienkaemper (2005).

DeMersseman and Meyers), near the outflow of Flynn and Deer Creeks in the Alsea, and from several small streams, including one at its confluence with the Nestucca River, in the Trask area. Owing to thick vegetation and a lack of exposed soil, little channel bank material was collected: two samples from low down in Watershed 1, one from near North Fork Hinkle gauge, and two in the Trask area.

Soil and vegetation were not collected in transects as in the Alptal, due to the greater area of the watersheds and the difficulties of traversing the terrain except by roads. However, locations were chosen to cover a wide geographic area, range of elevations and different eco-geomorphologic settings, including ridge, slope and depression. Separate surface soil samples and soil profiles were collected in Watershed 1 and Trask; only profiles were taken in Hinkle; and only surface samples in Lookout Creek and the Alsea. Trask surface soils were collected in the Trask watershed itself by Alex Irving of Oregon State University, while profiles were taken in the neighbouring catchment: one on the drainage divide, one at the confluence with the Nestucca River, and one on the scarp face of a landslide that allowed sampling to a depth of 200 cm. A sample of landslide debris, from the top of the slip, was also collected. At Hinkle, soil profiles were located at each of the gauges and on the high ridge forming the eastern catchment divide. Soil profiles were sampled every 10–50 cm, to a depth (except for the Trask landslide scarp face) of between 30 and 80 cm.

Foliage samples consisted of leaves or needles and thin twigs, while thicker branches provided standing wood samples. Samples of all plants mentioned in Section 2.3.5 (page 41) were collected, with the exception of the true firs, *Pteridium sp.*, *Rhododendron sp.* and *Vaccinium parvifolium*: all relatively minor species. Moss from channel banks and hillslopes was also collected in Watershed 1 and Hinkle. It was assumed that location within Oregon would not have a large effect on vegetation chemistry and so vegetation collection was concentrated at H.J. Andrews. However, four species—*Pseudotsuga menziesii*, *Tsuga heterophylla*, *Alnus rubra* and *Polystichum munitum*—were collected at all watersheds in order to verify this assumption. Charcoal, not evident in the Alptal because of different forest management practices and a lower occurrence of natural wildfire, was common at Hinkle and also occurred elsewhere. Four samples were collected in total, from soil profiles and the forest floor.

Litter and stream-conditioned plant matter were collected at several sites at H.J. Andrews in December 2012. Representative material was gathered from the litter layer using a clean trowel. Stream-conditioned plant matter was collected from channel edges, and consisted of both obviously biogenic material, such as leaves, and organic-rich fines. Thus, these samples inevitably also included some clastic material.

3.2.3 Hydrometric and climatic data

To maximise their usefulness, suspended sediment samples must be accompanied by concurrent discharge and climate data. This allows particular suspended load characteristics, including SSC, organic carbon content, and elemental and stable isotopic composition, to be related to different flow and atmospheric conditions. Ultimately, robust mean export fluxes of total, fossil and non-fossil organic carbon can then be calculated using long-term records.

Monitoring activity at each of the study watersheds has been described in general terms in Chapter 2; this section states how these data are used, and gives more detail regarding collection methods.

3.2.3.1 Alptal

Discharge and water temperature are measured and recorded automatically every 10 minutes via v-notch weirs at the Vogelbach and upper and lower Erlenbach gauges. Every week, stage is also recorded manually and the discharge calculated from it to compare to the automated value. If necessary, a correction is applied to the week's data. In this study, data from the upper Erlenbach station is used because this is where suspended sediment samples were collected. During events in the Erlenbach (that is, when there is bedload transport as determined by the geophones installed in the channel bed immediately above the retention basin), discharge is recorded every minute. Discharge values were assigned to suspended sediment samples as follows: for compound samples, mean discharge during the preceding seven days, assuming that collection occurs at 10am Swiss winter time every Monday (in reality the time varies slightly, but this has minimal effect on the calculated discharge); for instantaneous samples, the value at the exact time of collection if 1-minute data exist, and a value interpolated between the two closest 10-minute values if not.

Measurements of air temperature and precipitation are automatically recorded every 10 minutes at the Erlenbach and Vogelbach climate stations (Figure 2.1, page 20). These parameters are also checked manually once a week.

All hydrometric and climatic data used henceforth in this study were provided directly by WSL via Jens Turowski of the Mountain Hydrology research unit.

3.2.3.2 Oregon

Gauges currently in use at H.J. Andrews are trapezoidal flumes, with v-notch weirs attached from June to October to increase sensitivity during low flow (Creel & Henshaw, 2005). They measure stage height, which is converted to discharge using well-

constrained rating curves. Historical data are freely available to download from the H.J. Andrews website at 15-minute intervals for the small watersheds and 30-minute intervals for Lookout Creek (Johnson & Rothacher, 2012), but they take several years to appear in final form there. Discharge data for the storms sampled in November 2011 were obtained separately. For Lookout Creek, provisional discharge data at 15-minute intervals were obtained from the USGS National Water Information System website (http://waterdata.usgs.gov/nwis/uv?site_no=14161500). For Watershed 1, raw stage data at 5-minute intervals were obtained from Fred Bierlmaier of Oregon State University, and converted to discharge data using rating curve equations provided by Don Henshaw, also of Oregon State University (Henshaw, 2002). Stage data for the period covered by the WS2 compound samples (November 2011 to April 2012) were obtained and converted in the same way. Discharge values were assigned to compound samples by calculating the mean discharge in the period since the time of the last sample, and to instantaneous suspended sediment samples by interpolating between the two closest values where necessary.

Discharge data for the other study watersheds is not readily available, but an instantaneous discharge value for each suspended sediment sample was provided for Hinkle and Trask by Amy Simmons of the Department of Forest Engineering, Resources & Management, College of Forestry, Oregon State University. No discharge data tied to the suspended sediment samples could be obtained for the Alsea.

Extensive climatic data, including air temperature and precipitation, are collected at multiple weather stations across H.J. Andrews, of which two are used in this study (Figure 3.4). The CS2 meteorological station near the site headquarters (elevation ∼480 m) has the longest records, so data from here are used in determining the long-term climate characteristics reported in Section 2.3.3 (page 34). However, data from this and most other stations are not yet available to download for November 2011. Therefore, data from the HI5 station near Blue River Ridge (elevation ∼925 m) is used to construct pluviographs for the events (Figure 6.13, page 163). Although HI5 is not near the gauges of Lookout Creek and Watershed 1, it is within the Lookout catchment and at an elevation comparable to the top of Watershed 1, so is likely to accurately represent the rainfall input to these systems. There may be a small discrepancy in the timing of precipitation at different sites within the forest, but because the events were large regional storms, this is likely to be minor.

3.3 Sample preparation

3.3.1 Homogenisation

Only the suspendable fraction (<2 mm) of soils and sediments was subjected to further analysis, since any larger particles do not contribute to the suspended load under normal circumstances, and could introduce a bias into the source characterisation. In soil science, such particles are referred to as rock fragments and not considered as part of soil (Atkinson, 2005). The <2 mm fraction was isolated through sieving. For well-consolidated soils and sediments, particularly very clay-rich ones from the Erlenbach, initial wet-sieving using a pressurised jet of de-ionised water to push the clays through a 63 μm sieve was necessary to break up the sediment enough to be dry-sieved. Sediments were separated into <63 μm, 63-500 μm, 500-2000 μm and >2000 μm fractions and weighed, and the latter discarded. The remaining fractions were re-combined in their correct proportions to produce bulk <2 mm samples. These were then homogenised by grinding using an agate ball mill grinder, with the pots and balls washed thoroughly between samples.

Bedrock and vegetation samples were analysed in bulk. Bedrock samples were first crushed to <5 mm fragments using a jaw-crusher—plates cleaned thoroughly between samples—then homogenised using the ball mill grinder as before. Vegetation is too fibrous to be effectively homogenised by the ball mill, and for this a blade mill grinder was used instead, courtesy of Steve Boreham and Chris Rolfe at the Physical Geography Laboratories, Department of Geography, University of Cambridge. For standing wood samples, outer bark was first removed with a sharp metal knife and discarded, because its isotopic composition may reflect local influences, and is also more likely to become contaminated. For litter and stream-conditioned plant matter, large clastic particles were removed before homogenisation, but large organic fragments were retained. These were decayed enough that blade mill grinding was unnecessary; for most samples, grinding with a pestle and mortar was sufficient.

Suspended sediment was removed from filters in a variety of ways. Scraping with a metal spatula was adequate for nylon filters with a good amount of sediment, but a higher rate of return was achieved by washing the sediment into a glass dish or beaker using a gentle spray of de-ionised water, evaporating the water in an oven at 80°C, and scraping the sediment out of the beaker with a spatula. This also prevented ripping of the filters and was the preferred method for small samples. However, this method could not be used on glass fibre filters, which disintegrate when sprayed with water: careful scraping was the best that could be done here (see Section 3.4.1.3 for

discussion). Sediment was then homogenised by grinding with an agate pestle and mortar, resulting in the loss of a small amount of material. For very small samples, no homogenisation was necessary because the whole sample had to be analysed in order to obtain a significant signal. Suspended sediment occasionally contained material >2 mm; these particles, mainly large organic material such as spruce or fir needles, were excluded from chemical analysis in order to prevent bias, but their weight was recorded and included in calculation of SSC.

3.3.2 Carbonate removal

As detailed in Chapter 1, the central aims of this project involve determining the composition of organic carbon in various types of sample. Thus, inorganic carbonate must be removed prior to analysis. Although significant amounts of carbonate were unlikely to be present in any sample given the nature of the geology underlying the study catchments described in Chapter 2, it was necessary to ensure that none was present because carbonates have positive $\delta^{13}C$ values that could cause the measured $\delta^{13}C$ to deviate significantly from the true value of the organic component. The method followed here is based on procedures developed by France-Lanord & Derry (1994) and refined by Galy *et al.* (2007a), Hilton *et al.* (2008a), and Sparkes (2012).

If available, between 0.5 and 1 g of each sample, or otherwise the entire sample, was weighed into a glass beaker, mixed with 21.3 ml de-ionised water and stirred with a metal spatula to aid mixing if necessary. Samples were then transferred to a fume cupboard where 2 ml of 11.65N HCl was added to form a 1N acid concentration. Samples were covered with watch glasses and heated to 80°C on a hotplate for 3 hours. The supernatant was then removed using a pipette and replaced with 40 ml de-ionised water. After settling, this was also removed and the samples rinsed twice more. Finally, covered samples were oven-dried at 80°C, scraped out of beakers using a spatula, re-homogenised using a spatula or agate pestle and mortar, and decanted into clean glass vials.

Vegetation samples were not initially subjected to the de-carbonation procedure because they contain no carbonate. Despite this, it was noticed that the de-carbonation process affected the chemical parameters returned by the mass spectrometer for vegetation samples, particularly $\delta^{15}N$ (Figure 3.5). The effect was subsequently reported by Brodie *et al.* (2011) and attributed to isotopic fractionation during the acid reaction. All vegetation samples that had already been run were therefore re-run following the acid treatment. The differences were not large, but enough to be significant (Table 3.4), and further vegetation samples were reacted with acid. In determining sources,

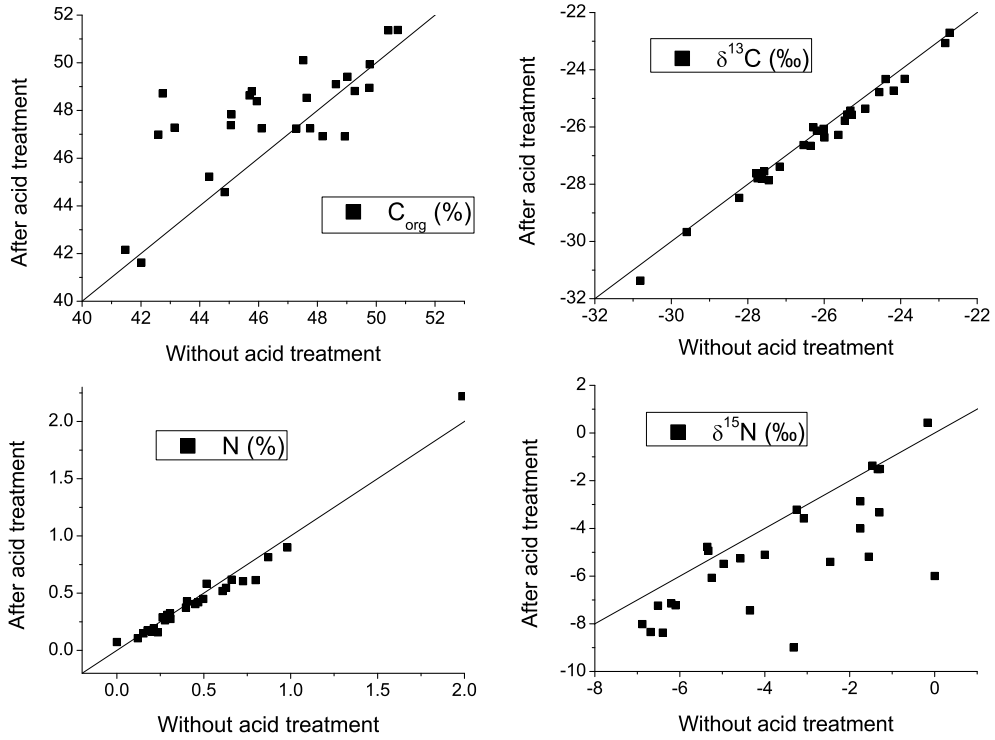

Figure 3.5: Effect of acid treatment to 26 vegetation samples on chemical parameters. Line in each panel is 1:1, for comparison.

	C (%)	**N (%)**	δ^{13}**C (‰)**	δ^{15}**N (‰)**
Mean	47.4	0.461	-26.25	-4.51
Difference	0.20	-1.28	0.02	1.69
Relative difference	-0.03	<0.01	-0.01	-0.55
Standard deviation	1.20	0.04	0.17	1.28

Table 3.4: Effect of acid treatment to vegetation samples on chemical parameters. "Mean" is the mean for each parameter of all vegetation samples from the Erlenbach, including decarbonated and non-decarbonated analyses. Other values are means of the difference, relative difference and standard deviation of the paired decarbonated and non-decarbonated analyses of all vegetation samples collected from the Erlenbach.

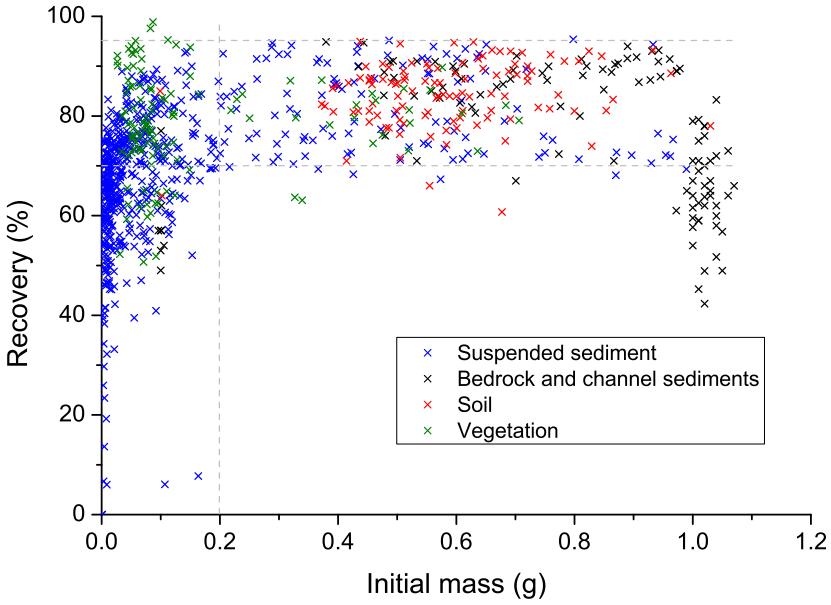

Figure 3.6: Sample recovery from the carbonate removal process plotted against initial sample mass for 925 samples which underwent the procedure during this study.

absolute values matter less than relative differences between carbon pools, and in carrying out the same carbonate removal procedure on all samples, any fractionation effects are universally applied and the results internally consistent. However, comparisons with independent datasets must be made with care and awareness of these effects.

By recording sample weights before and after carbonate removal, the sample loss caused by the process can be investigated (Figure 3.6). The proportion of the original sample recovered after the procedure depends on the initial mass up to about 0.2 g, which suggests that some relatively constant mass of material is always lost through the mechanical transfer of material between containers. Thereafter, the proportion recovered is steady, but covers a broad range: between 70% and 95% for nearly all samples. This and the colour of the acid after the reaction suggests that in addition to the constant mechanical loss there is also loss of a fraction which dissolves or floats in acid and is pipetted out with the waste, an effect also noted by Galy *et al.* (2007a). This fraction is likely to be largely labile carbon, but fulvic acids—which are a stable form of carbon originating from soil humus—may also be mobilised by acidification (Tipping, 2002). However, this is difficult to quantify, and this study follows the assumption of Galy *et al.* (2007a) that their contribution to the dissolution loss is minimal. Although variable, this loss does not vary systematically between sample types. The group of bedrock samples with initial mass of ∼1 g with a lower recovery

percentage are from the Alptal and likely did contain some carbonate, which accounts for their different behaviour.

Although the mechanical transfer loss affects all components equally and so is unlikely to result in any significant bias, the carbonate removal process results in the unavoidable loss of the labile fraction of organic C, and the results subsequently reported relate to the non-labile fraction only. Although this means the calculated fluxes underestimate what leaves the catchments, it is the more recalcitrant fraction that is most likely to be ultimately buried in the ocean, and therefore of interest in this study.

3.4 Analysis

3.4.1 C and N concentrations and stable isotopes

Each processed, powdered sample was measured into a tin capsule and combusted with oxygen using a Costech flash Elemental Analyser (EA). The amount of material required to give suitable C and N peaks depended on the type of material, and corresponded to ∼20 mg for C-containing bedrock, ∼10 mg for suspended sediment, ∼5–6 mg for soil and ∼1–2 mg for vegetation. The EA was coupled through a Conflo IV gas bench for gas separation to a Nier-type mass spectrometer in continuous flow mode: either a Thermo MAT253 (before January 2012) or a Thermo DELTA V Plus. The long-term precision is the same for both instruments (Rolfe, 2012).

Carbon and nitrogen concentrations are reported in weight percent (%) of dry material, and stable isotopic ratios as $\delta^{13}C_{VPDP}$ and $\delta^{15}N_{AIR}$ in parts per thousand(‰) (see Section 1.3.2, page 7). In subsequent chapters, the following terminology is used: C_{org} and N for the concentrations of acid-insoluble organic carbon and nitrogen; C/N and N/C for the ratios of these parameters; and $\delta^{13}C$ and $\delta^{15}N$ for the stable isotope ratios of acid-insoluble organic carbon and nitrogen.

3.4.1.1 External standards and analytical error

Two external standards for $\delta^{13}C$ and $\delta^{15}N$, CAFFEINE and USGS-40, issued by the International Atomic Energy Agency in Vienna, were used (Table 3.5). These were analysed a total of 69 and 70 times respectively, spread over 16 sample runs between April 2010 and January 2013. Figure 3.7 shows the deviation over time of these standards from their published isotopic compositions. Only one point falls well outside the error range (defined as twice the long-term standard deviation, 2σ; Table 3.5): CAFFEINE $\delta^{15}N$ for run 15. USGS-40 and CAFFEINE $\delta^{13}C$ behave normally

		Publ.	n	Mean	2σ	Mean diff.
MAT253						
CAFFEINE	δ^{13}C	-27.5	52	-27.52	0.125	-0.02
CAFFEINE	δ^{15}N	1.0	52	1.07	0.131	0.07
USGS-40	δ^{13}C	-26.2	53	-26.19	0.241	0.02
USGS-40	δ^{15}N	-4.5	53	-4.54	0.140	-0.05
DELTA V Plus						
CAFFEINE	δ^{13}C	-27.5	17	-27.51	0.122	-0.02
CAFFEINE	δ^{15}N	1.0	17	1.08	0.316	0.06
USGS-40	δ^{13}C	-26.2	17	-26.21	0.094	-0.01
USGS-40	δ^{15}N	-4.5	17	-4.51	0.142	-0.01

Table 3.5: Published ("Publ.") and measured ("Mean") values of external standards, the long-term analytical error on them (quantified as twice the standard deviation (2σ) of all analyses associated with this study, "n"), and the mean difference to the published value. All parameters are quoted separately for the two machines used.

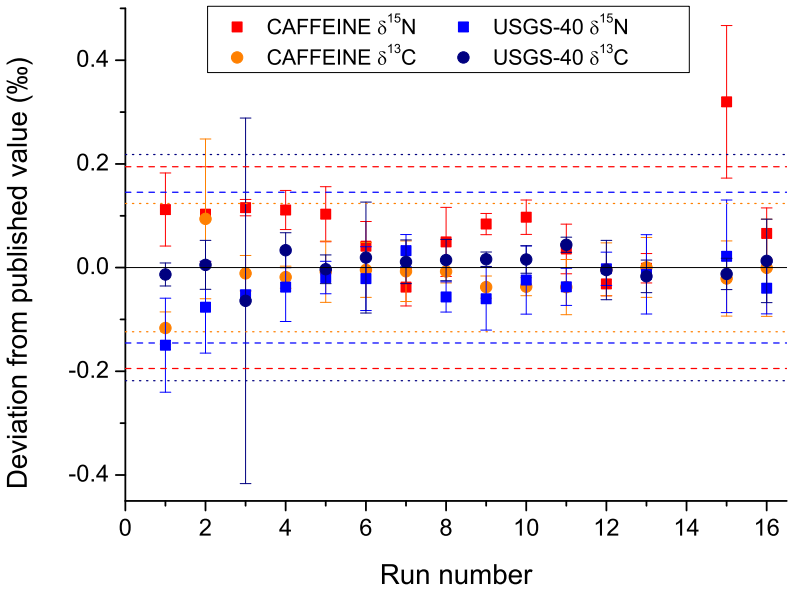

Figure 3.7: Deviation of external standards, CAFFEINE and USGS-40, from published values over time. Each point is the mean value of 3-4 analyses for each run; error bars are twice the standard error on the mean for each run. Lines indicate long-term 2σ range for δ^{15}N (dashed) and δ^{13}C (dotted). DELTA V Plus was used from run 12.

in this run, so there is no systematic error present. The cause remains unknown and therefore cannot be corrected for.

In a further test for long-term machine drift, 10 homogenised, powdered samples were analysed a second time one year after the first analysis. Differences were negligible: the average relative difference was 0.05% for C and 0.07% for N, and average standard deviation (σ) was 0.05‰ for δ^{13}C, and 0.3‰ for δ^{15}N.

Sample heterogeneity was tested by multiple analyses of 4–5 aliquots of five homogenised samples of varying material. The average relative difference was $\ll$0.001% for C and N, and average standard deviation (σ) was 0.05‰ for δ^{13}C, and 0.3‰ for δ^{15}N, suggesting that the samples have been well-homogenised and the aliquots measured give chemical parameters representative of the true values for each sample.

In most cases, error bars denoting long-term precision—derived from 2σ for δ^{13}C, δ^{15}N, C/N and N/C, and twice the relative difference for C_{org} and N—are smaller than the point size in the subsequent figures, and in all cases the overall picture and conclusions are unaffected. Analytical error bars are therefore not added to figures where individual samples are plotted.

3.4.1.2 Internal blank characterisation and correction

An internal blank correction was applied to all carbon and nitrogen elemental concentrations and isotopic ratios following the methods of Hilton *et al.* (2010, 2012b). Standards CAFFEINE and USGS-40 were each mixed with torched sand to dilutions ranging from one in 2 to one in 1000 and analysed as before. The isotopic ratio returned was found to be dependent on the peak amplitude (Figure 3.8, plotted as 1/amplitude to give straight lines). Because there is a good relationship between amplitude and peak area, it is more precise to use the amplitude because this does not require very accurate measurement at low amplitudes in the peak tails (Galy, 2013). The intersection of regression lines for CAFFEINE and USGS-40 gives both the amplitude ($1/x$-value) and isotopic composition (y-value) of the blank. Points lying well outside 95% confidence bands after the first regression (a total of six) were not included in the final regression. Following this procedure revealed that the internal blank had a C amplitude of 80.9 mV and δ^{13}C of -25.3‰, and an N amplitude of 19.9 mV and δ^{15}N of 0.09‰.

For each sample, the conversion factor from amplitude to amount of C or N in weight percent was determined, and multiplied by the corrected amplitude (=measured amplitude−blank amplitude) to obtain the corrected amount. The isotopic

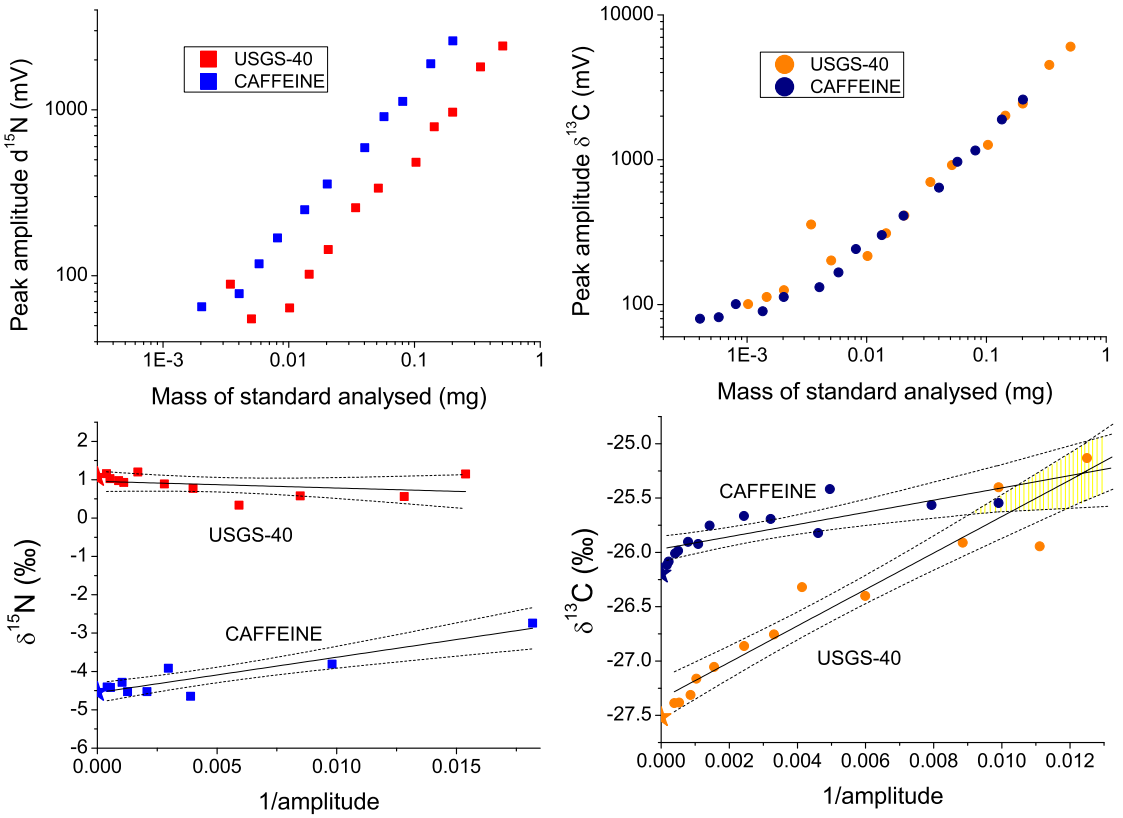

Figure 3.8: Internal blank characterisation for C and N concentrations and isotopic ratios using USGS-40 and CAFFEINE. Top panels show mass of standard versus amplitude. Bottom panels show isotope ratios of standard aliquots diluted with torched sand plotted against 1/peak amplitude in mV. Solid lines are regression lines through each group of standard dilutions and dashed lines are 95% confidence bands. Stars indicate long-term mean values of standards (not included in regression). The regression lines represent mixing lines between the true isotopic ratios of the standards (Table 3.5) and the internal blank. The blank is the point (area) where the lines (confidence bands) for the two standards intersect. It is shown as a yellow-striped area for δ^{13}C, but is well off the axes for δ^{15}N.

ratio was then corrected using the following equation:

$$\delta_{corr} = \frac{\delta_{meas}.A_{meas} - \delta_{blk}.A_{blk}}{A_{corr}} \tag{3.1}$$

where δ is δ^{13}C or δ^{15}N, A is the peak amplitude in mV, *corr.* is the corrected value, *meas.* is the measured value and *blk.* is the blank value.

3.4.1.3 Envelopes and glass fibre filters

Concerns regarding the accurate analysis of compound samples from Oregon were allayed by laboratory tests. Firstly, the samples had been stored for several years in paper envelopes, a potential source of contamination. Although the filters had been

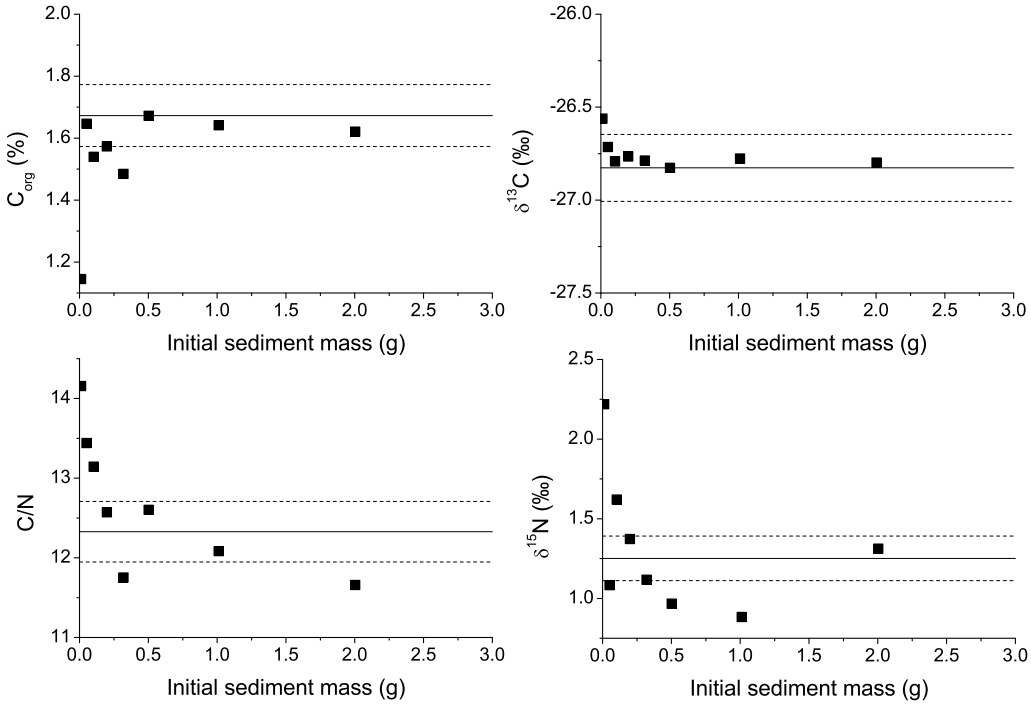

Figure 3.9: Effect of initial sediment mass on chemical parameters measured after samples were mixed with de-ionised water, filtered through glass fibre filters, removed from the filters and de-carbonated. Values have been blank-corrected. The sediment used was VO-CF-6; lines show values obtained from an aliquot of VO-CF-6 filtered through a nylon filter, with dashed lines showing long-term errors (2σ for isotopes and C/N; twice the average relative difference for C_{org}). These do not necessarily represent the values that the points should approach because the suspensions had to be made up before homogenisation by grinding; however, points do approach the lines, indicating that there is a real sample size effect beyond natural heterogeneity.

folded to enclose and protect most of the sediment, some from the larger samples had fallen into the bottom of the envelope. A 20 mg-piece of envelope was analysed, and contained 0.21% N with δ^{15}N of 0.06, while the carbon peak saturated the collector. To test whether this did influence samples stored in them, suspensions made up with various amounts of a bedload sediment sample from the Vogelbach, VO-CF-6, in de-ionised water, were filtered through glass fibre filters and stored in equivalent envelopes for two months, then analysed. Results were identical to un-stored VO-CF-6, indicating that there is no contamination from the envelope over this time period. Longer storage is impractical to simulate, but it is assumed that any envelope contamination will be negligible at most.

Secondly, the glass fibre filters themselves represent a possible source of contamination because of their tendency to disintegrate and become difficult to separate from sediment when scraped during the removal process. Pieces of three filters were

analysed to characterise their chemistry, all returning non-measurable N but containing 0.07%–0.14% C_{org} with $\delta^{13}C$ of -30.8‰to -34.0‰. Although the $\delta^{13}C$ is lighter than that of most Oregon suspended sediment samples, it is not significantly so, and the low concentrations mean that it is unlikely to have a noticeable effect on sample chemistry. Indeed, results from several aliquots of VO-CF-6 filtered through glass fibre filters were well within error of one filtered through a nylon filter in all chemical parameters, with the $\delta^{13}C$ heavier if anything, suggesting that variability is due to natural sediment heterogeneity rather than contamination.

Finally, there was a concern that bias might arise from a particular component of the suspended sediment getting preferentially stuck in the filter pores and thus being excluded from analysis. A dependence on sediment mass was observed for all chemical parameters, but they only significantly deviated from the values of the VO-CF-6 aliquot filtered through a nylon filter for the smallest sample with initial mass ∼0.01 g (Figure 3.9). This is well below the lower limit of starting mass that could be analysed after it had been through the carbonate removal process, and most samples were at least an order of magnitude larger.

3.4.2 Radiocarbon analysis

14 samples from the Erlenbach were graphitised at the NERC Radiocarbon Laboratory (RCL) in East Kilbride, Scotland, and ^{14}C measurements on these obtained at the Scottish Universities Environmental Research Centre (SUERC) accelerator mass spectrometry (AMS) laboratory, also in East Kilbride. These comprised six samples of suspended sediment at different points on the rising limb of a storm hydrograph, including the largest discharge sampled, four surface soil and four old wood samples (Table 4.2, page 81). The analysis was carried out under NERC Radiocarbon Facility allocation number 1573.0911.

All samples had previously been processed as described in earlier sections, and had undergone carbonate removal. At the RCL, conversion to graphite followed the method described in Wand *et al.* (1984). Powdered samples were weighed into quartz glass tubes, placed in a vacuum overnight and combusted at 900°C in a furnace. CO_2 was released and isolated by breaking the tube on a vacuum rig, condensing out water and other components using dry ice and methylated spirit, and condensing the CO_2 using liquid nitrogen. The CO_2 thus obtained for each sample was split into three aliquots: one each for ^{14}C analysis, $\delta^{13}C$ analysis, and archive. The first was converted to graphite via heating on another vacuum rig and passage through first copper, forming CO, and then iron, forming C. The resulting graphite was made

into a pellet and passed to the AMS laboratory, where analysis followed the methods described in Litherland (1984). One suspended sediment sample at low discharge, 12.7 1748, was too small for routine analysis and was run at low current on the AMS to obtain a result.

Reported results comprise the proportion of ^{14}C atoms in each sample compared to that present in the atmosphere in the year 1950 (F_{mod}), $\Delta^{14}C$ in ‰ (equal to (F_{mod} -1) x 1000), and conventional radiocarbon age. Standards were analysed with the samples and used to calculate 1σ uncertainties. The standard IAEA-C5, subjected to the same carbonate removal procedure as the samples, returned a radiocarbon age within 1σ of the consensus value, showing that no discernible bias is introduced to ^{14}C measurement by the acid treatment.

3.4.3 Qualitative analytical methods

In addition to the quantitative geochemical methods described above, several other techniques were used on a subset of samples. Due to constraints on time and resources, these were not developed to their full potential in this study; nevertheless, they provide additional qualitative information that is useful in refining the inferences made from the geochemical dataset. These techniques are described briefly below.

3.4.3.1 Lignin biomarker analysis

Eight soil and sediment samples and five plant samples from the Erlenbach underwent lignin biomarker analysis using microwave-assisted alkaline cupric oxide (CuO) oxidation and gas chromatography mass spectrometry under the supervision of Chris Vane at the British Geological Survey (BGS). Samples had been previously dried but not homogenised or decarbonated. Details of the method are given in (e.g.) Goñi & Montgomery (2000); Hedges & Ertel (1982); Kögel & Bochter (1985). Briefly, complete samples were microwaved at 150°C with CuO powder, ferrous ammonium sulphate and sodium hydroxide solution for 60 minutes. After cooling, they were centrifuged with a pyridine-based recovery standard and the supernatant acidified using concentrated HCl. Liquid-liquid extraction was performed by shaking with ethyl acetate and allowing to separate. The organic layer was pipetted off and moisture removed using anhydrous sodium sulphate. The solvent was removed and the residue spiked with an internal standard and made up with pyridine before derivitisation. Samples were analysed using a Varian 3800 gas chromatograph coupled to a Varian 1200L triple quadrupole mass spectrometer. An oak wood standard and procedural blanks were used throughout.

A number of organic compounds are identified by this method, and the most useful derived parameters of these are described here. Lambda (Λ) is the sum of vanillyl, syringyl and cinnamyl compounds, providing a measure of lignin content normalised to total organic carbon (e.g. Hedges & Mann, 1979b; Vane *et al.* , 2001a). The ratio of syringyl to vanillyl compounds (S/V) and cinnamyl to vanillyl compounds (C/V) are used to distinguish lignin from angiosperm and gymnosperm sources and woody and non-woody sources respectively (e.g. Hedges & Mann, 1979a; Vane *et al.* , 2001b). The ratio of vanillic acid to vanillic aldehyde ((Ad/Al)v) is an indicator of microbial decay, particularly oxidative fungal decay (e.g. Vane *et al.* , 2001b).

3.4.3.2 Raman spectroscopy

Raman spectra for four Alptal bedrock samples, two each from the Erlenbach and the Vogelbach, were obtained using a Renishaw spectrometer at the Department of Materials Science and Metallurgy, University of Cambridge. Raman spectroscopy is a tool for analysing the structure of individual particles of carbonaceous material, which provides information about the maximum temperature to which the material has been exposed and thus about its geological evolution (e.g. Beyssac *et al.* , 2003). The theory behind the technique and its application to geological and environmental samples is thoroughly described by Sparkes (2012) and references therein.

Powdered but non-de-carbonated samples were used. Around 0.2 g of each sample was pressed between glass slides and observed through a 50x magnification lens to locate each graphite particle (around 5–10 for each sample) before analysis. A 514 nm Ar-ion laser beam was then fired at the sample and analysed for a change in photon frequency after interacting with it, with changes reported in wavenumber units (cm^{-1}). Spectra from disordered carbon show multiple broad peaks, especially at 1350 cm^{-1} and 1600 cm^{-1}, while crystalline graphite shows a single sharp peak at 1580 cm^{-1} (Sparkes, 2012). Peak height reflects Raman intensity and is measured in relative units. Curves are then fitted to the spectra and background noise removed. Cross-plots of the sum of peak widths versus estimated temperature are used to compare samples to space occupied by typical graphite, very disordered and somewhat disordered carbon. For each sample, one of two methods, R2 or RA2, is used for estimating temperature, depending on the degree of ordering. All data collection and processing methods are described in detail by Sparkes (2012).

Chapter 4

Organic carbon export in the Erlenbach from instantaneous summer storm sampling

4.1 Introduction

The Erlenbach, in Switzerland, is an extensively studied and instrumented headwater catchment typical of much terrain in the European Prealps (Section 2.2, page 19). A series of instantaneous suspended sediment samples collected over a range of discharge from Q/Q_{mean}=0.4 to Q/Q_{mean}=59, together with samples of organic carbon stores through the catchment, is used to investigate the sources and pathways of riverine POC and the ways in which these vary under different hydrologic conditions. Organic carbon and nitrogen concentrations and stable isotope ratios are the principal methods used, but radiocarbon, biomarker and Raman spectroscopic analysis are used to add further details and confirm inferences. Two initial sections, 4.2 and 4.3, describe the chemistry and nature of organic matter in source materials and suspended sediment respectively. Section 4.4 uses these results to discuss i) the mixing relationships shown by riverine POC, ii) the determination of end members, iii) modelling the fraction of non-fossil carbon in the suspended sediment samples, and iv) organic carbon routing in the catchment. Finally, the long-term export of suspended sediment and total, fossil and non-fossil POC is considered in Section 4.5, including the calculation of mean fluxes for the period 1983–2011 inclusive. A summary of the main conclusions is included at the end of the chapter.

4.2 Organic carbon in source materials

Mean composition data for riverine suspended sediment, hillslope runoff input and major catchment carbon stores are summarised in Table 4.1. Radiocarbon data, comprising F_{mod} (the fraction of modern carbon in the sample), $\Delta^{14}C$ and conventional radiocarbon age, can be found separately in Table 4.2. When not stipulated, uncertainties are ± twice the standard error on the mean ($\pm 2\bar{\sigma}$); σ=standard deviation. Visual representation of the composition of catchment organic carbon pools and how they relate to each other and suspended sediment, are shown at the end of this section in Figure 4.7. In the following sub-sections, each major carbon pool will be reviewed in turn.

4.2.1 Bedrock

Bedrock samples from the Erlenbach had organic carbon concentration (C_{org}) values ranging from 0.16%–1.15%, with a mean of 0.54%±0.11 (n=22). This is within the range of C_{org} measured in other sedimentary rocks. In general, bedrock samples had low C/N (7.81±1.7) and heavy C ($\delta^{13}C$=-25.71‰±0.36) and N ($\delta^{15}N$=3.34‰±0.26) compared to other carbon stores in the catchment, but they were also highly variable (C/N σ=3.98; $\delta^{13}C$ σ=0.84‰).

Because of this variability, definition of a truly average catchment bedrock composition would require a weighting according to outcrop area. However, this is not feasible because sample composition does not appear to follow any geographic or lithologic patterns, according to either published geological maps or the appearance of the samples. Even if this could be achieved, it would not necessarily represent what ends up in the suspended load: the stream is just as unlikely as a geologist to sample the bedrock representatively, although it may be biased towards softer lithologies, while field sampling is biased towards the more resistant layers that form outcrops. The mean composition given above, then, is as reasonable an approximation as any of the local store of petrogenic carbon.

Raman spectra and cross-plot (Figure 4.1) show that the Erlenbach bedrock samples contain a range of organic carbon particles from very disordered (multiple broad peaks) to graphite (single sharp peak at 1580 cm^{-1}). This reflects the input of fresh POC at the time of flysch formation and admixture of POC that had been metamorphosed during previous orogenic episodes.

No ^{14}C measurements were made on bedrock, but its Eocene age means it can be assumed to have an F_{mod} of ∼0.

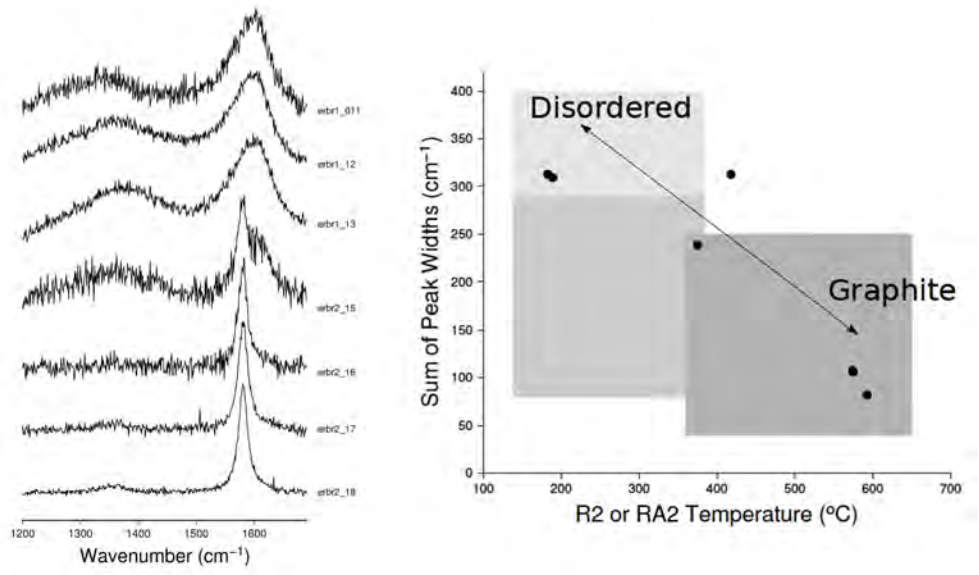

Figure 4.1: Raman spectra from carbon in Erlenbach bedrock samples (left) and cross-plot showing peak width versus temperature (right). The spectra are stacked from least ordered carbon at the top to most ordered at the bottom; peak height is relative and reflects Raman intensity. In the cross-plot, grey boxes reflect the space typically occupied by very disordered (light grey), somewhat disordered (medium grey) and ordered (dark grey) organic carbon. "Temperature" is an estimate of the maximum temperature that a particular carbon particle has been exposed to; R2 and RA2 refer to methods of estimating this parameter. For details, see Sparkes (2012).

4.2.2 Bedload

Bedload is used as a broad term for any material collected from the channel bed, including relatively coarse-grained sediment from the stream itself and finer material deposited within the wider channel after floods. Despite this wide definition, there is little chemical variation: all samples had relatively low C_{org} with a mean of 0.87%±0.21 (n=11). With mean C/N of 9.78±0.9, mean δ^{13}C of -25.84‰±0.10 and mean δ^{15}N of 2.13‰±0.23, they show a similar composition to bedrock. Unlike other source sediments, bedload samples were not dominated by a fine fraction, but had equal proportions of coarse, medium and fine material (Figure 4.2(b)). Also unlike other source sediments, the fine fraction (<63 μm) contained slightly more organic carbon than the bulk (<2 mm) sediment (Table 4.3). In terms of composition, the fine fraction had higher C/N and heavier N than the bulk values, but there was no difference in δ^{13}C (Figure 4.2(a)).

	n	C_{org} (%)		C/N		$\delta^{13}C$ (‰)		$\delta^{15}N$ (‰)	
		Mean	σ	**Mean**	σ	**Mean**	σ	**Mean**	σ
Bedrock	22	0.54±0.11	0.26	7.81±1.7	3.98	-25.71±0.36	0.84	3.34±0.26	0.60
Bedload	11	0.87±0.21	0.36	9.78±0.9	1.57	-25.84±0.10	0.17	2.13±0.23	0.38
Channel banks	8	0.87±0.22	0.32	8.12±1.1	1.58	-25.89±0.40	0.57	2.91±0.29	0.40
Landslide profile	22	0.64±0.06	0.15	7.38±0.4	0.87	-26.03±0.12	0.28	2.67±0.30	0.71
Deep soil	10	2.15±1.2	1.85	11.8±2.3	3.64	-25.98±0.34	0.54	3.56±1.99	3.14
Surface soil	17	16.5±6.3	12.9	17.9±2.2	4.45	-26.84±0.48	0.98	-1.33±0.77	1.59
Foliage	8	46.9±2.0	2.88	55.5±17	24.2	-28.30±1.13	1.60	-5.87±1.67	2.36
Standing wood	5	47.5±0.6	0.71	185±83	92.3	-25.98±1.57	1.75	-7.44±3.26	3.64
Woody debris	12	49.1±1.8	3.18	173±98	170	-25.25±0.69	1.19	-3.99±1.29	2.24
Non-fossil	-	*2.75±4.8*	-	*15.8±6.8*	-	*-27.15±0.53*	-	*0.61±1.40*	-
Forest runoff SS	38	7.99±0.9	2.77	12.5±0.7	2.28	-26.40±0.08	0.23	2.33±0.30	0.93
Meadow runoff SS	10	17.6±1.7	2.67	14.7±1.8	2.91	-26.06±0.50	0.79	3.30±1.04	1.64
Riverine SS	122	1.52±0.06	0.32	10.6±0.2	1.34	-26.58±0.08	0.45	1.78±0.16	0.87
Rising limb	*72*	*1.52±0.07*	*0.29*	*10.7±0.3*	*1.35*	*-26.56±0.08*	*0.32*	*1.77±0.13*	*0.56*
Falling limb	*50*	*1.54±0.09*	*0.33*	*10.5±0.4*	*1.29*	*-26.61±0.15*	*0.54*	*1.80±0.31*	*1.09*
Raining	*85*	*1.53±0.06*	*0.29*	*10.7±0.3*	*1.32*	*-26.60±0.07*	*0.34*	*1.76±0.12*	*0.53*
Dry	*37*	*1.36±0.12*	*0.37*	*9.19±0.4*	*1.07*	*-26.20±0.15*	*0.47*	*2.23±0.38*	*1.15*

Table 4.1: Organic carbon concentration (C_{org}), organic carbon to nitrogen ratio (C/N), organic carbon isotopic composition ($\delta^{13}C$) and nitrogen isotopic composition ($\delta^{15}N$) of major carbon stores within the Erlenbach, and hillslope runoff and riverine suspended sediment. Surface soil samples were collected from the top ∼10 cm (without overlying vegetation); deep soil samples were collected from below 10 cm in two vertical profiles. *Non-fossil* is the hypothetical non-fossil end member modelled in Section 4.4.1. SS=suspended sediment, subdivided into samples collected during i) rising and falling limbs and ii) active rainfall and dry periods (subsets shown in italics). Means for riverine and runoff suspended sediment are weighted by SSC (see Section 4.3).

Sample type		**Sample ID**	**Publication code**	$\mathbf{C}_{org}$	$\mathbf{F}_{mod}$ **(fraction of modern C)**	Δ^{14}**C**	**Conventional radiocarbon age (years BP)**
	Q (l s^{-1})						
Suspended sediment	77	12.7 1748	SUERC-40494	2.2	0.68±0.004	-317.9±3.5	3073±41
	394	12.7 1719	SUERC-39226	1.2	0.67±0.003	-328.0±3.2	3193±38
	517	29.7 1768	SUERC-39232	1.3	0.47±0.002	-530.5±2.3	6074±39
	1170	12.7 1711	SUERC-39229	2.2	0.74±0.004	-256.5±3.5	2381±38
	2060	12.7 1707	SUERC-39230	1.9	0.69±0.003	-314.4±3.2	3033±38
	2290	12.7 1729	SUERC-39231	1.8	0.67±0.003	-333.8±3.2	3262±38
Surface soil		ER-ST-1-L-0	SUERC-39216	1.2	0.53±0.003	-471.7±2.6	5123±39
		ER-ST-2-L-15	SUERC-39219	6.0	1.00±0.005	-3.5±4.7	Modern
		ER-ST-1-R-350	SUERC-39220	25	1.06±0.005	64.8±5.0	Modern
		ER-ST-1-R-20	SUERC-39221	11	1.05±0.005	53.9±5.0	Modern
Wood entrained in bedload		ER-V-19	SUERC-39222	50	0.81±0.004	-186.5±3.8	1658±37
		ER-V-11	SUERC-39223	50	1.00±0.005	-0.1±4.5	Modern
Wood entrained in landslides		ER-V-17	SUERC-39224	52	0.87±0.004	-132.1±4.1	1138±38
		ER-V-20	SUERC-39225	50	0.61±0.003	-392.9±2.7	4009±36

Table 4.2: Results of radiocarbon analysis on selected samples. Errors are $\pm 1\sigma$. The reference date for F_{mod} is 1950; therefore F_{mod} can be >1 in plants and soils due to incorporation of ^{14}C from nuclear weapons testing during the second half of the twentieth century.

	Fraction (X)	Average difference (X-bulk) in: C (%)	C/N	δ^{13}C (‰)	δ^{15}N (‰)
Bedload	Fine	0.14±0.14	-2.22±0.77	0.02±0.12	0.51±0.48
Landslide	Fine	-0.09±0.03	-2.02±0.30	0.11±0.08	0.20±0.44
Deep soil	Fine	-0.56±0.50	-2.16±0.96	0.28±0.17	0.85±0.44
Surface soil	Fine	-5.76±2.02	-5.08±2.26	0.46±0.19	0.92±0.52
	Medium	1.99±1.98	0.84±1.67	-0.04±0.16	0.03±0.65
	Coarse	4.42±1.72	4.66±2.14	-0.17±0.12	-0.60±0.39

Table 4.3: Compositional differences between grain size fractions in some Erlenbach source sediments. Differences shown are parameters measured in bulk sediment subtracted from equivalents measured in the stated fraction (X). Fractions are defined as follows: bulk, <2000 μm; fine, <63 μm; medium, 63–500 μm; coarse, 500–2000 μm. Analysis was not carried out on different size fractions for all samples collected; the above data derive from 8 bedload, 9 landslide, 6 deep soil and 15 surface soil samples.

4.2.3 Channel banks

Material directly adjacent to the stream is a likely source of sediment to the suspended load. In many places, channel banks are midway between landslide complexes and stable slopes in appearance, and samples from such banks form the bulk of this group. A light-brown, low-viscosity mud running over the clay banks and into the stream during rain was also sampled, although its chemistry did not differ from the rest of the group. As a whole, these channel bank samples were very similar to bedrock and bedload in both C_{org} content and composition, with mean values of 0.87%±0.22 (n=8) (C_{org}), 8.12±1.1 (C/N), -25.89‰±0.40 (δ^{13}C) and 2.91‰±0.29 (δ^{15}N).

The results from biomarker analysis of selected Erlenbach samples are shown in Figure 4.3. Channel bank samples—ER-CS-4 from the lower catchment and ER-CS-6 and ER-CS-7 from the upper reaches—had low total concentrations of lignin (Λ values of 0.09 mg to 0.15 mg per 100 mg of organic carbon). Low C/V ratios indicate that the organic matter present was derived from wood rather than needles, leaves and grasses. In two samples with low S/V ratios, this was from gymnosperm species such as *Picea abies* and *Abies alba*, while in the third, ER-CS-4, with higher S/V, the wood was from angiosperms or a mixture. ER-CS-4 also showed comparable (Ad/Al)v to fresh vegetation, indicating minimal fungal decay. The other two samples had (Ad/Al)v values greater than 0.6, consistent with a moderate degree of degradation (e.g. Hastings *et al.* , 2012).

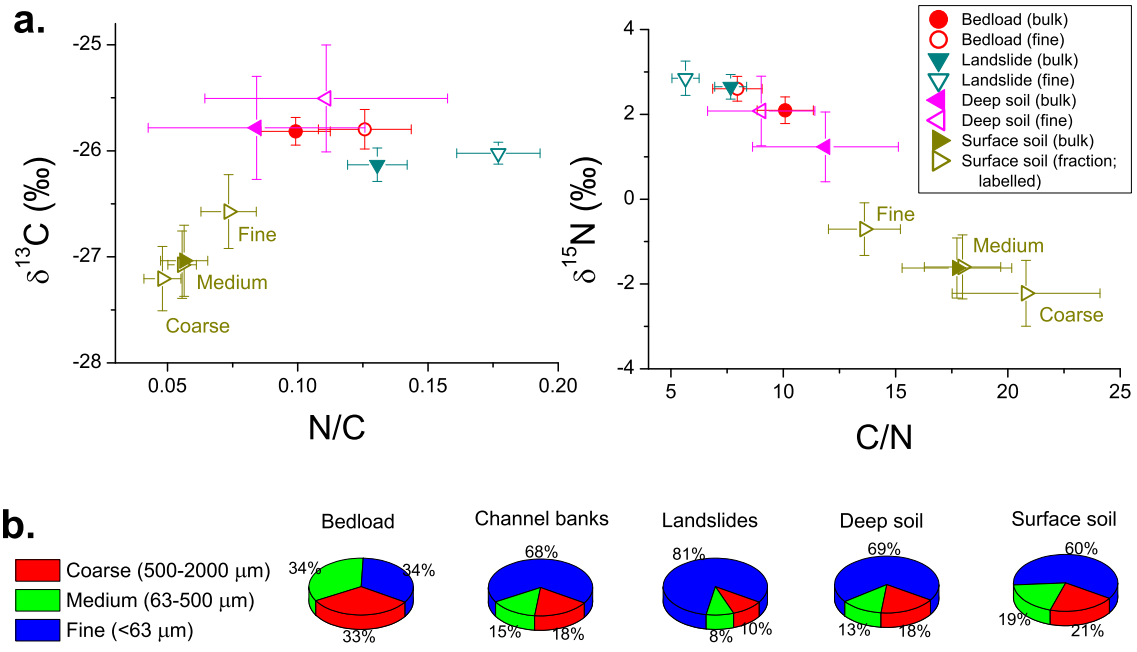

Figure 4.2: (**a**) Chemistry and (**b**) distribution of grain size fractions in Erlenbach source sediments. Top left shows nitrogen to organic ratio (N/C) versus organic carbon isotopic composition (δ^{13}C); top right shows organic carbon to nitrogen ratio (C/N) versus nitrogen isotopic composition (δ^{15}N). Fractions are defined as follows: bulk, <2000 μm; fine, <63 μm; medium, 63–500 μm; coarse, 500–2000 μm.

4.2.4 Landslide complexes and soil profiles

Landslides varied significantly, forming a continuum from active and bare to dormant with vegetated soil developed on the surface. More than any other source sediment, landslide samples were dominated by fine-grained material, which made up 81% by weight (Figure 4.2). This explains why the fine fraction differed little in C_{org}, δ^{13}C and δ^{15}N from bulk landslide material, although it did have lower C/N.

Profiles through two relatively fresh landslides, both within 10 m of the main channel, were sampled (Figure 4.4). Samples from both landslides had a mean C_{org} of 0.64%±0.06 (n=22). Their composition was within error of bedrock, with similarly low C/N (7.38±0.4) and heavy C (δ^{13}C=-26.03‰±0.12) and N (δ^{15}N=2.67‰±0.30). Figure 4.5 shows that these landslide complexes had very homogeneous compositions throughout their depth, with no systematic variations in chemistry.

In contrast, the profiles through deep stable soils (Figure 4.5) showed a decrease in C_{org} and C/N and increase in δ^{15}N at 40–60 cm depth to levels comparable to the landslides, although there are no clear patterns in δ^{13}C. They document a transition from surface soil-like upper horizons to more fossil-like layers at depth. This matches

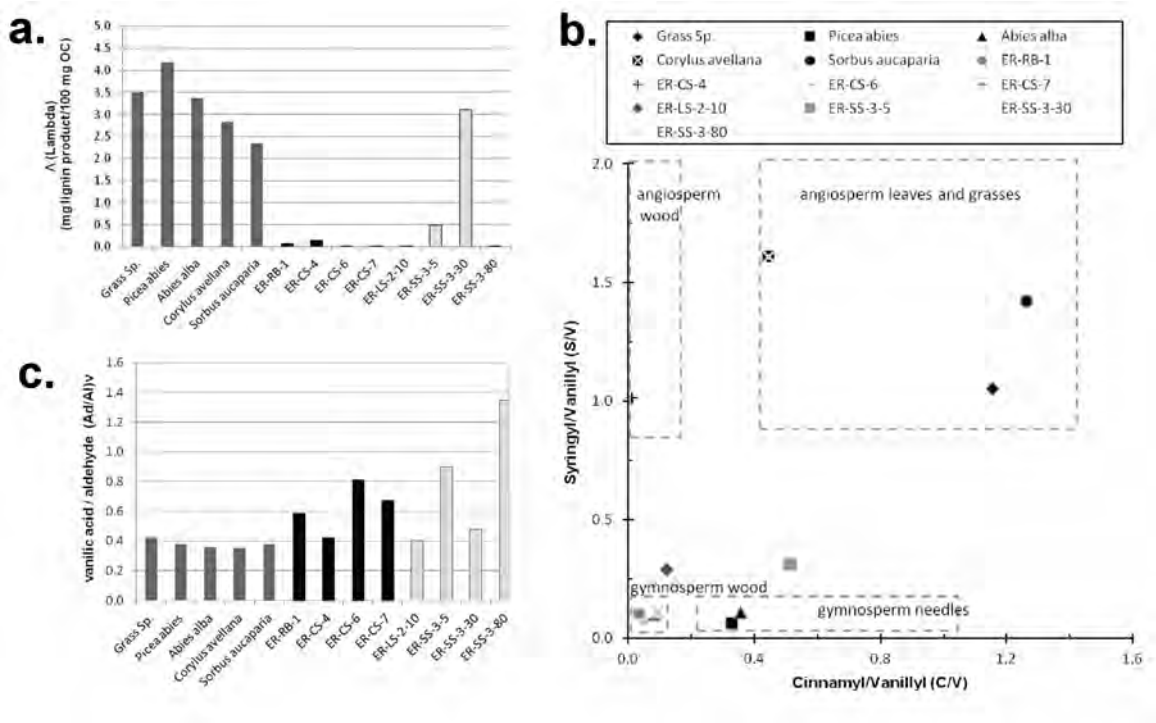

Figure 4.3: Biomarker analysis of selected Erlenbach samples (all figures from Vane, 2012a). ER-RB-1 is a sample from the retention basin, ER-CS-4, ER-CS-6 and ER-CS-7 are channel bank samples, ER-LS-2-10 is a landslide sample from 10 cm depth, and ER-SS-3-5, ER-SS-3-30 and ER-SS-3-80 are deep soils taken from the same profile at 5 cm, 30 cm and 80 cm respectively. (**a**) Lignin concentration. Λ is the sum of syringyl and vanillyl and cinnamyl phenols normalised to 100 mg of organic carbon. (**b**) Plot of cinnamyl/vanillyl versus syringyl/vanillyl phenol ratios. Ranges of major vascular plant groups, shown by dashed boxes, are from Goñi & Montgomery (2000); Hedges & Mann (1979a); Hedges *et al.* (1985); Vane *et al.* (2001a). (**c**) Ratio of vanillic acid to vallinin ((Ad/Al)v).

the vertical progression in their appearance from dark, organic-rich soils to pale gley (Figure 4.4). The same patterns in C_{org}, C/N and δ^{15}N are reported by Mariotti *et al.* (1980) in a French soil sequence derived also from flysch. Excluding the uppermost profile samples, which are considered as surface soils, C_{org} in deep soil ranged from around 4% in the top half to 0.5% at the bottom, with a mean of 2.15%±1.2 (n=10). They were isotopically similar to bedrock and landslides (δ^{13}C: -25.98‰±0.34; δ^{15}N: 3.56‰±1.99) but had considerably higher C/N (11.8±2.3).

The fine fraction of deep soil had lower C_{org} than bulk sediment (Table 4.3), as well as lower C/N and less negative δ^{13}C and δ^{15}N (Figure 4.2). The variability in composition with depth was independent of grain size. The grain size distribution of deep soils was very similar to that of channel banks, with 69% falling in the fine fraction, 13% in the medium and 18% in the coarse (Figure 4.2(b)).

Only one landslide sample underwent biomarker analysis (Figure 4.3). It had a

Figure 4.4: Photographs of Erlenbach landslide and stable slope profiles. Depths shown are ∼50–70 cm except (**c**) which is 160 cm; trowel is 30 cm long. (**a**) ER-LS-1: Active, unvegetated landslide complex showing vertical homogeneity. (**b**) An older, vegetated landslide (not analysed) still has no internal structure. (**c**) ER-SS-2 and (**d**) a representative soil profile (ER-SS-3, analysed for biomarkers only): Stable slopes, with soil horizons marked, showing colour changes reflecting decreasing C_{org} with depth.

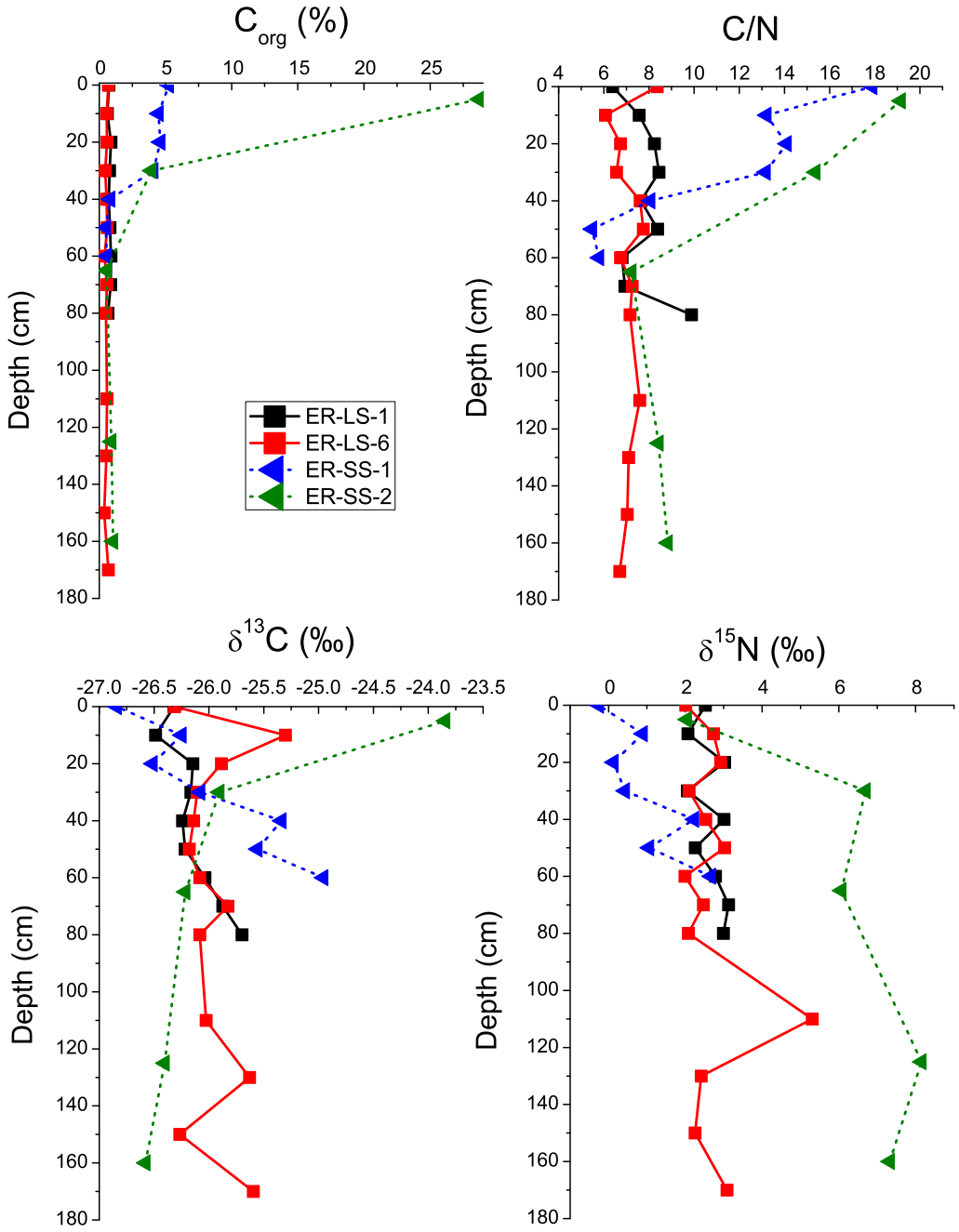

Figure 4.5: Chemical profiles through Erlenbach landslides (solid lines) and stable slopes (dashed lines), showing concentration of organic carbon (C_{org}), organic carbon to nitrogen ratio (C/N), carbon isotopic composition ($\delta^{13}C$) and nitrogen isotopic composition ($\delta^{15}N$).

similarly low Λ value to the channel bank samples, and a comparable (Ad/Al)v value to ER-CS-4, only slightly higher than fresh plant material. Its S/V and C/V ratios indicate lignin from both gymnosperm and angiosperm sources.

Three soil samples, one each from the F, O and B horizons of ER-SS-3 (Figure 4.4) underwent biomarker analysis, with variable results (Figure 4.3). Λ was 0.5 mg in the uppermost F sample, 3.1 mg in the middle O sample (comparable lignin concentration to the values returned by the plant samples), and 0.09 mg in the bottom B sample. The O sample showed least microbial alteration (lowest (Ad/Al)v), with F somewhat higher and B showing the greatest decay of any sample, with a (Ad/Al)v value of nearly 1.4. The three were also variable in their S/V and C/V ratios, with the deepest sample showing evidence of only gymnosperm wood, while the top sample contained a mixture of angiosperm and gymnosperm non-woody material, and the middle sample, though dominated by gymnosperm wood, showed influence from all four components.

4.2.5 Surface soil

Surface soil (top ∼10 cm) showed highly variable C_{org}, with a range of 1.2% to 45% and σ of 12.9%, reflecting the wide variety of soil types and ecological settings within the catchment. The mean C_{org} was 16.5%±6.3 (n=17.) In contrast, organic carbon composition in these samples was much more uniform, with relatively small uncertainties on the mean values. Surface soil had a relatively high mean C/N of 17.9±2.2 and light C (δ^{13}C=-26.76‰±0.48) and N (δ^{15}N=-1.31‰±0.76).

Surface soils were slightly less dominated by fines than many of the other source sediments, with 60%, 19% and 21% of material classed as fine, medium and coarse respectively (Figure 4.2(b)). There is a clear compositional progression with grain size (Figure 4.2): C/N decreases and δ^{13}C and δ^{15}N become heavier as grain size decreases. The medium fraction had an identical composition to the bulk value. C_{org} also decreased with grain size, the largest drop coming between the medium and fine fractions (Table 4.3).

The ^{14}C results from four surface soils (Table 4.2) showed that they are essentially modern; the one soil F_{mod} value of less than 1 is explained by its close association with a landslide, lack of overhead forest canopy and a C_{org} content many times lower than the other surface soils analysed for ^{14}C.

4.2.6 Vegetation

Three classes of vegetation were analysed: foliage, standing wood and woody debris; see Section 3.2.2 (page 57) for details.

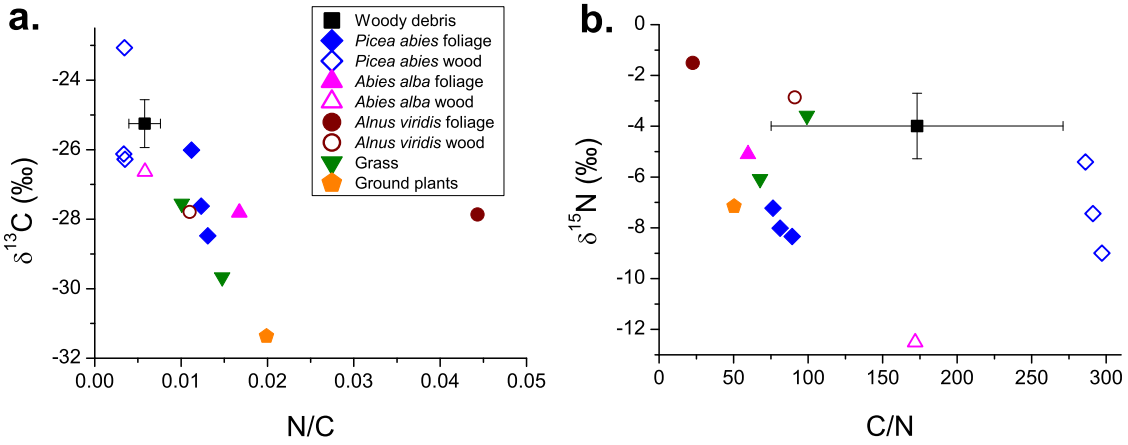

Figure 4.6: Chemical composition of Erlenbach vegetation samples. (**a**) Nitrogen to organic carbon ratio (N/C) versus organic carbon isotopic composition (δ^{13}C); (**b**) organic carbon to nitrogen ratio (C/N) versus nitrogen isotopic composition (δ^{15}N).

4.2.6.1 Foliage

Foliage samples included the two main types of conifer present in the catchment (*Picea abies* and *Abies alba*), a deciduous tree (probably *Alnus viridis*), an unknown species of grass, and representative mixed-vegetation ground cover, including broadleaf plants and moss. As a group they had mean C_{org} of 46.9%±2.0 (n=8), high mean C/N (55.5±17) and light C (δ^{13}C=-28.30‰±1.13) and N (δ^{15}N=-5.87‰±1.67). Figure 4.6 illustrates the differences between species as well as between foliage and wood. *Picea abies* foliage had relatively light δ^{15}N and heavy δ^{13}C compared to the rest of the foliage samples. *Abies alba* did not have a significantly different composition to *Picea abies*. *Alnus viridis* foliage plots distinctly, with high N/C and heavy N compared to other species, while the ground plants had the most negative δ^{13}C. Grass plots centrally.

4.2.6.2 Wood

Standing wood and woody debris, with C_{org} values of 47.5±0.6 (n=5) and 49.1±1.8 (n=12) respectively, were compositionally much more similar to each other than they were to same-species foliage, with significantly higher C/N and heavier δ^{13}C. Their values of C/N (185±83 and 173±98), δ^{13}C (-26.0‰±1.57 and -25.2‰±0.69) and δ^{15}N (-7.44‰±3.26 and -3.99‰±1.29) were the same within error. The range of isotopic values obtained for *Picea abies* wood were consistent with those determined at WSL, where separately collected samples of *Picea abies* wood were found to have δ^{13}C of -24.8‰ and δ^{15}N of -6.8‰ (Krause, 2010).

According to ^{14}C analysis, the woody debris ranges from modern to 4000 years old, suggesting that wood can reside in both landslides and the channel bed for a considerable period. Wood stored in soil in a similar catchment in the French Alps has been found by ^{14}C dating to be as old as 6700 years (Carcaillet, 2001).

The compositional similarity between fresh and old wood confirms that it is largely the chemical differences between lignin in wood and starch, lipids and other organic components in foliage (Guehl *et al.* , 1998; O'Leary, 1981) that causes the compositional difference between woody debris and foliage, rather than the process of ageing by microbial activity. These differences, namely that lignin and therefore wood has higher C/N, less negative $\delta^{13}C$ and similar $\delta^{15}N$ (O'Leary, 1981; Ometto *et al.* , 2006), are borne out by the relationships shown in Figure 4.6. Note that a direct comparison with relevant literature is difficult because of the acid treatment used on these samples that removes a labile fraction (see Section 3.3.2, page 66).

4.2.6.3 Analysis of biomarkers in plant material

Vegetation samples subjected to biomarker analysis (*Picea abies*, *Abies alba*, *Corylus avellana*, *Sorbus aucaparia* and an unknown species of grass) were nominally mixtures of woody stem and needles or leaves. Their positions in the S/V versus C/V plot (Figure 4.3) suggest that all were in fact more dominated by non-woody material. Other than this, all samples plot within the expected boxes, with the gymnosperms having low S/V values compared to the angiosperms. All plant materials had high lignin concentration compared to most of the sediments, with Λ ranging from 2.35 mg to 4.19 mg, and (Ad/Al)v values of less than 0.42, consistent with values expected from fresh plant matter (Vane, 2012b).

4.2.7 Relationships within and between catchment stores

The compositional relationships between organic carbon in the pools discussed above are illustrated in Figure 4.7. Although bedrock is the ultimate fossil source, landslide and channel bank samples plot within error of it, suggesting that the organic carbon in these pools comes directly from bedrock more or less entirely. In N/C–$\delta^{13}C$ space, both bedload and deep soil plot above positions expected if they were simple mixtures of bedrock-derived and soil-derived organic carbon, suggesting that there is also incorporation of wood within these pools.

In all source sediments for which different size fractions were analysed (bedload, landslides, deep soil and surface soil), the fine fraction had a more "fossil-like" signature (i.e. lower C/N and less negative isotopic ratios) than the bulk sediment. All

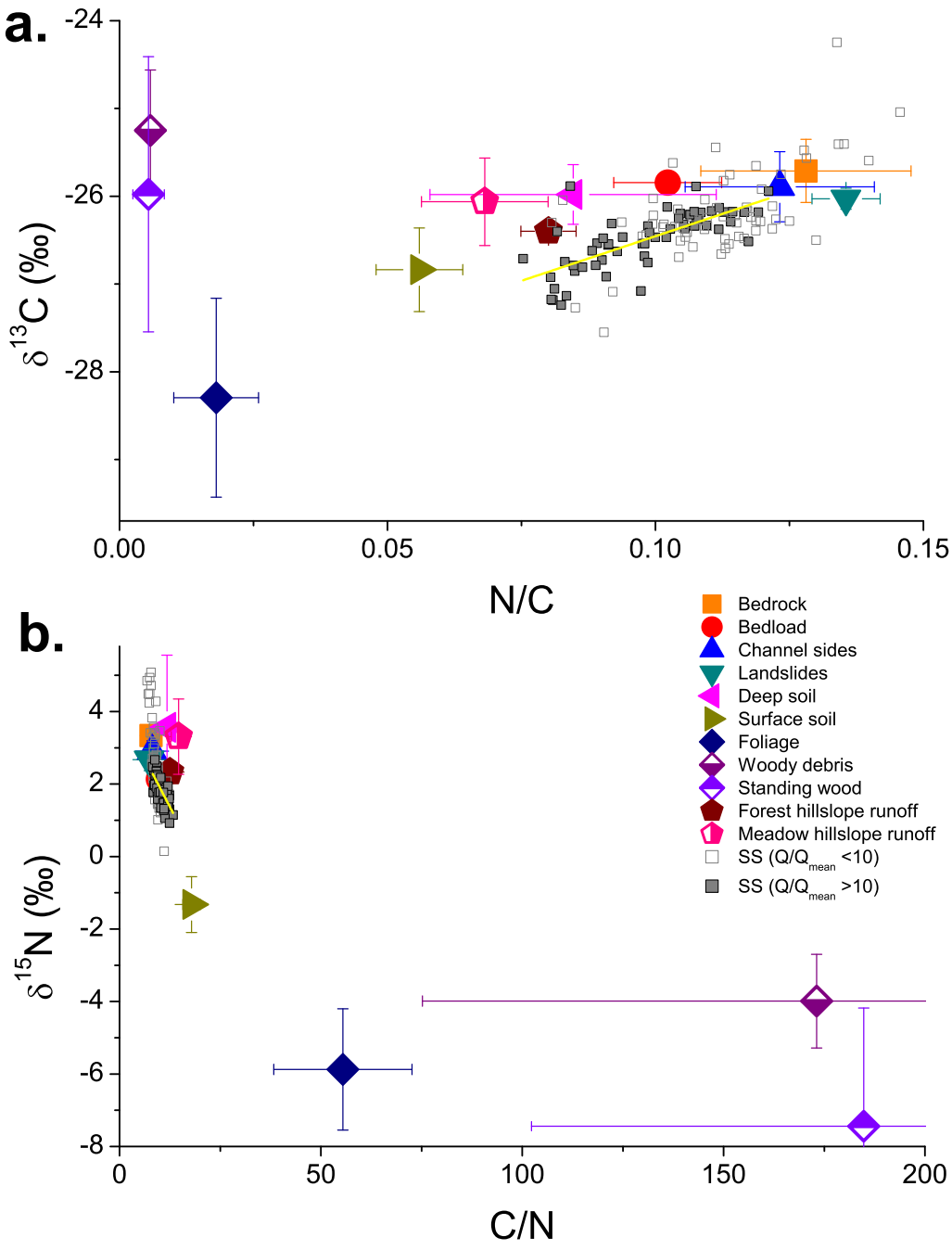

Figure 4.7: Chemical composition of POM in Erlenbach riverine suspended sediment (SS) and catchment-wide carbon stores. (**a**) Nitrogen to organic carbon ratios (N/C) and organic carbon isotopic composition (δ^{13}C) of Erlenbach riverine suspended sediment, hillslope runoff suspended sediment and major stores of carbon within the catchment. (**b**) Organic carbon to nitrogen ratios (C/N) and nitrogen isotopic composition (δ^{15}N) of the same pools. An enlarged version of the most crowded part of each plot can be found in Figure 4.10. Also shown are lines of best fit (yellow) through SS samples with Q/Q_{mean} >10.

except bedload also contained a lower proportion of organic carbon in the fine fraction than the bulk; in the case of surface soil substantially lower. This is a consequence of the fine-grained, clay-rich lithology: bedrock erosion products will naturally fall into the fine fraction, while soil and plant material, at least initially, will likely be in the form of larger grains or aggregates. For example, surface soils were slightly less dominated by the fine fraction than deep soils, likely reflecting the presence of larger organic particles that are broken down at depth—although the runoff erosion of fines could be a factor. The grain size distribution also indicates that grafting of organic matter onto fines in soils and elsewhere does not dominate the carbon budget at source. This contrasts with downstream studies, where organic carbon bound to fine particles is dominant (e.g. Hatten *et al.* , 2012; Hilton *et al.* , 2010).

4.3 Organic carbon in the suspended load

Organic carbon in the suspended load includes free-phase POM (floating vegetation) as well as organic carbon attached to mineral grains. Mean compositional parameters have been weighted by SSC, as this gives a more accurate representation of the bulk material being exported than a straight arithmetic mean.

4.3.1 Concentration of organic carbon in the suspended load

The range of C_{org} in suspended sediment samples was 0.78%–2.52%, with a mean of 1.52%±0.06 (n=122) and σ of 0.32%. Within each event, there is no consistent pattern in C_{org} over the hydrograph (Figure 4.8). However, when all data are considered together, there is a clear parabolic pattern in the variation of C_{org} with both Q and SSC, with negligible difference between rising and falling limbs. The product of Q and SSC combines both effects in the parameter "total suspended load" (TSL, in g s^{-1}), shown in Figure 4.9. At low TSL, C_{org} is initially variable, then decreases with increasing TSL. Beyond a threshold of ∼500 g s^{-1} (corresponding to Q∼400 l s^{-1}, Q/Q_{mean} ∼10 and SSC∼1600 mg l^{-1}), C_{org} increases: this trend continues up to at least ∼40000 g s^{-1} (∼2500 l s^{-1}; Q/Q_{mean} ∼60). The threshold is reached under moderate conditions, occurring several times per year, and in four of the five events sampled. Because of this change in behaviour, flows of Q/Q_{mean} <10 are taken to represent background conditions, after Gomez *et al.* (2010). Both the dilution and the addition are relationships with significant correlations at the 0.05 level (Kendall's τ=-0.30 and 0.67 respectively). The increase in C_{org} of the particulate load is mirrored by an increase in DOC export during storms in the Erlenbach (Hagedorn *et al.* , 2000).

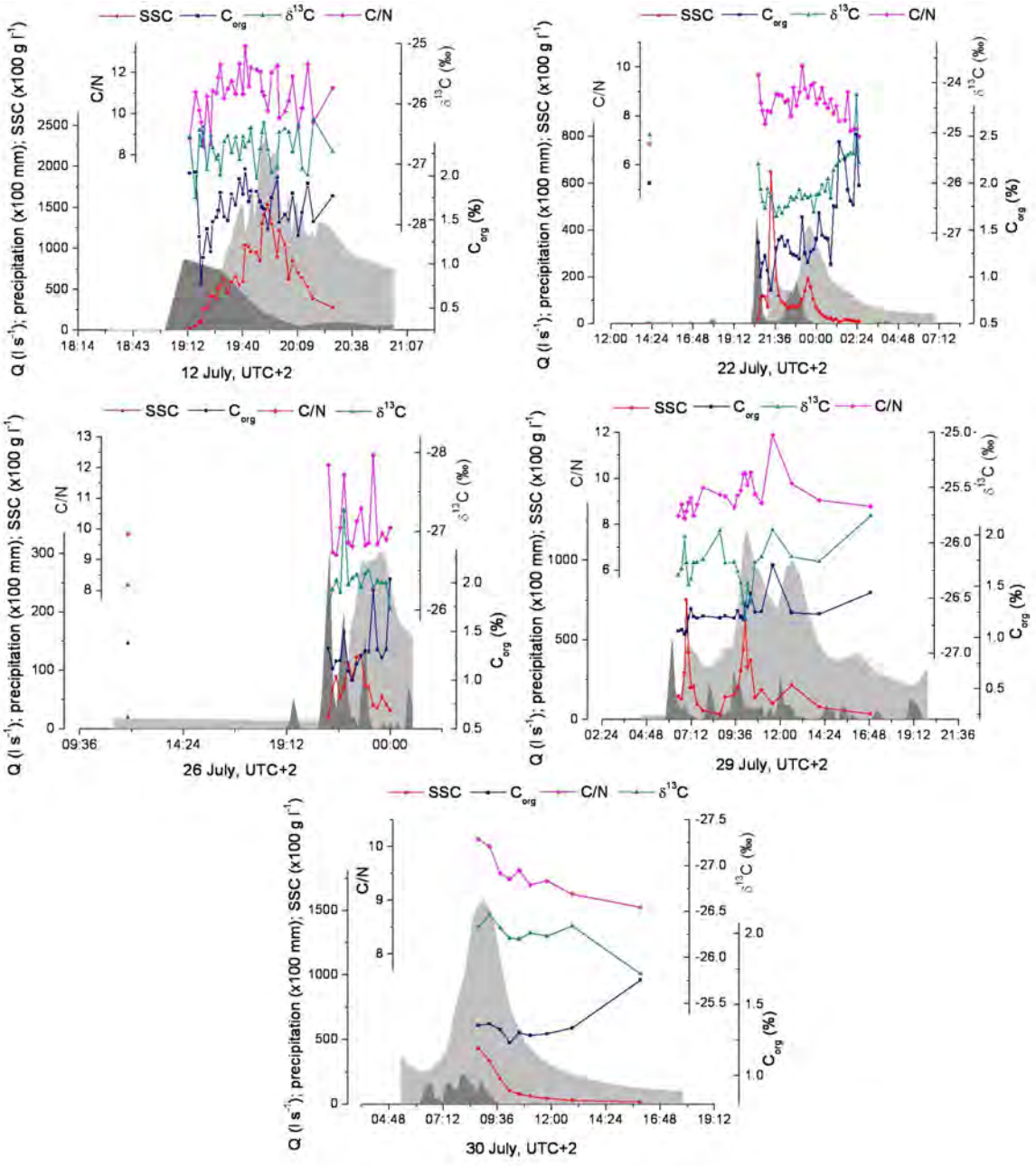

Figure 4.8: Hydrographs for five storm events sampled in July 2010. Dark grey area is precipitation (x100, in mm); light grey area is discharge (Q, in $\mathrm{l\,s^{-1}}$). Superimposed are four parameters measured or calculated for each sample (represented by a symbol): suspended sediment concentration (SSC, x100, in g $\mathrm{l^{-1}}$; red circles), organic carbon concentration (C_{org}; blue squares), carbon isotopic composition (δ^{13}C; turquoise triangles), and organic carbon to nitrogen ratio (C/N; pink diamonds).

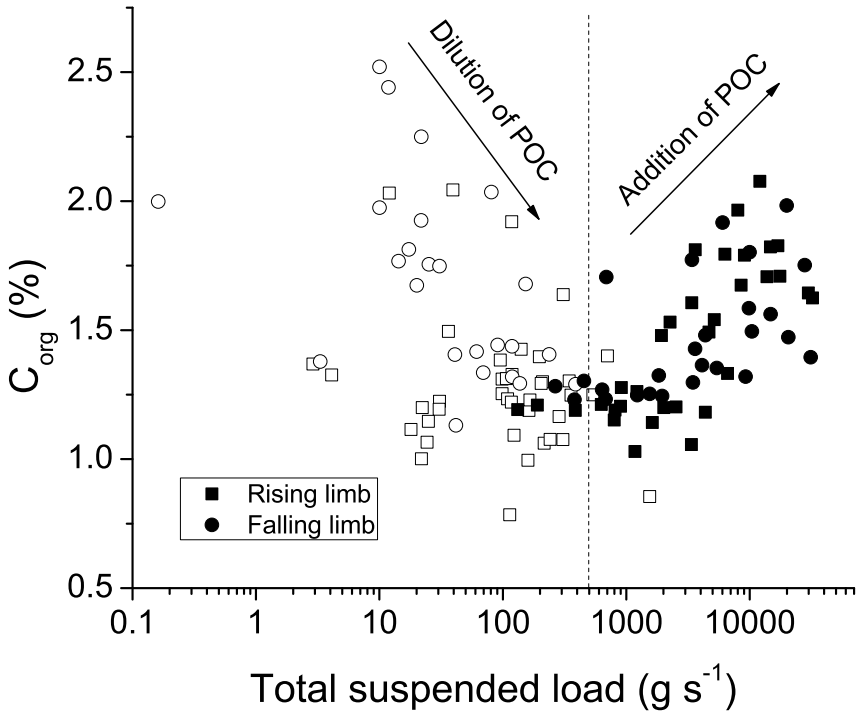

Figure 4.9: Variation of organic carbon concentration (C_{org}) in riverine suspended sediment with total suspended load (note logarithmic x-axis). Open symbols denote background flow (Q/Q_{mean} <10).

4.3.2 Composition of organic carbon in the suspended load

C/N in riverine suspended sediment ranged from 6.9 to 13, with a mean of 10.6±0.24 (n=122); δ^{13}C ranged from -27.55‰to -24.25‰with a mean of -26.58‰±0.08; and δ^{15}N ranged from 0.15‰to 5.08‰with a mean of 1.78‰±0.16. There were compositional differences between samples collected during rain and dry periods (Table 4.1), with the former having lower N/C, higher C/N and more negative δ^{13}C and δ^{15}N. However, there was no compositional difference between samples collected on the rising and falling limbs. In both N/C–δ^{13}C and C/N–δ^{15}N space, where mixing relationships are linear, POM in riverine suspended sediment samples plots in a broadly linear range bounded approximately by bedrock and soil (Figure 4.7). Suspended sediment samples with higher δ^{15}N than the bedrock range are a further indication that the stream is sampling bedrock compositions that were not collected and analysed. The mean F_{mod} for the six suspended sediment samples sent for Δ^{14}C analysis was 0.68±0.08.

4.3.2.1 Runoff suspended sediment

Forest and meadow runoff samples collected from the sub-plots (Section 3.2.1.1, page 51) had mean compositions just within error of each other. In N/C–δ^{13}C space, they lie at the low-N/C end of the riverine suspended sediment range, but with higher δ^{13}C. In C/N–δ^{15}N space, they are again off the trend defined by riverine suspended sediment (Figure 4.7). Both sets of runoff samples have higher mean C_{org} values than riverine suspended sediment, of 7.99%±0.9 (n=38; forest) and 17.6%±1.7 (n=10; meadow). This reflects the general appearance of the sediment samples, which were brown compared to grey riverine sediment, and often contained free-floating organic matter such as spruce and fir needles.

4.3.2.2 Retention basin

Sediment from the retention basin was used as a loose proxy for suspended sediment in biomarker analysis because this technique requires several orders of magnitude more material than was available from suspended sediment sampling. The retention basin was sampled once, around 36 hours after a large flood on 1 August 2010 with a peak discharge of 9.3 m^3 s^{-1} (Q/Q_{mean} =240). The sampled material was fine-grained, collected far enough from the edge not to be affected by soil bank composition but likely to have been largely deposited during the recent event. It had a comparable C_{org} (1.5%) to the suspended sediment mean, slightly higher C/N (14), slightly heavier C (δ^{13}C=-26.1‰) and slightly lighter N (δ^{15}N=1.5‰). Overall, the chemistry of this material indicates that it does reflect the suspended load to a substantial degree.

Results of biomarker analysis (Figure 4.3) confirm the affinity of retention basin sediment with channel sides rather than soils. It had a low value of Λ, S/V and C/V ratios that place it in the composition range of gymnosperm woods, and an (Ad/Al)v value of ∼0.6.

4.4 Sources and pathways of organic carbon

Both the compositional distribution and F_{mod} values of riverine suspended sediment are consistent with mixing between fossil and non-fossil end members. Mixing relationships, and their variation with discharge, are shown in Figure 4.10. These plots include the same data as Figure 4.7, but zoomed in to focus on the mixing zone, and with riverine suspended sediment coloured according to TSL—a parameter which scales with discharge. Although C_{org} in suspended sediment is always higher than that of bedrock, indicating that there is some non-fossil input at all times, this input

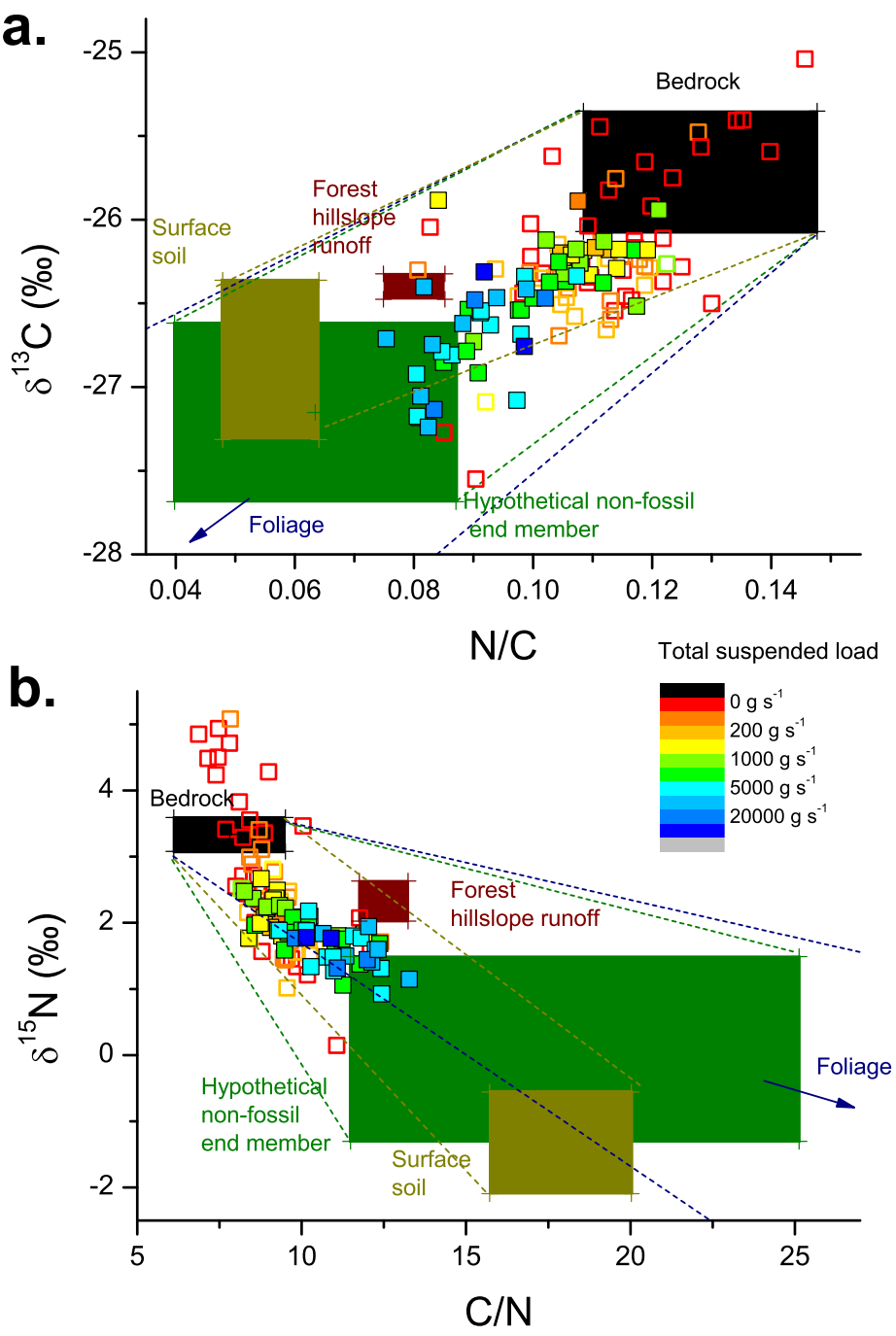

Figure 4.10: Chemical composition of POM in Erlenbach riverine suspended sediment. These are zoomed-in views of the plots in Figure 4.7, showing suspended sediment samples in detail and colour-coded according to total suspended load (warm colours represent low values; cold colours represent high values). Open squares are background flow (Q/Q_{mean} <10). Determination and nature of the hypothetical non-fossil end member is discussed in Section 4.4.1.

becomes increasingly significant at higher TSL. Samples collected at low TSL cover the whole compositional range, but are strongly concentrated towards high N/C and less negative δ^{13}C and δ^{15}N (that is, a "fossil" composition). During larger events, there is a bulk shift away from the fossil towards the non-fossil end of the mixing zone.

4.4.1 Nature of the end members

Because the composition of the POM exported from the catchment plots in the space between several different carbon pools, careful definition of the fossil and non-fossil end members is necessary. Although the chemical composition of bedload, landslides and channel banks suggests that these pools all derive from bedrock, bedrock alone is taken as the unequivocal fossil end member. In reality, all three are likely to be sources of fossil carbon, while contributing minimal non-fossil material, if any. For example, the lack of internal structure in the landslide profiles (Figures 4.4 and 4.5) indicates that large-scale mixing must be involved in their formation, yet the low C_{org} and near-bedrock composition show that such churning does not incorporate significant non-fossil organic material. Material of the fossil end member, then, can be harvested by several geomorphologic mechanisms without significant impact on its composition.

Of the non-fossil carbon pools, surface soil and foliage are closest to the mixing trend defined by the suspended sediment samples, but mixing zones between these and the fossil end member are slightly misaligned with the actual distribution in N/C–δ^{13}C and C/N–δ^{15}N space respectively. Because of this, and because it is likely that non-fossil material comes from a range of sources, the non-fossil end member is not taken to be either of these distinct pools. Instead, a hypothetical non-fossil end member is calculated using the procedure defined by Hilton *et al.* (2010). Briefly, the δ^{13}C of the non-fossil end member for each of six suspended sediment samples with known F_{mod} from ^{14}C analysis is calculated according to the mixing relationship

$$\delta^{13}C_{sample} = F_{mod}.\delta^{13}C_{nf} + (1 - F_{mod}).\delta^{13}C_{fos} \tag{4.1}$$

where $\delta^{13}C_{sample}$, $\delta^{13}C_{nf}$ and $\delta^{13}C_{fos}$ are the δ^{13}C value of the sample, a hypothetical non-fossil end member and the average δ^{13}C of bedrock samples respectively. The mean of the six calculated values of $\delta^{13}C_{nf}$ is taken.

Lines of best fit, calculated using only points with Q/Q_{mean} >10 (Figure 4.7), are then used to find the corresponding N/C, C/N and δ^{15}N. The same method is used with a plot of δ^{13}C versus $1/C_{org}$ to determine the C_{org} of the non-fossil end member. Uncertainties of twice the standard error on the mean of the initial

δ^{13}C value are propagated through these calculations. The resulting hypothetical end member (Figure 4.10) has C_{org} of 2.75%±4.8, C/N of 15.8±6.8, δ^{13}C of -27.15‰±0.53 and δ^{15}N of 0.61‰±1.40. Despite the low C_{org}, this is compositionally much more similar to surface soil than foliage, suggesting that soil is heavily implicated in the non-fossil POC input. The low C_{org} value may suggest that only a certain fraction of the organic carbon stored in soil is actually mobilised.

Other evidence also suggests that surface soil rather than foliage is the principal non-fossil end member, if less conclusively. Vegetation is hugely scattered in the δ^{13}C component, and this would be reflected in a far wider spread for suspended sediment if vegetation were being directly incorporated. A very strong correlation between SSC and POC in mg l^{-1} (R^2=0.98) suggests that POC is closely associated with or behaves in the same way as lithic particles, rather than existing as a separate free-floating phase as plant-derived material would. Finally, biomarker analysis of retention basin sediment, as a proxy for suspended load, shows no compelling evidence for direct incorporation of plant material.

Plotting the modern carbon concentration (F_{nf} x C_{org}, in %) of riverine suspended sediment against total carbon concentration (C_{org}, in %) can also give insights into the nature of the end members. F_{nf} is the modelled fraction of modern carbon in each suspended sediment sample; its determination is described in Section 4.4.2. In this plot (Figure 4.11), the gradient of the regression line is equal to the F_{nf} of the non-fossil end member, while the x-intercept gives the C_{org} of the fossil end member (Galy *et al.* , 2008). These parameters are broadly in agreement with previous inferences: the gradient of 1.09±0.11 confirms that the non-fossil end member is modern, while the x-intercept of 0.74%±0.23 is within error of the sampled bedrock mean of 0.54%±0.11.

4.4.1.1 The role of wood

Woody debris lies well off the main mixing trends (Figure 4.7), and it is assumed to constitute a minimal input to the carbon in the riverine suspended load, although it may be a significant input to soil at deeper levels. It is likely that pieces of wood entrained within channel banks and bedload are indeed mobilized during events, but are too large to be picked up by the sampling method. Although considerable amounts of large woody debris have been recovered from the basket samplers following events, the catchment is apparently too small for shredding of coarser woody debris to have a significant effect on the composition of POM in the suspended load between source and gauging station. Initial calculations using this material suggest that coarse POM (pieces <0.1 g) constitute 30%–50% of the total carbon flux out of the catchment

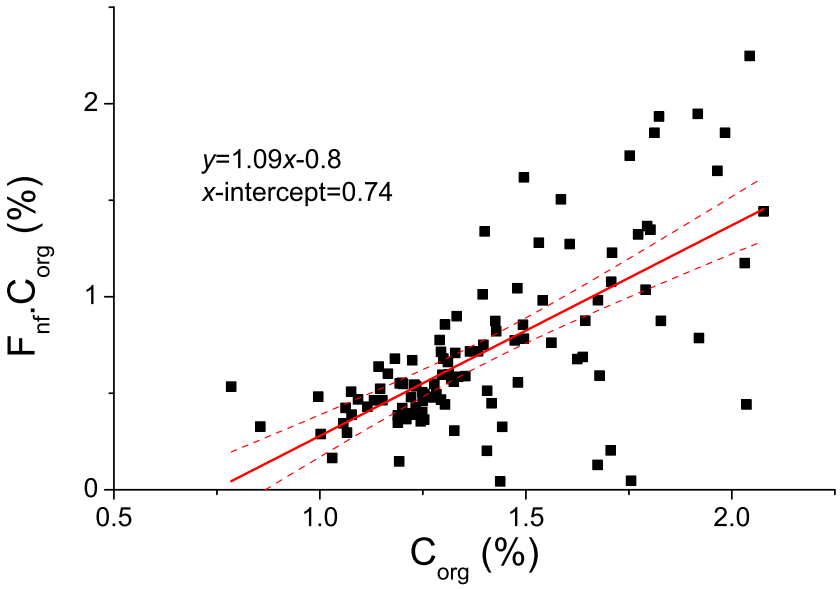

Figure 4.11: Modern carbon concentration (F_{nf} x C_{org}) of Erlenbach riverine suspended sediment versus total carbon concentration (C_{org}). Solid line shows best fit; dashed lines are 95% confidence bands. Nine samples with F_{nf} of zero are omitted from this plot.

(Turowski, 2012a). It is clear that large woody debris can be an important component of riverine organic carbon export in certain circumstances (e.g. West *et al.* , 2011), but it is not considered further here because of the lack of constraints. There is some further discussion on this in Section 7.4.1.1.

4.4.2 Modelling F_{mod}

If the proportion of organic carbon derived from non-fossil sources is known, the concentrations of fossil and non-fossil POC in milligrams per litre can be obtained for each sample, and then used to determine independent relationships with discharge. Separate long-term export rates of fossil and non-fossil POC can then be calculated: an important objective because only burial of non-fossil POC acts to draw down CO_2. It is not practical to obtain F_{mod} for every sample by radiocarbon dating. However, given the simple mixing exhibited by the system, it is possible to model this parameter for each suspended sediment sample, denoted F_{nf} to distinguish it from F_{mod} measured using ^{14}C (Hilton *et al.* , 2010). The method uses the $\delta^{13}C$ of the sample and two end members, bedrock and the hypothetical non-fossil end member determined above, and a rearrangement of Equation 4.1:

$$F_{nf} = \frac{\delta^{13}C_{fos} - \delta^{13}C_{sample}}{\delta^{13}C_{fos} - \delta^{13}C_{nf}} \tag{4.2}$$

Owing to scatter in the system, calculated F_{nf} values for 9% of samples fell outside the limits 0–1.1, the range found in natural systems (e.g. Levin & Hesshaimer, 2006). For these, a value of 0 or 1.1 was substituted as appropriate. On the samples sent for ^{14}C analysis, F_{nf} showed reasonable agreement with F_{mod}, reproducing it to within 0.25 at the 95% level.

4.4.3 Organic carbon routing during storms

In order to draw more general conclusions from the detailed study of POC export in the Erlenbach, its origins and harvesting mechanism need to be better understood.

When there is a small overall load, local incidental mobilisation dominates and suspended sediment shows the natural variability of catchment composition and process (Figures 4.9 and 4.10). As load increases, subsequent POC dilution to a minimum of ∼1% (Figure 4.9) must be due to an increased input of material with low C_{org}, by a mechanism that does not require high-energy flows. This is likely due to higher discharge causing an increase in bed shear stress, which mobilises fossil-derived material already in the channel. This lithic material (left by previous events, delivered to the channel by creep landslides, or eroded from bedrock exposed within the channel) contains small amounts of fossil C_{org}: bedrock mean C_{org} is 0.54%±0.11 (n=22) and bedload, landslide and channel bank pools all have mean C_{org} <1%.

Beyond the 500 g s^{-1} threshold (at Q/Q_{mean} ∼10), material with a higher C_{org} than bedrock or any of the groups derived from it must be added to the suspended load. Addition of fossil organic carbon, either directly from bedrock or via landslides or channel banks, cannot explain the compositional trends observed in the suspended load with increasing discharge (Figures 4.7 and 4.10). Instead, the sourcing mechanism must mobilize surface soil, litter and vegetation, in a way that gives the composition of the hypothetical non-fossil end member calculated in Section 4.4.1. This strongly suggests that surface runoff processes are responsible, but there is a compositional discrepancy in $\delta^{13}C$ and $\delta^{15}N$ between runoff suspended sediment and the hypothetical end member. However, the sub-plots (where the runoff samples were collected) are situated towards the edge of the catchment, whereas runoff entering the stream comes from lower, steeper hillslopes. Here, the bed shear stress is higher and runoff may penetrate deeper via transient gullying (Horton, 1945), allowing overland flow to pick up more soil and reducing $\delta^{13}C$ and $\delta^{15}N$ values to the hypothetical composition. There may also be a seasonal fractionation effect related to the decomposition state of the litter: runoff samples collected during the summer (June, July and August) have lower $\delta^{13}C$ and $\delta^{15}N$ values than during the rest of the year. Considering these

processes, hillslope activation driven by surface runoff can account for the change in composition of riverine POM above background flow, and so for the material added in this hydrological phase. This is supported by end member mixing analysis using dissolved nutrient tracers in the Erlenbach catchment which suggests that, at moderate summer storm peak discharges, over half the runoff in the stream comes directly from precipitation (Hagedorn *et al.* , 2000). The Q/Q_{mean}=10 threshold, therefore, appears to reflect a critical shear stress at which slope material is mobilised by overland flow on steep hillslopes adjacent to trunk channels.

The flood hydrographs (Figure 4.8) suggest that as soon as discharge has peaked (i.e. when precipitation slows or stops), hillslopes are deactivated and delivery of non-fossil organic carbon to the stream is staunched, shown by decreasing C/N and increasing $\delta^{13}C$. This reflects the differing compositions of suspended sediment collected during rain and dry periods (Table 4.1). Similarly, F_{nf} is significantly higher for samples collected during rainfall (0.62±0.05, n=85) than when not raining (0.35±0.06; n=37). The 22 July and, to a lesser extent, 26 July events also show a strong increase in C_{org} over the falling limb, indicating that fossil organic carbon continues to be mobilized from channel or bank sources; a similar transition is reported by Gomez *et al.* (2010) for a catchment in New Zealand. None of the sampled "fossil" pools have high enough C_{org} concentrations to account for the 22 July increase, but such a small event is likely to mobilise very localised, non-representative sources and this one may have tapped a disproportionately C_{org}-rich fossil layer. The larger 12 July and 29 July events, showing constant C_{org} on the falling limb, are likely to be much more characteristic of sediment- and POC-transporting flows in their behaviour and reflect increasingly distributed sourcing. In contrast, the contribution of organic carbon originating from surface soil to the dissolved load is greatest over the falling limb of storms (Hagedorn *et al.* , 2000), likely reflecting the role of shallow groundwater in soil-derived DOC supply as groundwater flow rates remain high for some time after precipitation.

4.4.3.1 Higher flow mechanisms

So far, only processes operating during moderate to large flows have been considered: samples up to Q/Q_{mean} ~60 provide no insight into the geomorphologic dynamic at very high flow rates. Although an 11-month study on landslides in the Erlenbach catchment found no rapid rainfall-triggered movements (Schuerch *et al.* , 2006), it was carried out during an unusually dry period when discharge did not exceed 1600 l s^{-1} (Q/Q_{mean}=41). It is possible that extreme precipitation, beyond that seen in either

that study or this one, could trigger rapid landslides. A study of rainfall intensity and duration thresholds for landslide initiation in Europe (Guzzetti *et al.* , 2007) suggests that this is plausible in the Erlenbach during events such as the 12 July storm and larger. If fast landsliding is triggered, then the system may cross a threshold into a more "active margin-like" mode of behaviour, where mass wasting during storms causes progressive dilution of modern organic carbon (Blair & Aller, 2012; Kao & Liu, 1996; Masiello & Druffel, 2001). However, under the moderate conditions characterised in this study, the rising proportion of material derived from non-fossil sources as discharge increases excludes this mode of operation, and if such a threshold exists, it must be at Q/Q_{mean} >60.

4.5 Long-term export fluxes

It is important to consider not only the export of total carbon, but of fossil carbon and non-fossil carbon separately, because only non-fossil carbon burial has an effect on contemporary CO_2 drawdown (e.g. Berner, 1982; Blair & Aller, 2012). Because distinct pools of organic carbon behave differently, shown by the changing composition of POC at different discharges, their long-term export should be considered independently (Wheatcroft *et al.* , 2010).

The calculated F_{nf} values can be used to construct rating curves describing the relationships between discharge and load of four components: suspended sediment (SS), total POC (tPOC), fossil POC (fPOC) and non-fossil POC (nfPOC). These are all power laws of the form $a(Q/Q_{mean})^b$ (Figure 4.12). Because of the threshold switch to POC addition at Q/Q_{mean} >10, and the fact that flows above background conditions are disproportionately important in transporting sediment and POC, only samples at Q/Q_{mean} >10 would ideally be used to fit the rating curves. However, this is mathematically unsatisfactory as it restricts the range of Q/Q_{mean} to less than one order of magnitude and results in large uncertainties on a and b. Relationships are therefore determined using the full sample set (three orders of magnitude in Q/Q_{mean}), but their geomorphological validity is checked by comparing with those determined using only samples with Q/Q_{mean} >10. In all cases a and b are well within error (Table 4.4).

The larger exponent for tPOC (b=1.33) compared to SS (b=1.19) means that relatively more POC is exported at higher discharges than SS, in contrast to the relationships seen in the Waipaoa River (New Zealand) and Alsea River (Oregon) (Wheatcroft *et al.* , 2010). The effect is even more pronounced for nfPOC (b=1.45) than for tPOC. The exponent for fPOC (b=1.08) is within error of that for SS,

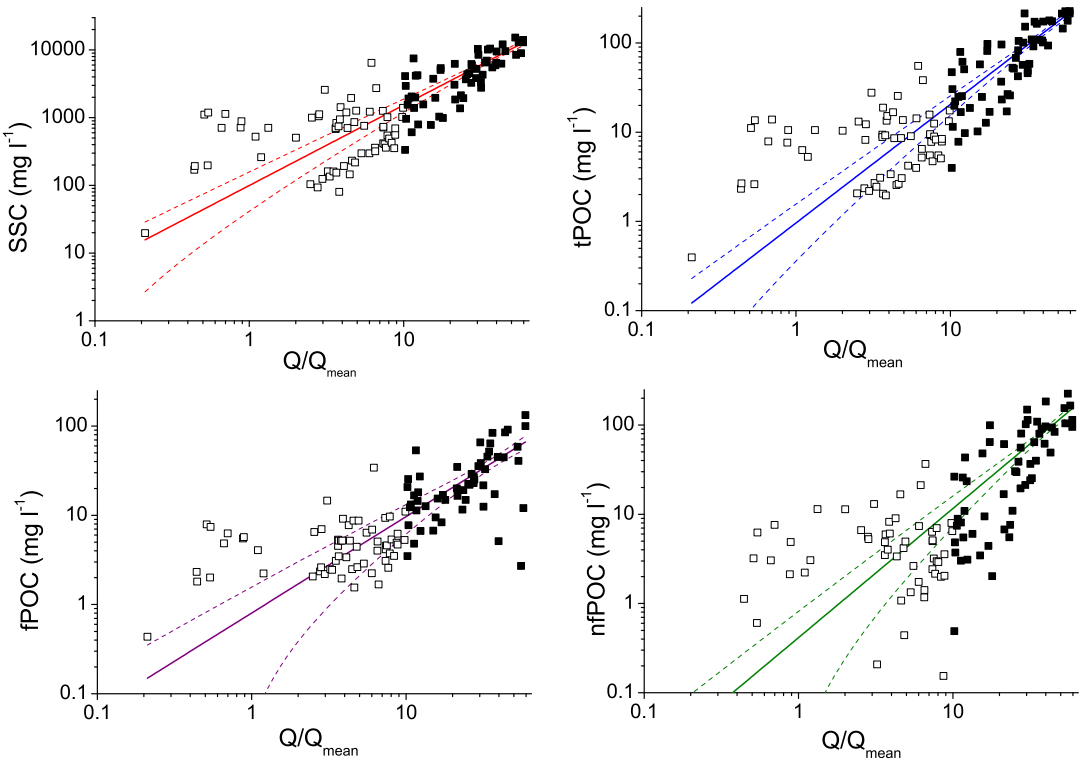

Figure 4.12: Rating curves showing power law relationships between Q/Q_{mean} and concentrations, in mg l^{-1}, of suspended sediment, total POC (tPOC), fossil POC (fPOC) and non-fossil POC (nfPOC). POC is particulate organic carbon concentration. Small squares represent individual samples; open symbols are background flow (Q/Q_{mean} <10). Dashed lines are 95% confidence bands.

reflecting their shared clastic origin. By equating the rating curve equations for fPOC and nfPOC it can be shown that equal amounts of these components are exported at Q/Q_{mean}=6.1; above this, F_{nf} will be >0.5, and below it will be <0.5.

Differences in the rating curve exponents are mirrored by those in effective discharge (Q_e); the discharge that, on average, transports the largest proportion of a given constituent load (Andrews, 1980; Nash, 1994; Wheatcroft *et al.* , 2010). In rivers with high Q_e, large floods with long return times are important to the total export of the constituent in question, whereas in systems with low Q_e (close to 1), frequently occurring, low-discharge conditions transport the majority of it. In the Erlenbach, Q_e is greatest for nfPOC (corresponding to Q/Q_{mean} of 13.4±3.7), and lowest for fPOC (6.1±1.7)—although there may be a second, much higher discharge at which fPOC could peak (see discussion in Section 4.4.3.1). Q_e for all four components relative to Q_{mean} (Table 4.4) is within and towards the lower end of the range observed in other small mountain rivers (Wheatcroft *et al.* , 2010).

	a	**b**	$\mathbf{R^2}$	$\mathbf{Q_e}$ (l s^{-1})	$\mathbf{Q_e}$ ($\mathbf{Q/Q_{mean}}$)
SS	99.7±29.4 *96.0±44.2*	1.19±0.08 *1.20±0.12*	0.78 *0.68*	300±50	7.7±1.3
tPOC	0.96±0.30 *0.96±0.48*	1.33±0.08 *1.33±0.13*	0.81 *0.71*	400±70	10.4±1.8
fPOC	0.80±0.39 *0.75±0.64*	1.08±0.13 *1.10±0.23*	0.50 *0.32*	240±50	6.1±1.7
nfPOC	0.41±0.20 *0.44±0.33*	1.45±0.13 *1.43±0.20*	0.70 *0.57*	520±140	13.4±3.7

Table 4.4: Rating curve parameters for power law relationships between Q/Q_{mean} and suspended sediment (SS) or particulate organic carbon (POC), of the form SS or POC=$a(Q/Q_{mean})^b$. Values in regular type (used for flux calculations) are based on the whole sample set; values in italics (given for information) are based only on samples with Q/Q_{mean} >10. There are three classes of POC: total (tPOC), fossil (fPOC) and non-fossil (nfPOC). Correlation coefficients are given as R^2. Q_e is the effective discharge, as defined by Wheatcroft *et al.* (2010). Q/Q_{mean} is the discharge relative to the average discharge over the period 1983–2011 inclusive (39 l s^{-1}).

The export of the four components over the period 1983–2011 inclusive was modelled by applying these rating relationships to the 10-minute discharge record for the Erlenbach, with full results shown in Table 4.5. The mean annual yields (in tonnes per year) and export fluxes (in tonnes per square kilometre per year) of each component were: 1220±232 t yr^{-1} and 1648±313 t km^{-2} yr^{-1} (SS); 17.3±4.3 t yr^{-1} and 23.3±5.8 t km^{-2} yr^{-1} (tPOC); 7.4±1.2 t yr^{-1} and 10.1±1.6 t km^{-2} yr^{-1} (fPOC); and 10.4±3.2 t yr^{-1} and 14.0±4.4 t km^{-2} yr^{-1} (nfPOC).

The yield of fPOC calculated in this way is identical to the "expected" mean annual yield of fossil carbon (7.4±1.3 t yr^{-1}), reached by multiplying the average C_{org} of the bedrock samples (assuming these accurately represent catchment-wide bedrock) by suspended sediment yield. This suggests that there is no significant remineralisation of fossil organic carbon during bedrock erosion and export from these headwaters, in common with findings from the French Alpes-de-Haute-Provence (Graz *et al.* , 2011), although oxidation may occur during onward transport and floodplain storage in large river systems (Bouchez *et al.* , 2010).

	Mean annual yield (t)	**Mean annual yield (t) according to Q/Q_{mean} ($l\ s^{-1}$). Proportions in each class are given in brackets.**				**Export flux (t km^{-2} yr^{-1})**
		$Q/Q_{mean} \leq 1$ (77%)	$1<Q/Q_{mean} \leq 10$ (22%)	$10<Q/Q_{mean} \leq 60$ (1%)	$Q/Q_{mean} >60$ (<0.01%)	
SS	1220±232	12.0±0.79 (1.1%)	376±35.3 (32%)	740±91.8 (61%)	91.1±61.3 (5.8%) *215±171 (10%)*	1648±313
tPOC	17.3±4.3	0.11±0.01 (0.7%)	4.57±0.44 (28%)	11.0±1.40 (64%)	1.57±1.06 (6.9%) *4.21±3.43 (12%)*	23.3±5.8
fPOC	7.44±1.2	0.10±0.01 (1.5%)	2.56±0.24 (36%)	4.30±0.53 (58%)	0.47±0.32 (5.1%) *1.02±0.79 (8.6%)*	10.1±1.6
nfPOC	10.4±3.2	0.04±0.00 (0.5%)	2.39±0.23 (26%)	6.85±0.88 (67%)	1.10±0.74 (7.3%) *3.29±2.73 (13%)*	14.0±4.4
F_{nf}	0.61±0.02	0.30±0.00	0.48±0.00	0.61±0.00	0.70±0.00 *0.76±0.02*	-

Table 4.5: Modelled export fluxes of the four main components in Erlenbach suspended load, averaged over 29 years (1983–2011 inclusive). SS is suspended sediment; tPOC, fPOC and nfPOC are total, fossil and non-fossil particulate organic carbon respectively. F_{nf} is the modelled fraction of organic carbon derived from non-fossil sources, given overall in the first column and then for separate discharge classes. For $Q/Q_{mean} >60$, the top line (normal type; used in calculating overall yields and fluxes) conservatively assumes that the rating curves are flat from $Q/Q_{mean}=60$; the bottom line (italics; given for comparison only) assumes that the same rating relationships apply above this limit. The overall mean F_{nf} of 0.61 is for the conservative scenario.

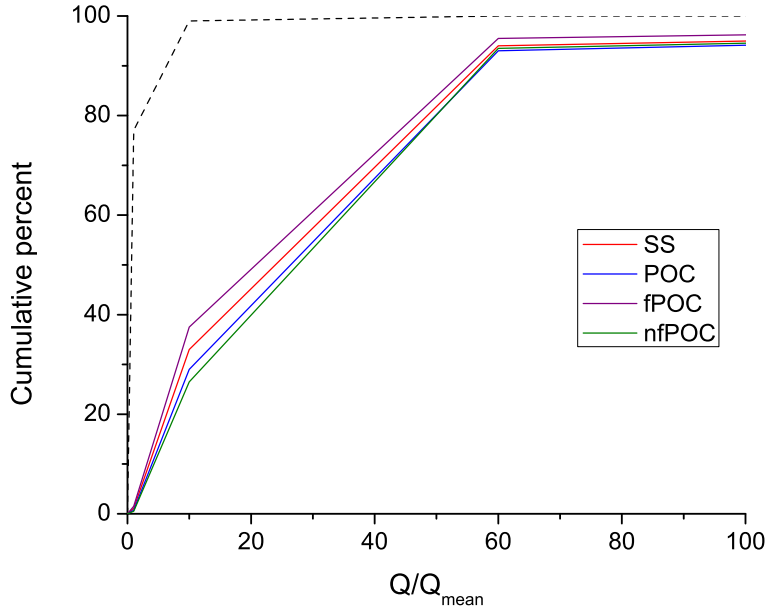

Figure 4.13: Cumulative percent yields of suspended sediment (SS) and total, fossil and non-fossil POC from the Erlenbach as a function of Q/Q_{mean}. The black dashed line shows the cumulative proportion of time spent by the stream in each discharge class.

The effect of the different rating curve exponents is illustrated by comparing the proportional yields of each component at different discharges, with the largest flows transporting a greater proportion of nfPOC than tPOC, and a greater proportion of tPOC than SS and fPOC (Table 4.5; Figure 4.13). Three discharge class boundaries are defined, corresponding to Q/Q_{mean}=1, 10 and 60. Q/Q_{mean}=10 (~310 l s^{-1}) is the threshold above which POC is added, while Q/Q_{mean}=60 (~2300 l s^{-1}) is the approximate limit of discharges sampled. This limit is not exceeded very often (higher values are recorded for just 81 10-minute segments out of over 1.5 million), but can be exceeded substantially: the largest discharge recorded in the 10-minute dataset during the monitoring period was 11950 l s^{-1} (Q/Q_{mean} ~309), on 25 July 1984. Even higher discharges occur on shorter timescales: measurements at a frequency of 1 minute show a peak of ~14600 l s^{-1} (Q/Q_{mean} ~378) on 20 June 2007.

The results show that the lowest discharge class (Q/Q_{mean} ≤1; the state of the stream for over three quarters of the time) is insignificant in terms of both SS and POC export. Conversely, if the same rating curve applied above the upper limit, discharges of Q/Q_{mean} >60 would transport considerable quantities of sediment, POC and particularly nfPOC (10%, 12% and 13% of total transport respectively), despite occurring less than 0.01% of the time. However, because of the lack of constraints on

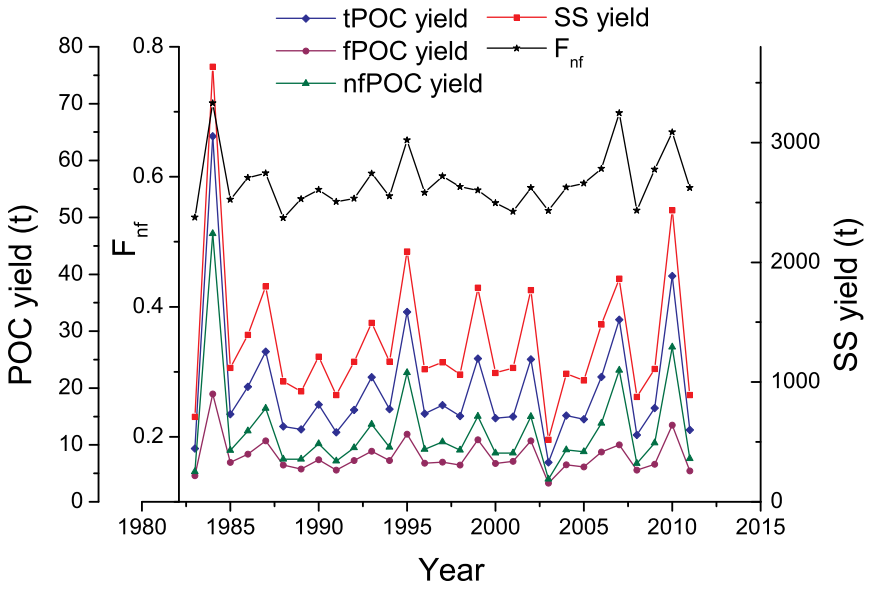

Figure 4.14: Annual variation in F_{nf} and yields of SSC and total, fossil and non-fossil POC (tPOC, fPOC and nfPOC respectively) from the Erlenbach.

processes or suspended load at these flows, this assumption is not conservative; for example, if landslides are activated as discussed earlier, there may be an increase in the proportion of fPOC. Instead, a constant load of all four components for Q/Q_{mean} >60 is assumed, giving a conservative estimate for the total yields.

The modelled amounts of fossil and non-fossil POC exported were used to calculate a mean F_{nf} value for each year, both overall and at different discharges (final row of Table 4.5). According to the model, 61%±2 of all the organic carbon exported from the Erlenbach over this 29-year period came from non-fossil sources. F_{nf} varied significantly between discharge classes, from 0.30±0.00 during the lowest flow (Q/Q_{mean} <1) to 0.61±0.00 for 10<Q/Q_{mean} ≤60. Beyond Q/Q_{mean}=60, F_{nf} would be 0.76±0.02 if the same rating relationship applied, but 0.70±0.00 in the conservative scenario where the curve is assumed to flatten.

Variation in SS and POC export and F_{nf} over the monitoring period is illustrated in Figure 4.14. Export fluxes varied by around an order of magnitude. Yearly maxima in tPOC export (64 t km^{-2} yr^{-1}), nfPOC export (47 t km^{-2} yr^{-1}) and F_{nf} (0.71) all occurred in 1984, while minima of 6.9 t km^{-2} yr^{-1}, 4.0 t km^{-2} yr^{-1} and 0.55 respectively occurred in 2003. Yields of all types of POC, and F_{nf}, are strongly correlated with SSC yield.

4.5.1 Discussion of potential biases

The calculated F_{nf} of POC exported from the catchment is systematically biased by not including bedload, because bedload is closely related to bedrock (Figure 4.7) and contains dominantly fossil carbon. This is particularly true in small catchments with high sediment load like the Erlenbach, where bedload is relatively more important than in large mountain rivers (Rickenmann *et al.* , 2012). Bedload was excluded from this study in order to enable comparison with other sites, since only suspended load data are available at most locations. However, because bedload transport is constrained to some extent in the Erlenbach, the implications are briefly discussed. The total sediment volume accumulated in the retention basin between August 1982 and October 2012 was 17730 m^3, including pore space and suspendable fines. Using a bulk density of 1750 kg m^{-3} (Rickenmann & McArdell, 2007), and assuming that 75%–80% of the material is larger than 2 mm (Rickenmann & McArdell (2007) estimate that 50% of material in the retention basin is >1 cm; 90% is >0.3 mm (Turowski, 2012b)), this gives ∼800 tonnes bedload per year. Using the bedrock C_{org} of ∼0.5%, this equates to an additional ∼4 tonnes of organic carbon per year on top of the 17 tonnes exported in the suspended load. An alternative estimate, assuming that bedload volume is approximately equal to suspended load volume in the Erlenbach (Turowski *et al.* , 2010), gives an additional ∼7 tonnes of organic carbon per year. These figures suggest that, if bedload as well as suspended load is considered, the overall F_{nf} would decrease from 0.6 (Table 4.5) to between 0.4 and 0.5. A further consideration is the probability that non-fossil carbon in the form of coarse woody debris is transported in the bedload (Turowski, 2012a), meaning that total non-fossil POC export is also underestimated by this analysis (see also Section 4.4.1.1).

Because the rating curves and flux estimates are based on samples collected during the summer only, they are biased towards processes acting in summer only and take no account of possible seasonal changes in the relationships between discharge and tPOC, fPOC and nfPOC concentrations. However, it is likely that significantly different processes to those constrained is this study occur only during the winter and early spring, when there is snow on the ground or melting. Figure 2.7(a) (page 27) shows that, although discharge is highest during snow melt in April–May, suspended sediment concentrations are relatively low throughout winter and spring. Multiplying mean discharge by mean SSC gives mean total suspended load values of ∼3 g s^{-1} for winter/spring (December–May) and ∼15 g s^{-1} for summer/autumn (June–November). Thus, the mass of material exported under the conditions constrained in this study is likely approximately five times greater than that exported at other times. Even if

somewhat different processes were shown to operate in winter and taken into account, the long-term fluxes would probably not change substantially.

4.6 Chapter summary

The processes responsible for transferring organic carbon from hillslope to stream in an alpine headwater catchment with C_{org}-rich bedrock, a high degree of hillslope-channel coupling and no extreme mass wasting over the timescale of the study, have been characterised. Additionally, the long-term yields of suspended sediment, total POC, fossil POC and non-fossil POC from this system under moderate conditions have been determined.

Suspended sediment exported from the Erlenbach catchment has a mean C_{org} of 1.45%±0.06. Both concentration and composition of this organic carbon vary systematically with hydrological conditions, although variations over any single hydrograph are highly individual. At low discharge, POC concentration and composition is highly variable, due to natural heterogeneity in the small amount of material transported. As discharge increases (along with total suspended load), in-channel clearing causes initial dilution of POC. At a moderate, frequently-crossed threshold (Q/Q_{mean}=10), the hillslope becomes active and runoff delivers additional POC to the stream in the form of largely soil-derived biomass, causing a bulk shift to higher C/N and lower $\delta^{13}C$ and $\delta^{13}N$. This is associated with an increase in the F_{nf} from 0.30 during background flow to 0.70 at the highest discharges sampled in this study (Q/Q_{mean} ∼60). Active precipitation is crucial to the mechanism, with riverine suspended sediment showing greater non-fossil influence and significantly higher F_{nf} during rain and on the rising limb than when the rain has stopped and flow is waning. Landslides and channel bank collapse do not regularly contribute to the POC exported under these conditions, but may be activated at extremely high flow rates.

Rating curves show power law relationships between discharge and four components: suspended sediment, total POC, fossil POC and non-fossil POC. All exponents are >1, with fossil POC the lowest at 1.08±0.13. Total POC has a significantly higher exponent than suspended sediment, and non-fossil POC has one greater still. C conservative estimates of average export fluxes over the past 29 years of suspended sediment, total POC, fossil POC and non-fossil POC (in tonnes km^2 yr^{-1}) were 1648±313, 23.3±5.8, 10.1±1.6 and 14.0±4.4 respectively.

Chapter 5

Further insights from the Alptal

5.1 Introduction

Chapter 4 used only data from the instantaneous samples collected from the Erlenbach during summer storms. While much insight can be gained into POC mobilisation in Switzerland from this dataset, the Erlenbach may be an atypical catchment in terms of its rapid erosion rate, extensive creep landsliding, sensitive response to rainfall and high bedrock C_{org}. To determine how these peculiarities might influence POC export, and to examine POC mobilisation in the Swiss Prealps in a more general way, the neighbouring Vogelbach catchment is studied as a contrasting setting. Similar methods are used to those employed in Chapter 4, with organic carbon and nitrogen concentrations and stable isotopic compositions providing insights into the distribution and pathways of organic carbon within the catchment. However, because the Vogelbach dataset consists only of discharge-proportional compound samples, it is first necessary to investigate the potential differences between the discharge-proportional and instantaneous sampling methods by comparing results from the two Erlenbach datasets. The compound samples also offer additional information about seasonal patterns of POC harvesting in the Erlenbach. In the final section, export fluxes of total, fossil and non-fossil POC from the Vogelbach are quantified. A comparison between fluxes calculated from the two Erlenbach datasets is used to evaluate the degree to which using compound samples may underestimate the true yield.

As in the previous chapter, quoted uncertainties on source compositions—and error bars on figures—are ± twice the standard error on the mean, σ=standard deviation, and means for suspended sediment are weighted by SSC.

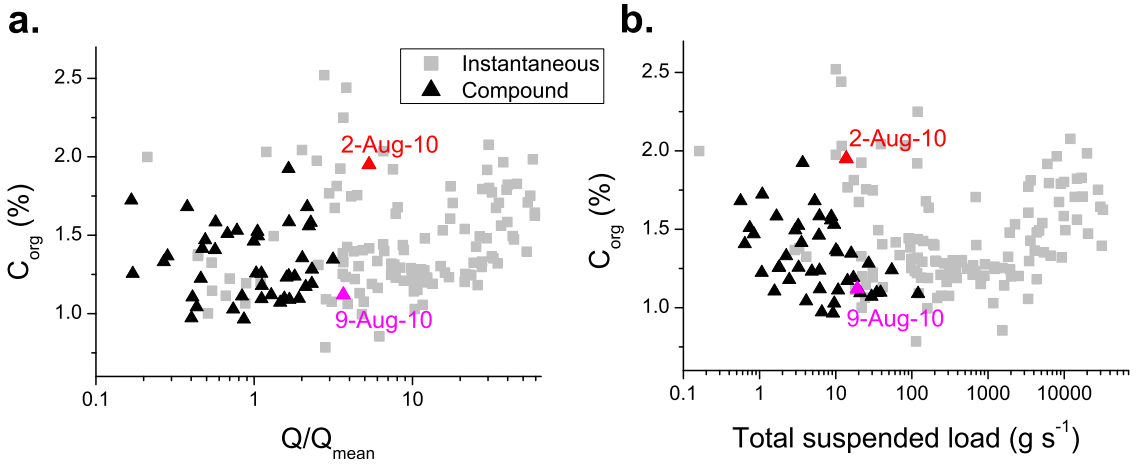

Figure 5.1: Organic carbon concentration (C_{org}) in Erlenbach compound samples compared to instantaneous samples, as a function of (**a**) discharge (Q/Q_{mean}) (**b**) and total suspended load. Coloured triangles indicate compound samples collected on the date shown; see Section 5.2.1 for details. Note logarithmic x-axes.

5.2 Erlenbach compound samples

5.2.1 Organic carbon concentration and composition

The discharge-proportional compound samples had a slightly lower mean C_{org} than the instantaneous dataset of 1.22%±0.07 (n=45), and were less variable, with a range of 0.96%–1.95% and a standard deviation of 0.24%. They show a significant decrease in C_{org} with increasing total suspended load (Kendall's τ=-0.29), but no significant correlation with Q/Q_{mean} (τ=0.04) (Figure 5.1). These plots also show the extent to which events are diluted out of the compound record, even though compound sampling is weighted towards them through the discharge-proportionality built into the method (Schleppi *et al.* , 2006): the instantaneous samples, collected during very moderate events, represent discharges on average an order of magnitude greater than the compound set. By way of example, the compound samples taken on 2 August and 9 August 2010 are highlighted; the former was collected the day after a very large event with a peak discharge of 9.3 m^3 s^{-1} (equivalent to Q/Q_{mean} of 240), the latter a week later when discharge was still elevated. Although at the high end of the distribution, neither show an elevated total suspended load compared to the other samples, and while the 2 August sample had the highest C_{org}—though only marginally—the 9 August sample had one of the lowest.

The compositional distribution of Erlenbach compound samples is shown and compared to that of the instantaneous samples in Figure 5.2. They lie on a slightly different trend to the instantaneous samples, having more negative isotopic ratios

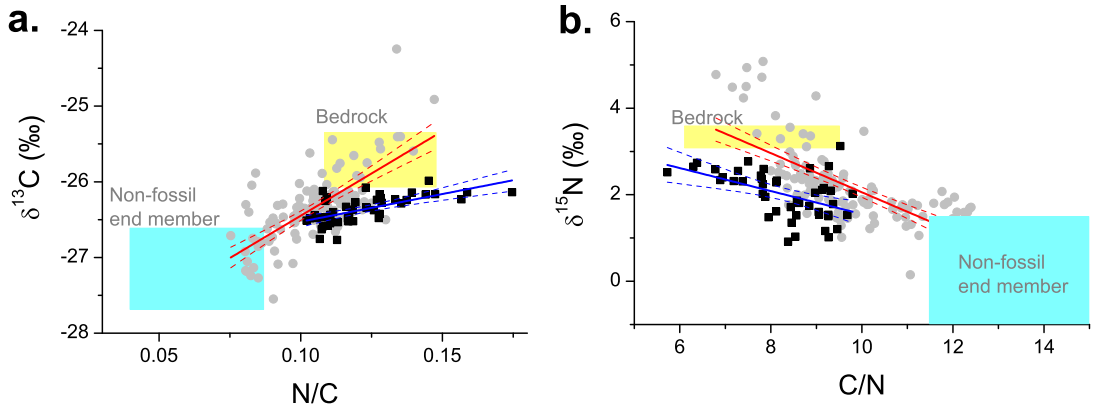

Figure 5.2: Chemical composition of POM in Erlenbach compound samples, compared to the instantaneous sample set. Solid lines are linear fits to each dataset; dashed lines are 95% confidence bands. Parameters are given later in Table 5.1. (**a**) Nitrogen to organic carbon ratio (N/C) versus carbon isotopic composition (δ^{13}C); (**b**) organic carbon to nitrogen ratio(C/N) versus nitrogen isotopic composition (δ^{15}N).

for a given N/C or C/N value; the possible reasons for this are discussed in Section 5.2.2. Notwithstanding this apparent shift, they cluster around the fossil end of the mixing zone, consistent with a mean F_{nf} (modelled in the same way as for the instantaneous sample set) of 0.42±0.04, somewhat less than the instantaneous mean F_{nf} of 0.60±0.05. Figure 5.3 shows a slight shift towards bedrock with increasing total suspended load—and bed shear stress—in both N/C–δ^{13}C and C/N–δ^{15}N space. This is as expected given the dilution apparent in Figure 5.1(b).

5.2.1.1 Seasonality in POM concentration and composition

Figure 5.4 shows the temporal variation of suspended load C_{org} and composition (represented by C/N and δ^{13}C), together with discharge, over the sampling period. In general, all parameters follow the same trends, with low C/N and less negative δ^{13}C—both signalling a greater "fossil" influence—occurring when C_{org} is low, and the opposite when C_{org} is high. Seasonal trends are also apparent. Through the autumn and winter, C_{org} was relatively low and there was a strong fossil input, although this was quite variable in 2009. From May, C_{org} increased systematically until the summer storm season, and there was a concomitant compositional shift towards non-fossil carbon. There was a decrease in all parameters immediately following the large event of 12 July (Q/Q_{mean}=59), then a recovery and another, larger drop immediately after the 2 August event (Q/Q_{mean}=240). After this, there was a partial recovery in C/N but C_{org} and δ^{13}C stayed low into the winter.

The increase in C_{org} and non-fossil influence during spring is explained by the en-

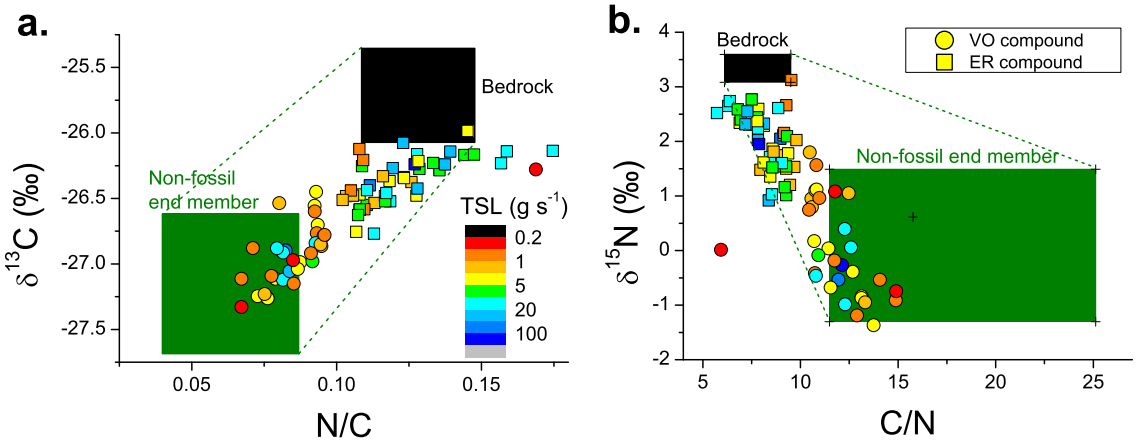

Figure 5.3: Chemical composition of POM in Vogelbach (circles) and Erlenbach compound (squares) samples, coloured according to total suspended load (TSL). Warm colours represent low values; cold colours represent high values. (**a**) Nitrogen to organic carbon ratio (N/C) versus carbon isotopic composition (δ^{13}C); (**b**) organic carbon to nitrogen ratio(C/N) versus nitrogen isotopic composition (δ^{15}N). "Bedrock" and "Hypothetical non-fossil end member" are those defined in the previous chapter for the Erlenbach.

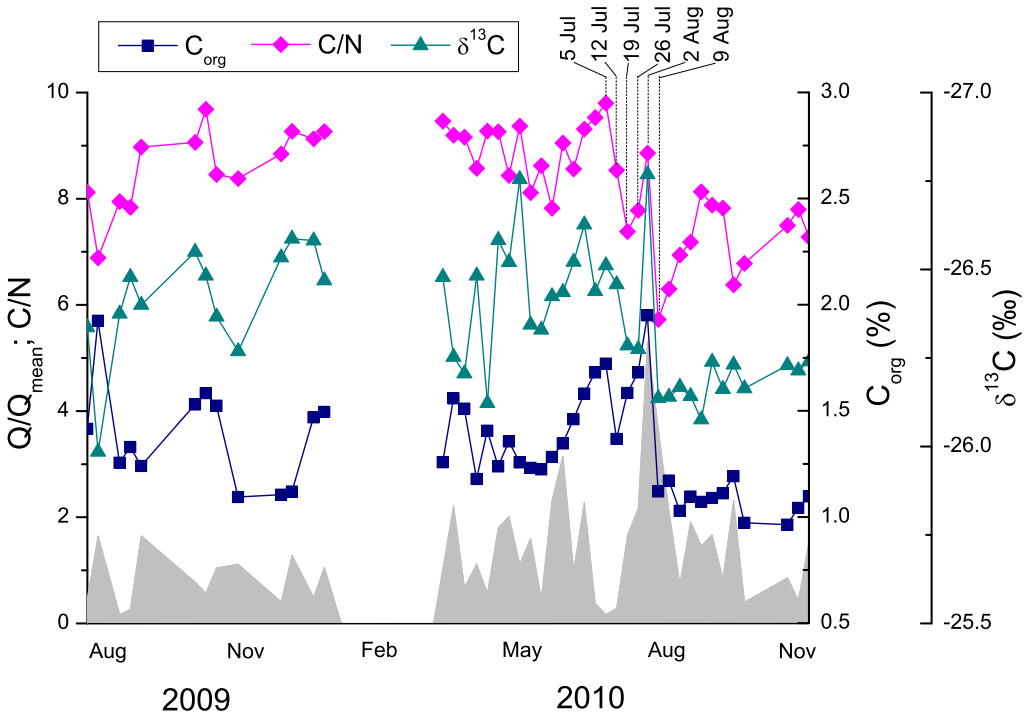

Figure 5.4: Seasonal variation in organic carbon concentration (C_{org}; blue squares), ratio of organic carbon to nitrogen (C/N; pink diamonds), and organic carbon isotopic composition (δ^{13}C; turquoise triangles) in Erlenbach compound samples. Also shown in grey is the mean discharge (as Q/Q_{mean}) for the week represented by each sample. The samples covering the period of instantaneous sample collection are indicated with dates.

	N/C–δ^{13}C			C/N–δ^{15}N		
	a	**b**	$\mathbf{R^2}$	**a**	**b**	$\mathbf{R^2}$
Compound	-27.3±0.2	7.30±1.3	0.42	4.21±0.60	-0.27±0.07	0.22
Instantaneous	-28.7±0.2	22.3±2.1	0.49	6.57±0.42	-0.45±0.04	0.48

Table 5.1: Parameters for the linear trends in composition of POM in Erlenbach compound and instantaneous samples, shown in Figure 5.2 and of the form y=a+bx. Correlation coefficients are given as R^2.

hanced growth of plants during this period, increasing the supply of leaves to the channel where they may directly join the suspended load or become incorporated into the bedload to be mobilised subsequently, in either case supplementing the non-fossil content. Snow cover during winter also prevents mobilisation of non-fossil material from the hillslopes; this starts again with spring snow melt, which may additionally help to flush material into the channel. There are two mechanisms which may explain the decrease following large events. Biogenic material, steadily built up in the channel under background conditions, could be flushed out by short-lived high flows. Immediately afterwards, only fossil-derived material would be available for mobilisation until non-fossil stocks had replenished. Alternatively, it could result from dilution. Section 4.4.3 (page 99) describes how hillslope input is switched off when the rain stops and discharge has peaked (falling limb samples have much lower F_{nf} than rising limb samples). If SSC remains high then fossil material with low C_{org} will dominate. However, Figure 4.8 (page 92) shows that SSC is not generally elevated for more than a few hours after the event peak, and so this effect would be suppressed in a compound sample representing an entire week. Therefore, the first hypothesis is preferable.

5.2.2 Relationship between compound and instantaneous suspended sediment samples

Figure 5.2 and Table 5.1 show that the compound samples lie on a different trend line to the instantaneous samples, having the same non-fossil end member but a slightly different fossil one. This deviation is problematic: if compound samples comprise different proportions of carbon from the same end members, because they include more low-discharge signal, they should still lie on the same mixing line. One possibility is that the bedrock (or bedrock-derived material, such as landslides) eroded at low flow is systematically different to that mobilised during storms. On average, landslide samples do have lower C/N and more isotopically negative compositions than mean Erlenbach bedrock (Table 4.1, page 80). If landslide material is picked up under

background conditions while higher flows access bedrock in situ, and the bedrock that they access has the same composition as the sampled catchment mean, then the difference in the two sample sets could be accounted for. However, this is difficult to test, and there is no particular geomorphological reason why it should occur.

A second possibility is that the suspended sediment composition could change during storage through processes such as bacterial alteration (Bonin *et al.* , 1999), in which case the data cannot be taken at face value. Although attempts to minimise bacterial alteration were made by constantly refrigerating the accumulation bottles at 5°C, this could still have occurred. If it did, then it is more likely that C/N was altered than δ^{13}C and δ^{15}N. This is because bacteria tend to cause enrichment in heavier isotopes (e.g. Dijkstra *et al.* , 2006; Melillo *et al.* , 1989), the opposite to the change that would be required to produce the shifts observed in Figure 5.2. In addition, a large enough shift in δ^{15}N to put the compound samples back on the instantaneous trend would also put them all on the wrong side of bedrock. Bacterial breaking or weakening of carbon bonds, leading to a C-rich, N-poor component becoming labile and hence more likely to be lost during the acid carbonate removal process, could provide a mechanism. Alternatively, if organic matter in the dissolved load has a different composition, it could cause alteration of POM by reacting with or attaching to particulate matter during storage. This possibility could be tested by finding the composition of dissolved and particulate organic matter in paired samples.

Some of the 12 July instantaneous samples that were not filtered until nearly two weeks after collection did not show any deviation from the trend defined by the rest of the instantaneous samples, but since the composition of these was towards the non-fossil end of the range where the two trends overlap, this is inconclusive. As a further test of the potential effects of storage, three pairs of samples were collected over discharges ranging from Q/Q_{mean}=0.1 to Q/Q_{mean}=3.8; one was filtered immediately and the other left in a refrigerated bottle for at least two months before filtration. They were otherwise treated identically. The differences between the pairs are shown in Table 5.2. No consistent patterns are apparent that could explain the observed trends: in the first case, the sample left to stand had higher C_{org}, higher C/N and less negative δ^{13}C and δ^{15}N than the sample filtered immediately (in agreement with behaviour expected from bacterial activity, but opposite to the shifts required), while in the pair collected at the highest discharge, the trend for C_{org}, C/N and δ^{15}N was reversed. In conclusion, no available evidence indicates that protracted storage of river water samples before filtration has an effect on POC composition.

A third possible explanation for the difference between the instantaneous and compound trends is that the compound sampling procedure could result in a loss of organic

Date	Discharge ($l\ s^{-1}$)	Difference (left to stand−filtered instantly) C_{org} (%)	C/N	$\delta^{13}C$ (‰)	$\delta^{15}N$ (‰)
26-Sep-11	4.3	1.20	0.67	0.27	0.72
25-May-12	25.9	0.82	2.63	0.66	-0.74
04-Jun-12	148	-0.15	-0.65	0.07	-0.83

Table 5.2: Effect of protracted pre-filtration storage on the organic carbon concentration (C_{org}), organic carbon to nitrogen ratio (C/N), carbon isotopic composition ($\delta^{13}C$) and nitrogen isotopic composition ($\delta^{15}N$) Erlenbach suspended sediment samples. Differences shown are parameters measured in samples filtered immediately subtracted from equivalents measured in those left for at least two months.

matter, perhaps related to the lower density of such material and hence its different behaviour during flow through pipes. Although complex, this could potentially be investigated further by a careful comparison of instantaneous samples collected at the same time time as impulses triggered by the automated system: in effect, creating a "compound" sample from instantaneous ones. However, there was no time to do so during this project, and so data from the compound samples are accepted at face value.

5.2.3 Long-term fluxes from Erlenbach compound samples

It is necessary to attempt the calculation of long-term fluxes from Erlenbach compound samples in order to provide a direct comparison for similarly calculated fluxes from the Vogelbach later in the chapter. This cannot be done in the same way as for the Erlenbach instantaneous samples because there is no correlation between discharge and tPOC, fPOC or nfPOC (Figure 5.5(a)); however, several other approaches may be used. Differences between the two sets of Erlenbach fluxes calculated in this and the previous chapter serve to highlight the limitations of using compound samples in flux estimates.

5.2.3.1 Direct integration

Because the compound samples represent the total sediment load for the entire period since the last sample, yields can be calculated by integrating POC concentration and mean discharge over a week's time interval, and summing them. For the Erlenbach, this can be done for the 12-month period from August 2009 to July 2010. Unfortunately there are many weeks (15 out of a total of 52) that are not represented by a sample because there was not enough water or sediment. For these, SSC of 10 mg l^{-1}, C_{org} of 1%, and F_{nf} of 0.2 were inserted: these are typical values of samples collected

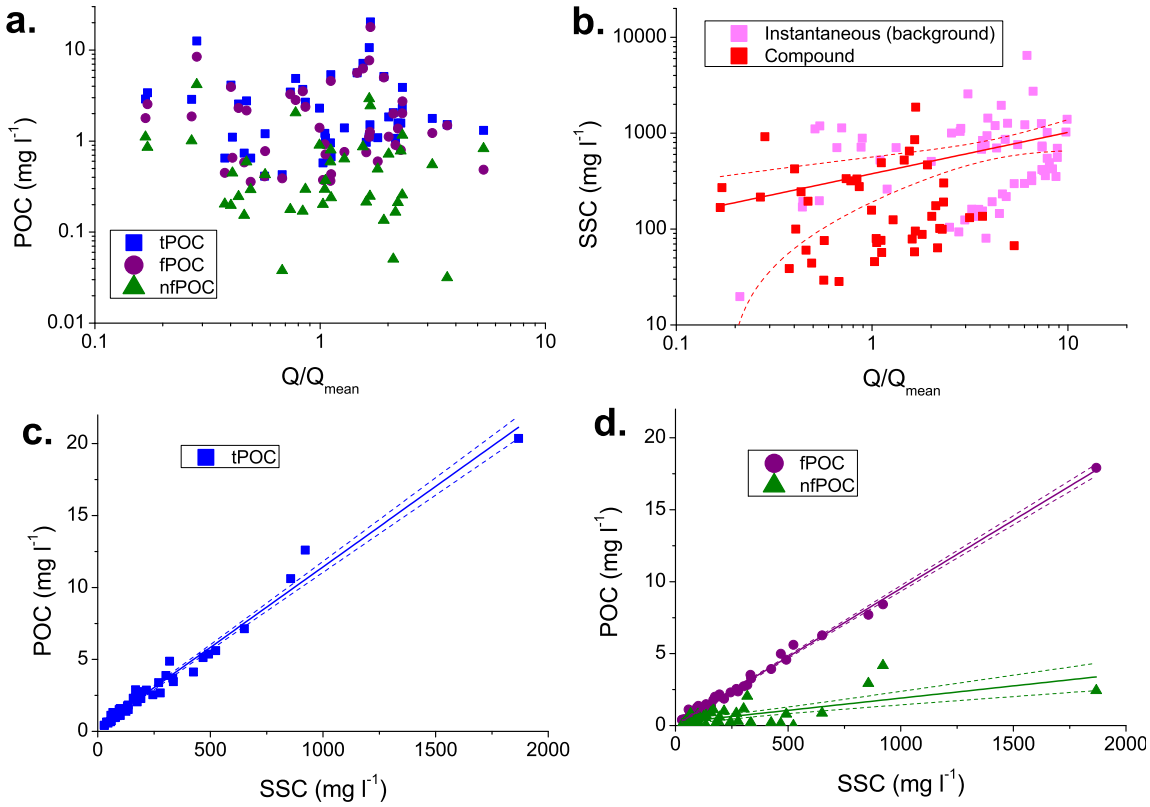

Figure 5.5: Relationships between discharge, SSC and POC using data from the Erlenbach compound samples. (**a**) Total, fossil and non-fossil POC plotted against Q/Q_{mean}. (**b**) SSC plotted against Q/Q_{mean}; both the compound samples and the instantaneous samples with Q/Q_{mean} <10 were used to fit the curve. (**c**) Total POC plotted against SSC. (**d**) Fossil and non-fossil POC plotted against SSC. Solid lines are power (for (**b**)) or linear fits to the data; dashed lines are 95% confidence bands.

	a	**b**	**c**	**d**	$\mathbf{R^2}$
Q/Q_{mean}–SS	378±94	0.43±0.16	-	-	0.08
SSC–tPOC	-	-	0.24±0.09	0.011±0.00	0.98
SSC–fPOC	-	-	0.04±0.05	0.009±0.00	0.99
SSC–nfPOC	-	-	0.21±0.12	0.002±0.00	0.44

Table 5.3: Erlenbach rating curve parameters for a power law relationship between Q/Q_{mean} and suspended sediment (SS) of the form $SS=a(Q/Q_{mean})^b$, and for linear relationships between POC and SSC, of the form $POC=c+d$SSC. There are three classes of POC: total (tPOC), fossil (fPOC) and non-fossil (nfPOC). Correlation coefficients are given as R^2. These are based only on the compound sample set, except for the relationship between SS and Q/Q_{mean}, which is based on the compound sample set plus instantaneous samples with Q/Q_{mean} <10.

	1983–2011, modelled from rating curves			**Flux 2009-2011** ***(compound samples)***
	Export flux (t km^{-2} yr^{-1})	**Conservative flux**	**Very conservative flux**	
SS	1100±640	730±300	510±190	200
tPOC	13±7.3	8.5±3.5	6.1±2.2	2.8
fPOC	11±6.2	7.0±2.9	4.9±1.8	1.9
nfPOC	2.3±1.2	1.5±0.7	1.2±0.5	0.9
F_{nf}	0.2±0.0	0.2±0.0	0.2±0.0	0.2

Table 5.4: Modelled fluxes of SS and total, fossil and non-fossil POC from the Erlenbach using the compound sample set. All figures are mean annual fluxes, given in t km^{-2} yr^{-1}. The first three columns are modelled over the period 1985–2011 inclusive using the relationships shown in Figure 5.5. "Export flux" is the total modelled flux assuming that the same relationships apply at all discharges; "Conservative flux" is the modelled yield assuming that the rating curve flattens at Q/Q_{mean}=5.3, the highest discharge sampled; "Very conservative flux" assumes that the contribution of flows higher than Q/Q_{mean}=5.3 is zero, i.e. the modelled flux for discharges of Q/Q_{mean} <5.3. Final column is the flux estimated over the period August 2009 to July 2010 calculated by integrating concentrations from the compound sample set. F_{nf} is the fraction of POC derived from non-fossil sources.

at similarly low-flow conditions that were analysed. By this method, the total flux of POC from the Erlenbach between August 2009 and July 2010 was 2.6 t km^{-2} yr^{-1}, and equivalents for fPOC and nfPOC were 1.8 t km^{-2} yr^{-1} and 0.8 t km^{-2} yr^{-1}. These are almost an order of magnitude lower than the more robust fluxes calculated using the instantaneous sample set in Section 4.5 (23±6 t km^{-2} yr^{-1} of tPOC, with an overall F_{nf} of 0.6±0.0), and severely underestimate the proportion of POC from non-fossil sources. The comparison suggests that this method does not accurately approximate fluxes in the Alptal system.

5.2.3.2 Modelling using rating curves

This approach uses a weak power law relationship between Q and SSC, together with relatively well-defined linear relationships between SSC and tPOC, fPOC and nfPOC (Figure 5.5; Table 5.3), to model the export of these parameters over the 29-year period covered by the discharge records. Assuming these relationships hold at all discharges, the fluxes obtained are: 1100±640 t km^{-2} yr^{-1} (SS), 13±7.3 t km^{-2} yr^{-1} (tPOC), 11±6.2 t km^{-2} yr^{-1} (fPOC) and 2.3±1.2 t km^{-2} yr^{-1} (nfPOC), with an overall F_{nf} of 0.2±0.0. A more conservative picture is given by assuming a plateau in the rating curves beyond the highest discharge sampled, Q/Q_{mean}=5.3, and no further increase in POC concentration with increasing flow. A third model, assuming that

no material is contributed to the flux by flows with Q/Q_{mean} >5.3, since processes operating beyond this limit are unknown, takes this caution to its extreme. In reality this is very unlikely, but it puts a lower bound on the fluxes. The outcomes of all three models are given in Table 5.4. Again, all are lower than the more robust fluxes and F_{nf} calculated in the previous chapter, and none are within error, despite the large errors on the fluxes derived from compound samples resulting from propagation of large uncertainties on rating curve parameters. This is likely primarily due to the sampling method's suppression of short-duration storm events that are disproportionately important in mobilising POC and particularly nfPOC.

5.3 Organic carbon in the Vogelbach

As Section 2.2 (page 19) describes, the Vogelbach catchment represents a different geomorphologic setting to the Erlenbach, despite their close proximity: it is steeper, drier and less prone to creep landsliding. Although the samples collected here (both source materials and suspended sediment) are far less numerous, they provide an important contrast to the Erlenbach and insights into the influence of geomorphology on POC export style.

5.3.1 Organic carbon in source materials

Multiple samples of bedrock, bedload and surface soil were collected; their chemical compositions are summarised in Table 5.5, and shown graphically in Figure 5.6.

5.3.1.1 Bedrock

Bedrock samples from the Vogelbach had mean C_{org} of 0.30%±0.31 (n=4), C/N of 9.28±5.1, and heavy C and N (δ^{13}C and δ^{15}N values of -26.11‰±0.23 and 2.72‰±0.89 respectively). The composition is adequately constrained in δ^{13}C relative to Erlenbach sources, but not so well constrained in δ^{15}N (Figure 5.6). There is an even larger variability—and hence error on the mean—in C/N (Figure 5.6). This makes it unsuitable for use as an end member when considering mixing processes, and for this reason the Erlenbach bedrock composition, within error of the Vogelbach mean in all chemical parameters, is used instead to represent the fossil input.

	n	**C_{org} (%)**		**C/N**		**δ^{13}C (‰)**		**δ^{15}N (‰)**	
		Mean	σ	**Mean**	σ	**Mean**	σ	**Mean**	σ
Bedrock	4	0.30±0.31	0.31	9.28±5.1	5.12	-26.11±0.23	0.23	2.72±0.89	0.89
	22	*0.54±0.11*	*0.26*	*7.81±1.7*	*3.98*	*-25.71±0.36*	*0.84*	*3.34±0.26*	*0.60*
Bedload	8	0.99±0.28	0.40	10.3±1.3	1.87	-26.30±0.13	0.18	2.57±0.45	0.63
	11	*0.87±0.21*	*0.36*	*9.78±0.9*	*1.57*	*-25.84±0.10*	*0.17*	*2.13±0.23*	*0.38*
Surface soil	12	15.1±7.6	13.2	17.0±1.6	2.74	-26.99±0.42	0.72	-3.29±0.93	1.61
	17	*16.5±6.3*	*12.9*	*17.9±2.2*	*4.45*	*-26.84±0.48*	*0.98*	*-1.33±0.77*	*1.59*
Suspended sediment	32	5.15±0.65	1.84	12.1±0.59	1.67	-26.98±0.09	0.25	-0.29±0.31	0.87
	45	*1.22±0.07*	*0.24*	*8.03±0.30*	*0.99*	*-26.31±0.05*	*0.18*	*1.98±0.16*	*0.54*

Table 5.5: Organic carbon concentration (C_{org}), organic carbon to nitrogen ratio (C/N), organic carbon isotopic composition (δ^{13}C) and nitrogen isotopic composition (δ^{15}N) of bedrock, bedload, surface soil and riverine suspended sediment sampled from the Vogelbach catchment. The equivalent values for the Erlenbach are given in italics beneath each line, for comparison; both suspended sediment values are for the discharge-proportional compound sample sets.

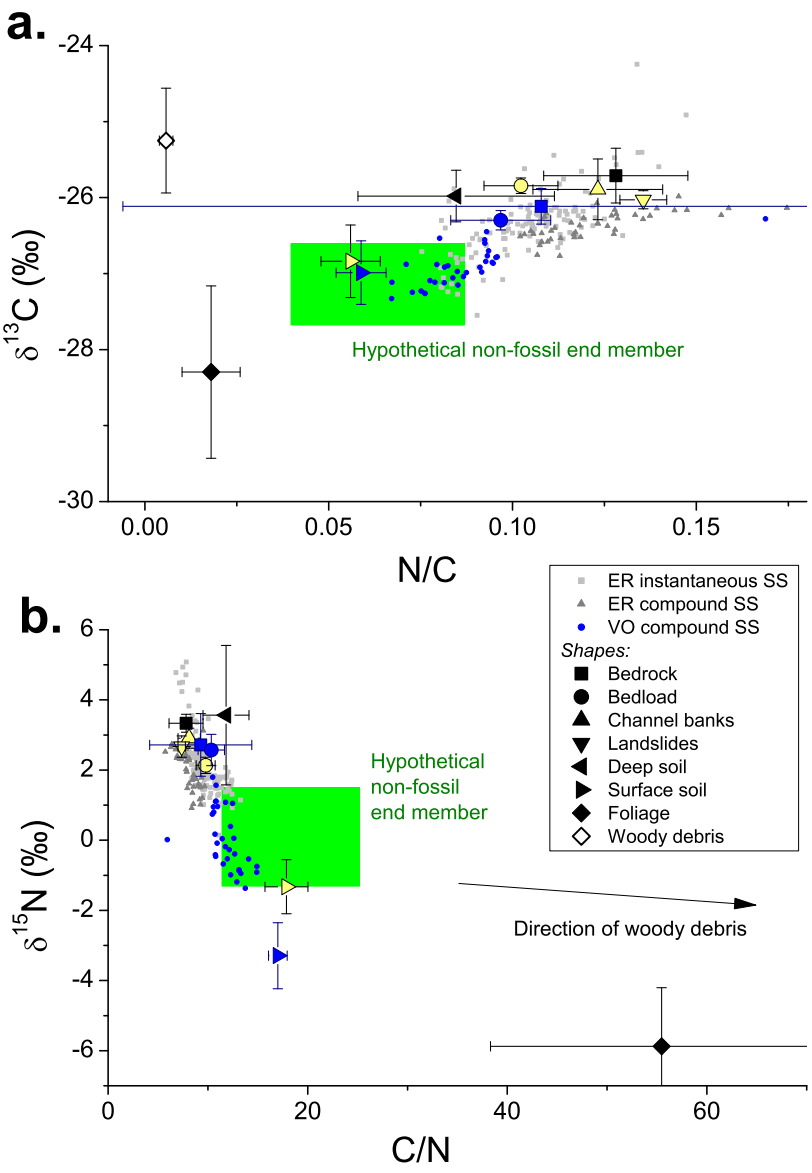

Figure 5.6: Chemical composition of organic matter in catchment stores and riverine suspended sediment (SS) from the Vogelbach (VO) and Erlenbach (ER) compound and instantaneous samples. (**a**) Nitrogen to organic carbon ratio (N/C) versus carbon isotopic composition (δ^{13}C); (**b**) Organic carbon to nitrogen ratio(C/N) versus nitrogen isotopic composition (δ^{15}N). Blue source symbols represent samples taken directly from the Vogelbach, black represents Erlenbach samples considered to be good proxies for the equivalent Vogelbach stores, and yellow represents Erlenbach samples not used as proxies for the Vogelbach, either because Vogelbach equivalents have been collected, or because they may be affected by the geomorphologic differences between the catchments (discussed in Chapter 2). The hypothetical non-fossil end member is the one calculated for the Erlenbach in Section 4.4.1.

Figure 5.7 shows a plot of modern C_{org} versus total C_{org}, where the x-intercept gives the C_{org} of the fossil end member (Galy *et al.* , 2008) as 1.52%±0.94, within error of the Erlenbach fossil C_{org} derived in the same way (0.74±0.23). Although this is higher than the measured mean value of 0.30%±0.31 (n=4), emphasising the lack of representativeness of the collected samples in terms of what the stream erodes, both estimates have large errors, and no real conclusions can be drawn.

Raman spectra and cross-plot for Vogelbach bedrock (Figure 5.8) show that the fossil organic carbon it contains is, in general, more disordered than in Erlenbach bedrock (Figure 4.1, page 79): here there is scant evidence of any graphite. Since Vogelbach bedrock is Cretaceous in age and Erlenbach bedrock is largely Eocene, this indicates that the source for the flysch changed over time. During the early phase, particles came only from sedimentary cover, resulting in recycling of some organic carbon but no graphite. By the Eocene, metamorphic rocks had been exhumed and contributed graphitised organic carbon to flysch deposits.

5.3.1.2 Bedload and surface soil

In contrast to bedrock, Vogelbach-specific bedload and surface soil are well-constrained source pools, with very similar errors to their Erlenbach counterparts.

Bedload C/N was similar in the Vogelbach to the Erlenbach, with a mean of 10.3±1.3 (n=8). Vogelbach bedload mean δ^{15}N of 2.57‰±0.45 was more positive than the Erlenbach value, though still within error of it, but it was distinguished by a significantly lower δ^{13}C of -26.30‰±0.13. It also had a slightly higher C_{org} of 0.99%±0.28.

Vogelbach surface soil composition is almost identical to that in the Erlenbach in N/C–δ^{13}C space, but plots slightly differently in C/N–δ^{15}N space (Figure 5.6) owing to its lighter N (δ^{15}N=-3.29‰±0.93 (n=12)). Samples had mean C/N of 17.0±1.6 and δ^{13}C of -26.99‰±0.42. The C_{org} values of surface soils from the two catchments were well within error of each other, Vogelbach surface soil having a value of 15.1%±7.6. This chemical coincidence reflects the similarity of soil types, and hence soil formation processes, between the two catchments (Section 2.2.5, page 24).

5.3.1.3 Other sources

It is apparent (Figure 5.6) that the source materials collected independently in the Vogelbach are not vastly disparate from the Erlenbach equivalents, with only minor differences outside of within-pool variation. Deep soil is a derivative of bedrock and surface soil, so it is probable that this will also be similar in both catchments. In-

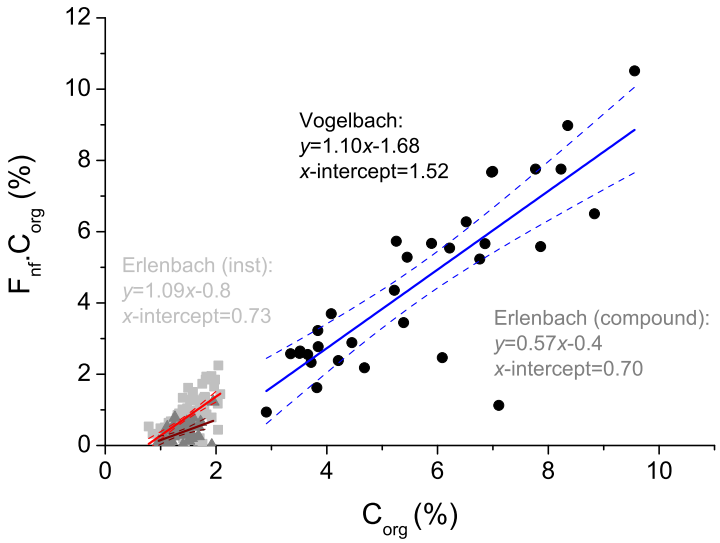

Figure 5.7: Modern carbon concentration (F_{nf} x C_{org}) of riverine suspended sediment versus total carbon concentration (C_{org}) for Vogelbach samples (black circles) and compared to Erlenbach compound samples (dark grey triangles) and instantaneous ("inst") samples (light grey squares; also shown in Figure 4.11, page 98). Solid lines show best fit; dashed lines are 95% confidence bands.

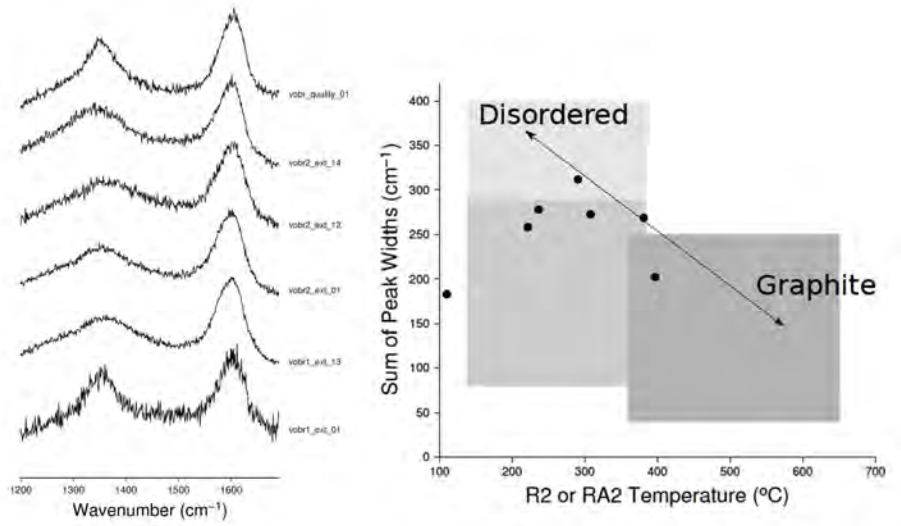

Figure 5.8: Raman spectra from organic carbon in Vogelbach bedrock samples (left) and cross-plot showing peak width versus temperature (right). The spectra are stacked from least ordered carbon at the top to most ordered at the bottom; peak height is relative and reflects Raman intensity. In the cross-plot, grey boxes reflect the space typically occupied by very disordered (light grey), somewhat disordered (medium grey) and ordered (dark grey) organic carbon. "Temperature" is an estimate of the maximum temperature that a particular carbon particle has been exposed to; R2 and RA2 refer to methods of estimating this parameter. For details, see Sparkes (2012).

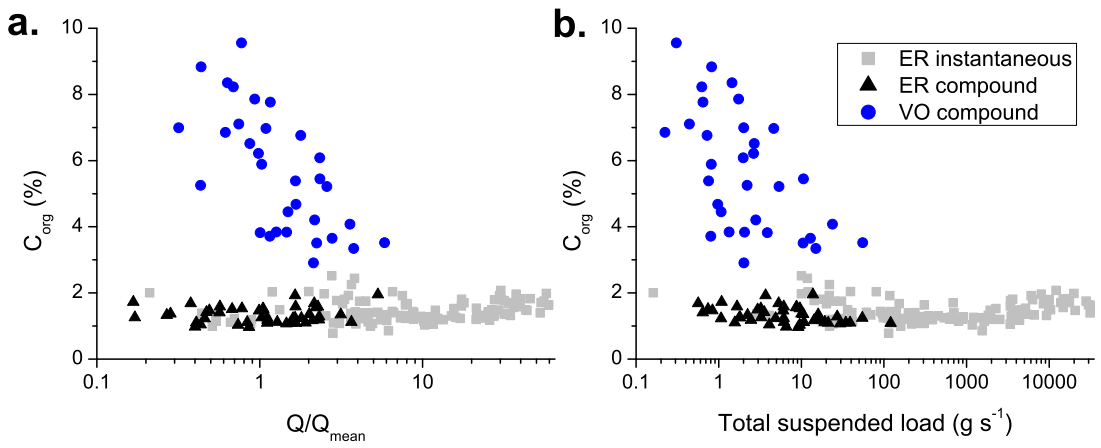

Figure 5.9: Organic carbon concentration (C_{org}) in Vogelbach (VO) and Erlenbach (ER) compound suspended sediment samples, plotted against (**a**) discharge (expressed relative to Q_{mean}) and (**b**) total suspended load. Erlenbach instantaneous samples, discussed in Chapter 4, are also shown for comparison. Note logarithmic x-axes.

dividual plant species are also likely to show comparable values, and although the proportions may differ slightly, this is not likely to have a significant effect on the catchment-averaged values of foliage or wood. Landslides, especially those which regularly feed into the channel, are not developed in the Vogelbach as they are in the Erlenbach, and are unlikely to be a significant source for suspended POM under the conditions sampled.

If the same relationship holds as in the Erlenbach, then channel bank sources will be derived from, and have a similar composition to, bedrock. However, this cannot be assumed, because there is a strong geomorphological element to the development of channel banks and the geomorphologic regimes of the two catchments are different (Section 2.2.4, page 22). Therefore, the composition of channel banks in the Vogelbach is unknown.

5.3.2 Organic carbon concentration and composition in the suspended load

Suspended sediment samples for the Vogelbach consist of 32 discharge-proportional compound samples collected between August 2009 and September 2011. As a group, they contained significantly higher proportions of organic carbon than either of the Erlenbach suspended sediment sample sets, with a mean C_{org} of 5.15%±0.65 (n=32). The range in C_{org} was 2.91% to 9.56%, and σ was 1.84%.

Figure 5.9 shows Vogelbach C_{org} plotted against discharge and total suspended

load. Both show decreasing C_{org} as flow and turbidity increase. These inverse relationships are significant at the 0.05 level, with Kendall's correlation coefficients of -0.50 and -0.43 respectively. These plots suggest that the sample set collected may represent the equivalent of the initial dilution phase for the Erlenbach indicated in Figure 4.9 (page 93), with discharges and sediment loads high enough to trigger the switch to POC addition by hillslope activation never reached. They also demonstrate the much higher C_{org} in the Vogelbach compared to both Erlenbach sample sets, which must be a consequence of lower SSC. Figure 2.7 (page 27) shows that the Vogelbach typically has SSCs which are ten times lower than in the Erlenbach, and this is reflected in the mean SSC values of each of the sample sets: 35 mg l^{-1} for the Vogelbach, 251 mg l^{-1} for Erlenbach compound samples, and 2920 mg l^{-1} for Erlenbach instantaneous samples. If SSC in the Vogelbach is ten times lower, yet C_{org} is only three times higher, then this suggests that input of organic carbon to the Vogelbach stream is actually lower than it is in the Erlenbach by approximately two thirds.

In terms of composition, suspended sediment from the Vogelbach had higher C/N and lighter C and N than suspended sediment from the Erlenbach, with mean values of C/N=12.1±0.59, δ^{13}C=-26.98‰±0.05 and δ^{15}N=-0.29‰±0.16. The samples plot on broadly the same linear trend as both sets of Erlenbach samples in both N/C–δ^{13}C and C/N–δ^{15}N space, but closer to surface soil (Figure 5.6). Figure 5.3 suggests that there is no systematic change in composition with TSL.

5.3.3 Sources and pathways of organic carbon

5.3.3.1 F_{nf} of organic carbon in the suspended load

As shown in Figures 5.3 and 5.6, many Vogelbach suspended sediment samples plot within the range of the hypothetical non-fossil end member calculated for the Erlenbach in Section 4.4.1 (page 96). Given the observed similarity of surface soil in the two catchments, and predicted similarity of vegetation end members, this is likely to be a good proxy for the non-fossil end member in the Vogelbach in the absence of any radiocarbon measurements that would allow its direct calculation. This is supported by Figure 5.7, where the regression line has a gradient, representing F_{mod} of the non-fossil end member (Galy *et al.* , 2008), of 1.10±0.14—well within error of the Erlenbach equivalent.

It appears, then, that close to 100% of the organic carbon in many of these samples comes from non-fossil sources. Modelling F_{nf} using Erlenbach bedrock and hypothetical non-fossil end member compositions gives a mean F_{nf} value for these samples of 0.88±0.06. This is higher than for the instantaneous Erlenbach sample set (mean

F_{nf} of 0.60±0.05), and much higher than for the compound Erlenbach dataset (mean F_{nf} of 0.42±0.04), which is a more appropriate comparison. This result fits with the observed higher C_{org} of Vogelbach suspended sediment: since fossil sources contain only around 0.5%–1.5% organic carbon (depending on whether chemical analysis of samples or the regression in Figure 5.7 is taken), C_{org} values of ∼5%–6% require the input of substantial amounts of non-fossil material.

It is worth briefly considering how changing the bedrock composition affects F_{nf}. If the Vogelbach mean bedrock composition from the four samples collected is used, the mean F_{nf} of the suspended sediment samples becomes 0.83±0.08: still significantly higher than either of the Erlenbach sample sets.

5.3.3.2 POC mobilisation in the Vogelbach

Under low-to-moderate flow conditions, the POC exported from the Vogelbach is much more influenced by non-fossil sources than the POC exported in the Erlenbach under the same conditions. Not enough samples could be collected from the Vogelbach to track patterns of seasonality as in the Erlenbach. It is unclear whether the non-fossil material comes from soil, foliage or a mixture, although the lack of any suspended sediment compositions falling between foliage and surface soil is slim evidence for a dominance of the former, and this has been assumed in using the Erlenbach hypothetical non-fossil end member.

As argued in Section 5.3.2, organic carbon inputs to the stream are lower in the Vogelbach than under similar conditions in the Erlenbach, represented by the compound samples. However, they are not uniformly lower: to account for the higher F_{nf} in the Vogelbach, fossil organic carbon input must be reduced by ∼90%, while non-fossil input must remain constant.

How is the fossil organic carbon input reduced? This is likely to have a geomorphological explanation arising from lithological differences. Because the substrate in the Vogelbach is sandier, hillslopes are better-drained and more stable, so there is no creep landsliding to maintain a regular supply of bedrock-derived POC to the channel. Non-fossil inputs—fallen leaves; soil that has gradually worked its way into the channel under gravity or in the runoff during previous rainfall—are the same as in the Erlenbach under similar conditions (i.e. when the hillslopes are not active). Given the steeper slopes and beech-suppressed understory (von Wühlisch, 2008), which would not soak up minimal runoff as effectively as a fully-vegetated slope, the transfer of such material may be somewhat easier than in the Erlenbach.

An explanation reconciling the apparent dilution shown in Figure 5.9 with the lack

of compositional shift exhibited in Figure 5.3 is still elusive. This discrepancy could be resolved if there is large compositional variability in the bedrock: in that case, there could be a decrease in C_{org} without a discernible trend in composition over the number of samples collected. Similarly, if the true mean C_{org} of bedrock was very low, then implausibly large amounts of lithic material would need to be added to systematically affect the composition, but increased mobilisation of it would still explain the dilution. However, Figure 5.7 suggests that Vogelbach bedrock C_{org} is higher than Erlenbach bedrock C_{org}. The alternative is that the decrease in C_{org} with discharge and TSL is not a dilution by lithic material, but a reduction in input. However, it is difficult to see why this should be so, and why the same is not observed in the Erlenbach. Characterising the organic carbon content and composition of Vogelbach bedrock more comprehensively could help to solve this, but as has been shown in the Erlenbach (Section 4.2.1), this would not be an easy task. More useful would be to collect instantaneous suspended sediment samples over a series of large storm events: the hysteresis in C_{org} and compositional parameters should shed light on the mechanisms of POC mobilisation. Unfortunately, the opportunity to do this did not arise within the timescale of the project.

5.3.4 Long-term POC export

Because the direct integration method has been shown not to accurately approximate long-term fluxes in the Alptal system (Section 5.2.3.1), and because a higher proportion of weeks in the Vogelbach than in the Erlenbach are missing samples, only the rating curve modelling method is used here to estimate export fluxes.

Rating curves and their numerical parameters for relationships between discharge, suspended sediment and POC in the Vogelbach compound sample set are shown in Figure 5.10 and Table 5.6. The line for nfPOC has a considerably higher gradient than the one for fPOC, indicating that nfPOC is mobilised at a faster rate than fPOC as SSC increases. This is in agreement with the observation—discussed in Section 5.3.3.2—that the progressive dilution of POC shown in Figure 5.9 is not accompanied by a shift of the POC from non-fossil to fossil composition; indeed, these rating curves suggest the opposite.

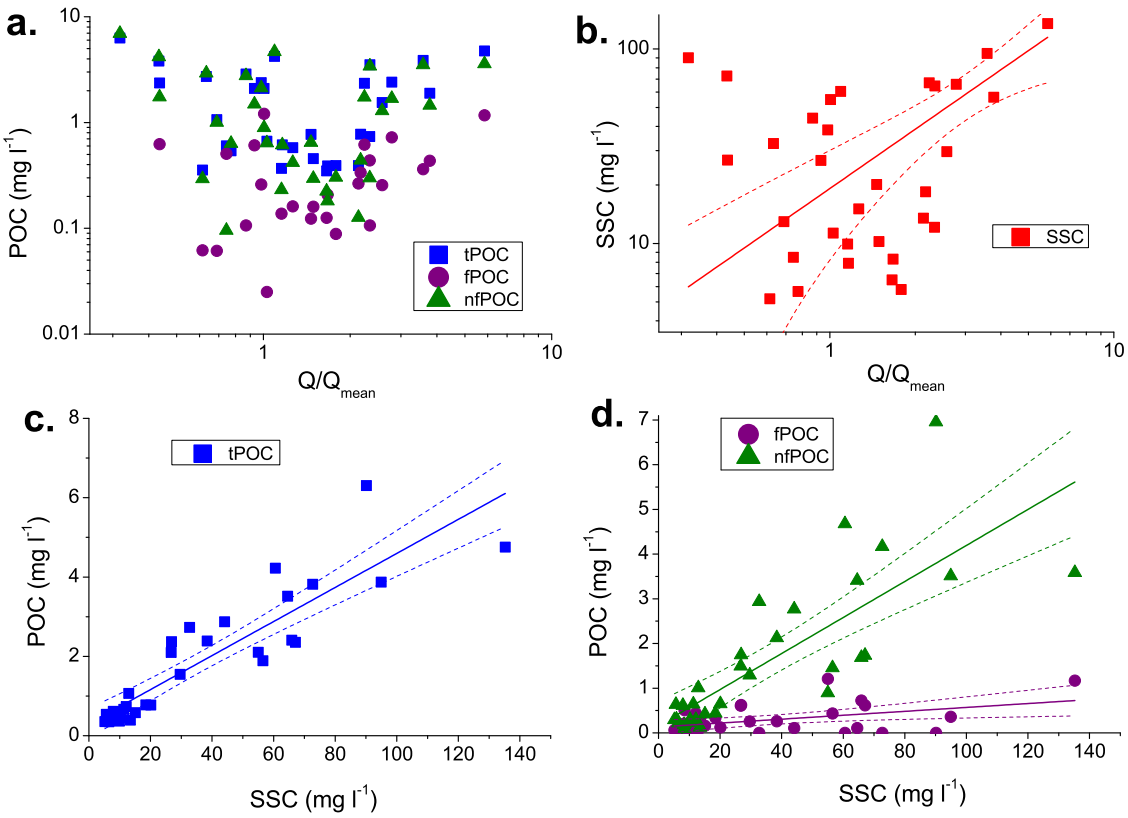

Figure 5.10: Relationships between discharge, SSC and POC in the Vogelbach. (**a**) Total, fossil and non-fossil POC plotted against Q/Q_{mean}. (**b**) SSC plotted against Q/Q_{mean}. (**c**) Total POC plotted against SSC. (**d**) Fossil and non-fossil POC plotted against SSC. Solid lines are power (for (**b**)) or linear fits to the data; dashed lines are 95% confidence bands.

	a	**b**	**c**	**d**	**R^2**
Q/Q_{mean}–SS	19.2±5.4	1.01±0.23	-	-	0.22
SSC–tPOC	-	-	0.30±0.19	0.043±0.00	0.79
SSC–fPOC	-	-	0.13±0.08	0.004±0.00	0.17
SSC–nfPOC	-	-	0.16±0.27	0.040±0.01	0.62

Table 5.6: Vogelbach rating curve parameters for a power law relationship between Q/Q_{mean} and suspended sediment (SS) of the form $SS=a(Q/Q_{mean})^b$, and for linear relationships between POC and SSC, of the form $POC=c+d$SSC. There are three classes of POC: total (tPOC), fossil (fPOC) and non-fossil (nfPOC). Correlation coefficients are given as R^2.

Using the same modelling approach as for the Erlenbach compound samples, fluxes based on the Vogelbach compound sample set are: 140±130 t km^{-2} yr^{-1} (SS), 6.6±5.8 t km^{-2} yr^{-1} (tPOC), 0.8±0.7 t km^{-2} yr^{-1} (fPOC) and 6.0±7.5 t km^{-2} yr^{-1} (nfPOC), with an overall F_{nf} of 0.9±0.3. These and results from two more conservative models (with the same criteria as used for the Erlenbach compound samples in Section 5.2.3.2) are shown in Table 5.7. The large errors again result from large uncertainties on the rating curve parameters.

Following these calculations, it can be said that, *under background conditions*, on the order of 3–4 t km^{-2} yr^{-1} of POC are exported from the Vogelbach, of which ∼90% is derived from non-fossil sources. This estimate should be representative on long time scales, as it is not prone to the effects of extreme events, but the large errors mean that it can at best be taken as a very rough estimate.

The modelled Vogelbach fluxes are likely to be an underestimate for the same reasons as for fluxes derived from Erlenbach compound samples: principally, that the compound sampling method minimises the contribution of short-lived storms that are disproportionately important in mobilising sediment and particularly POC. Because of the suppressed response of Vogelbach discharge and SSC to rainfall compared with the Erlenbach, the underestimation is likely to be less dramatic, but beyond this it is impossible to tell its magnitude because the carbon dynamics operating during such events are unconstrained. The difference between the Erlenbach fluxes calculated from compound and instantaneous sample sets can be used as a rough correction to account for hillslope activation during storms. From the compound samples, the Vogelbach exports per unit area around ∼50% of the tPOC exported by the Erlenbach. From the Erlenbach instantaneous samples, this would equate to ∼11 t km^{-2} yr^{-1} of tPOC and (using an F_{nf} of 0.9) ∼10 t km^{-2} yr^{-1} of nfPOC, ∼70% of the Erlenbach nfPOC export. However, because of the sampling limitations, it is unclear whether POC is added through hillslope activation during storms as in the Erlenbach, in which case such a correction should be applied, or continues to be diluted, in which case there should be no correction. Hence, both the corrected and uncorrected figures must be used to bound the estimated export fluxes, giving values of ∼100–200 t km^{-2} yr^{-1} for SS, ∼3–11 t km^{-2} yr^{-1} for tPOC, ∼0.5–1 t km^{-2} yr^{-1} for fPOC and ∼3–10 t km^{-2} yr^{-1} for nfPOC.

The large number of assumptions necessary means that these flux estimates should be regarded only as an indication of the order of magnitude of the quantities of sediment and total, fossil and non-fossil POC exported from settings like the Vogelbach.

	1985-2011, modelled from rating curves		
	Export flux (t km^{-2} yr^{-1})	**Conservative flux**	**Very conservative flux**
SS	140±130	65±37	44±22
tPOC	6.6±5.8	3.2±1.9	2.3±1.2
fPOC	0.8±0.7	0.5±0.3	0.4±0.2
nfPOC	6.0±7.5	2.9±2.6	2.0±1.8
F_{nf}	0.9±0.3	0.9±0.3	0.9±0.3

Table 5.7: Modelled fluxes of SS and total, fossil and non-fossil POC from the Vogelbach. All figures are mean annual fluxes, given in t km^{-2} yr^{-1}, modelled over the period 1985-2011 inclusive using the relationships shown in Figure 5.10. "Export flux" is the total modelled flux assuming that the same relationships applies at all discharges; "Conservative flux" is the modelled flux assuming that the rating curve flattens at Q/Q_{mean}=5.2, the highest discharge sampled; "Very conservative flux" assumes that the contribution of flows higher than Q/Q_{mean}=5.2 is zero, i.e. the modelled flux for discharges of Q/Q_{mean} <5.2.

5.4 Chapter summary

Despite the slightly differing compositional trends of Erlenbach instantaneous and compound samples, there is no evidence that the latter data should not be taken at face value: they are not systematically affected by protracted storage. Although these discharge-proportional compound sample sets from the Erlenbach and Vogelbach greatly dilute the effects of large, short-lived events, they still offer insights into POC mobilisation in Switzerland that cannot be gained from the Erlenbach instantaneous dataset examined in Chapter 4.

POC mobilisation in the Erlenbach has a seasonality beyond the effects of discharge. C_{org} and relative input of non-fossil material in the suspended load is low or variable over the autumn and winter, before increasing through spring as the snow melts, leading to accumulation of non-fossil material from the hillslope in the channel, augmented by new plant growth. Sharp drops in both C_{org} and non-fossil influence occur after the large summer storms, which sweep the channel clear of this material leaving bedrock-derived sediment to dominate.

Most organic carbon stores in the Vogelbach catchment are compositionally the same as those in the Erlenbach to first order, yet Vogelbach suspended load contains around three times as much organic carbon as a percentage of total sediment. Because SSC is around ten times lower in the Vogelbach, this actually corresponds to a decrease in organic carbon input compared to the Erlenbach. The reduction occurs entirely in fossil POC, and is a result of higher geomorphologic stability leading to reduced lithic supply to the channel. Consequently, Vogelbach suspended sediment, even in

background conditions, has a much higher F_{nf} than the Erlenbach of over 0.8. As flow increases, more lithic material is mobilised, resulting in a progressive dilution of organic carbon. However, unlike in the Erlenbach, this is not accompanied by a compositional shift towards fossil material, possibly indicating that bedrock entering the Vogelbach suspended load has highly variable composition.

There is no correlation between discharge and POC concentration in the Vogelbach samples, but a weak power law rating curve relating SSC to discharge and good linear relationships between POC and SSC can be used to estimate export fluxes of total, fossil and non-fossil POC. In reality these are only lower bounds because the compound samples exclude or severely reduce the contribution of storm events and therefore underestimate total annual yields, as shown by a comparison of export fluxes calculated from the Erlenbach instantaneous and compound datasets. A correction based on this comparison can be made to estimate a ball-park upper bound for the true fluxes of material from the Vogelbach. These methods indicate that on the order of 3–11 t km^{-2} yr^{-1} of POC are exported from the Vogelbach, of which ∼90% is derived from non-fossil sources. As in the Erlenbach, this export is entirely runoff-driven, occurring under very moderate climatic conditions and requiring no rapid or deep-seating mass wasting. Mechanisms operating when these do occur remain unconstrained, but such times are likely to be infrequent.

Chapter 6

Organic carbon mobilisation and export in Oregon's uplands

6.1 Introduction

The previous two chapters established the major sources of organic carbon in the riverine suspended load of two neighbouring catchments in the Swiss Prealps, the mechanisms by which this material is transferred from hillslopes, and the export fluxes of total, fossil and non-fossil POC from these catchments. In this chapter, the same is done for a large catchment in the Oregon Cascades, Lookout Creek, and a smaller nested catchment, Watershed 1, both part of H.J. Andrews Forest observatory. Less comprehensive sample- and datasets from three other catchments, Hinkle in the Cascades, and Trask and Alsea in the Oregon Coast Range, are discussed alongside. The primary aim is to characterise organic carbon mobilisation and export in a second location geographically distant from Switzerland, in order to check the applicability of findings already described. Like Switzerland, Oregon offers the opportunity to study temperate, forested hillslopes in relatively undisturbed condition, but there are differences in ecosystem, geomorphologic regime and geology, which provides insights into the effects of specific factors on POC concentration, composition and routing. The substrate is largely volcanic; only Alsea is substantially underlain by sedimentary bedrock containing fossil organic carbon, and this is sandy rather than clay-rich as in the Alptal. Following the characterisation of processes operating in Oregon, Chapter 7 will compare POC dynamics in Switzerland and Oregon, and discuss how findings from these two studies may be extrapolated globally.

Catchment abbreviations used in figures in this chapter are as follows. WS1= Watershed 1, WS2=Watershed 2, LO=Lookout Creek; all are located at HJA=H.J. Andrews Forest. NFH=North Fork Hinkle (referred to in the text as Hinkle); TR=Trask and surrounding area; ALS=Alsea. When discussing Alsea suspended sediment, distinction is made between Flynn Creek and Deer Creek because of Deer Creek's history of intensive logging (Section 2.3.5, page 41) and the contrasting behaviour that results. River sampling methods are distinguished as follows: inst=instantaneous samples; compound or comp=discharge-proportional samples collected every two or three weeks; others collected by turbidity threshold sampling. See Chapter 3 for general sampling methods and catchment-specific details. As previously, uncertainties on mean source compositions are twice the standard error, σ=standard deviation, and means for suspended sediment are weighted by SSC in order to more accurately represent the bulk suspended load exported.

6.2 Organic carbon in source materials

Mean data for carbon stores in individual catchments, where at least three samples of the same type were taken, are presented in Table 6.1 and Figure 6.1(a) and (b). In most cases, equivalent pools in different catchments are within error of each other, and so in subsequent discussion the different catchment source materials are combined into an overall "Oregon" dataset, summarised in Table 6.2 and Figure 6.1(c) and (d). In the following sections, each organic carbon pool is reviewed individually. Refer to Section 3.2.2.2 (page 60) for sample location details.

6.2.1 Bedrock

Because much of the rock underlying the Oregon catchments is volcanic (Walker & King, 1969), fossil organic carbon is rarely present and hence plays a minimal role in POC dynamics here. As expected, given the wholly igneous geology of the Cascades (Section 2.3.2, page 31), bedrock samples from H.J. Andrews and Hinkle contain non-measurable amounts of organic carbon. No bedrock samples were obtained from Trask, where the substrate is largely volcanic but includes some siltstone and sandstone outcrops. Bedrock core samples from the Alsea watershed, underlain by estuarine and marine sandstones and siltstones, had C_{org} ranging from 0.04%–1.50%, with a mean of 0.43%±0.19 (n=23). They had low C/N (11.1±2.1), and relatively heavy C (δ^{13}C=-26.30‰±0.20) and N (δ^{15}N=1.04‰±0.84).

	n	C_{org} (%)		C/N		δ^{13}C (‰)		δ^{15}N (‰)	
		Mean	σ	**Mean**	σ	**Mean**	σ	**Mean**	σ
Bedrock ALS	23	0.43±0.19	0.45	11.1±2.1	4.96	-26.30±0.20	0.48	1.04±0.84	2.02
Bedload HJA-WS1	3	1.72±0.95	0.83	16.8±6.8	5.93	-26.75±0.42	0.37	2.17±2.46	2.13
Bedload HJA-LO	3	1.26±0.57	0.49	16.5±4.2	3.65	-27.13±0.33	0.29	5.37±0.87	0.75
Bedload NFH	3	1.50±0.71	0.62	23.3±4.3	3.70	-26.63±0.93	0.81	-1.36±2.37	2.05
Bedload TR	3	6.31±5.82	5.04	25.3±9.2	7.97	-26.37±0.85	0.74	-0.41±3.05	2.64
Deep soil HJA-WS1	15	2.30±1.2	2.41	30.7±14.9	28.9	-25.54±0.48	0.93	5.69±1.13	2.18
Deep soil NFH	16	2.39±1.9	4.01	23.3±3.9	8.04	-25.39±0.51	1.05	4.87±2.05	4.22
Deep soil TR	9	5.21±2.1	3.02	20.7±2.6	3.91	-24.97±0.23	0.34	2.79±0.70	1.05
Surface soil HJA-WS1	16	6.46±2.5	4.95	28.5±13.7	27.3	-26.93±0.49	0.98	1.06±1.08	2.16
Surface soil HJA-LO	11	7.71±4.2	7.03	26.8±34.8	57.6	-27.12±0.41	0.68	2.23±0.73	1.20
Surface soil TR	11	9.93±2.6	4.38	20.0±3.6	5.92	-26.47±0.52	0.86	1.97±0.64	1.06
Surface soil ALS	6	9.21±5.4	6.61	16.7±2.4	2.95	-27.37±0.85	1.05	1.81±1.43	1.75
Foliage HJA-WS1	22	51.0±1.7	4.06	47.6±21	48.8	-30.11±0.74	1.74	-1.50±0.66	0.81
Foliage HJA-LO	11	48.7±1.9	3.17	36.0±14	22.6	-30.64±1.11	1.84	-2.86±1.15	1.91
Foliage NFH	8	51.0±1.8	2.56	34.5±12	17.2	-30.87±1.64	2.32	-2.66±0.98	1.38
Foliage TR	6	51.3±1.9	2.36	22.0±7.0	8.52	-30.42±1.24	1.52	-2.10±1.29	1.59
Foliage ALS	5	51.0±2.8	3.09	29.9±16	18.4	-30.40±1.16	1.30	-2.57±1.58	1.77
Standing wood HJA-WS1	8	50.6±1.4	2.00	283±216	305	-27.95±1.72	2.43	-0.76±0.16	0.22
Standing wood HJA-LO	10	48.1±1.6	2.46	187±190	300	-27.82±1.13	1.79	-4.26±1.88	2.98
Standing wood NFH	4	48.9±1.4	1.42	216±118	118	-28.24±2.81	2.81	-3.64±1.50	1.50
Standing wood TR	3	47.5±1.5	1.29	203±150	130	-29.14±1.80	1.56	-4.22±4.81	4.16
Standing wood ALS	3	48.2±1.7	1.43	186±316	273	-27.98±2.08	1.81	-5.53±3.76	3.26
Woody debris HJA-WS1	4	51.8±6.5	6.46	221±102	102	-25.39±0.58	0.58	-3.64±1.31	1.31

Table 6.1: Organic carbon concentration (C_{org}), organic carbon to nitrogen ratio (C/N), organic carbon isotopic composition (δ^{13}C) and nitrogen isotopic composition (δ^{15}N) of major carbon stores from individual Oregon watersheds, where at least three samples of the same type were taken from the same watershed.

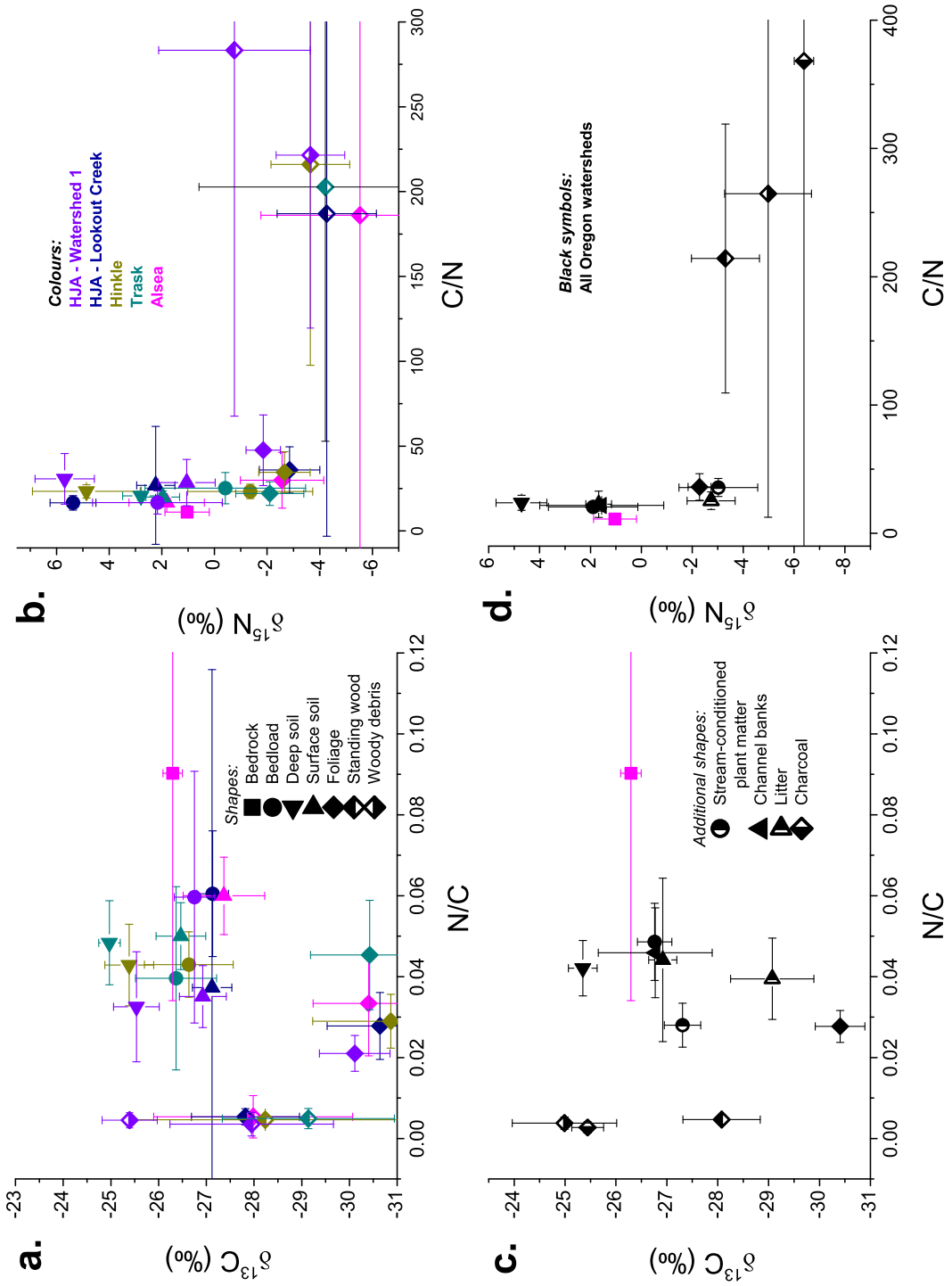

Figure 6.1: Chemistry of carbon pools in Oregon. (**a**) and (**b**) Pools in individual watersheds; (**c**) and (**d**) pools averaged across all Oregon watersheds. (**a**) and (**c**) Nitrogen to organic carbon ratio (N/C) versus organic carbon isotopic composition (δ^{13}C); (**b**) and (**d**) Organic carbon to nitrogen ratio (C/N) versus nitrogen isotopic composition (δ^{15}N). The shape of the symbols reflects the type of carbon pool; the colour reflects the watershed represented.

	n	C_{org} (%)		C/N		δ^{13}C (‰)		δ^{15}N (‰)	
		Mean	σ	**Mean**	σ	**Mean**	σ	**Mean**	σ
Bedload	14	2.76±1.5	2.86	20.6±2.8	5.23	-26.76±0.31	0.58	1.77±1.65	3.08
Stream-conditioned plant matter	7	6.07±3.9	5.15	35.7±7.0	9.22	-27.31±0.36	0.47	-3.02±1.55	2.05
Channel banks	5	7.91±6.8	7.63	21.8±4.5	5.02	-26.77±1.12	1.25	1.56±2.44	2.72
Deep soil	41	2.98±1.1	3.44	23.8±5.8	18.7	-25.35±0.28	0.90	4.71±1.00	3.20
Surface soil	44	8.02±1.7	5.62	22.7±10	34.0	-26.92±0.28	0.92	1.68±0.51	1.68
Litter	4	26.7±12	12.8	25.3±6.9	6.87	-29.07±0.82	0.82	-2.74±0.94	0.94
Foliage	52	50.5±1.0	3.45	36.1±10	37.4	-30.40±0.49	1.75	-2.29±0.45	1.62
Standing wood	28	48.9±0.8	2.22	214±105	277	-28.08±0.76	2.01	-3.31±1.34	3.54
Woody debris	7	52.0±3.8	5.07	265±252	333	-24.99±1.03	1.36	-4.98±1.70	2.25
Charcoal	4	69.8±6.2	6.18	368±526	526	-25.44±0.31	0.31	-6.39±0.38	0.38

Table 6.2: Organic carbon concentration (C_{org}), organic carbon to nitrogen ratio (C/N), organic carbon isotopic composition (δ^{13}C) and nitrogen isotopic composition (δ^{15}N) of major carbon stores averaged across all the Oregon watersheds in this study.

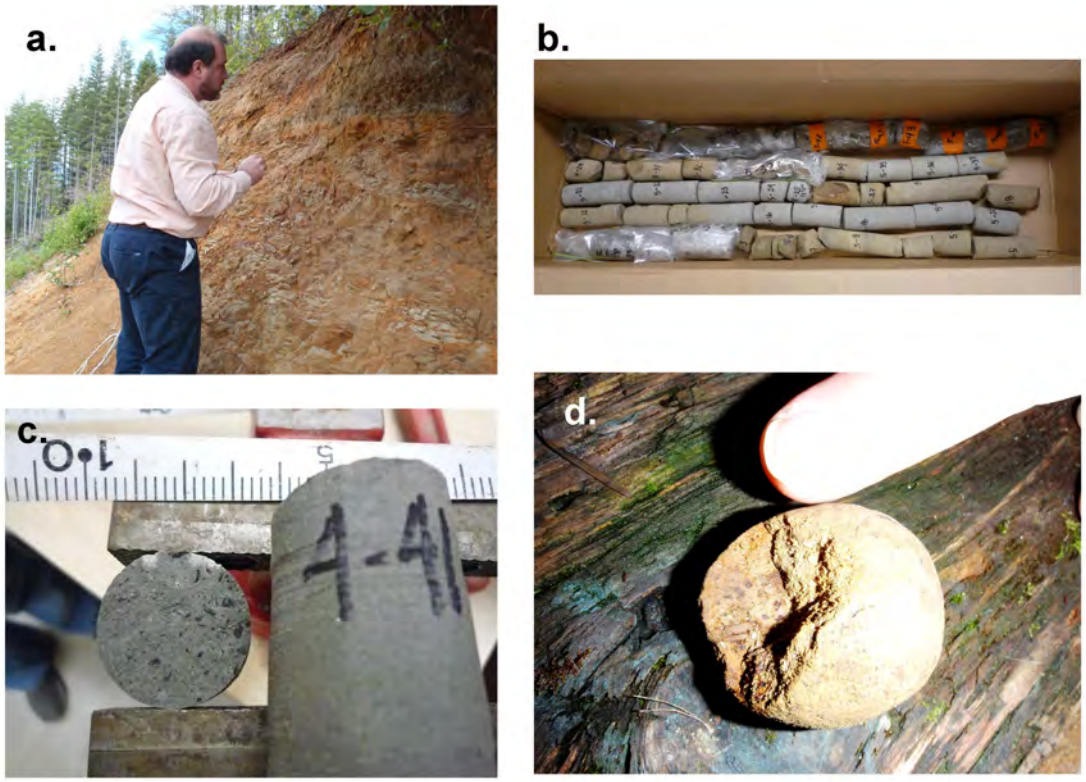

Figure 6.2: Fossil organic carbon oxidation in the Alsea watershed, Coast Range. (**a**) Bedrock outcrop showing extensive oxidation. (**b**) Core UNB-5, showing alternating oxidised and reduced sections, with more oxidation in the fractured sections. Pieces are numbered consecutively, ascending with depth. The length of the box is ∼60 cm. (**c**) Reduced section of core UNB-4 (piece 41), showing substantial fragments of organic matter. (**d**) Oxidised pebble from Flynn Creek bedload, showing remnants of organic matter.

6.2.1.1 Fossil organic carbon oxidation in the Coast Range

Although it is not directly related to the main aims of this chapter, the Alsea cores offer insight into the fate of bedrock organic carbon at depth (see Section 3.2.2.2 on page 60 for details of core sampling).

Many of the rock outcrops in the Coast Range, particularly in the Alsea watershed, are heavily oxidised (Figure 6.2(a).). In contrast, the cores have both oxidised and non-oxidised layers, identified by yellow to grey colour changes. Although oxidation is more prevalent close to the surface and reduction dominant at greater depths (in these cores, no oxidation occurs below ∼250 cm), there are some reduced zones near the surface, and places where oxidised and reduced layers alternate (e.g. core UNB-5; Figure 6.2(b).). This suggests that the situation is more complex than a single oxida-

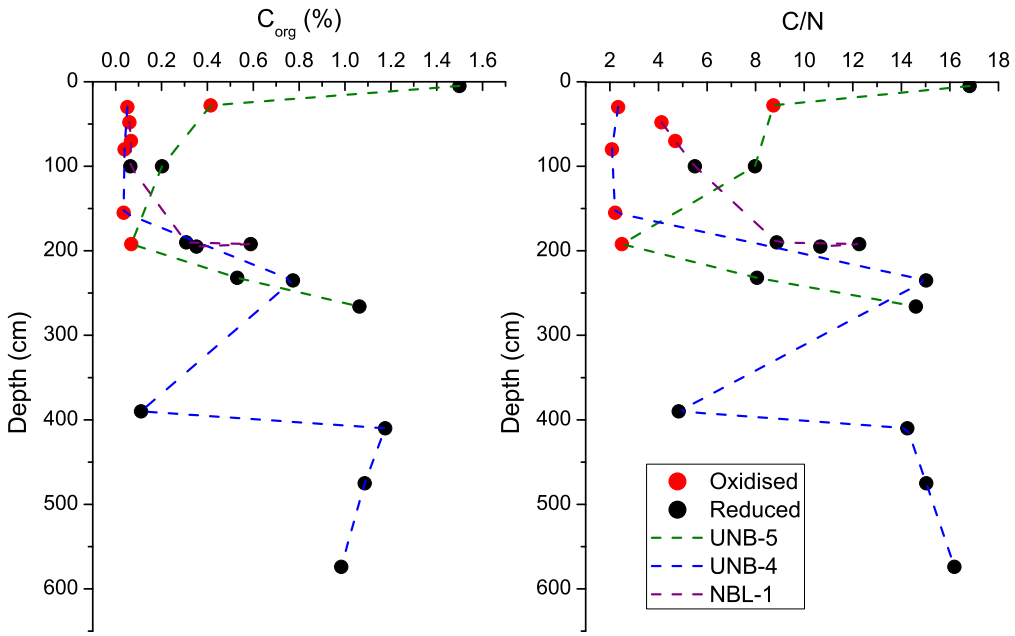

Figure 6.3: Organic carbon concentration (C_{org}) and organic carbon to nitrogen ratio (C/N) in organic matter from three bedrock cores from the Needle Branch catchment of Alsea watershed (UNB-5, UNB-4 and NBL-1). Samples from oxidised and reduced sections of the cores are indicated.

tion front moving downwards from the surface. A likely explanation is that oxidation also occurs along fracture zones, which act as conduits for oxygen-rich groundwater; indeed, the oxidised sections of the cores appear to be more broken up than the reduced sections (Figure 6.2(b)).

In many of the reduced sections, substantial fragments of organic matter were clearly visible, but there were also some organic remnants present in oxidised rocks (Figure 6.2(c) and (d)). These observations are reflected in the chemical analysis (Figure 6.3): while organic carbon was present at some level for all samples, there were strong differences in the C_{org} of the oxidised and reduced samples, with the oxidised samples having values in all cases less than 0.5%, and in all but one case less than 0.07%. The reduced samples had C_{org} values ranging from 0.06% to 1.5%. C/N values reflect these patterns, with reduced samples having on average greater C/N values than oxidised samples, indicating that N was affected to a much lesser extent by oxidation processes. There are no systematic changes in C or N isotopic composition, suggesting that there was no significant fractionation associated with the oxidation process.

In summary, some organic carbon loss has occurred in oxidised layers, concentrated in the top few metres of the rock mass. This has implications for riverine suspended

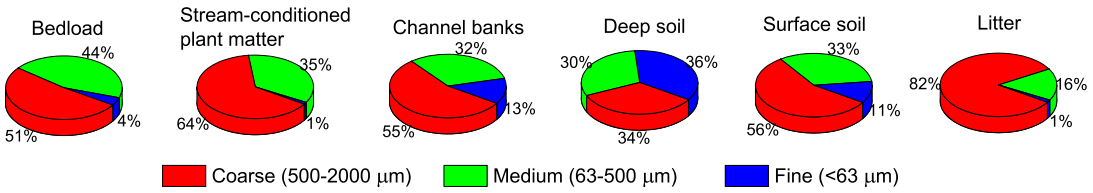

Figure 6.4: Distribution of grain size fractions in source sediments from all Oregon catchments.

sediment. If the stream erodes these oxidised surface layers, then input of fossil organic matter is likely to be low. But rivers cut deeper into the stratigraphy than the surrounding hillslopes; if the weathering front in the channel is closer to the surface because of faster erosion, then more fossil organic matter will enter the suspended load and POM chemistry will also be altered.

6.2.2 Bedload

Taking all catchments together, bedload samples from Oregon had mean C_{org} of 2.76%±1.5 (n=14), low mean C/N of 20.6±2.8 and relatively heavy C and N (δ^{13}C= -26.76‰±0.31; δ^{15}N=1.77‰±1.65). The mean compositions of bedload from H.J. Andrews, Hinkle, Trask and Alsea (the latter from only two samples) were within error of each other, except with regard to δ^{15}N, which was significantly higher at H.J. Andrews and slightly higher in the Alsea. The grain size distribution of bedload, along with other source sediments, is illustrated in Figure 6.4; only a minor proportion (4%) falls into the fine fraction (<63 μm), while just over half the remainder is coarse (500–2000 μm) and the rest medium-grained (63–500 μm).

6.2.2.1 Stream-conditioned plant matter

When plant material falls into or otherwise enters the channel, it can remain on the stream bed for some time undergoing decomposition, a process known as "stream conditioning" (Finlay, 2001). These samples, treated separately from bedload, consisted of both channel material obviously derived from plant matter—such as leaves—and organic-rich fines. They had higher C_{org} (6.07%±3.9 (n=7)) than the bulk bedload samples, and a significantly different composition in both N/C–δ^{13}C and C/N–δ^{15}N space (Figure 6.1). Their mean C/N of 35.7±7.0 was relatively high, and both δ^{13}C (slightly) and δ^{15}N (considerably) were more negative than wider bedload and channel bank samples, with mean values of -27.31‰±0.36 and -3.02‰±1.55 respectively. Stream-conditioned plant matter samples contained 64% coarse material and 35% medium-grained material, with almost no fines (Figure 6.4).

6.2.3 Channel banks

Few samples were collected from channel banks, reflecting the fact that they are commonly overhung by vegetation with little sediment visible. Those samples that were collected had higher C_{org} (7.91%±6.8 (n=5)) than bedload, but an indistinguishable chemical composition: C/N=21.8±4.5; δ^{13}C=-26.77‰±1.12; δ^{15}N=1.56‰±2.44. The C_{org} value (and hence C/N) is skewed by one sample from Trask with C_{org} of 20%, but even discounting this sample the compositional similarity to bedload remains. Channel bank samples had a slightly higher proportion of fine material (13%) than bedload, but were still dominated by coarse (55%) and medium (32%) fractions (Figure 6.4).

6.2.4 Soil

Surface soil (top ∼10 cm) and deep soil (10–200 cm) plot distinctly in both N/C–δ^{13}C and C/N–δ^{15}N space, and again, means from different catchments overlap within each category. Surface soil had higher C_{org} than deep soil: 8.07%±1.7 (n=43) compared to 2.66%±1.2 (n=28).

C/N mean values for surface and deep soils (22.7±10 and 25.4±6.8 respectively) had relatively large errors, which substantially overlap. However, the uncertainties on their mean isotopic compositions are much smaller, and it is by these that they are distinguished. They had δ^{13}C values of -26.94‰±0.28 (surface) and -25.42‰±0.32 (deep), and δ^{15}N values of 1.69‰±0.52 (surface) and 5.12‰±1.11 (deep). Surface soil plots close to and well within error of bedload and channel banks in both N/C–δ^{13}C and C/N–δ^{15}N space, while deep soil shows little affinity with these. The grain size distribution of deep soil (Figure 6.4) also suggests that it is distinct from any other source sediment, with roughly equal proportions of coarse, medium and fine material and by far the highest proportion of fines (36%) of all sediments characterised. On the other hand, the surface soil samples had an identical grain size distribution to channel bank material.

6.2.4.1 Stable slope soil profiles

Figure 6.5 shows the changes in chemistry that occur with depth for several soil profiles in Watershed 1, Hinkle and Trask. They show a decrease in C_{org} with depth, reflecting a variety of possible processes including reduced deposition, bacterial digestion and abiotic oxidation of organic carbon, and increased admixing of lithic material. However, while the lower layers have relatively uniform C_{org}, there is a large variation

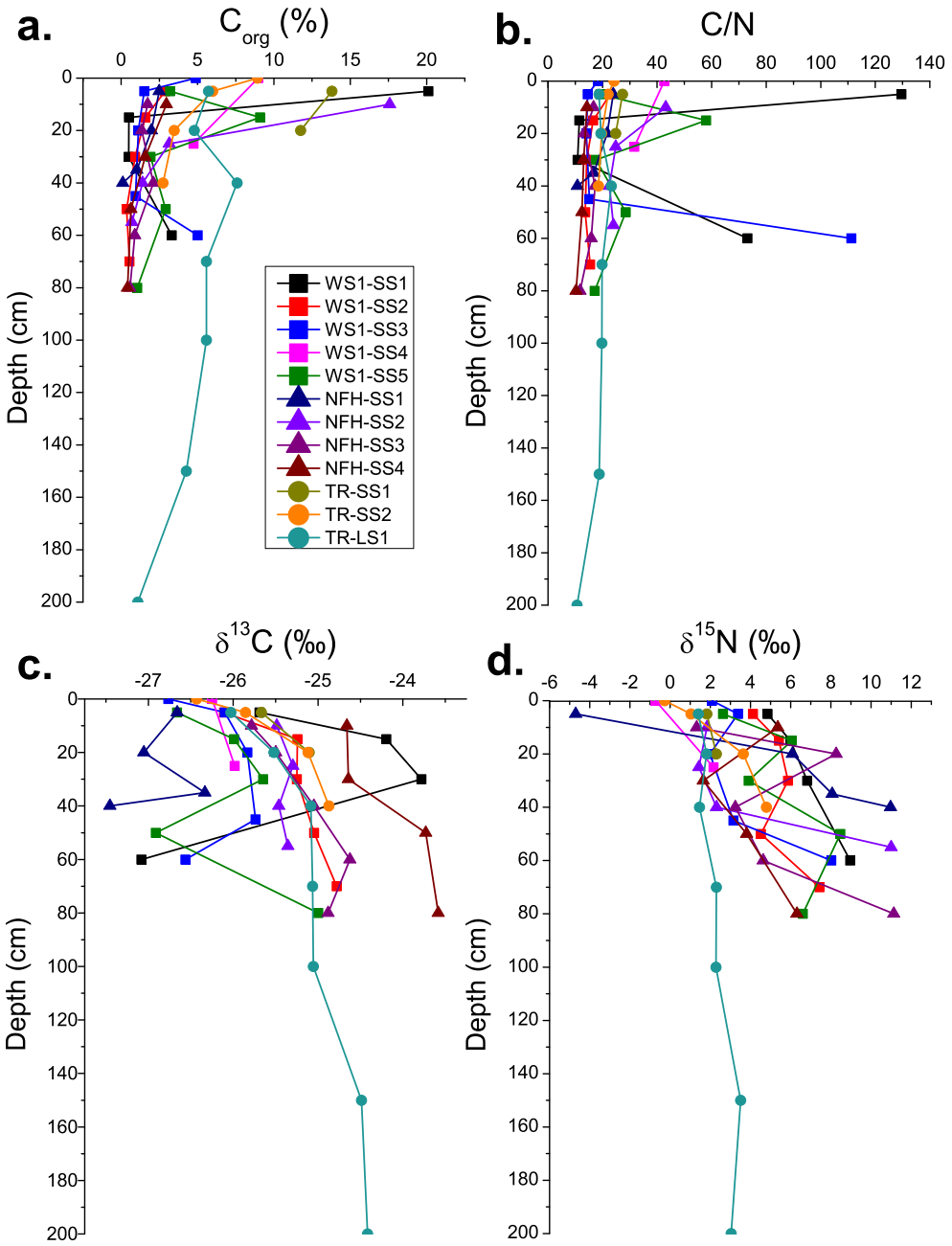

Figure 6.5: Profiles through stable slopes, showing (**a**) concentration of organic carbon (C_{org}); (**b**) organic carbon to nitrogen ratio (C/N); (**c**) organic carbon isotopic composition ($\delta^{13}C$); and (**d**) nitrogen isotopic composition ($\delta^{15}N$). SS=stable slope, LS=landslide (collected on a landslide scarp face, but still showing progression through a stable slope).

between profiles in the C_{org} of the uppermost layers, which ranges from 0.3% to 20%. The C/N curve for each profile has a similar shape to the corresponding C_{org}, showing that the concentration of nitrogen decreases less with depth than that of carbon. The patterns in $\delta^{13}C$ and $\delta^{15}N$ are less clear-cut, but the dominant trends are towards heavier isotopes of both C and N with depth, as a result of the fractionations associated with bacterial activity. All depth-related chemical trends described here are consistent with observations in soil profiles from a wide range of environments (e.g. Balesdent *et al.* , 1993; Wynn *et al.* , 2005, 2006).

6.2.4.2 Landslides

Active landslides are uncommon in the Coast Range and even more so in the Cascades. Only one recent landslide was encountered, in the Trask region. The landslide itself was not directly sampled, but a sample from the top of the rotated block, likely representing mixed debris originating from the scarp face, was collected (not shown on any figures). This sample was very similar to the mean soil profile values in all chemical parameters. The landslide appeared to be simply a block of the stable slope, displaced but retaining its internal structure.

6.2.4.3 Litter

Litter consists of dead plant material that has fallen to the ground and may have begun to decompose. It can be thought of as the top layer of soil, but surface soil samples in this study were collected after first removing overlying litter, and so it is considered separately here. Litter samples had mean C_{org} of 26.7%±12 (n=4), midway between that of fresh vegetation and surface soil. In C/N–$\delta^{15}N$ space, mean litter composition plots just within error of foliage and close to stream-conditioned plant matter, with mean C/N of 25.3±6.9 and mean $\delta^{15}N$ of -2.74‰±0.94. In N/C–$\delta^{13}C$ space litter plots between foliage and surface soil, with mean $\delta^{13}C$ of -29.07‰±0.82. Samples were dominated by coarse material (82%) and, like stream-conditioned plant matter, included virtually no fines (Figure 6.4).

6.2.5 Vegetation

Different types of vegetation, including major tree and ground plant species, were analysed in order to determine whether any of them have a particular individual influence on the composition of carbon in riverine suspended sediment (see Section 3.2.2.2 on page 60 for detailed sampling information). Results are shown in Table 6.3

and Figure 6.6. Although there are compositional differences between species (Table 6.3), the scatter is generally large and the uncertainties on the means correspondingly so. Hence, consideration of each species as an individual carbon pool is not practicable. However, it is worth noting which species plot at the extremities of the distribution (Figure 6.6). *Alnus rubra* foliage, *Polystichum munitum* and *Rubus sp.* tend to give the lowest C/N (highest N/C) values, while the conifer woods (*Tsuga heterophylla*, *Pseudotsuga menziesii* and *Thuja plicata*), along with woody debris, have the highest. *Gaultheria sallon* has particularly negative δ^{13}C; woody debris and the conifer woods have more positive δ^{13}C. No one species dominates high or low δ^{15}N.

There was a marked difference in the overall mean composition of wood and foliage, and additionally between standing wood and woody debris. Woody debris had higher C/N, heavier C and lighter N than foliage, both overall and within each species and watershed (Tables 6.2, 6.3, and 6.1; Figure 6.6). Standing wood sits between the two.

Samples of four widespread and representative species (*Tsuga heterophylla*, *Pseudotsuga menziesii*, *Alnus rubra* and *Polystichum munitum*) were collected from all watersheds in the study to check geographic dissimilarity in same-species composition. No discernible differences above same-location within-species variation were apparent.

6.2.6 Charcoal

Due to the prevalence of natural and anthropogenic forest fires, as well as controlled burning (Section 2.3.5, page 41), charcoal is a potentially important source of riverine organic carbon in Oregon. Four samples were collected; three from mid-catchment soil profiles and forest floor at Hinkle and one from a soil profile at the top of Watershed 1. These had a distinctive composition, with very high C/N (368±526 (n=4; the large error is due to one sample with C/N of 1354)), heavy C (δ^{13}C=-25.44‰±0.13) and light N (δ^{15}N=-6.39‰±0.38). In both N/C–δ^{13}C and C/N–δ^{15}N space, charcoal plots within error of woody debris, but it has much higher C_{org} (70% compared to 52%).

	n	C_{org} (%)		C/N		δ^{13}C (‰)		δ^{15}N (‰)	
		Mean	σ	**Mean**	σ	**Mean**	σ	**Mean**	σ
Tsuga heterophylla—needles	7	53.2±1.7	2.28	39.7±5.8	7.62	-31.46±1.30	1.73	-2.87±1.10	1.46
Tsuga heterophylla—wood	9	49.9±2.0	3.00	152±219	328	-28.81±1.56	2.35	-3.38±1.91	2.86
Pseudotsuga menziesii—needles	6	51.6±4.0	4.89	39.2±5.8	7.12	-30.13±0.97	1.19	-3.57±1.09	1.33
Pseudotsuga menziesii—wood	7	50.0±2.7	3.54	326±128	169	-26.63±1.25	1.65	-4.20±2.63	3.49
Thuja plicata—needles	4	53.1±2.4	2.40	37.6±8.9	8.93	-28.96±2.39	2.39	-3.76±2.19	2.19
Thuja plicata—wood	4	49.0±1.3	1.34	512±377	377	-26.83±1.42	1.42	-3.79±6.21	6.21
Alnus rubra—leaves	6	52.7±1.6	1.91	21.6±5.9	7.23	-30.70±0.91	1.11	-1.50±0.66	0.81
Alnus rubra—wood	5	47.9±1.2	1.39	177±93.8	105	-29.33±1.09	1.22	-1.71±2.08	2.33
Polystichum munitum—leaves	5	49.4±1.4	1.58	23.3±2.66	2.98	-30.98±0.65	0.72	-1.29±0.56	0.62
Polystichum munitum—stem	4	48.6±0.6	0.61	72.1±16.8	16.8	-29.57±1.03	1.03	-2.85±1.22	1.22
Acer circinatum—foliage	4	47.5±2.2	2.21	73.8±134	134	-30.10±1.32	1.32	-0.67±1.01	1.01
Moss	4	46.5±1.6	1.60	62.0±17.8	17.8	-28.93±1.70	1.70	-2.86±2.02	2.02
Gaultheria sallon—foliage	3	49.0±1.4	1.22	45.4±71.6	62.0	-33.40±1.03	0.90	-3.72±0.73	0.64
Rubus sp.—foliage	3	47.2±0.9	0.74	24.7±35.1	30.4	-31.92±1.26	1.09	-1.44±1.01	0.88
Woody debris	6	51.2±4.1	5.03	252±298	365	-24.86±1.18	1.44	-5.03±2.01	2.46

Table 6.3: Organic carbon concentration (C_{org}), organic carbon to nitrogen ratio (C/N), organic carbon isotopic composition (δ^{13}C) and nitrogen isotopic composition (δ^{15}N) of different types of vegetation averaged across all the Oregon watersheds in this study. Only species where more than three samples of the same type were collected are included.

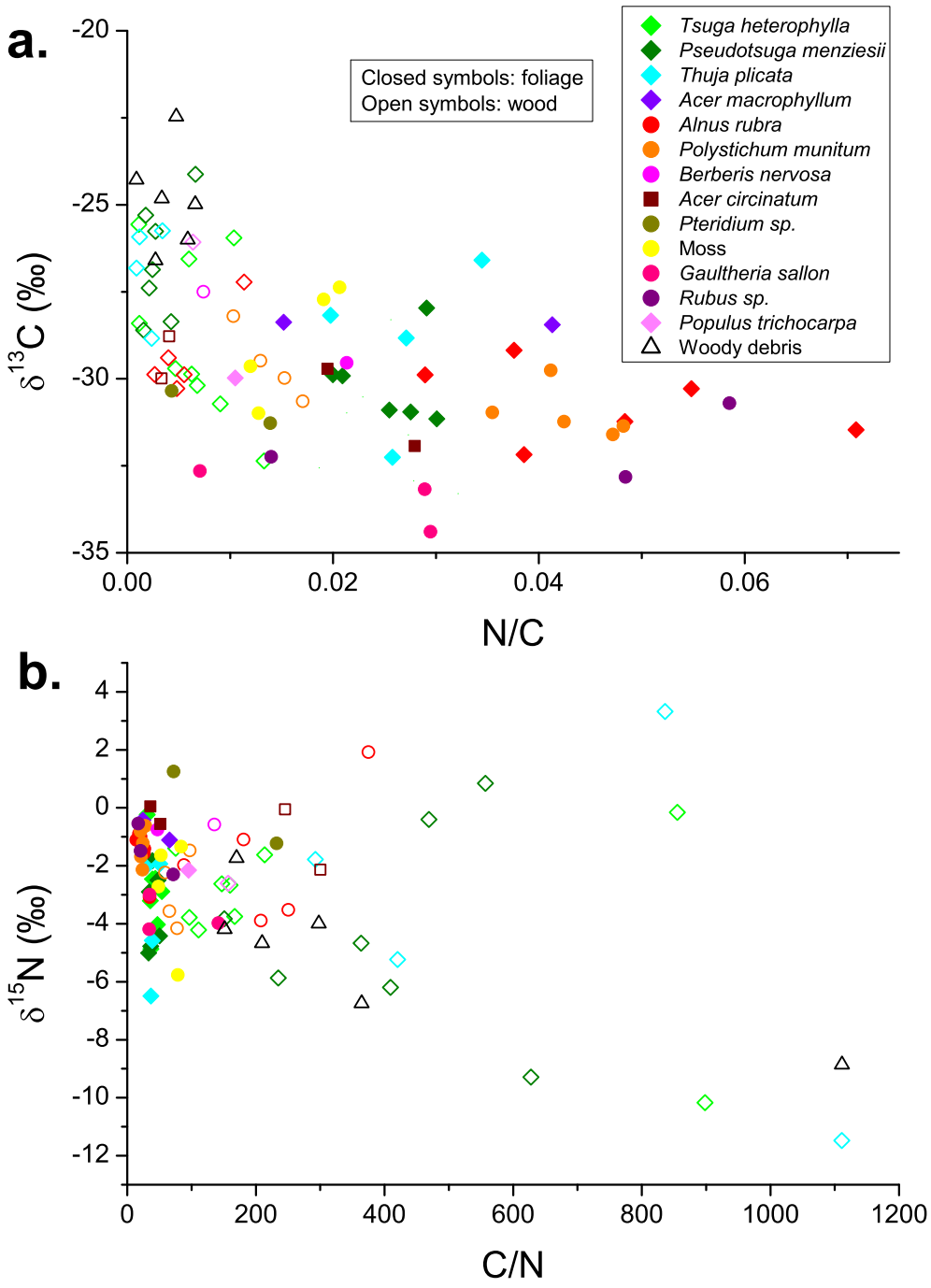

Figure 6.6: Chemical composition of Oregon vegetation samples. (**a**) Nitrogen to organic carbon ratio (N/C) versus organic carbon isotopic composition (δ^{13}C); (**b**) Organic carbon to nitrogen ratio (C/N) versus nitrogen isotopic composition (δ^{15}N). Colours represent different species (as in legend); closed symbols are foliage, open symbols are wood. Shapes reflect the type of plant: diamonds are trees, circles are ground plants, squares are shrubs, and triangles are woody debris.

6.2.7 Diatoms

Diatoms are an extremely widespread group of phytoplankton, and freshwater varieties are the cause of autochthonous algal blooms in productive rivers (Finlay *et al.* , 1999). Although such blooms do not generally occur in flashy, frequently turbid headwaters, diatoms are observed in the streams at H.J. Andrews whenever it rains, presumably washed from the hillslopes or pools within the riparian zone (Frentress & McDonnell, 2011), or disturbed from the stream bed. Diatoms were not directly analysed in this study, and their organic chemistry is poorly documented elsewhere. Isotopic analysis of diatoms is a relatively new technique and no data exist for Oregon. However, available evidence suggests that their composition can be highly variable, even in a single location (e.g. Finlay, 2001; Hurrell *et al.* , 2011). In East African lacustrine sediments, δ^{13}C ranges from -27.5‰ to -36.5‰ (Hurrell *et al.* , 2011), while in Narragansett Bay, Rhode Island, it is -20.3‰(Gearing *et al.* , 1984). A study of epilithic algal δ^{13}C in Californian rivers (Finlay *et al.* , 1999) found values that varied from -17.9‰ in pools to -27.5‰ in riffles. In unproductive tributary streams, invertebrate herbivore δ^{13}C was used as a proxy for algal δ^{13}C, yielding values of around -32‰, and in some cases up to -44‰ (Finlay *et al.* , 2011). No information exists regarding the δ^{15}N of riverine diatoms, but Cloern *et al.* (2002) found values of ∼3‰ to ∼11‰ in benthic diatoms of the San Francisco Bay estuary. The C_{org} content of diatoms is again not widely known, but seems to be low, in many cases less than 1% (Hurrell *et al.* , 2011). Therefore, their contribution to the suspended load would have to be volumetrically significant in order to exert a strong influence on its composition. Previous studies (e.g. Finlay, 2001) have shown that δ^{13}C of coarse and fine benthic particulate and dissolved organic matter in Californian rivers do not correlate with algal δ^{13}C, unlike dissolved inorganic carbon. Because of this, together with the lack of any information regarding the composition of local species, diatoms are not further considered as a significant input to the suspended load of the headwater samples in this chapter. However, they cannot be entirely ruled out, and if more time and resources were available, it would be worth using biomarker methods (e.g. Hatten *et al.* , 2012) to try to identify their contribution—if any—to these samples.

6.3 Organic carbon in the suspended load

This section begins with some general observations regarding patterns of suspended sediment behaviour in Oregon, which is discussed in more detail with respect to POC

fluxes later in the chapter (Section 6.5). Concentration of organic carbon in the suspended load of all Oregon catchments, and then their compositional parameters, are subsequently reported. This part of the chapter is largely descriptive; detailed interpretation and discussion of results is left for the next section.

6.3.1 Sediment in Oregon streams

Oregon rivers transport generally low levels of sediment, resulting in the clear waters observed during both summer and autumn visits to the area. Figure 6.7 shows the relationship between discharge and SSC for all watersheds except those in the Alsea, for which no discharge records could be obtained. For the remaining watersheds, there is at best a weak relationship between SSC and discharge. Calculation of Kendall's correlation coefficient shows that there is no significant correlation at the 0.05 level for Lookout Creek and Watershed 1 (either compound or instantaneous sample sets), and weak significant correlations for Hinkle (τ=0.34) and Trask (τ=0.37). This relative lack of correlation, especially at H.J. Andrews, suggests that factors other than discharge affect the amount of sediment carried, such as sediment supply and transport capacity, which is linked to channel roughness as well as discharge (Stoffel & Wilford, 2012).

These relationships are at odds with the well-defined (R^2 >0.9) discharge–sediment rating curves reported by Goñi *et al.* (2013) for the Umpqua River and Hatten *et al.* (2012) for the Alsea River, in terrain with similar erosion rates and over a similar range of Q/Q_{mean}, but at larger scales. Although more scatter is expected in smaller streams because of the stochastic nature of sediment supply (Benda & Dunne, 1997), this seems unlikely to explain such a large disparity in correlation. However, it is not clear what other factors could cause this effect.

Figure 6.8 shows SSC for all catchments, including Flynn Creek and Deer Creek, in the top panel. SSC tends to be higher in the samples obtained by turbidity threshold sampling (Hinkle, Trask and Alsea) rather than discharge-proportional sampling (H.J. Andrews) because they represent only peak sediment transport conditions. Samples from Deer Creek (pink left-facing triangles in Figure 6.8) had the highest SSC values, reflecting the influence of more recent intensive clear-cutting (Section 2.3.5, page 41).

6.3.2 Concentration of organic carbon in the suspended load

Figure 6.8 shows organic carbon concentrations (C_{org}), plotted against SSC and discharge for all Oregon samples where suitable data exists. C_{org} was considerably higher than in most rivers, with many samples reaching 20%–30%, and much more variable.

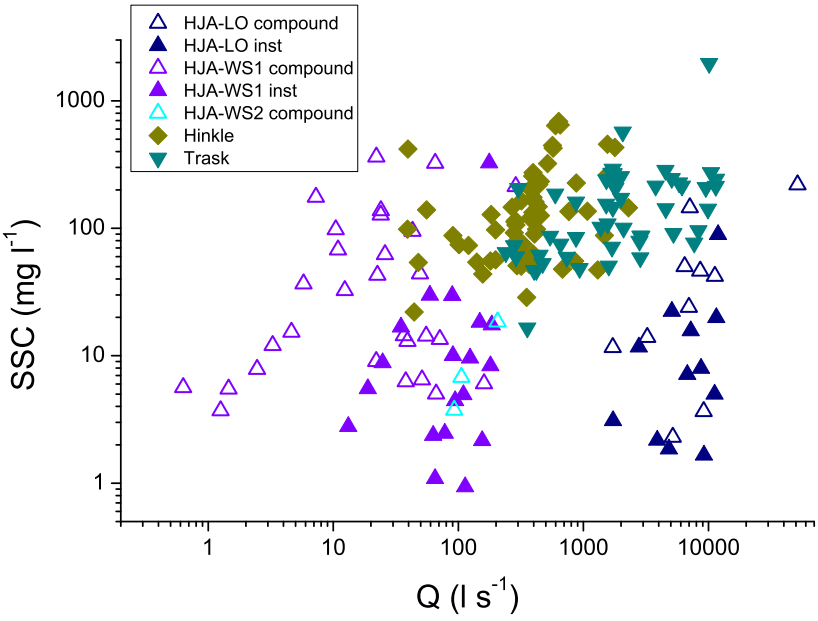

Figure 6.7: SSC plotted against discharge in Oregon watersheds, showing lack of significant relationships.

Mean values are presented in Table 6.4.

These data show a large amount of scatter, but significant inverse correlations at the 0.05 level exist between SSC and C_{org} for Watershed 1 compound samples, Hinkle and Flynn Creek, and between Q and C_{org} for both H.J. Andrews instantaneous datasets. The latter two have the highest values of Kendall's correlation coefficient (τ=-0.61 and -0.72 for Lookout Creek and Watershed 1 respectively).

The highest individual values of C_{org} occurred at Trask, but the mean values for Trask, Hinkle, all H.J. Andrews samples combined and Flynn Creek were within error of each other. These were 10.2%±2.5 (n=51), 9.28%±1.4 (n=60), 6.13%±1.9 (n=73) and 6.35%±1.8 (n=38) respectively. Deer Creek, the intensively logged catchment in the Alsea, had the lowest C_{org} values with a mean of 0.45%±0.9 (n=20).

Higher C_{org} values in instantaneous samples from both Lookout Creek and Watershed 1 compared to compound samples are likely to result from a sampling method bias. For example, instantaneous samples could pick up more large organic particles, which may be missed by "sipping" through the small tube used in the compound sampling (Johnson, 2012). Mean C_{org} in all samples from Lookout Creek (5.63%±3.3) and in all from Watershed 1 (6.15%±2.4), on the other hand, are within error of each other.

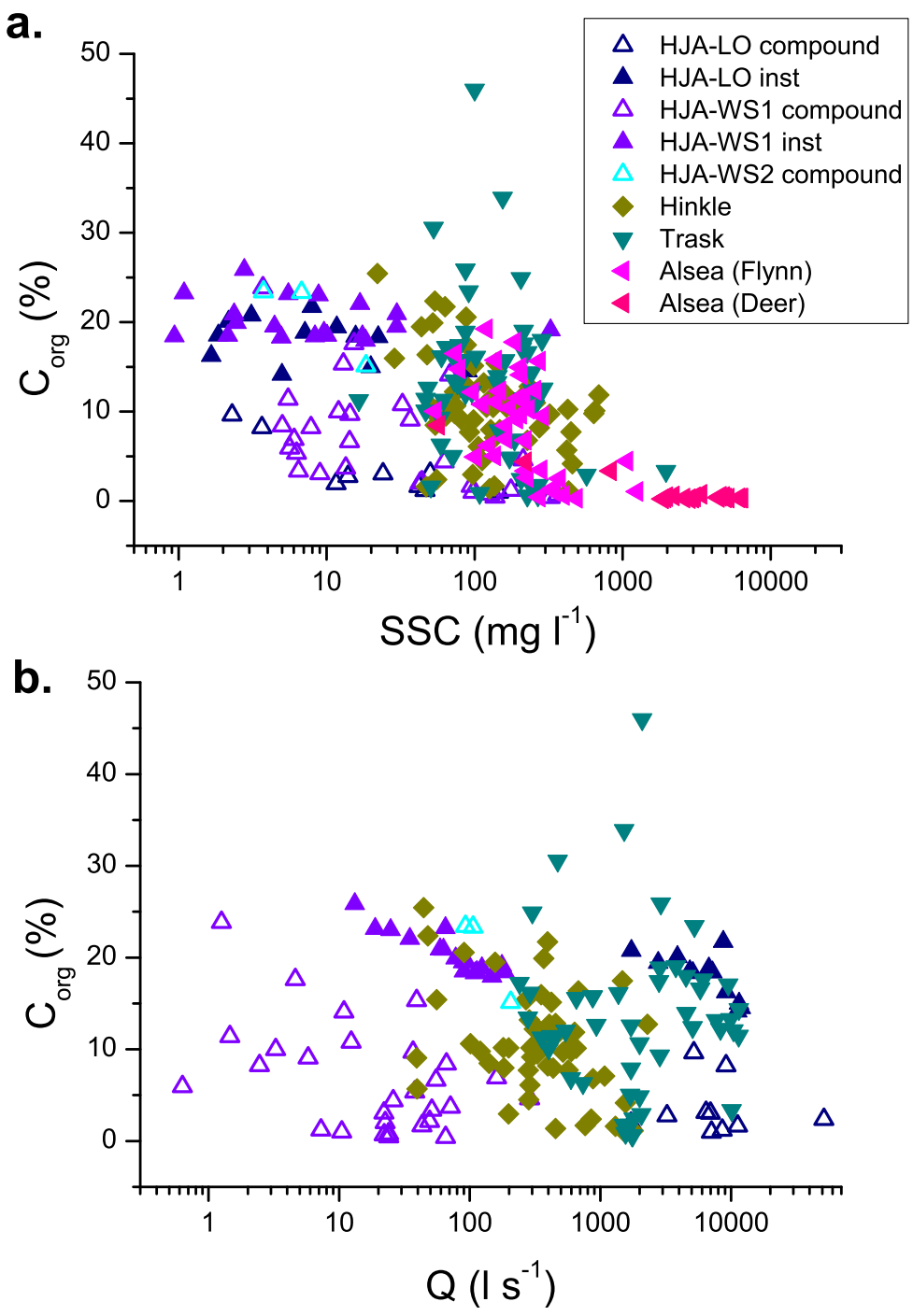

Figure 6.8: Organic carbon concentration (C_{org}) in Oregon suspended sediment versus (**a**) SSC and (**b**) discharge. Note logarithmic x-axes.

	n	**C_{org} (%)**		**C/N**		**δ^{13}C (‰)**		**δ^{15}N (‰)**	
		Mean	σ	**Mean**	σ	**Mean**	σ	**Mean**	σ
HJA all	*73*	*6.13±1.9*	*8.10*	*22.5±1.5*	*6.44*	*-27.36±0.26*	*1.11*	*-1.43±0.46*	*1.96*
HJA-LO compound	10	2.03±1.9	2.97	17.2±2.0	3.09	-27.68±0.84	1.33	1.33±0.72	1.14
HJA-LO inst	12	16.3±1.4	2.49	20.0±1.2	2.06	-26.84±0.28	0.49	-0.11±0.46	0.80
HJA-LO all	*22*	*5.63±3.3*	*7.85*	*19.2±1.2*	*2.87*	*-27.47±0.47*	*1.09*	*0.97±0.43*	*0.51*
HJA-WS1 compound	29	2.75±2.1	5.78	21.8±2.2	5.79	-27.48±0.47	1.28	-2.72±0.74	1.98
HJA-WS1 inst	19	19.4±1.0	2.24	24.1±0.8	1.72	-26.71±0.25	0.54	-0.02±0.40	0.88
HJA-WS1 all	*48*	*6.15±2.4*	*8.19*	*23.2±1.3*	*4.61*	*-27.33±0.33*	*1.14*	*-2.17±0.61*	*2.10*
HJA-WS2	3	18.1±5.5	4.76	42.3±7.6	6.60	-26.88±0.57	0.49	-1.06±0.20	0.18
Hinkle	60	9.28±1.4	5.38	30.0±2.0	7.92	-26.69±0.28	1.07	-1.86±0.81	3.13
Trask	51	10.2±2.5	8.83	19.4±2.2	7.98	-27.57±0.18	0.64	-0.32±0.27	0.98
Alsea (Flynn)	38	6.35±1.8	5.44	18.5±1.5	4.60	-27.45±0.15	0.48	-0.57±0.39	1.20
Alsea (Deer)	20	0.45±0.91	2.04	9.44±1.5	3.42	-27.12±0.25	0.56	-1.30±0.52	1.16

Table 6.4: Organic carbon concentration (C_{org}), organic carbon to nitrogen ratio (C/N), organic carbon isotopic composition (δ^{13}C) and nitrogen isotopic composition (δ^{15}N) of POM in Oregon headwaters.

6.3.3 Composition of organic carbon in the suspended load

Figure 6.9 shows the distribution of POM from different Oregon watersheds in N/C–δ^{13}C and C/N–δ^{15}N space, exhibiting a very wide spread in both cases. Mean values are presented in Table 6.4.

Notwithstanding a few outliers, populations from Hinkle and Deer Creek are compositionally distinct in both plots: Hinkle samples have high C/N (range 13–57; mean 30.0±2.0) and relatively heavy C (δ^{13}C range -25‰to -33‰; mean -26.7‰±0.3), while Deer samples have very low C/N values (range 5–17; mean 9.4±1.5). The regions where samples from the other watersheds plot overlap substantially, roughly in the middle of the overall distribution.

Within H.J. Andrews, however, some variation is apparent, reflected in the mean values given in Table 6.4. Samples from Watershed 1 had higher C/N and considerably more negative δ^{15}N than those from Lookout Creek, outside the uncertainties on the means; possible reasons for this are speculated upon in Section 6.4.2. In addition, the compound samples for both Lookout Creek and Watershed 1 had much lighter C than the corresponding instantaneous datasets; this was also the case for N for Watershed 1, but not Lookout Creek. Like the disparity in C_{org} values, this could be due to a sampling bias, but if so then the large organic particles that are excluded from compound samples cannot consist of fresh plant material. This seems unlikely, but is not unimaginable; needles and micro-fibres in particular might get through more easily than clumps of soil. In addition, fresh plant material is likely to be transported at the surface of the flow, while the autosampler takes water from the middle. There could also be a post-collection treatment or storage effect.

Unexpectedly, Watershed 2 samples occupy the same domain as Hinkle samples in both plots, although as there are only three samples it is impossible to tell whether this is significant.

6.4 Sources and pathways of organic carbon

Now that the concentrations and compositions of organic matter in source and sediment sample sets have been established, they can be used to explore the routing of organic carbon in Oregon headwaters. This section is split into three subsections. Firstly, all watersheds are considered together. The nature of end member sources is examined in light of the compositional distribution of suspended sediment samples, and the relative contributions of mixing and decomposition to this distribution is discussed. The procedure and results of an end member mixing analysis are reported, and

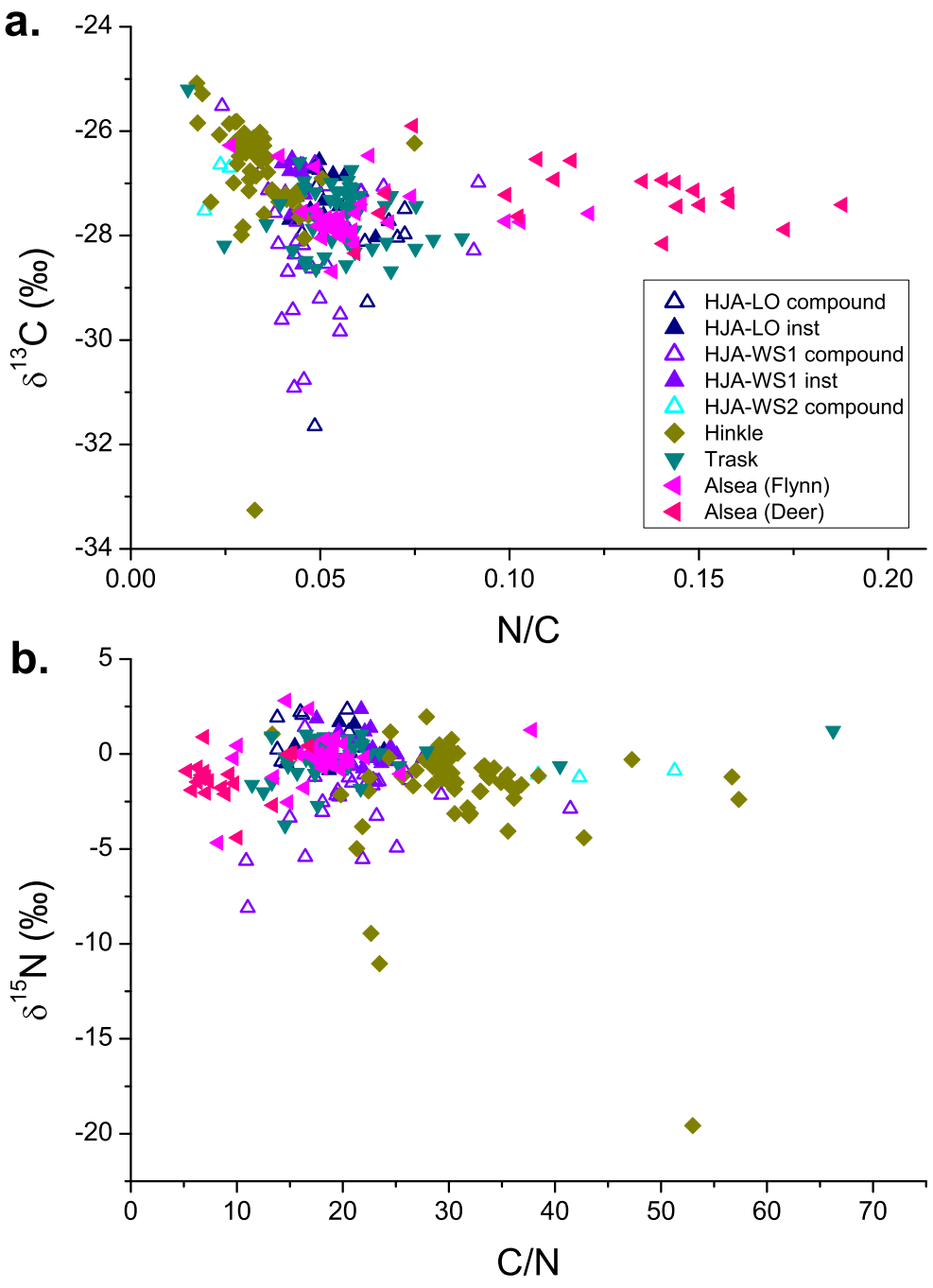

Figure 6.9: Chemical composition of POM in Oregon suspended sediment. (**a**) Nitrogen to organic carbon ratios (N/C) versus organic carbon isotopic composition (δ^{13}C); (**b**) Organic carbon to nitrogen ratios versus nitrogen isotopic composition (δ^{15}N).

there is also a discussion of compositional trends with changing SSC. The two later subsections present separate discussions of organic carbon dynamics in the Cascades and the Coast Range, drawing on the analysis and discussion of the first subsection, and linking geochemical results and interpretation to geomorphological observations. To accommodate the additional information available for H.J. Andrews, the Cascades subsection also includes discussions on temporal trends over the flood hydrographs sampled in November 2011, and seasonal patterns evident in the compound samples from Watershed 1.

6.4.1 General chemical trends

The relationships in N/C–δ^{13}C and C/N–δ^{15}N space between organic matter in the suspended load and catchment stores are illustrated in Figure 6.10. Note that the lower panel is zoomed in compared to Figures 6.1, 6.6, and 6.9.

In both plots, suspended sediment samples—other than those from Deer Creek—almost entirely occupy a compositional space bounded by the error bars of purely biogenic end members, with surface soil, channel banks and bedload at one corner, and vegetation forming an arc at the other end. There is no evidence of clustering within this space, indicating that plant material is not homogenized before incorporation into the suspended load. Instead, individual plant foliage or wood is assimilated directly, leading to a wide sector of suspended sediment compositions.

6.4.1.1 The bedrock end member

As described in Section 2.3.2 (page 31), sedimentary bedrock containing fossil organic carbon entirely underlies the Alsea watershed, and is therefore likely to contribute to the suspended load of Deer Creek and Flynn Creek. Similar sedimentary units underlie part of the Trask watershed, and so must be considered there also. However, the distribution of Deer Creek samples in Figure 6.10 suggests that the bedrock composition determined from the Alsea cores in Section 6.2.1 does not accurately represent the bedrock eroded by Deer Creek, and by inference the other Coast Range streams: this must have lower C/N, δ^{15}N and δ^{13}C than the core samples, but by how much remains unknown. Given the lack of any statistical evidence for binary mixing in the Deer Creek samples in either N/C–δ^{13}C or C/N–δ^{15}N space, and their very low C_{org} values (mean 0.45%±0.91), taking the average composition of Deer Creek suspended sediment is likely to be one reasonable approximation for bedrock—an assumption that could be checked by ^{14}C analysis of Deer suspended load. The similarity of sedimentary units found in the Trask and Alsea watersheds (Section 2.3.2, page 31)

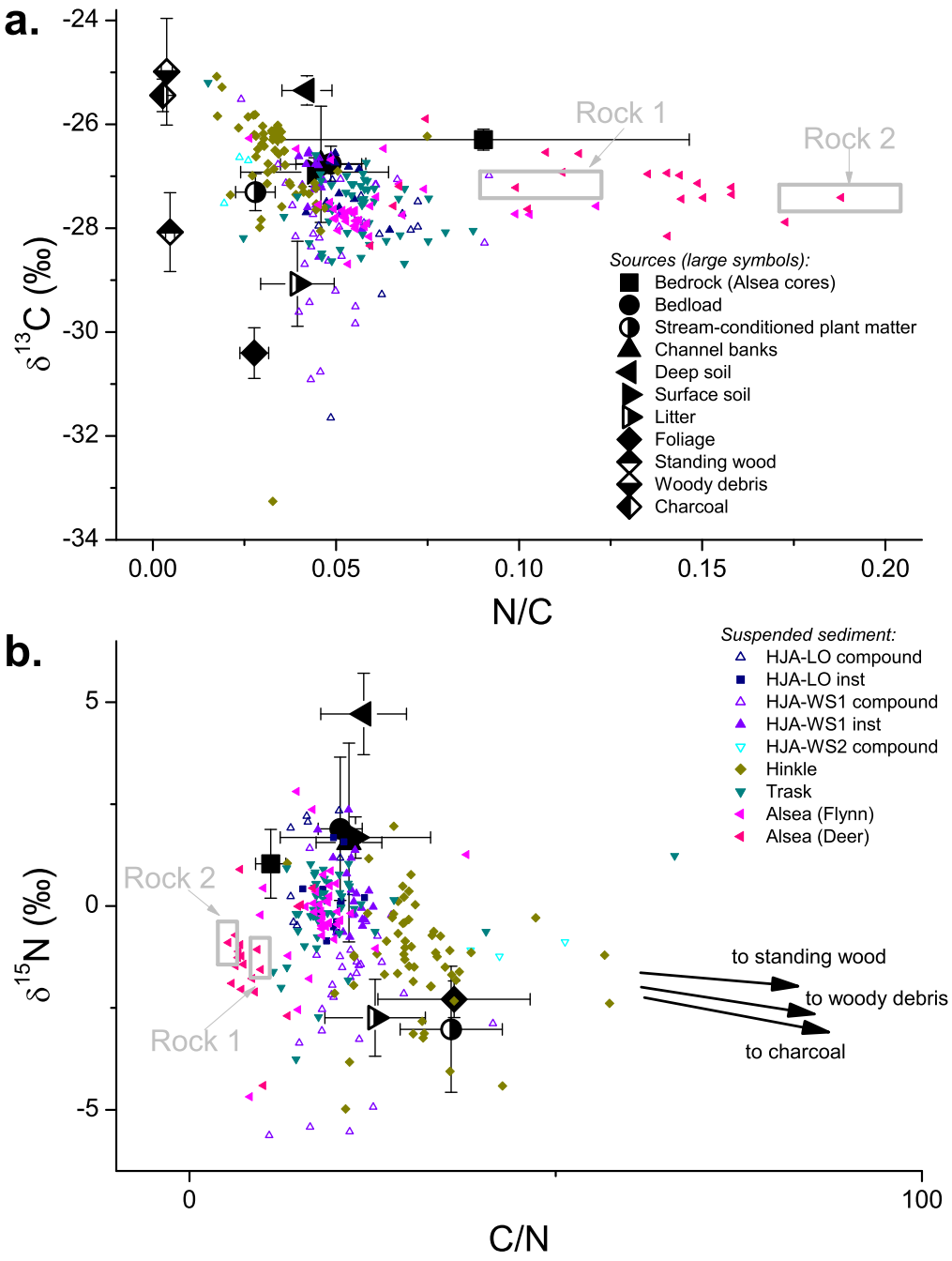

Figure 6.10: Chemical composition of organic matter in Oregon-wide (except bedrock) sources and catchment-specific riverine suspended sediment. (**a**) Nitrogen to organic carbon ratios (N/C) versus organic carbon isotopic composition (δ^{13}C); (**b**) Organic carbon to nitrogen ratios versus nitrogen isotopic composition (δ^{15}N). Rock 1 and Rock 2 are estimates of the composition of organic matter in bedrock eroded by Coast Range streams (see Section 6.4.1.1).

means that this is also valid as a first-order proxy for Trask bedrock composition. An alternative estimate of the composition of organic matter in bedrock is given by the Deer Creek suspended sediment sample with the most extreme C/N value. Both are indicated on Figure 6.10, where the more extreme estimate based on a single sample is given the same uncertainty as the one based on the average Deer Creek suspended load composition.

6.4.1.2 Relationships between source materials

Oregon bedload and channel bank samples are indistinguishable in their composition from surface soil, even in the Alsea, where the composition of bedload organic matter is quite different from that of bedrock organic matter. This suggests that fossil organic matter, even where present, makes at most a minor contribution to these source sediments, leaving biogenic material to dominate. In most cases, carbon in bedload, channel banks and soil at all depths must be simply due to decomposed vegetation. These three pools have different C_{org} values, presumably owing to the variable admixing of carbon-free clastic material, but this has no effect on C/N or isotopic composition. The differences in composition with respect to fresh vegetation (heavier C and N and lower C/N due to loss of C) are a result of fractionation processes during decomposition and are relatively well-documented (Coyle *et al.* , 2009; Dijkstra *et al.* , 2006; Finlay, 2001; Melillo *et al.* , 1989).

The overlap in bedload, channel bank and surface soil composition in both N/C–δ^{13}C and C/N–δ^{15}N space (Figure 6.1), and in their grain size distributions (Figure 6.4), suggests that the carbon in these pools has undergone a similar degree and type of degradation. The additional processes involved in degrading the carbon found in deep soil must be slightly different, resulting in a greater proportion of fine material and further ^{13}C and ^{15}N enrichment, but little change in C/N (see also Figure 6.5). That stream banks are more similar to surface soil than deep soil reflects the observation that, in most Oregon headwaters, hillslope surfaces merge into channels without a significant step. Thus, deeper parts of the soil profile that exist on hillslopes are not systematically exposed in the channel walls. Material adjoining the channel is most likely to be recently accumulated alluvium. Surface soil, channel banks and bedload are effectively the same material, and in the following sections, the term "surface soil" encompasses all three source pools.

Litter represents a half-way stage in the compositional change from fresh foliage to surface soil/bedload/channel banks (Figure 6.10(a)). Stream-conditioned plant matter plots off this trend and must consist of decomposed foliage with a litter-like

composition mixed with woody debris. Thus, neither is a primary source. In C/N–δ^{15}N space (Figure 6.10(b)), both litter and stream-conditioned plant matter appear to be much more closely associated with foliage, despite having significantly lower C_{org} content. This could indicate that nitrogen fractionation occurs at a later stage of decomposition than loss of carbon and carbon fractionation, as has been modelled for soils in Taiwan (Hilton *et al.* , 2012b).

6.4.1.3 Mixing versus decomposition

The suspended sediment compositions shown in Figure 6.10 and their relationships to potential sources could result from either mixing or a fractionation process, i.e. plant decomposition. Unlike the processes and accompanying fractionations by which biogenic material is transformed into fossil organic matter, the transformation of fresh foliage to refractory soil organic matter occurs over timescales of months to years (e.g. Melillo *et al.* , 1989), so partial decomposition can easily occur between plant matter ceasing to be part of a living entity and being exported from the catchment. This could happen either in the litter layer in the riparian zone, or in the stream bed itself, and the composition of riparian litter and stream-conditioned plant samples provides confirmation of the process occurring in both locations.

The fact that suspended sediment samples generally have more positive δ^{15}N values than the means of both litter and stream-conditioned plant material, and more positive δ^{13}C than the former, suggests that in the general case there is still mixing of plant matter with surface soil (or soil-derived bedload and channel banks), even if there is decomposition first. However, the wide compositional spread of vegetation samples makes it extremely difficult to properly deconvolve the relative effects of mixing and decomposition. In the following sections, relationships are discussed in terms of mixing between primary end members, but it should be borne in mind that there may also be a purely decompositional component: the effects of a greater contribution from soil and the addition of more degraded foliage are interchangeable. This is one likely reason for the disparity between the proportional contributions of end members to riverine POC as determined by mixing analysis using δ^{13}C and C_{org}, and δ^{15}N and N concentration, described in the next section.

6.4.1.4 End member mixing analysis of source contributions

Although the wide compositional spread of suspended sediment samples means that little is gained from estimating source contributions to the organic carbon in each of them as in the Alptal, it is instructive to do this for the mean POM compositions of

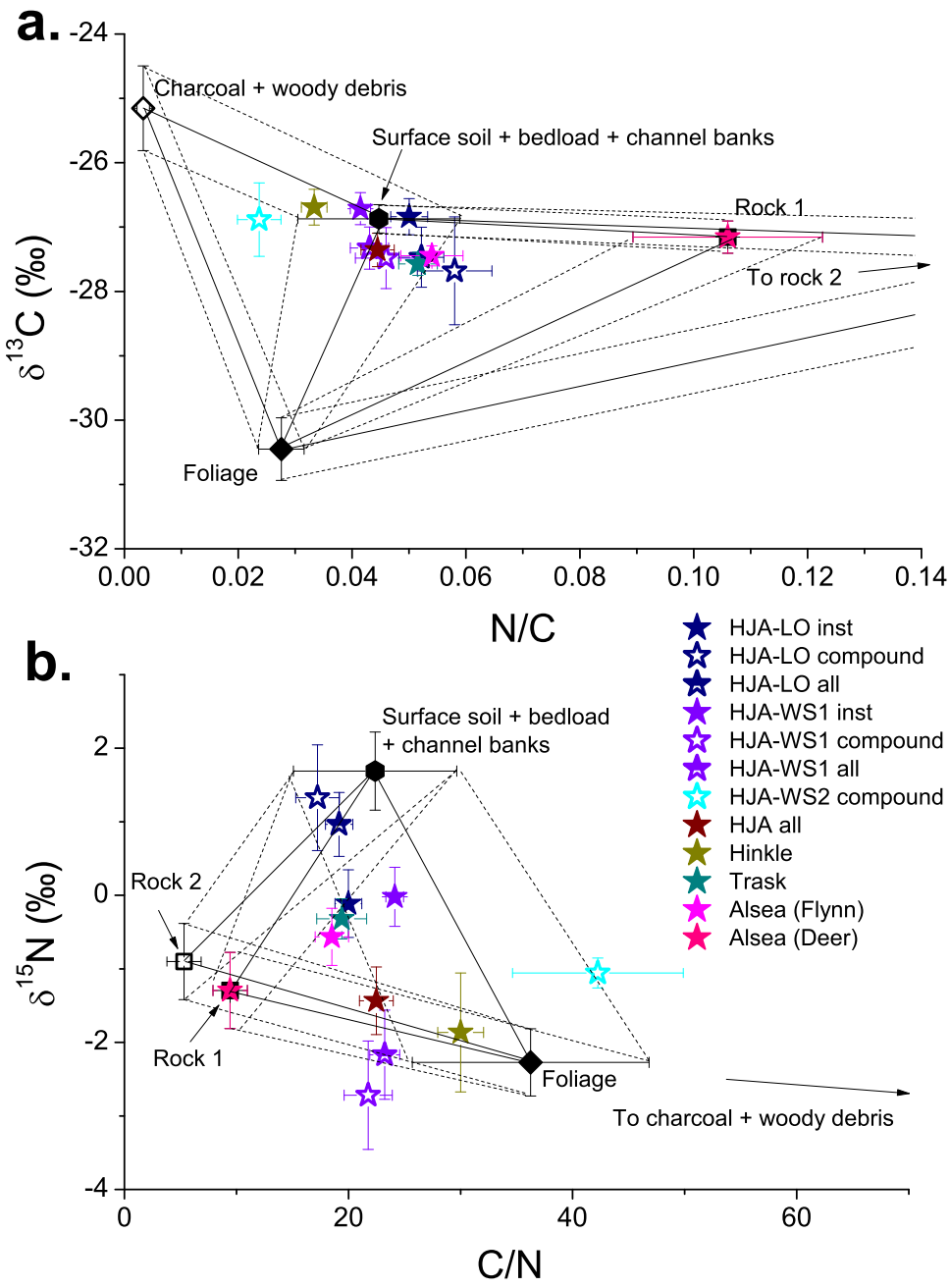

Figure 6.11: Mean suspended sediment composition in Oregon watersheds, together with end member sources used in mixing analysis, and mixing lines (solid lines) and zones (delineated by dashed lines) between them. Rock 1 and Rock 2 are estimates of the composition of organic matter in bedrock eroded by Coast Range streams (see Section 6.4.1.1). (**a**) Nitrogen to organic carbon ratios (N/C) versus organic carbon isotopic composition (δ^{13}C); (**b**) organic carbon to nitrogen ratios versus nitrogen isotopic composition (δ^{15}N).

each watershed, illustrated in Figure 6.11.

Given the discussion in Section 6.4.1.2, surface soil, bedload and channel banks were combined to form the first end member for all calculations. Other end members varied according to watershed. For most datasets from H.J. Andrews, mean suspended sediment composition lies within error of the binary mixing line between the surface soil end member and foliage in both N/C–δ^{13}C and C/N–δ^{15}N space (Figure 6.11). Those that do not—other than Watershed 2—lie on the bedrock side of it. However, since there is no organic carbon in H.J. Andrews bedrock, this cannot be a third source and only these two end members were used. In these cases, the proportions of organic carbon contributed by each end member can be found by solving equations 6.1 and 6.2 simultaneously, where F_x and F_y are the proportions of end members 1 and 2 respectively, and subscript *1*, *2* and *SS* denote parameters of end members 1 and 2 and the suspended load of the watershed in question. They can also be found by solving equations 6.3 and 6.4 simultaneously, then converting x and y using equation 6.5 and normalising to 1, where F_C is the proportional contribution of the end member to the organic carbon in the suspended load, F_{EM} is the proportional contribution of the end member to bulk suspended load (i.e. x or y), and subscripts *EM* and *SS* denote parameters of the end member and suspended load respectively. These approaches give different answers; the difference between them serves to indicate the error on the proportions, since in most cases this is larger than the errors arising from the propagation of uncertainties on end member compositions.

$$\delta^{13}C_{ss} = F_x.\delta^{13}C_1 + F_y.\delta^{13}C_2 \tag{6.1}$$

$$F_x + F_y = 1 \tag{6.2}$$

$$\delta^{15}N_{ss}.N_{ss} = x.\delta^{15}N_1.N_1 + y.\delta^{15}N_2.N_2 \tag{6.3}$$

$$x + y = 1 \tag{6.4}$$

$$F_C = \frac{F_{EM}.C_{org(EM)}}{C_{org(SS)}} \tag{6.5}$$

For the other catchments, a three-end member mixing analysis was performed, again separately using first δ^{13}C and C_{org} as in the equations below, then substituting δ^{15}N and N concentration. The proportional contributions of each end member are

found by solving equations 6.6, 6.7 and 6.8 simultaneously; the proportion of organic carbon contributed by each end member is then given by equation 6.5. Again, the difference between results from the two approaches gives a better idea of the uncertainties on them than error propagation through the calculations.

$$C_{ss} = x.C_1 + y.C_2 + z.C_3 \tag{6.6}$$

$$\delta^{13}C_{ss}.C_{ss} = x.\delta^{13}C_1.C_1 + y.\delta^{13}C_2.C_2 + z.\delta^{13}C_3.C_3 \tag{6.7}$$

$$x + y + z = 1 \tag{6.8}$$

For Watershed 2 and Hinkle, the three end members used were the combined surface soil end member, foliage, and woody debris and charcoal combined. There is no evidence that standing wood contributes significantly to the suspended load of any catchment, so this was ignored. For Trask, Flynn and Deer, the third end member was bedrock. For Flynn and Deer, results were unaffected by which of the two bedrock composition estimates discussed in Section 6.4.1.1 was used, but there was a substantial difference for Deer Creek. Considering both for the latter catchment gives an indication on the uncertainties on the proportion of fossil organic carbon in the suspended load of this system.

As discussed in Section 6.4.1.2, there is no mechanism for deep soil to systematically enter the suspended load, and no evidence in the compositional distribution of any of the suspended sediment sample sets that it does, so this end member was ignored for all catchments.

The results of the end member mixing analysis are shown in Table 6.5, and discussed in subsequent sections on the Cascades and Coast Range in turn.

				C_{org} and $\delta^{13}C$			N and $\delta^{15}N$			Averaged		
SS dataset	**EM1**	**EM2**	**EM3**	**G_1**	**G_2**	**G_3**	**H_1**	**H_2**	**H_3**	**F_1**	**F_2**	**F_3**
HJA all	*soil*	*foliage*	-	*0.87*	*0.13*	-	*0.29*	*0.71*	-	*0.58±0.29*	*0.42±0.29*	-
LO inst	soil	foliage	-	1.01	-0.01	-	0.41	0.59	-	0.71±0.30	0.29±0.30	-
LO comp	soil	foliage	-	0.77	0.23	-	0.56	0.44	-	0.67±0.10	0.33±0.10	-
LO all	soil	foliage	-	0.83	0.17	-	0.67	0.33	-	0.75±0.08	0.25±0.08	-
WS1 inst	soil	foliage	-	1.04	-0.04	-	0.44	0.56	-	0.74±0.30	0.26±0.30	-
WS1 comp	soil	foliage	-	0.83	0.17	-	0.31	0.69	-	0.57±0.26	0.43±0.26	-
WS1 all	soil	foliage	-	0.87	0.13	-	0.24	0.76	-	0.56±0.31	0.44±0.31	-
WS2	soil	foliage	wood	0.29	0.23	0.48	0.14	0.26	0.60	0.22±0.07	0.25±0.02	0.53±0.06
Hinkle	soil	foliage	wood	0.70	0.06	0.24	0.07	0.08	0.85	0.39±0.38	0.07±0.07	0.54±0.31
Trask	soil	foliage	rock	0.82	0.20	-0.01	0.37	0.63	0.00	0.59±0.23	0.41±0.21	0.00±0.00
Flynn	soil	foliage	rock	0.83	0.16	0.02	0.32	0.66	0.02	0.57±0.26	0.41±0.25	0.02±0.00
Deer	soil	foliage	rock 1	0.00	0.00	1.00	0.00	0.00	1.00	0.00±0.00	0.00±0.00	1.00±0.00
Deer	soil	foliage	rock 2	0.48	0.00	0.52	-0.09	0.64	0.44	0.20±0.29	0.32±0.32	0.48±0.04

Table 6.5: Proportional contributions of sources to the organic carbon in Oregon suspended sediment from end member mixing analysis. EM1, EM2 and EM3 are Oregon-wide end members: "soil" is the mean of all surface soil, bedload and channel bank samples; "wood" is the mean of all charcoal and woody debris samples; "rock 1" is the mean of Deer Creek suspended sediment samples; and "rock 2" is the Deer Creek suspended sediment sample with highest C/N (see Section 6.4.1.1 for discussion). For Trask and Flynn, results were the same whether rock 1 or rock 2 was used. G_1, G_2 and G_3 are the proportions of organic carbon in the suspended load of the given watershed that originate from end members 1, 2 and 3 respectively, as calculated using C_{org} and $\delta^{13}C$; H_1, H_2 and H_3 are equivalents calculated using N concentration and $\delta^{15}N$; and F_1, F_2 and F_3 (used in subsequent discussion) are the averages of the two methods.

6.4.1.5 Trends in composition with increasing SSC

Figure 6.12 shows the variation in composition of organic matter in the suspended load with increasing SSC. Although patterns are not clear-cut, there are some indications in N/C–δ^{13}C space that at higher SSC (cold colours), samples increasingly cluster around the centre of the distribution, with fewer outliers. This suggests that surface soil becomes a more significant source. Deer Creek is the exception to this; here, carbon in the suspended load is increasingly pulled towards bedrock at high SSC. Samples at the extremities of each distribution occur at medium (H.J. Andrews, Trask and Alsea) or low (Hinkle) SSCs. This makes sense: at quiet times, individual inputs from discrete sources are likely to remain visible in the bulk composition. The same patterns are not apparent in C/N–δ^{15}N space, except for the Alsea, reflecting the complexity of processes involved in the source–sediment system in Oregon headwaters.

6.4.2 Organic carbon dynamics in the Cascades

On average, POC in suspended sediment from H.J. Andrews has exactly the same make-up as that from Trask and Flynn Creek—that is, ∼60% from surface soil and ∼40% from foliage (Table 6.5). However, the Cascades sample sets contain more examples at the compositional extremes, particularly in N/C–δ^{13}C space (Figure 6.10).

At H.J. Andrews, these take the form of very low δ^{13}C and δ^{15}N values. This trend is likely due to the increasing dominance of individual pieces of foliage at very low SSC, particularly needles from abundant species such as *Tsuga heterophylla*, *Pseudotsuga menziesii* and *Thuja plicata* (Figure 6.6). Because they generally occur at low SSC, they are not significant in the bulk material exported, and this is reflected in such samples being "diluted out" of the mean suspended load composition when it is weighted by SSC.

Possible reasons for compositional differences between compound and instantaneous samples have already been discussed (Section 6.3.3). There are also apparent differences between Lookout Creek and Watershed 1, reflecting the compositional differences described earlier, although, because of the large uncertainties, the proportional contributions of surface soil and foliage in each are within error (75%±8 and 25%±8 for Lookout Creek; 56%±31 and 44%±31 for Watershed 1). If the difference is real, it suggests that homogenisation of biomass via soil, channel bank material or bedload occurs more extensively in the larger catchment. Since there is more scope for material to sit in the channel before being exported in Lookout Creek, and no reason why soil formation processes should be different, the latter is more likely. Additionally, it is possible that the vegetation density in Watershed 1 may be higher

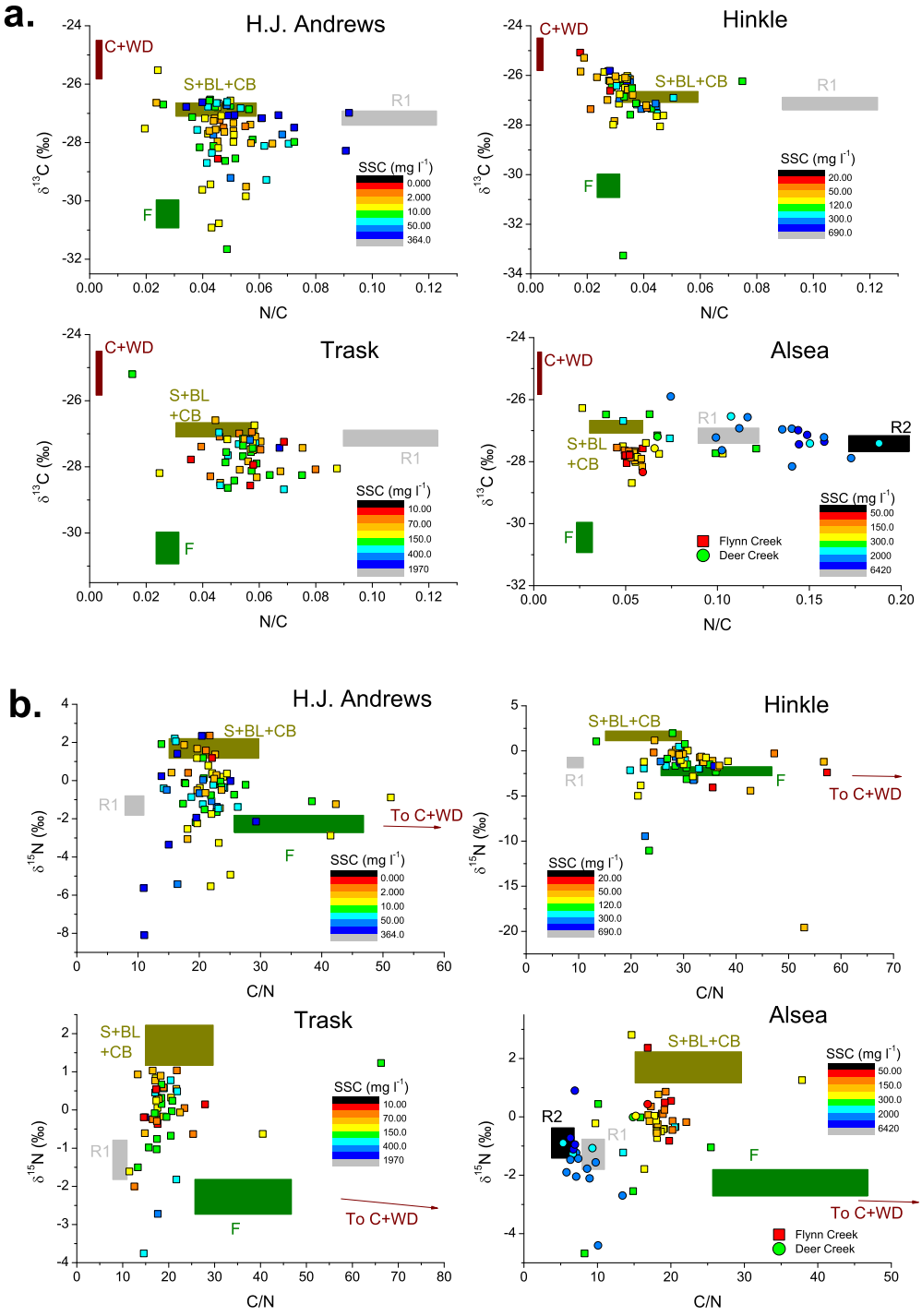

Figure 6.12: Composition of Oregon POM, colour-coded according to SSC. (**a**) Nitrogen to organic carbon ratios (N/C) versus organic carbon isotopic composition (δ^{13}C); (**b**) Organic carbon to nitrogen ratios (C/N) versus nitrogen isotopic composition (δ^{15}N). H.J. Andrews includes suspended sediment from Lookout Creek and Watersheds 1 and 2. Boxes in each plot indicate Oregon-wide end members as used in mixing analysis (Section 6.4.1.4): surface soil, bedload and channel banks (S+BL+CB); foliage (F); charcoal and woody debris (C+WD) and rock 1 (R1) and rock 2 (R2). Limits are defined by error bars in earlier figures.

than that in Lookout Creek as a whole, and also that, because of the much smaller size of stream in Watershed 1, a higher proportion of it is overhung by vegetation which can fall directly into it.

POC in Watershed 2 is unique at H.J. Andrews for having a significant contribution (53%±6) from charcoal and woody debris, with around half the remainder from foliage and half from surface soil. No observations made at H.J. Andrews explain why this should be so.

Hinkle suspended sediment has, on average, a similar composition to that from Watershed 2, but one distinct from that of the rest of H.J. Andrews and the Coast Range watersheds: around half (54%±31) of the organic carbon in it derives from charcoal and woody debris, with only 7%±7 coming from foliage and the rest from surface soil. As there is no immediately obvious reason for woody debris to be more readily incorporated into Hinkle suspended load than the other Oregon headwaters, charcoal is likely to be the primary explanation. Observations, including the presence of charcoal-rich horizons in some Hinkle soil profiles, and local knowledge support the idea that charcoal is particularly influential at the Hinkle. Located further south, Hinkle has a drier and hotter climate (Section 2.3.3, page 34), resulting in more frequent wildfire in the natural regime, and perhaps a higher likelihood of fires reaching the riparian zone from where charcoal could find its way into the channel (Wondzell, 2012). In addition, Hinkle has seen intensive industrial forestry with broadcast burning over the last 80 years (Swanson, 2012).

6.4.2.1 Temporal trends over flood events at H.J. Andrews

Two flood events in November 2011 were sampled at both Lookout Creek and Watershed 1 gauging stations (see Section 3.2.1.2 on page 54 for sampling details). Groups of samples collected on the rising and falling limb of flood hydrographs have identical compositions in all chemical parameters measured. However, the trends over the hydrographs (Figure 6.13) are definite and consistent.

In both Lookout Creek and Watershed 1, the first event—16–17 November—is characterised by SSC increasing and peaking ahead of discharge, indicating that suspended sediment mobilisation occurs primarily in or near the channel. The chemical parameters also begin to change before discharge does and some reach their peak or trough earlier, but others coincide with the discharge peak. Event 2—21–22 November—shows more variable chemistry, but with peaks and troughs generally coincident with the discharge peak. This is also true of SSC, which is vastly elevated at the discharge peak in both Lookout Creek and (particularly) Watershed 1, compared to prior and

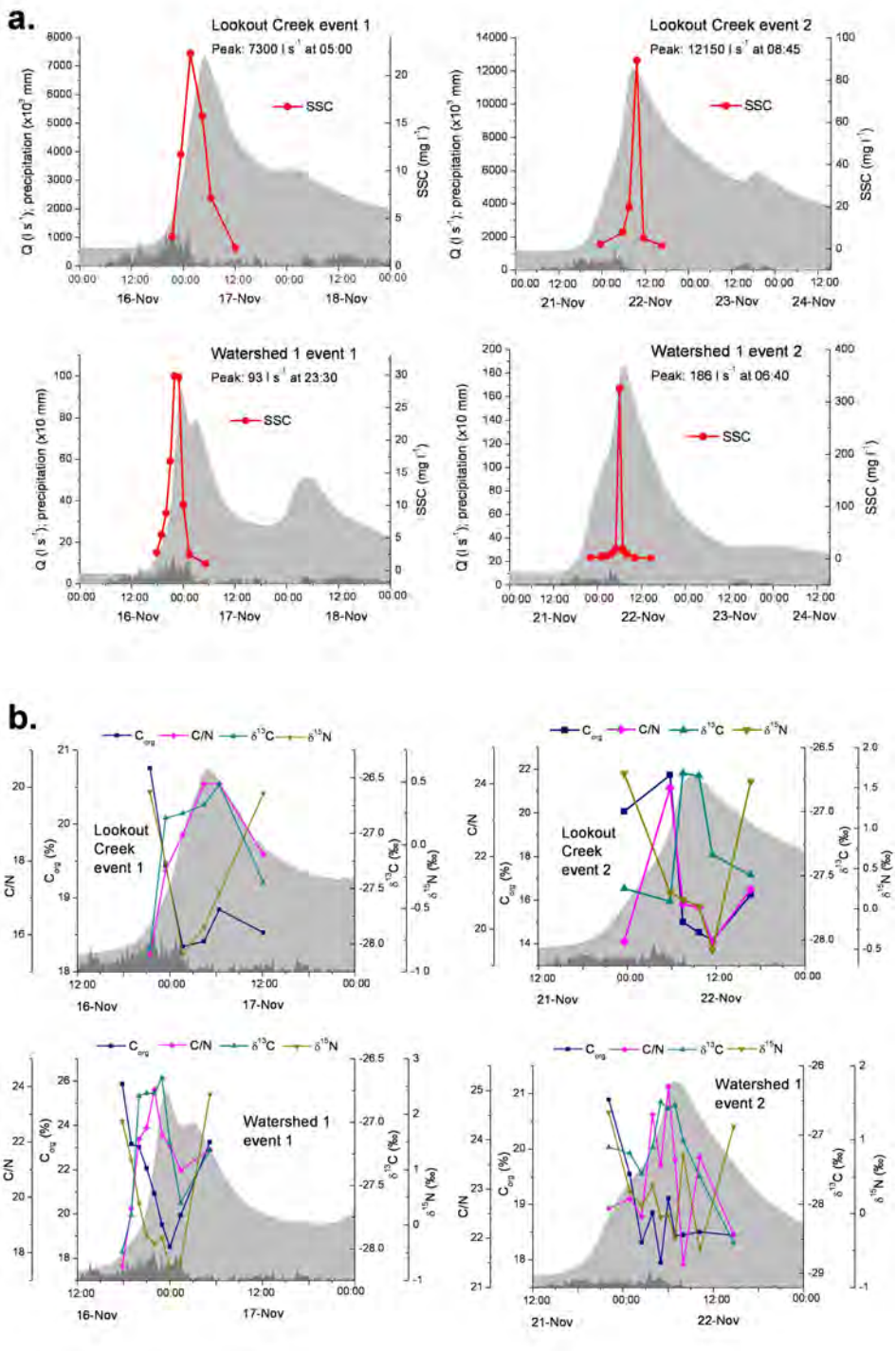

Figure 6.13: Hydrographs for the two flood events sampled simultaneously at Lookout Creek and Watershed 1. Dark grey area is precipitation (data from the H15 met station near Blue River Ridge (Daly & McKee, 2012); see Figure 3.4 (page 61) for location and Section 3.2.3.2 (page 63) for discussion. Light grey area is discharge (Q). Times are in PST (UTC–8); dots represent individual samples. (**a**) Full flood duration with peak discharges given, showing SSC. (**b**) Zoomed in on the sampling period, showing organic carbon concentration (C_{org}), organic carbon to nitrogen ratio (C/N), organic carbon isotopic composition ($\delta^{13}C$) and nitrogen isotopic composition ($\delta^{15}N$).

subsequent samples and the peak in event 1. Because it occurs at both small and large scales, this is more likely to reflect a systematic effect than a localised mobilisation event.

In general, C_{org} and $\delta^{15}N$ decrease then increase during a flood, while C/N and $\delta^{13}C$ increase then decrease. The low C_{org} during peak flow indicates dilution of POC by material with C_{org} of less than the lowest concentration reached during the floods (14%), which includes bedrock (no C_{org}), bedload (C_{org}=2.9%), channel banks (C_{org}=4.8%), deep soil (C_{org}=2.7%) and surface soil (C_{org}=8.1%). At the same time, chemical shifts (lighter N, heavier C and higher C/N at the peak) suggest that more woody debris is incorporated into the suspended load with increasing discharge. These two trends can be reconciled if the dilution is caused by addition of bedrock, while the source of the organic carbon that is still being mobilised shifts from foliage and surface soil to woody debris. It is likely that this is caused by increased mobilisation—or shredding—of woody debris already in the channel.

If this is the case, there is a disconnect between what is observed over these single events to the patterns apparent on longer timescales, since Figure 6.12 (discussed in section 6.4.1.5) hints that soil is increasingly mobilised at the expense of plant material as discharge increases. It is possible that progressive mobilisation of woody debris is an individual feature of these storms that is usually less important, but more likely, the operation of such a process may be of short enough duration that woody debris is not detectable in the compound samples.

6.4.2.2 Seasonal variation in concentration and composition of POM in Watershed 1

Figure 6.14 shows the temporal variation in SSC, C_{org} and composition (represented by C/N and $\delta^{13}C$) of Watershed 1 compound samples, together with discharge, over the sampling period. There are no obvious seasonal patterns in chemistry other than those relating to discharge already discussed: C heavier and C/N lower when flow is high, reflecting a stronger input from surface soil than plant material. However, there is some evidence that C_{org} is higher during the summer months than it is at similar discharges and SSCs during winter. This likely reflects the difference in snow cover between summer and winter, with extra biogenic material able to accumulate in the channel and feed into the suspended load when snow does not blanket the hillslopes. Such material will be flushed out by the first winter storms, possibly represented by relatively high C_{org} values in late October–early November in both 2004 and 2005, and accumulate more slowly during the winter, leading to low concentrations.

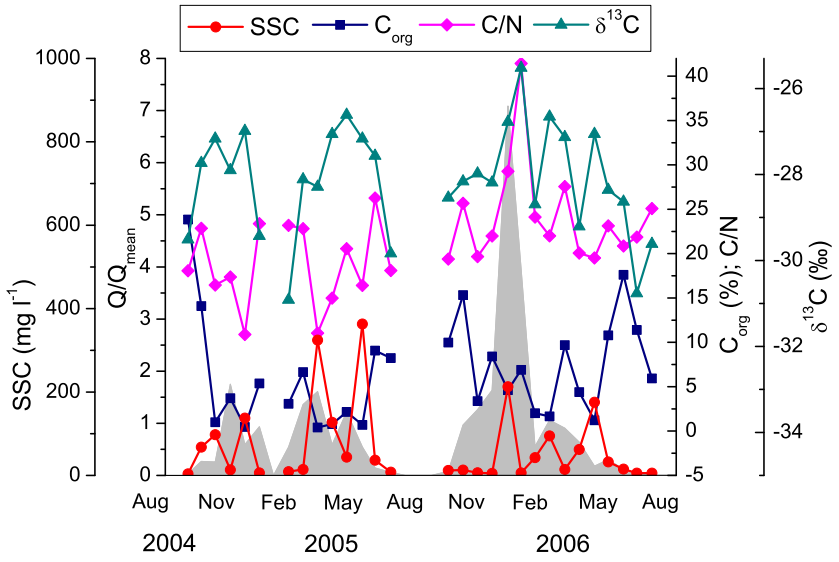

Figure 6.14: Seasonal variation in SSC (red circles), organic carbon concentration (C_{org}; blue squares), ratio of organic carbon to nitrogen (C/N; pink diamonds), and organic carbon isotopic composition ($\delta^{13}C$; turquoise triangles) in Watershed 1 compound samples. Also shown in grey is the mean discharge (as Q/Q_{mean}) for the week represented by each sample.

There are not enough samples for a useful investigation of seasonal patterns in the Lookout Creek samples, and the turbidity threshold sampling method used at Hinkle means that samples cluster around a few events, rather than showing behaviour spread out over the year.

6.4.2.3 Geomorphological observations

Cascades hillslopes are geomorphologically inert, and as a result, they are almost entirely decoupled from streams by a densely vegetated, low-gradient riparian zone. The landscape is smooth over short length scales (tens of metres); there is no widespread dissection (Figure 6.15). In the field, there is little evidence of active mass wasting on the hillslopes, such as tree creep and cracks in the ground. Trees grow right up to the channel banks (Figure 6.16(a)), indicating widespread stability on at least decadal timescales. Several earth flows, up to 2 km^2, do exist and can be identified from LiDAR topographic data (Figure 6.15). Under some conditions they could yield large amounts of sediment and organic carbon, but there is no evidence that they are currently active or reach the channels. It is probable that many of them are ancient, instigated by periglacial processes at the end of the last ice age, then dormant. Where historic landslides are known, they tend to start at roads (Snyder, 2000), indicating that such features may be even less common in the natural system.

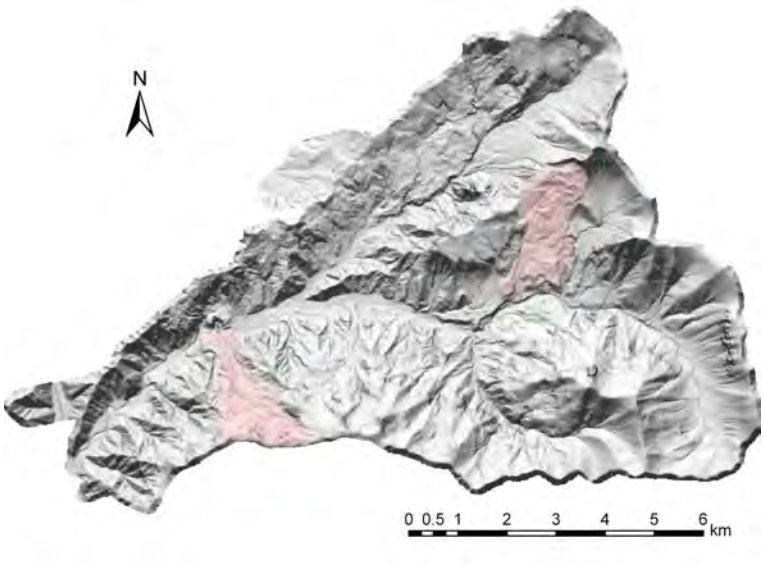

Figure 6.15: LiDAR picture of H.J. Andrews, showing lack of widespread landscape dissection and ancient earth flows highlighted in pink (compare Figure 2.17 on page 40). LiDAR data from Spies (2011).

Channels in both Watershed 1 and Lookout Creek are aggrading rather than incising. This results in flat valley floors much wider than the channels, without the undercut slope toes seen in actively incising areas where hillslopes are coupled directly to streams lacking an intervening riparian zone. Valley floors gradually fill up with colluvium, washed in from hillslopes and trapped by snags, baffles and pools before it can be removed by the stream. In addition, a thick carpet of moss and other ground vegetation both on the hillslopes and in the riparian zone acts like a sponge, soaking up rain and preventing overland flow from developing. The sponge effect is enhanced by the coarse nature of the underlying soil, which increases its porosity and ability to absorb and retain water (McDonnell, 2003). Indeed, no overland flows are known at H.J. Andrews except during rain-on-snow events (Montgomery *et al.* , 1997; Schulze, 2011). This protective ground plant layer may also reduce raindrop impact and hence soil erosion. In these ways, the contribution of hillslope soil to the suspended load is minimised. In contrast, ground plants overhanging the channel, as well as trees overhead, are directly connected to the stream. Delicate material entering the stream at the top of the catchment, such as needles and leaves, are easily broken up during downstream transport into pieces small enough to be picked up by the sampling methods at the catchment outflow. Yet, as discussed above, foliage accounts for only 42%±29 of inputs to average suspended POC: the remaining soil-like component must come principally from the channel banks or within the channel itself.

The cross-section of Watershed 2 (similar to that of Watershed 3 in Figure 6.16(b))

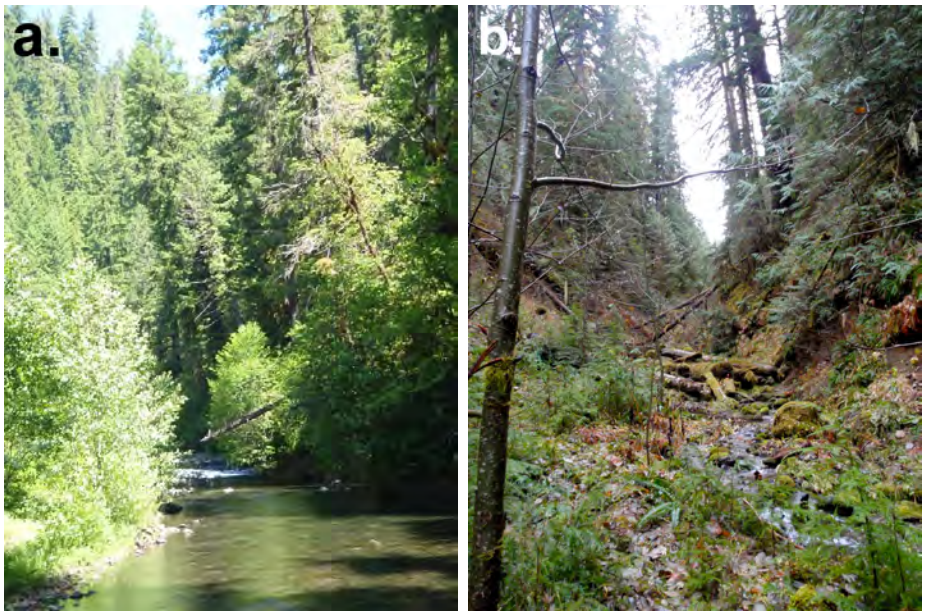

Figure 6.16: (**a**) Photograph of Lookout Creek. Riparian vegetation, including large trees, grows right up to the stream edge, indicating long-term bank stability. (**b**) Photograph of Watershed 3, showing hillslopes rising directly from channel and lack of flat riparian zone, in contrast to Lookout Creek and Watershed 1.

suggests that it is geomorphologically more active than Watershed 1 and Lookout Creek. There is a much-reduced riparian zone and evidence of undercut banks, especially in the lower reaches, indicating that incision is still occurring. The lack of riparian zone in some parts means that the moss carpet (still present further up the hillslopes) does not extend to the channel edge and more soil is exposed. With steep valley sides and no flat buffer, falling trees are likely to settle too high up to act as baffles for sediment, or break into short enough sections not to block the channel. The frequency of debris flows may be another factor: these clear out the channel and prevent colluvium from accumulating by removing the coarse woody debris that traps it. Once fallen trees begin to accumulate higher up in the catchment, large enough plugs to sweep out the lower channel are prevented from forming, meaning that baffles also accumulate lower down and channel incision is effectively switched off. It is possible that logging in Watershed 1 in the 1960s may have triggered this switching-off process, while Watersheds 2 and 3, never logged, have retained channel-cutting features. Fires and other natural events, as well as logging, could trigger the incision switch-off.

Unfortunately, obtaining samples from Watersheds 2 and 3 to test these hypotheses was not easy, and the three compound samples obtained from Watershed 2 suggest that less surface soil, not more, is mobilised here. This does not fit the hypotheses outlined above, but so few data points are inconclusive.

6.4.3 Organic carbon dynamics in the Coast Range

POM from Trask and Flynn Creek cluster more closely around surface soil composition than those from Cascades watersheds, but on average, the contributions to POC in the suspended load from surface soil and foliage are very similar to those at H.J. Andrews: 59%±23 and 41%±21 at Trask; 57%±26 and 41%±25 at Flynn Creek. The main difference to H.J. Andrews, therefore, is that SSC is rarely low enough for individual pieces of foliage, woody debris or fossil organic carbon to dominate a particular sample, although there are a few examples of each of these cases in the Trask sample set. Even this is probably mostly an effect of sampling method. A further difference to the Cascades catchments as a group is that there is no contribution on average from charcoal or woody debris, unlike at Hinkle and Watershed 2.

Although bedrock was included in the three end member mixing model for all the Coast Range catchments, the analysis showed that, whatever its composition, it makes on average no contribution to Trask suspended load. Only the Alsea exhibits any influence of petrogenic carbon, and in Flynn Creek this is a minimal 2%±0. The contribution of fossil organic carbon to Deer Creek POC, on the other hand, is indisputable, and is between ∼50% and 100% depending on which estimate of bedrock composition is used (see Section 6.4.1.1). Both surface soil and foliage contribute to the remainder of POC, in approximately a 2:3 ratio (Table 6.5): this, together with SSC values an order of magnitude higher (Figure 6.8), suggests that similar processes to those occurring in the natural Oregon catchments still operate at Deer Creek, but that the biogenic POC mobilised by them is swamped by additional lithic material. The same is observed in the Eel River in California, which has high SSC and transports significant petrogenic organic carbon, yet yields a comparable amount of biogenic carbon to the low-sediment Umpqua River into which Hinkle Creek drains (Goñi *et al.* , 2013).

6.4.3.1 Geomorphological observations

Field observations suggest that natural Coast Range environments are geomorphologically more active than the Cascades, likely a response to slightly higher rates of tectonic uplift (section 2.3.2). In the Trask area, there is evidence of limited active mass wasting in the form of recent landslides, and in both Trask and Flynn Creek, stream banks are more extensively undercut. The moss carpet is less ubiquitous, although overland flow still rarely happens. However, as discussed above, these differences appear to have a negligible effect on the composition and origins of the bulk suspended load exported from the headwaters. The presence of a vegetated riparian

zone is apparently enough to buffer these streams from any effects of the slightly more active hillslopes.

The only difference between Deer Creek and Flynn Creek is the recent intensive logging in the former (Section 2.3.5, page 41), so it must be concluded that it is this which causes the difference in the provenance of organic carbon in the suspended load. In areas which have been clear-cut and had stumps removed, there is likely to have been wholesale overturning of soil and regolith, with insufficient time since then for the organic carbon-rich surface soil and vegetation to have re-developed. Aided by the landslides known to have occurred from road-induced failures (Beschta & Jackson, 2008), runoff-driven erosion is then able to deliver this mixed material to channels. Thus, significant amounts of clastic sediment, largely derived from bedrock, are generated and propagate through the catchment to its outflow, and this happens to a greater extent during heavier rain. The generation process probably occurs higher up in the catchment where the riparian zone may be less well-established than in the lower reaches, which closely resemble Flynn Creek and likely behaves comparably with respect to carbon dynamics. Hatten *et al.* (2012) report that POC discharged into the Pacific Ocean by the Alsea River at Tidewater is virtually all modern, suggesting that the behaviour shown by Deer Creek is localised and not widespread throughout the Coast Range, while Flynn Creek and Trask behaviour is much more representative.

6.5 Long-term POC export fluxes

Long-term export of suspended sediment and POC in Oregon is difficult to constrain with the present dataset. However, it is possible to come up with some ballpark figures, albeit with caveats.

6.5.1 POC export fluxes in the H.J. Andrews Forest

Total POC export from Watershed 1 and Lookout Creek over the period covered by the compound sample sets can be calculated directly by integrating the mean discharge and POC concentration in mg l^{-1} for each sample over the preceding three-week period, and summing them. Where samples were too small to analyse, C_{org} was estimated by comparing the SSC value with those of the rest of the sample set, and a value for total POC exported over that particular 3-week period obtained as before. Including these samples has minimal effect on the fluxes because of their low discharges. For Watershed 1, 3.7 tonnes km^{-2} yr^{-1} of POC were exported, based on complete water years 2005 and 2006 (October 2004 to September 2006). For

Lookout Creek, the figure is 9.6 or 10.0 tonnes km^{-2} yr^{-1}, depending whether small samples with estimated C_{org} are included, based on complete water year 2006 (October 2005 to September 2006). However, it is impossible to say whether these fluxes are characteristic in the long term, because discharge—and with it the processes by which POC is mobilised and exported—varies significantly over decadal timescales (Figure 2.21, page 46). Relationships between discharge and POC concentration must be established in order to model the export of POC over the long-term discharge records available for Lookout Creek and Watershed 1.

Panels (a) and (b) of Figure 6.17 show POC concentration plotted against Q/Q_{mean} for Lookout Creek and Watershed 1. The relationships are poorly defined (R^2=0.09, 0.11 and 0.04 for Watershed 1, Lookout Creek and combined rating curves respectively) and will not give robust estimates of long-term POC export. This is reflected in the large errors resulting from propagation of the large uncertainties on the rating curve parameters (Table 6.6). However, there is little alternative: the linear relationships between SSC and POC are somewhat better-defined (Figure 6.17 (c)), with R^2 values of 0.18 for Lookout Creek, 0.24 for Watershed 1, 0.13 for all compound samples and 0.99 for all instantaneous samples, but no continuous long-term SSC records exist for Lookout Creek or Watershed 1, and the correlation between Q/Q_{mean} and SSC (Figure 6.17 (d), R^2=0.02 for all samples) is not strong enough to provide a suitable relation to discharge, thus preventing meaningful extrapolation.

Integrating the rating curves in Figure 6.17(a) over discharge records of 22 years for Lookout Creek (instantaneous readings every 30 minutes) and 30 years for Watershed 1 (mean readings every 15 minutes) gives mean POC export fluxes of 3.2±1.1 t km^{-2} yr^{-1} and 15.4±67 t km^{-2} yr^{-1} respectively. The fluxes for the years covered by compound sampling given by this method are 3.4 t km^{-2} yr^{-1} and 15.9 t km^{-2} yr^{-1}; comparing these to the values obtained directly suggests that the rating curves underestimate POC export from Lookout Creek, and overestimate it from Watershed 1. If the combined rating curve (Figure 6.17(b)) is used instead, the long-term export fluxes are 5.8±5.5 t km^{-2} yr^{-1} and 6.3±7.6 t km^{-2} yr^{-1} for Lookout Creek and Watershed 1 respectively, and those for the sampling periods are 6.3 t km^{-2} yr^{-1} and 5.8 t km^{-2} yr^{-1}. If the large errors are ignored, these are a much better match to the directly-obtained figures of 10 t km^{-2} yr^{-1} and 3.7 t km^{-2} yr^{-1}.

Given the broad agreement of these two methods, neither on their own robust enough to draw firm conclusions, it can be said with reasonable confidence that export of POC from settings like H.J. Andrews, on decadal timescales where discharge is within the "normal" range, is on the order of 6 tonnes km^{-2} yr^{-1}, although the large errors mean that this must be regarded as a ball-park figure.

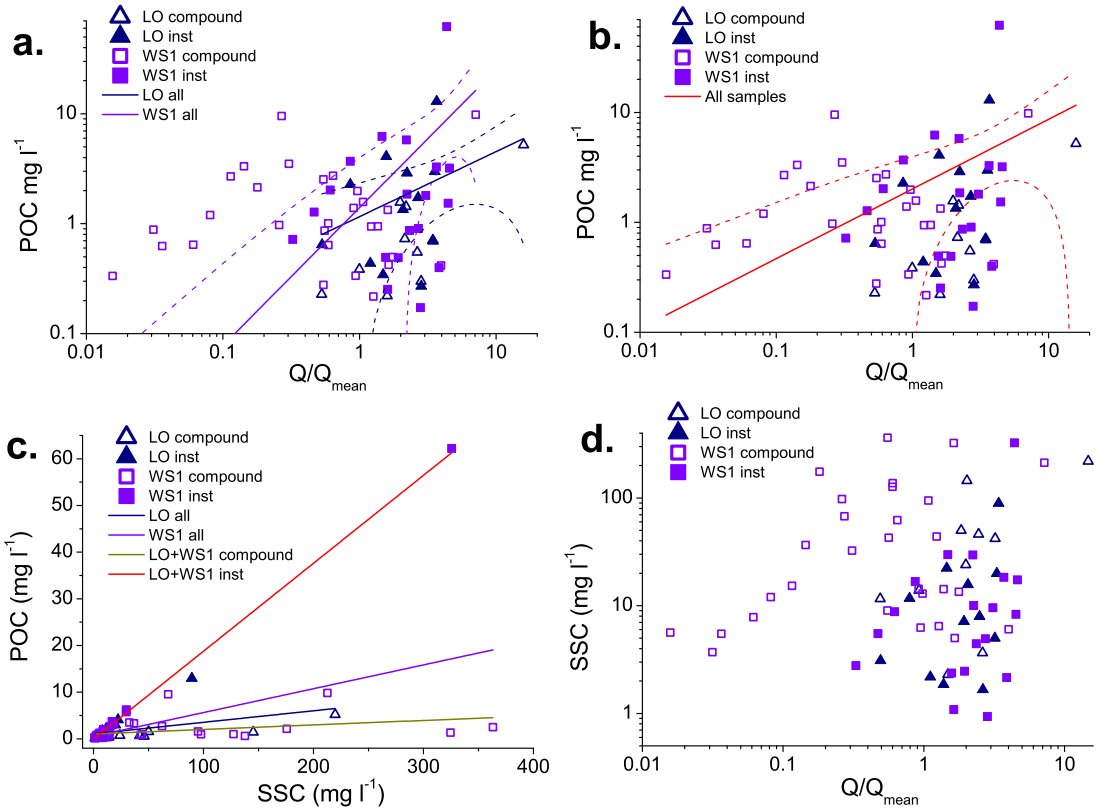

Figure 6.17: Rating curves showing power law relationships between (**a**) and (**b**) Q/Q_{mean} and POC concentration and (**d**) Q/Q_{mean} and SSC, and (**c**) linear relationships between SSC and POC for samples from H.J. Andrews. Navy triangles and blue squares represent individual samples from Lookout Creek and Watershed 1 respectively. Solid lines are best fits to the datasets indicated in each legend; dashed lines are 95% confidence bands.

	a	**b**	$\mathbf{R^2}$	$\mathbf{Q_e}$ **(l s^{-1})**	$\mathbf{Q_e}$ **(Q/Q_{mean})**
Combined	2.01±0.98	0.63±0.31	0.04	-	-
WS1	1.40±1.28	1.25±0.61	0.09	550±1740	14±44
LO	1.16±0.57	0.59±0.27	0.11	4150±1670	1.4±0.5

Table 6.6: Rating curve parameters for power law relationships between Q/Q_{mean} and POC, of the form $POC=a(Q/Q_{mean})^b$. The "Combined" curve uses samples from both Lookout Creek and Watershed 1. Correlation coefficients are given as R^2. Q_e is the effective discharge, as defined by Wheatcroft *et al.* (2010). Q/Q_{mean} is the discharge relative to the mean discharge for water years 1987–2008 for Lookout Creek (3250 l s^{-1}) and 1980–2009 for Watershed 1 (40 l s^{-1}). Long-term discharge data are from Johnson & Rothacher (2012).

6.5.1.1 Effective discharge and episodicity

The effective discharge (Q_e), the discharge that transports on average the largest proportion of a given constituent load (Andrews, 1980; Nash, 1994; Wheatcroft *et al.*, 2010) and expressed as Q/Q_{mean}, can only usefully be calculated for Lookout Creek; the large uncertainty on the rating curve exponent leads to a huge error on Q_e for Watershed 1 (Table 6.6). Lookout Creek has Q_e close to 1, indicating that frequently occurring, low-discharge conditions transport the majority of POC, and that extreme events may have little impact on POC export.

Variability can also be examined through the difference in annual discharge between years when there were large flood events and those when there were not. Major floods occurred at H.J. Andrews in the winter of 1964–1965 and February 1996: in water year 1996, mean Q was 64% and 53% higher than long-term Q_{mean} for Lookout Creek and Watershed 1 respectively. This information suggests that major floods have more impact on the overall export capacity in Lookout Creek than in Watershed 1. However, sediment-transporting events are not equal to discharge events, and behave differently because of the other factors involved, principally sediment supply. Based on work in western Oregon, Benda & Dunne (1997) suggest that variability of sediment output is optimised when catchment size is similar to that of the perturbation—in this case, a large rain storm. Thus, Lookout Creek would be expected to have a high variability, while Watershed 1 is too small to experience the full effects of a large storm and "saturates" earlier. This is at odds with the inferences made for POC from effective discharge, but it is clear from Figure 6.17 that POC does not always behave in the same way as bulk suspended sediment.

Additionally, it is worth noting that these metrics apply only over the few decades for which data exist. It is likely that episodicity also occurs with a much longer period, but constraining the POC exported by events with return times of 50 years or more is beyond the scope of this thesis. The processes and fluxes elucidated herein are applicable only over decadal timescales where no such events occur. Indeed, the occurrence of infrequent, episodic floods and debris flows causing the rapid release of large volumes of sediment and organic carbon that could be volumetrically significant in the long-term, limits the usefulness of the Oregon catchments for determining long-term sediment and POC yields (Grant & Wolff, 1991).

6.5.1.2 Coarse woody debris

The yields calculated above reflect only suspended material small enough to be sampled through tubes (for automated discharge-proportional samples) or bottle necks.

However, coarse woody debris is known to be abundant in Oregon's streams (Fetherston *et al.* , 1995; Johnson *et al.* , 2000) and it is likely that some of this material is mobilised and exported during storms (e.g. Bunte, 2001; Bunte & Swingle, 2003). No data are presently available on this for the catchments used in this study and so it is not considered further here. The implications of this omission are discussed in Section 7.4.1.1.

6.5.2 POC export flux in other Oregon catchments

Similar quantitative estimates, however weak, cannot be made for the other catchments because of the turbidity threshold sampling method and the lack of accessible continuous long-term discharge records for these catchments. In the turbidity threshold sampling datasets, a sampling date and instantaneous discharge for each sample is known, but frequently no sampling time. This and the paucity of samples means that even crude hydrographs cannot be constructed. The result is that it is impossible to assign a length of time and mean discharge to the conditions represented by each sample. In addition, long gaps are left between sampling clusters where there is no information. Too many assumptions would have to be made for any estimate of POC export for the period covered by these samples to be reliable. Hence, no constraints on POC export are given for Oregon landscapes other than those found at H.J. Andrews. Although it may be valid to extrapolate this throughout the Cascades, it cannot be assumed that the flux would be similar in the Coast Range, because the greater geomorphological activity observed there might lead to higher long-term sediment yields. Although there is little evidence of this at Flynn Creek (or F_{nf} would be lower), no further speculation is made.

In conclusion, the Oregon data presented in this chapter are more suited to investigation of the sources and routing processes of organic carbon than to a quantification of fluxes.

6.6 Chapter summary

The concentration and composition of organic matter in riverine suspended sediment and its potential sources was determined for several catchments in the Oregon Cascades and Coast Range. Equivalent carbon stores in each catchment are within error of each other, but riverine POM shows differing behaviour in some catchments, reflecting environmental and geomorphological factors.

SSC in natural Oregon streams is low, rarely exceeding 500 mg l^{-1}. Because there is

little clastic input, suspended load C_{org} is correspondingly high, and also highly variable, with mean values for relatively undisturbed catchments ranging from 6.13%±1.9 to 10.2%±2.5. Samples from Deer Creek, which has seen significant recent clearcutting and consequently has a much higher clastic input, have consistently much lower C_{org}, with a mean of 0.45%±0.91. Compositionally, the organic carbon in Deer Creek samples is bedrock-dominated: 50%–100% of it is of petrogenic origin, with the rest coming from both surface soil and foliage.

The suspended sediment samples from the other catchments contains almost entirely non-fossil carbon. This includes those from Flynn Creek, which is underlain by the same carbonaceous bedrock as Deer Creek, but whose suspended load POC contains only 2%±0 petrogenic carbon. Samples cluster around the composition of surface soil, bedload and channel banks (these three being indistinguishable), and within a sector between this and the arc formed by fresh plant matter (foliage and wood of many species). Individual plants are incorporated directly into the suspended load, with no prior homogenisation. On average, POC in the streams of H.J. Andrews, Trask and Flynn contains ∼60% carbon from surface soil and ∼40% from foliage. Samples from Hinkle, where wild and anthropogenic fires are more common, are strongly affected by the incorporation of charcoal, with approximately half of POC originating from this source. Deep soil is not a major source of carbon in the suspended load for any catchment. At H.J. Andrews, there is increased input of woody debris from in-channel shredding during storms. Over longer timescales, there is limited evidence from all watersheds that the proportion of soil relative to plant matter increases during times of high SSC.

Wide, flat riparian zones throughout all studied catchments act to decouple hillslopes and streams, meaning that inputs to the suspended load must come from in or directly adjacent to channels. In addition, porous soils and vegetation cover, including a moss carpet particularly pervasive in the Cascades, prevents overland flow. Although the Coast Range is geomorphologically more active than the Cascades, with more extensively undercut banks and evidence of recent mass wasting, this is not reflected in POM composition.

Long-term POC export fluxes from Oregon catchments are difficult to determine because of the low temporal resolution of the data, weak relationships between Q and POC/SSC, and lack of long-term discharge records. The major focus of this chapter is therefore on processes. However, the export flux from H.J. Andrews was estimated, using two different methods, to be on the order of 6 t km^{-2} yr^{-1} of POC, of which 100% derives from non-fossil sources.

Chapter 7

Synthesis

7.1 Introduction

This chapter has three aims. The first is to compare the systems studied in this project and hence determine the major controls on POC export style. The second is to consider how these findings could be extrapolated to a global scale. Finally, the significance of the processes observed and described in this thesis is assessed by placing them in the context of the global carbon cycle, including comparison to extant global flux estimates and discussion of potential climate feedbacks in which they may be implicated.

Symbols and abbreviations used in the figures in this chapter follow the same conventions as used in previous chapters.

7.2 Alptal and Oregon: comparisons and contrasts

7.2.1 Catchment organic carbon stores

The chemistry of POM in catchment carbon stores in the Alptal and Oregon is compared graphically in panels (a) and (b) of Figure 7.1.

Based on the samples collected in this study, bedrock from the Erlenbach and the Alsea has comparable C_{org} of 0.54%±0.11 and 0.43%±0.19 respectively. Both have low C/N and are enriched in the heavy isotopes, and samples cover a wide compositional spread, particularly in C/N. However, Alsea bedrock—both collected samples and estimated composition of rock eroded by streams—has slightly lighter C and N. In the Erlenbach, there is very little fossil organic carbon oxidation even at the surface because of sealing by near-permanently waterlogged gleysols. Consequently,

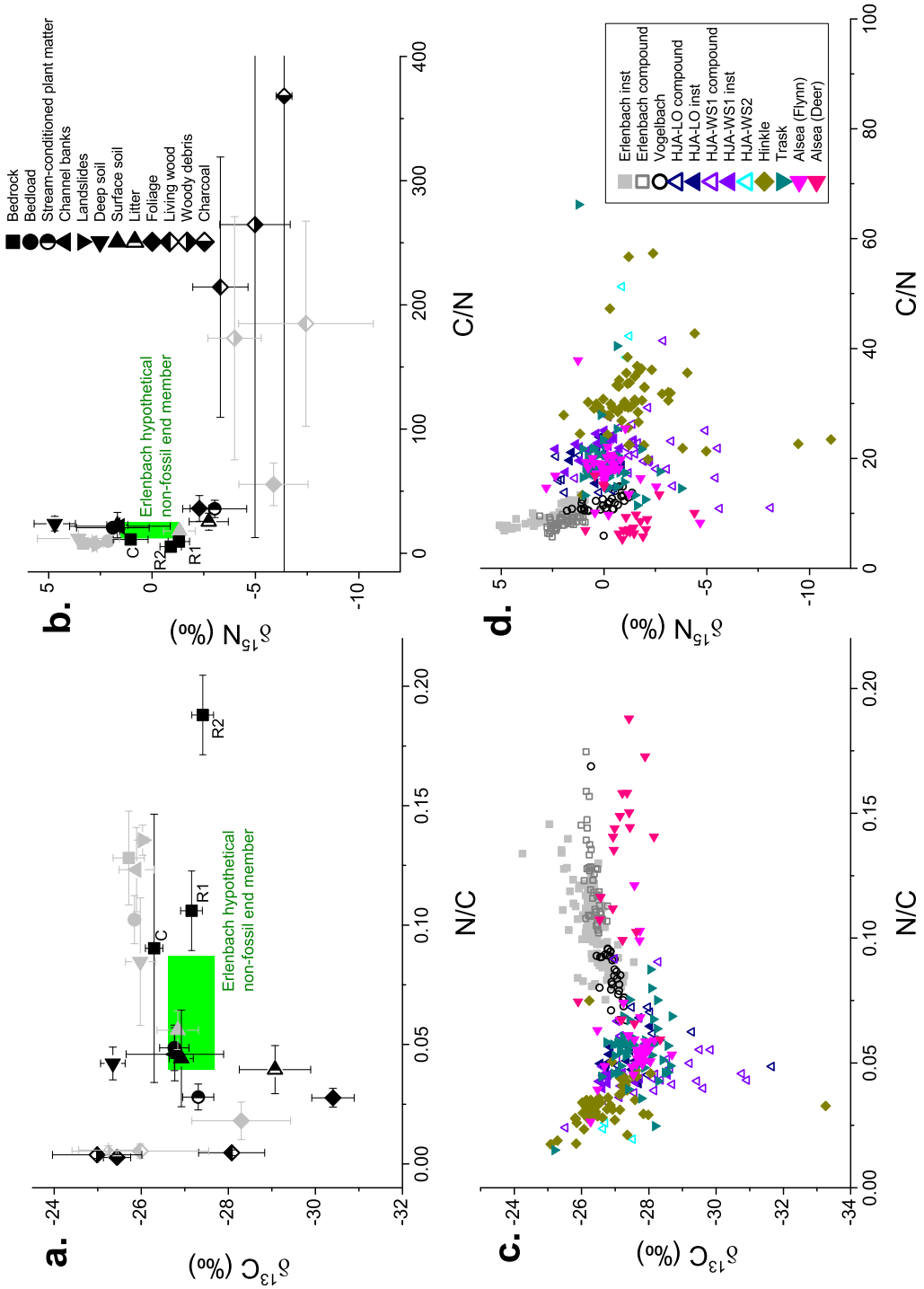

Figure 7.1: Chemistry of (**a**) and (**b**) organic carbon pools and (**c**) and (**d**) POM in suspended sediment in the Alptal and Oregon. Alptal sources are in grey and are represented by the Erlenbach only; Oregon sources are in black and are averaged across all watersheds. Three estimates of Oregon bedrock composition are included: that measured in Alsea cores (C), and two others, R1 and R2 (see Section 6.4.1.1 on page 152 for details). (**a**) and (**c**) Nitrogen to organic carbon ratios (N/C) versus organic carbon isotopic composition (δ^{13}C); (**b**) and (**d**) Organic carbon to nitrogen ratios (C/N) versus nitrogen isotopic composition (δ^{15}N).

there is a large fossil organic carbon contribution to the suspended load. In contrast, oxidation—extensive at the surface, concentrated along fractures at depth—in the Coast Range probably limits its contribution to the suspended load, especially in Flynn Creek. Some oxidation of bedrock in the Vogelbach is certainly observed, and the high F_{nf} values of suspended POC here (∼0.9) suggest that it may be quite pervasive. This variable oxidation is likely a function of substrate permeability.

Bedload and channel banks have higher C_{org} values in Oregon than Switzerland: they are dominated by biogenic material even where fossil organic carbon exists and channel banks contain as much organic carbon as surface soil. This is in direct contrast to the Erlenbach, where bedload and channel banks are compositionally "fossil" sources, overwhelmingly dominated by bedrock because of high exhumation rates, high clastic input to channels, and reducing conditions. In this respect, the Vogelbach is similar to the Erlenbach; its bedload plots much closer to bedrock than to surface soil. Differences are also apparent in the grain size distribution of these source sediments (Figure 4.2(b) on page 83 and Figure 6.4 on page 138): Oregon bedload and channel banks are dominated by coarse material, while in the Alptal fine material is much more significant. This likely arises from lithological differences between clay-rich Alptal flysch and Oregon volcanics, coupled with a larger input of coarse plant fragments and soil aggregates to Oregon bedload and channel banks.

Alptal surface soil contains twice the amount of organic carbon as Oregon surface soil (∼16% versus ∼8%) and has lighter N, but plots within error of it in N/C–δ^{13}C space. In both areas, surface soil has higher C_{org} than deep soil, although in Oregon the difference is smaller due to lower C_{org} in the surface soil. C_{org} in deep soil is the same, within error, in both locations, but they are compositionally distinct. Deep soil plots off the trend from bedrock through surface soil to vegetation in both areas, and does not make a major contribution to suspended POC in either. In Oregon, deep soil has the same C/N as surface soil but significantly heavier isotopic ratios. Alptal deep soil has lower C/N than surface soil (closer to bedrock), but only slightly heavier C and N. Profiles taken through stable slopes in the two areas show the same chemical patterns (compare Figure 4.5 on page 86 and Figure 6.5 on page 140). Fine material dominates both surface and deep layers in the Alptal gleysols (60% and 69% respectively), but is a relatively minor component in the coarse, open-structure soils of Oregon (11% at the surface; 36% at depth).

Despite the wholly dissimilar species assemblages found in the Alptal and Oregon, there are many parallels in the organic carbon concentration and composition of plant matter. In both areas, there is a marked difference in the composition of wood and foliage, and additionally in Oregon between standing wood and woody debris. In both

locations, woody debris has higher C/N, less negative δ^{13}C and similar δ^{15}N (slightly more negative in Oregon) compared to foliage. Standing wood plots between the two, although in the Erlenbach the separation between standing wood and woody debris is much less pronounced. Foliage from Oregon has considerably lighter C and heavier N than its counterpart in Switzerland, but there is negligible difference between woody debris from the two areas.

Significant carbon stores in Oregon that are absent or diminished in the Alptal include charcoal and stream-conditioned plant matter. Wildfire is not a frequent component of the natural regime in Switzerland, and there has been no forestry-related burning in the Alptal study catchments. While present in some reaches, stream-conditioned plant matter does not build up to the same extent as in Oregon streams, primarily due to steeper channel gradients and more regular channel-clearing during floods. Meanwhile, landslides are an important source of riverine POC in the Erlenbach, but less so in the Vogelbach and not at all in Oregon. Landslides observed on Coast Range hillslopes were in the form of slipped or rotated blocks with the internal soil layering preserved, in contrast to landslides in the Erlenbach where uniform composition with depth suggests that internal mixing has occurred.

7.2.2 Organic carbon in the suspended load

Oregon headwaters fundamentally differ from the Erlenbach in the amount of sediment they transport (Figure 7.2). Comparable river samples, i.e. those taken instantaneously by hand during storm events with return times of one year and less, have SSC values around three orders of magnitude lower at H.J. Andrews than the Erlenbach. SSC measurements obtained by turbidity threshold sampling at the other Oregon catchments, representing peak sediment transport conditions over several years, are still an order of magnitude lower than Erlenbach values. Only samples from Deer Creek approach comparable SSC, and these, as has been discussed, do not represent natural conditions because of intensive forest management there. The relationship between discharge and SSC is much stronger in the Erlenbach (Kendall's τ=0.62) than any of the Oregon watersheds, where τ=0.37 at best. The Vogelbach also exhibits a weak relationship (τ=0.14).

Unlike the Erlenbach, but similarly to the Vogelbach, C_{org} in Oregon watersheds does not follow a parabolic path with increasing SSC or Q (Figure 7.3). It is plausible that the Oregon data represent just the low-flow side of that pattern, and that there is a similar upturn at flows that have not been sampled in this project. For the Erlenbach, the upturn is at Q/Q_{mean} ~10: only one sample from Lookout Creek has

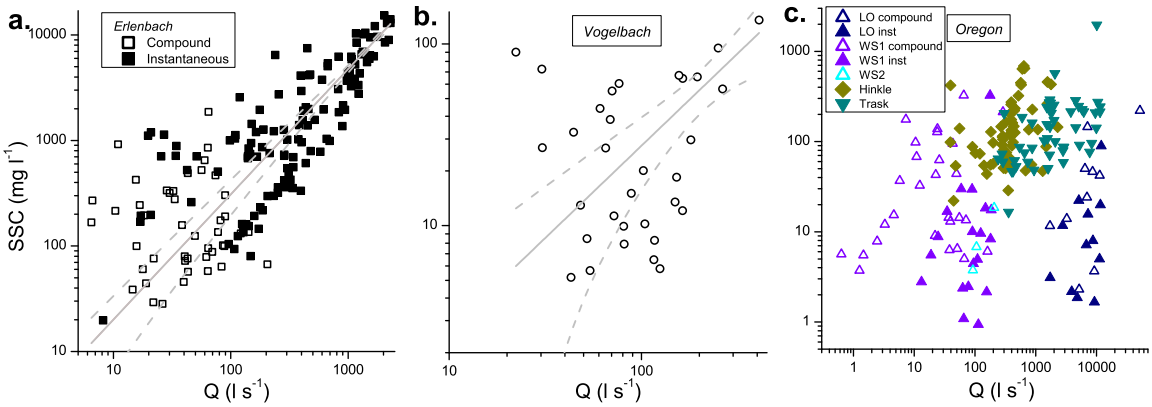

Figure 7.2: Relationship between discharge and SSC in (**a**) the Erlenbach, (**b**) the Vogelbach and (**c**) Oregon catchments where discharge records are available. The regression lines through the Alptal data are power laws (for the Erlenbach, fitted to both compound and instantaneous datasets combined); dashed lines indicate 95% confidence bands.

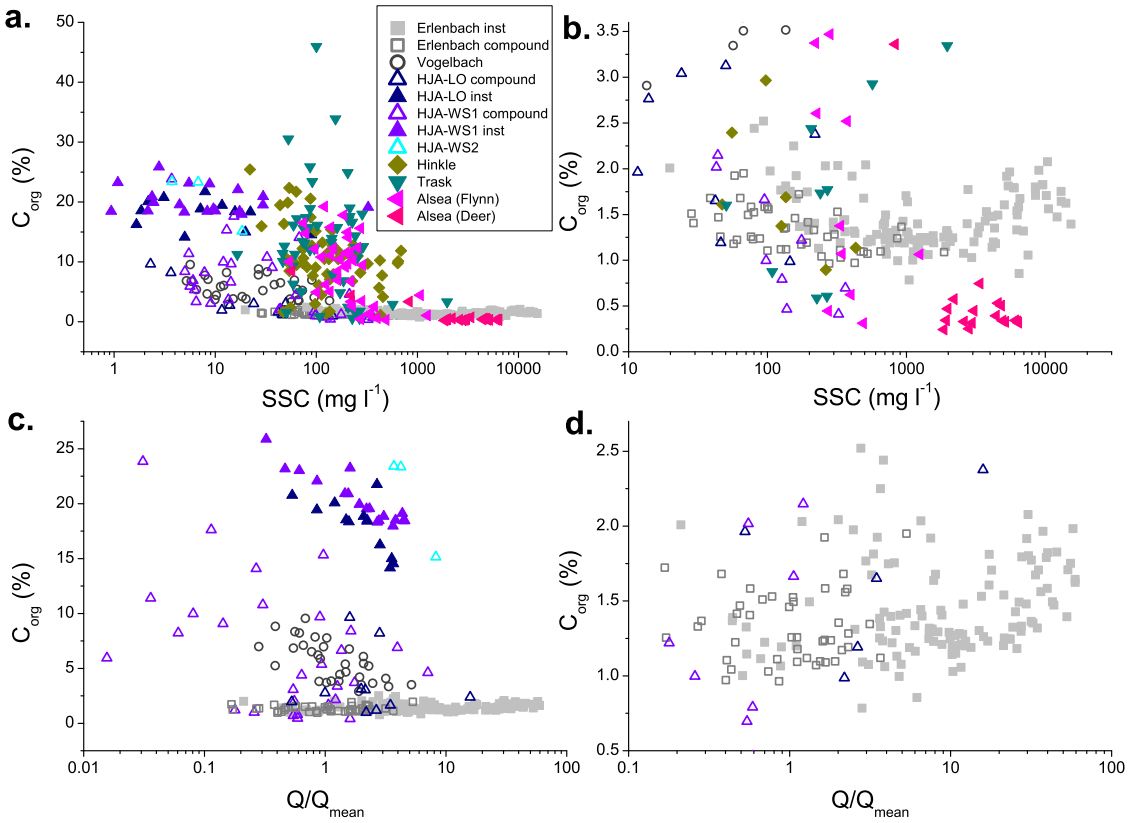

Figure 7.3: (**a**) and (**b**) Relationships between SSC and C_{org}. (**c**) and (**d**) Relationships between discharge (relative to Q_{mean}) and C_{org}. (**a**) and (**c**) show all catchments studied; (**b**) and (**d**) are zoomed in on the y-axis to enable parabolic distribution in the Erlenbach to be seen. Note logarithmic x-axes.

higher Q/Q_{mean}, but a comparison of Figure 2.6 (page 26) and Figure 2.22 (page 47) suggests that, at least in some Oregon watersheds, a similar proportion of flows at Q/Q_{mean} >10 may occur as in the Erlenbach. However, the channel–hillslope decoupling, caused by extensive riparian buffers, thick moss carpet and open soil structure, make it unlikely that Oregon hillslopes could be activated in the same way as in the Erlenbach, and there is no immediately apparent alternative mechanism for causing a similar threshold switch to POC addition. On the contrary, a threshold switch may occur in Oregon when debris flows are activated (Section 2.3.4, page 36), but this is unlikely to lead to increased C_{org} because most of the added material will come from deep soils and bedrock and hence contain relatively little organic carbon.

Figure 7.3 shows that C_{org} values of Oregon suspended sediment samples from natural catchments (mean values H.J. Andrews: 6.2%±0.9, n=73; Hinkle: 9.3%±1.4, n=60; Trask: 10.2%±2.5, n=51; Flynn Creek: 6.4%±1.8) are up to an order of magnitude higher than those in Erlenbach suspended load (mean 1.5±0.1, n=122 for the instantaneous dataset; 1.2±0.1, n=45 for the compound dataset), and twice as high as those from the Vogelbach (5.2±0.75, n=32). As with SSC, Deer Creek shows the most similarity with the Erlenbach, having an even lower mean C_{org} of 0.45%±0.9 (n=20), but higher variability. Compositional differences are illustrated in panels (c) and (d) of Figure 7.1. The vast majority of Oregon suspended sediment samples have higher C/N than those from the Erlenbach, and of those that do not, most are from Deer Creek. Most, including those from Deer Creek, also have lighter N. There is a wide spread in $\delta^{13}C$ at low N/C in the Oregon samples, reflecting the influence of both foliage and wood from many different species. This is greatest for H.J. Andrews, probably because this watershed has lower SSC; such conditions allow the natural heterogeneity of individual components to be preserved in the integrated signal.

Clear compositional shifts from fossil to non-fossil sources with increasing SSC, as seen in the Erlenbach instantaneous dataset (Figure 4.10, page 95), do not occur in Oregon (Figure 6.12, page 161) or the Vogelbach (Figure 5.3, page 112). Despite the POC dilution in these catchments evident from Figure 7.3, neither (except for Deer Creek) do they show the opposite shift from non-fossil to fossil, although for most Oregon catchments this is not expected since there is no fossil organic carbon present in the bedrock. There is some evidence, however, that in the Oregon catchments there is a shift from plant-dominated compositions to surface soil-, channel bank- and bedload-dominated compositions in more turbid flows, which could partially explain the dilution in addition to the admixing of lithic material.

Catchment/ Area	Export Flux (t km^{-2} yr^{-1}) SS	tPOC	fPOC	nfPOC	F_{nf}
Erlenbach	1650±310	23±6	10±2	14±4	0.6±0.0
Vogelbach	100–200	3–11	0.5–1	3–10	0.9±0.3
Coast excl. Deer	n.d.	n.d.	n.d.	n.d.	∼1
Deer Creek	n.d.	n.d.	n.d.	n.d.	0–0.5
Cascades	∼80	∼6	0	∼6	1

Table 7.1: Summary of calculated export fluxes of suspended sediment (SS) and total, fossil and non-fossil POC, in tonnes per square kilometre per year, from all studied catchments. The fraction of riverine POC derived from non-fossil sources (F_{nf}) is also given. "n.d."=not determined. The Cascades SS export flux is estimated from the data contained within Figure 2.23 (page 48).

7.2.3 Organic carbon fluxes and F_{nf}

Fluxes of sediment and total, fossil and non-fossil POC carried in the suspended load (not including coarse woody debris) from the Alptal and Oregon are compared in Table 7.1. Those from the Vogelbach and the Cascades are very similar; the main differences are slightly higher SS yield and slightly lower F_{nf} in the Vogelbach. Per unit area per unit time, the Erlenbach exports around ten times as much suspended sediment as the Vogelbach and Cascades, and, despite significantly lower C_{org} values, three to four times as much total POC and twice as much non-fossil POC. These figures show that, while catchments like the Erlenbach with high sediment yield are the most prolific exporters of POC, those with low suspended sediment concentrations can still yield substantial amounts, particularly of nfPOC, under moderate conditions.

Fluxes from the Coast Range are unconstrained for the reasons detailed in Section 6.5.2 (page 173). However, the chemical distribution of Coast Range suspended organic matter (Figure 7.1) shows that the POC that is exported is likely to be almost entirely non-fossil, and this is backed up by the end member mixing analysis (Section 6.4.1.4, page 155), in which 0%±0 of the carbon in Trask suspended load, and 2%±0 in Flynn Creek, is shown to be petrogenic.

Deer Creek records significantly higher peak storm SSC values than other Coast Range catchments, but these do not reach the highest values seen in the Erlenbach (Figure 7.3); therefore SS export is likely to be <1500 t km^{-2} yr^{-1}. F_{nf} for Deer Creek is difficult to constrain because of the lack of representativeness of the Alsea bedrock core samples, but using two estimates for the composition of bedrock eroded by the streams, end member mixing analysis puts it between 0 and 0.5 (Section 6.4.3, page 168). In addition, similar behaviour between the Erlenbach and Deer Creek—illustrated in Figures 7.1 and 7.3, noted in earlier sections of this chapter, and later

confirmed by Figure 7.4 in Section 7.2.4—suggests that it is certainly no more than 0.6, and very likely less because of the lack of evidence for addition of non-fossil POC by hillslope activation at higher flows.

Table 7.1 also shows that, to first order, F_{nf} is inversely correlated with suspended sediment yield, a pattern that has been noted globally (Leithold *et al.* , 2006).

7.2.3.1 Episodicity and effective discharge

In the Erlenbach, the year 1995 had the highest mean Q in the record, 26% higher than the long-term mean. In comparison, the Oregon flood of 1996 caused annual mean Q to be 64% and 53% higher than the long-term Q_{mean} for Lookout Creek and Watershed 1 respectively. The coefficient of variation of annual mean discharges reflects these trends, being lower for the Erlenbach (15%) and higher for Watershed 1 (27%) and Lookout Creek (33%). These figures suggest that total export capacity for sediment and carbon in a given year is highly dependent on whether there is a major flood for H.J. Andrews, but considerably less so for the Erlenbach, unless there exists a threshold for landsliding that has not been exceeded over the 29-year study period.

However, the same is not true for actual POC export. Effective discharge (Q_e) for nfPOC, expressed as Q/Q_{mean}, is 13.4±3.7 for the Erlenbach and 1.4±0.5 for Lookout Creek (the uncertainty on Q_e for Watershed 1 is too large for it to signify anything useful). Hence, large infrequent events are similarly important in mobilising and transporting nfPOC in the Erlenbach, but not at all important in Lookout Creek, perhaps because of some damping mechanism related to its considerably greater area. Not enough information is available to calculate these parameters for the other watersheds.

7.2.4 Contrasting sources and pathways of POC

With the exception of Deer Creek, organic carbon in Oregon suspended sediment is almost entirely non-fossil. Mixing is between purely biogenic end members (details below), rather than the case of soil-derived non-fossil carbon (61%±0) mixing with petrogenic carbon (39%±0) as in the Alptal. Although Vogelbach POC also exhibits compositions formed by mixing between bedrock and surface soil carbon, a higher proportion (90%±30) comes from the latter on decadal timescales than it does in the Erlenbach. In Oregon, many types of vegetation contribute directly to the suspended load, causing a wide spread in both axes, while in the Alptal, vegetation is only incorporated after homogenisation via a soil "window". In most natural Oregon watersheds, organic carbon in the suspended load is composed of ∼60% carbon derived from

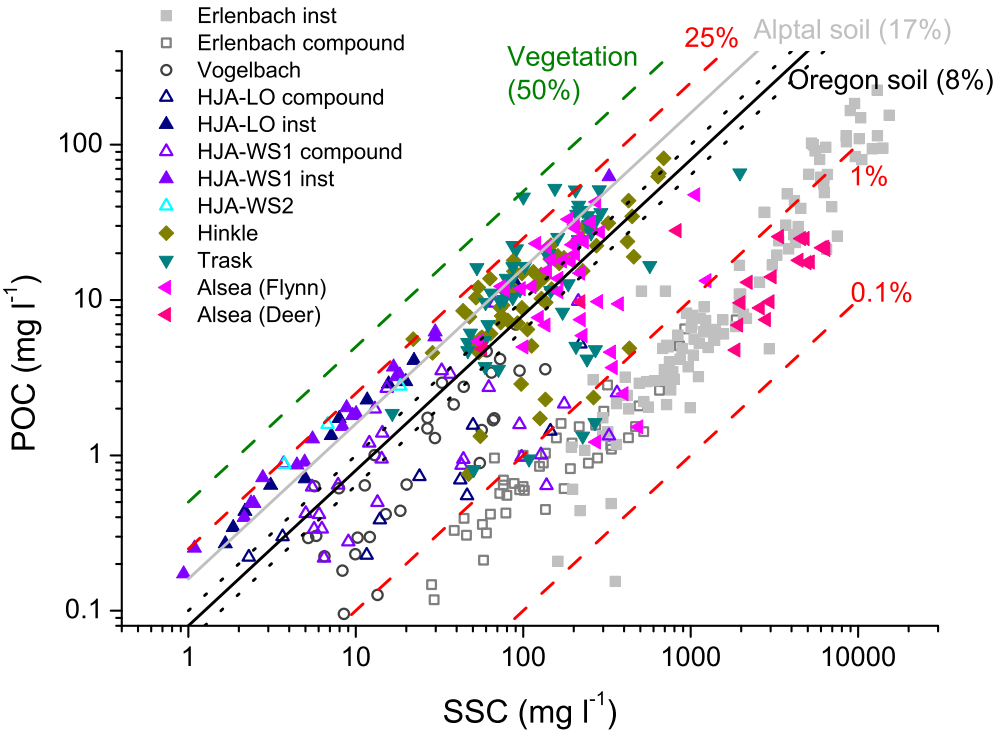

Figure 7.4: POC versus SSC for Oregon and Alptal catchments. Lines show expected relationship if suspended sediment was entirely sourced from pools containing the indicated proportions of organic carbon. Dotted lines on either side of the Oregon soil line indicate lowest and highest mean catchment proportions.

surface soil and ∼40% derived from foliage (H.J. Andrews: 58%±29 and 42%±29 respectively; Trask: 59%±23 and 41%±21; Flynn Creek: 57%±26 and 41%±25), while in watersheds where fire is particularly important—if Hinkle is representative—surface soil and charcoal are the two principal end members, with foliage contributing a minimal amount to suspended POC (Hinkle: 39%±38, 54%±31 and 7%±7 respectively).

Figure 7.4 illustrates a fundamental difference between Oregon and Alptal suspended sediment. In the Erlenbach, shown in grey squares, all suspended sediment samples plot well below the soil erosion line (that is, the line that would result if all suspended sediment came from average Alptal soil, with C_{org} of ∼17%). Vogelbach suspended sediment shows less dilution from soil, but nevertheless still plots below the Alptal soil line. In Oregon, however, well over half of all samples plot *above* the equivalent soil erosion line, clearly showing an enrichment in C_{org}. However, there is a distinct limit at 25%, with only three samples plotting above this.

What could cause such restricted enrichment? Mixing between soil and fresh plant matter could account for intermediate C_{org} concentrations, but this would result in C_{org} values covering the whole range from 8% to 50%, and C/N and $\delta^{15}N$ should

likewise more closely reflect plant compositions. One possibility is a biological process, operating only within the riparian soil accessible to the stream, that enriches it in C_{org} substantially beyond the level seen in surface soil elsewhere, to a concentration fundamentally limited by the process itself. But if that were the case, the channel bank samples should show some evidence of this C_{org} enrichment; instead, they are more depleted. Equally, the surface soil samples collected in the riparian zone or near the river should have higher C_{org} values, and there is no evidence for this. Alternatively, the apparent soil enrichment limit could be due to enforced dilution of fresh plant matter: there may be a mechanical constraint that means such material must be mixed with a certain proportion of clastics in order to be i) mobilised, or ii) sampled, but this would again result in some compositions closer to fresh plant matter than are observed.

There are two likely explanations. Mixing between litter, with a mean C_{org} of ∼27%), and soil would account for the distribution in Figure 7.4 while remaining consistent with the observed range of compositions. A density separation effect, in which only the organic material in soil, bedload or channel bank material is mobilised, would do likewise. Both are plausible, but observations of fresh plant matter floating in Oregon streams is evidence that foliage is not always degraded before incorporation into the suspended load; therefore the latter possibility is slightly preferred.

7.2.4.1 A POC export continuum

Differences in the amount and type of organic carbon mobilised—detailed in the previous sections—and the mechanisms by which it is harvested can be explained principally by geomorphological differences. The catchments studied form a continuum of POC export styles under the conditions covered by the sample sets in this study, with Deer Creek and the Erlenbach at one end and the Cascades at the other. These styles and the reasons behind them are summarised in the following paragraphs for each catchment, arranged in order of increasing mean F_{nf}.

Deer Creek generates large quantities of sediment, despite maintaining a riparian zone in the lower reaches and showing little evidence of active incision at least in the lower reaches. It is likely that soil and vegetation are poorly developed in some upper parts of the catchment following extensive logging in the second half of the twentieth century, and that through runoff-driven delivery of mixed hillslope material to upper channels, these areas are responsible for the high SSC values observed (Section 6.4.3, page 168). Consistent with this hypothesis, at least half the carbon in the suspended load derives from bedrock and F_{nf} is between 0 and 0.5. The rest comes from soil

and foliage, and it is likely that these are mobilised from within or next to channels in parts of the catchment not subjected to logging in the same way as in other Oregon catchments—but are simply swamped by lithic material containing fossil organic carbon. Unlike the Erlenbach, there is no commonly-crossed threshold beyond which non-fossil POC is added, because most hillslopes with substantial stocks of non-fossil organic carbon are decoupled from the channel, and rain soaks into the porous soil instead of delivering soil-derived material to the stream.

In the Erlenbach catchment, the stream is actively incising and steep hillslopes rise directly from the channel. Moreover, channel banks are cut into the hillslope profile and consist of relatively unweathered substrate. Continual mass wasting exposes bedrock-derived sediments, which are delivered to the channel by landslides and removed from there and from channel banks at low to moderate flow. This constant supply of clastic material is reflected in generally high SSC values, and, because organic carbon is present in the bedrock and not extensively oxidised, results in a low F_{nf} ($\sim$0.2–0.5) during "background" flow. However, the combination of steep slopes and mass wasting prevents thick vegetation growth, ensuring that, when it rains, overland flow is able to erode exposed surface soil and deliver it directly to the stream where it is immediately added to the suspended load and exported. This process raises the F_{nf} of suspended POC exported during storms to greater than 0.7.

The neighbouring Vogelbach is also actively incising, causing a similar lack of riparian zone and steep hillslopes maintaining a direct link between surface soil and the channel. Bedrock, again containing some organic carbon, can enter the stream with relative ease, either directly or by prior incorporation into bedload or channel banks as the landscape is denuded. However, this is a slower process than in the Erlenbach, largely because the substrate is sandier and therefore better-drained and more stable. There is no continual mass wasting adding bedrock-derived material to the channel, and consequently clastic input and SSC are lower, and F_{nf} higher ($\sim$0.9) as non-fossil inputs remain similar to those in the Erlenbach.

Like the Alptal catchments and Deer Creek, Flynn Creek is underlain by bedrock containing organic carbon. However, little of this enters the suspended load because streams are not rapidly incising—they cut only into layers of alluvium, not deeper—and because there is no mechanism for lithic material liberated by mass wasting higher on hillslopes to reach the channels. Clastic input is therefore low, resulting in consistently low SSC. Riparian zones have built up alongside the stream in the lower reaches, creating a buffer between hillslopes and channel. POC in the suspended load is derived from $\sim$60% soil and $\sim$40% foliage, both mobilised from within or adjacent to the channel. F_{nf} is mostly close to 1, but it is lower for a few samples evidently

containing fossil organic carbon (Figure 7.1); according to end member mixing analysis it is 0.98±0.0 on average.

Trask is geomorphologically similar to Flynn Creek, with evidence of mass wasting, but also vegetated riparian zones which limit clastic input and sediment yield. The major difference between the two is the lower proportion of carbonaceous bedrock underlying the catchment, but this has only a very minor effect. The result is almost identical: low concentrations of suspended sediment with high C_{org} consisting of soil- and foliage-derived biogenic carbon in similar proportions to Flynn Creek. A few more individual samples than in Flynn Creek have purely plant-like compositions, and F_{nf} is always ∼1.

In the Cascades catchments, F_{nf} is always ∼1. Channels run through wide, flat valley floors where alluvium accumulates and vegetation is allowed to flourish. In particular, the open-structure soil and ubiquitous moss carpet act like a sponge, soaking up rain and preventing overland flow from developing, let alone delivering any material to the channel. This again results in very low clastic input and SSC, and correspondingly high C_{org}. There is little soil exposed on hillslopes or channel banks, but soil-derived material does build up in the bedload. Carbon in the suspended load of H.J. Andrews results from mixing between this soil-like material and foliage, in roughly the same proportions as the natural Coast Range catchments. At Hinkle, around half the carbon in the suspended load derives from charcoal, with around four fifths of the rest coming from soil and the remainder from foliage.

7.2.5 Factors controlling POC export style

It has been established in earlier chapters that rainfall is key to POC export in the temperate forested headwater catchments in this study. Given that rainfall for all study sites is similar to first order (Sections 2.2.3, page 21, and 2.3.3, page 34), the aim here is to establish what controls the *style* of POC export—or in other words, explains the differences between them. The previous section described how the variations in SSC, C_{org} of the suspended load, and POC composition between catchments arise from geomorphological differences, such as whether channels are incising, the type and pervasiveness of mass wasting, steepness of slopes and soil structure. But these are secondary, and depend themselves on the more fundamental elements of lithology, uplift rate and ecosystem biology. The relative importance of these factors in controlling POC export style is discussed in the following subsections.

7.2.5.1 Ecosystem biology

Although the catchments studied form a continuum, both Figure 7.1 (showing mixing in the suspended load between one biogenic and one petrogenic end member versus two biogenic end members) and Figure 7.4 (showing soil dilution versus enrichment in the suspended load) indicate that the most significant difference is between the Alptal catchments plus Deer Creek, and the other Oregon catchments. The only primary difference between Deer Creek and Flynn Creek is the intensive logging activity in the former. This suggests that vegetation cover is a key factor controlling the flux and nature of POC export, a conclusion also reached by Goñi *et al.* (2013) after studying the contrasting Umpqua and Eel river systems in the Pacific Northwest. Similarly, the Vogelbach is intrinsically very similar to Flynn Creek: both are developed on sandy carbonaceous bedrock and are subjected to moderate uplift rates. Again, the difference is vegetation, this time in the type of ecosystem that has evolved in each location: the relatively squat *Picea abies* and barren *Fagus sylvatica* forest in Switzerland; the towering, luxuriant *Pseudotsuga menziesii* forest in Oregon.

A thick growth of vegetation, whatever the other conditions, will always act to trap sediment and halt channel incision, potentially leading to the development of a riparian zone and isolation of hillslopes. Vegetation is also important in slope stabilisation: reduced root strength leads to more shallow landslides (Roering *et al.* , 2003), and old growth roots stabilise more than second or subsequent growth (Stoffel & Wilford, 2012). Together with lithology, ecosystem biology also has a strong influence on soil structure, which controls rain infiltration capacity and rate, and hence determines whether overland flow is possible or likely.

7.2.5.2 Uplift rate

The Coast Range is uplifting at a faster rate than the Cascades (Section 2.3.2, page 31), and this is presumably responsible for the geomorphologic differences observed in the two areas—principally more evidence of active mass wasting in the Coast Range. However, this does not apparently manifest itself in any change in the origin of POC exported, with POC from H.J. Andrews, Trask and Flynn Creek showing on average identical end member contributions. Because of the different methods used to sample suspended sediment and scarcity of continuous long-term records, it is unclear whether uplift rate has any systematic effect on SSC—and hence total amount of POC exported—in these catchments.

What can be said is that uplift rates are the same (to first order) in the Alptal and Coast Range, and these areas show quite different POC export styles, lending

further support to the hypothesis that ecosystem biology is the principal control and suggesting that, if uplift rate does have any effect on POC export style, it is minor.

7.2.5.3 Lithology

Lithology plays a subordinate role in determining POC export behaviour. It is the main difference between the Erlenbach and Vogelbach, which have similar ecosystems and vegetation cover; as discussed, the sandier nature of Vogelbach flysch leads to better-draining, more stable soil and hillslopes. The Erlenbach, with its fine-grained, impermeable flysch leading to waterlogging and creep landsliding, is likely eroding faster than is tectonically stable: this rapid erosion rate is due to differences in lithology rather than uplift rate. However, substrate nature does not always have such a large effect as it does in the Alptal: the type of lithological disparity between Flynn Creek and Trask is not manifested in POC export behaviour. If fossil organic carbon is present in the bedrock, there is potential for it to enter the suspended load, but, as in Flynn Creek, this need not be the case if other factors preclude stream erosion of unweathered substrate.

7.3 Global significance and extrapolation

This thesis has identified two close-to-end member modes of POC export in temperate forested uplands under natural conditions, and has shown that ∼6–23 t km^{-2} yr^{-1} of tPOC is exported from such settings, of which ∼6–14 t km^{-2} yr^{-1} is non-fossil. It has also shown that the mechanisms by which this occurs require only rain on vegetated, soil-covered hillslopes. Extrapolating these findings to a global scale in a systematic and robust manner would require a very large amount of work, not achievable in the time-frame of this project. Therefore, this section is necessarily speculative, but should nevertheless serve to illustrate the potential global significance of such processes. It should be noted that in the following calculations it is assumed that the headwater inputs to the fluvial system constrained in this project are more or less unchanged on reaching the ocean. This is likely not the case, as is considered further in Section 7.4 and Chapter 8. Discussion is restricted to natural processes; therefore the behaviour shown by Deer Creek is not considered.

7.3.1 Comparison to POC export in active mountain belts

The export rate of non-fossil POC from the Erlenbach (14±4 t km^{-2} yr^{-1}) is broadly comparable to those reported from Taiwan (21±10 t km^{-2} yr^{-1}; Hilton *et al.* , 2012a)

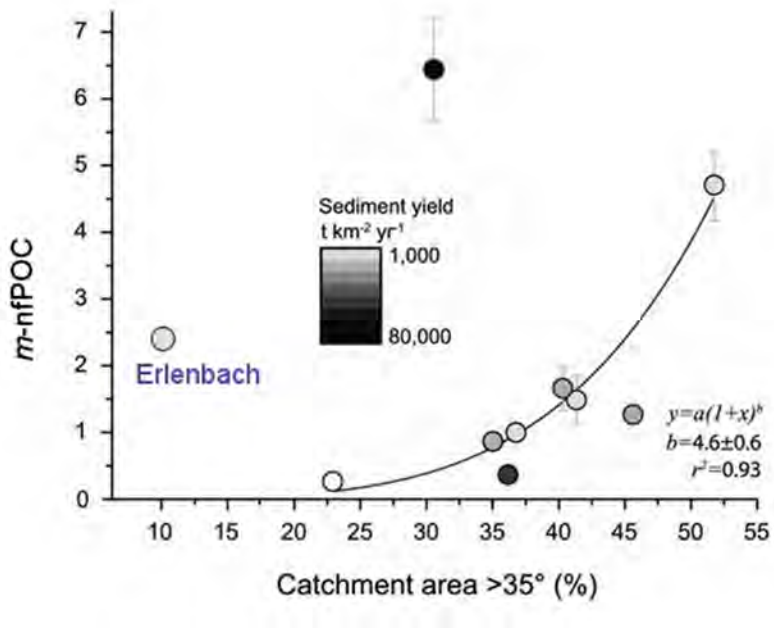

Figure 7.5: Effect of topography on nfPOC yield in Taiwan and the Erlenbach, modified from Hilton *et al.* (2012a). The gradient of the linear relationship between nfPOC and Q/Q_{mean} (m-nfPOC) is plotted against the proportion of the catchment area with slope angles >35°. Error bars on the Erlenbach point are smaller than the symbol size. A non-linear fit is shown to eight of the Taiwan catchments, excluding the Peinan River, whose behaviour Hilton *et al.* (2012a) attribute to recent tectonic activity.

and New Zealand (∼39 t km^{-2} yr^{-1}; Hilton *et al.* , 2008a). Even the nfPOC flux from the Cascades (∼6 t km^{-2} yr^{-1}) is greater than that from the Ganges–Brahmaputra basin (∼3 t km^{-2} yr^{-1}; Galy *et al.* , 2007b). However, the real significance lies in the contrasting processes responsible for these fluxes and their geographical scope. In active mountain belts, high rates of tectonic uplift, often combined with intense cyclonic storms, drive the deep-seated landsliding and flooding which mobilise most POC on a scale and frequency not seen elsewhere. In contrast, runoff-driven processes observed in the Alptal and Oregon are widely applicable and do not require catastrophic events to initiate significant POC export: similar processes are likely to occur wherever there is rain on soil-mantled hillslopes. While this likely includes some active mountain belts (e.g. Hilton *et al.* , 2008b, 2011b), many are probably less efficient than modest upland areas at exporting POC via runoff-driven processes, because steep gradients and high erosion rates are less conducive to soil development and vegetation growth.

Figure 7.5 gives some indication of the difference between areas where landslide-driven POC erosion dominates and those where runoff-driven POC erosion proceeds uninterrupted. Most catchments in this study cannot be plotted on this graph either

because not enough information is available or because the linear relationship between nfPOC and Q/Q_{mean} is too poorly defined. However, the Erlenbach can be plotted: it lies significantly off the trend defined by the Taiwan catchments, and confirms that nfPOC mobilisation there is not governed by the same processes.

7.3.1.1 Comparison to previously estimated global fluxes

Meybeck (1993) estimated that 18% of total atmospheric—i.e. modern—carbon (overall flux of 542x10^6 t yr^{-1}) is exported as soil-derived POC, or ~98x10^6 t yr^{-1}. Such a flux could be accounted for by 5% of the world's total land area of ~150 million km^2 behaving like the Erlenbach (nfPOC export=14 t km^{-2} yr^{-1}) or 11% behaving like the Cascades (nfPOC export=6 t km^{-2} yr^{-1}).

Figure 7.6 shows the global distribution of natural biomes. The Alptal falls under "temperate broadleaf and mixed forests", which constitute 9% of global land area (Mace *et al.* , 2005), while Oregon is categorised as "temperate coniferous forest", which makes up 3% of global land area (Mace *et al.* , 2005). Thus, ignoring for the moment all other constraints, these two biomes alone could account for Meybeck's flux.

But forest systems as a whole cover over 41 million km^2, or 27% of global land area (Dixon *et al.* , 1994). Including all biomes which have both soil coverage and the potential for significant rainfall (that is, all listed in Figure 7.6 except for tropical and subtropical dry broadleaf forests; flooded grassland and savannas; tundra; Mediterranean forests, woodland and scrub; deserts and xeric shrublands; mangroves; lakes; and rock and ice) brings the potential operating area available for runoff-driven POC export processes to ~96 million km^2, or 64% of global land area—well in excess of the 5%–11% required to account for Meybeck's flux. Anthropogenic disruption of these biomes will clearly reduce this potential area, but quantification of such effects is outside the scope of this project.

However, in addition to the biome requirement described above, there is a hillslope angle constraint on whether runoff-driven POC export will operate. All catchments in this study are characterised by relatively steep slopes: average hillslope angle is 20% in the Erlenbach (Hagedorn *et al.* , 2000), 37% in the Vogelbach (Milzow *et al.* , 2006) and 36% in H.J. Andrews Forest (Uhlenbrook *et al.* , 2007).

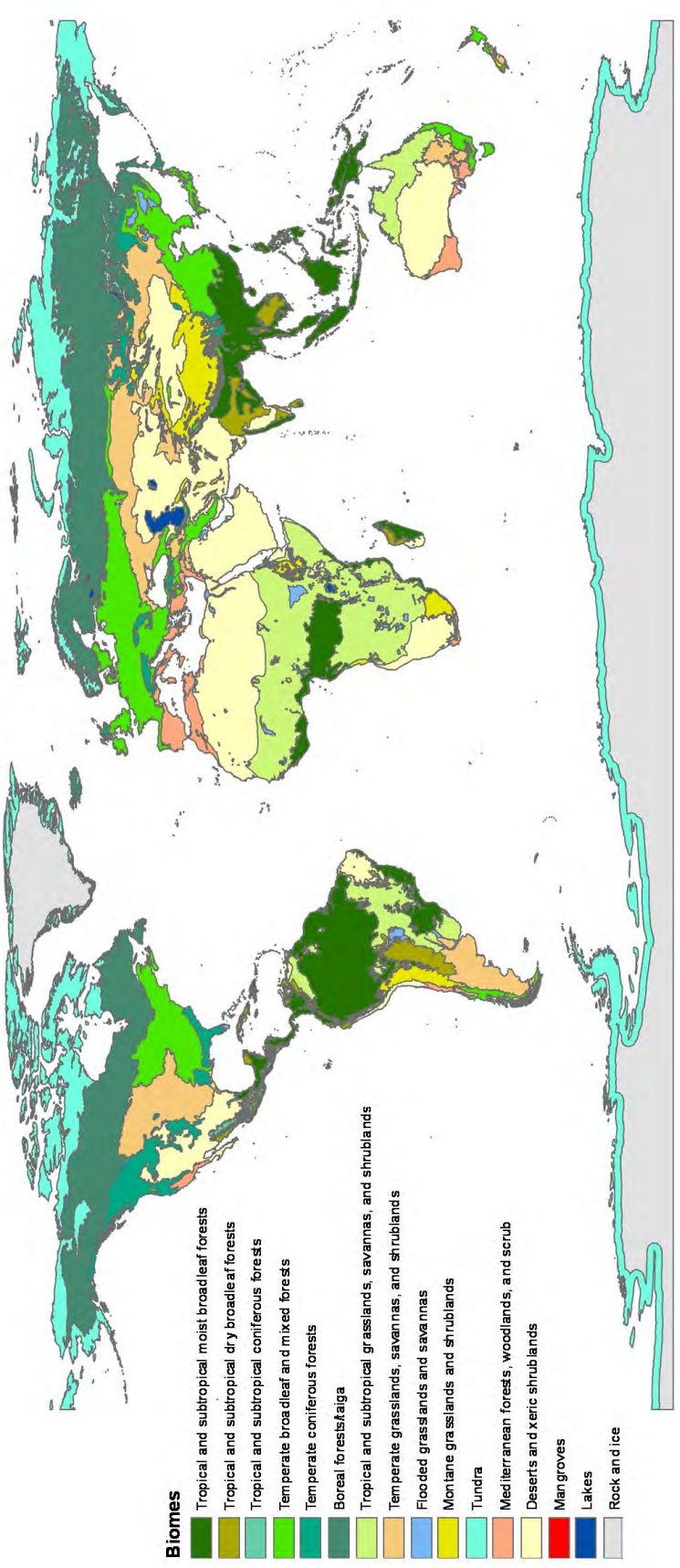

Figure 7.6: Global biome distribution. GIS data from The Nature Conservancy (http://maps.tnc.org/gis_data.html), based on Olson *et al.* (2001).

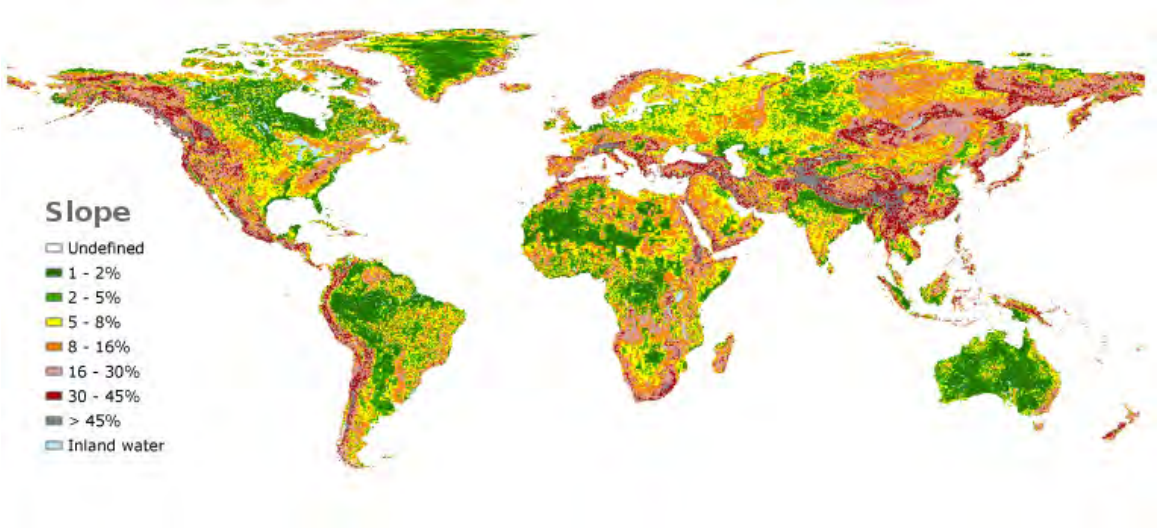

Figure 7.7: Global slope map, from the Food and Agriculture Organization of the United Nations (http://www.fao.org/nr/land/soils/en/). Slopes are derived from the U.S. Geological Survey's GTOPO30 digital elevation model.

It is clear from Figure 7.7 that the proportion of global land area having slopes of this order (∼16%–45%) within a suitable biome is considerably less than the 64% calculated using only the biome constraint. However, because no catchments with lower hillslope angles were studied, it is unclear what the slope threshold for the processes observed is, and it may be considerably lower. Figure 7.5 suggests that it is, at any rate, considerably lower than the threshold required for significant nfPOC mobilisation in active mountain belts where most nfPOC is mobilised by landslides. Hence, it is impossible to constrain the potential area for runoff-driven POC export further at present. The upper limit for runoff-driven processes is also unconstrained, but is of less importance because of the minimal area covered by slopes >45%, which will be in any case located mostly in mountainous, rocky terrain.

As an illustration, Table 7.2 presents modelled global fluxes of nfPOC that would result from different proportions of global land area hosting runoff-driven POC export processes. The table also shows the effect of varying global mean tPOC yield and F_{nf}, because the relative proportions of Erlenbach-like, Vogelbach-like, Coast Range-like and Cascades-like settings have not been determined. Fluxes calculated using a tPOC yield and F_{nf} mid-way between those of the two most extreme examples, the Erlenbach and H.J. Andrews, are shown in bold in Table 7.2, and range from 90x10^6 t yr^{-1} if runoff-driven POC export operates over 5% of global land area, to 900x10^6 t yr^{-1} if it operates over 50%. Given that these fluxes do not include alternative modes of POC export, such as those dominated by deep-seated landsliding, a comparison of these fluxes to Meybeck's figure of 98x10^6 t yr^{-1} tentatively suggest that the contribution of

Proportion of global land area (%):		**5**	**10**	**20**	**30**	**40**	**50**
tPOC flux= 5 t km^{-2} yr^{-1}	F_{nf}=*0.4*	15	30	60	90	120	150
	F_{nf}=*0.6*	23	45	90	135	180	225
	F_{nf}=*0.8*	30	60	120	180	240	300
	F_{nf}=*1*	38	75	150	225	300	375
tPOC flux= 10 t km^{-2} yr^{-1}	F_{nf}=*0.4*	30	60	120	180	240	300
	F_{nf}=*0.6*	45	90	180	270	360	450
	F_{nf}=*0.8*	60	120	240	360	480	600
	F_{nf}=*1*	75	150	300	450	600	750
tPOC flux= 15 t km^{-2} yr^{-1}	F_{nf}=*0.4*	45	90	180	270	360	450
	F_{nf}=*0.6*	68	135	270	405	540	675
	F_{nf}=0.8	**90**	**180**	**360**	**540**	**720**	**900**
	F_{nf}=*1*	113	225	450	675	900	1125
tPOC flux= 20 t km^{-2} yr^{-1}	F_{nf}=*0.4*	60	120	240	360	480	600
	F_{nf}=*0.6*	90	180	360	540	720	900
	F_{nf}=*0.8*	120	240	480	720	960	1200
	F_{nf}=*1*	150	300	600	900	1200	1500

Table 7.2: Modelled global fluxes of nfPOC, in millions of tonnes per year. Variables are the global mean flux of total particulate organic carbon (tPOC; first column) in t km^{-2} yr^{-1}, global mean fraction of tPOC derived from non-fossil sources (F_{nf}; second column) and proportion of global land area available for runoff-driven POC export, as observed in Switzerland and Oregon, in percent (first row). The row in bold type indicates fluxes expected if global mean tPOC yield and F_{nf} are approximately mid-way between the two end member watersheds of this study, the Erlenbach and H.J. Andrews. The row for F_{nf}=1 in each block also gives the predicted global fluxes of total POC, in millions of tonnes per year, for the given tPOC flux and proportion of global land area over which it is valid.

temperate forested areas to global riverine export of non-fossil POC, and consequently the global flux itself, may have been underestimated. Similarly, consideration of the predicted tPOC fluxes (given by the row for F_{nf}=1 in each block) shows that a relatively modest proportion of global land area hosting runoff-driven POC export fluxes (<10% for the mid-way tPOC export flux of 15t km^{-2} yr^{-1}; <30% for a much more conservative average flux of 5 t km^{-2} yr^{-1}) could single-handedly account for the currently accepted figure of ~200x10^{6} t yr^{-1} (Schlünz & Schneider, 2000; Seitzinger *et al.* , 2005, discussed in Section 1.3.3), and thus that the true global tPOC flux—and the contribution of areas outside active mountain belts to it—may be greater than extant estimates.

The concept that "mountains don't matter" for global POC export has strong parallels with the work of Dixon & von Blanckenburg (2012), who concluded that active mountain belts, with poorly developed soil and regolith leading to low weath-

ering efficiency, combined with small global area, may not contribute substantially to global weathering budgets compared to more geographically widespread soil-mantled uplands. This line of argument does, however, ignore the well-documented interdependence between climate, weathering and erosion in active mountain belts (e.g. France-Lanord & Derry, 1997; Hilton, 2008; Molnar & England, 1990; Raymo & Ruddiman, 1992; Raymo *et al.* , 1988), which is less clear in temperate uplands.

7.4 Linking POC export to the carbon cycle

While this project has focused on the upstream end of the organic pathway in temperate settings (that is, the initial mobilisation of organic carbon and its export from headwaters), it is useful to briefly consider its findings in the context of the wider carbon cycle, described in Section 1.2 (page 2). Like the previous one, this section is necessarily speculative, because a thorough treatment of these problems would require a very large amount of work.

7.4.1 Burial of terrestrial biogenic POC

Ultimately, it is the preservation and burial potential of the material exported that determines whether riverine organic carbon fluxes make significant contributions to global CO_2 drawdown. As described in Section 1.3.4.1 (page 11), much of the organic carbon entering the ocean appears to be rapidly oxidised before it can be buried in marine sediments (Hedges & Keil, 1995; Hedges *et al.* , 1997; Schlünz & Schneider, 2000), but high sediment yields increase the likelihood of preservation (Burdige, 2005; Galy *et al.* , 2007b; Hilton *et al.* , 2008b), and there is evidence for substantial preservation of biogenic POC in ancient sedimentary basins, originating from mountain belts similar to the present-day Alps (Sparkes, 2012, and in the Alptal and Alsea watersheds in this study). Here, then, is a qualification to the hypothesis that rapidly eroding active mountain belts are less important than general upland areas to the global draw down of CO_2 via the organic pathway: if the ballasting of POC by large amounts of suspended sediment is essential to preservation, then that may not be the case.

Long-term suspended sediment yield from the Erlenbach (∼1650 t km^{-2} yr^{-1}; Table 7.1) is comparable to the Ganges-Brahmaputra system (∼400 t km^{-2} yr^{-1}; Lupker *et al.* , 2011), but around an order of magnitude lower than Taiwan (13000-77000 t km^{-2} yr^{-1}; Hilton *et al.* , 2008b) and New Zealand (∼8770 t km^{-2} yr^{-1}; Hilton *et al.* , 2008a,b). The association of the POC exported from Erlenbach-like terrain with

clastic material may be enough to ensure that a significant amount is transferred to geological storage. The Erlenbach itself is distant from any marine depocentre, but overfilled foreland basins may also be viable sinks (e.g. Aufdenkampe *et al.* , 2011), and the catchment serves as an example of a particular style of POC export which elsewhere may discharge directly to the ocean.

POC exported from settings at the Cascades end of the spectrum suffer a less certain fate. Here, high organic carbon concentrations are accompanied by very low yields of clastic material (∼80 t km^{-2} yr^{-1}; Table 7.1), with the likely result that burial efficiency of this POC may be drastically reduced. Some indication of in-stream loss is given by a comparison of findings from this study with results from Goñi *et al.* (2013), who report that the total organic carbon flux for the Umpqua River, into which the Hinkle flows, is ∼1 t km^{-2} yr^{-1}. Assuming a headwater export flux of 6 t km^{-2} yr^{-1} is valid across the whole Umpqua watershed, then only ∼17% of the organic carbon that is mobilised ever reaches the ocean. What happens then is another issue, and although Hastings *et al.* (2012) report evidence for a depocentre containing terrestrial organic matter where the Umpqua River discharges to the Pacific margin, quantitative constraints on the burial efficiency of the system are lacking. The Alsea River discharges ∼3.8 t km^{-2} yr^{-1} to the Pacific Ocean (Hatten *et al.* , 2012), but no meaningful estimate of downstream transport efficiency can be made because POC mobilisation in Coast Range headwaters remains unconstrained.

7.4.1.1 Coarse woody debris

As explained in Sections 4.4.1.1 (page 97) and 6.5.1.2 (page 172), the contributions of coarse woody debris to the export flux of organic carbon from headwaters has not been considered in this project, and this is generally the case throughout the literature on riverine POC transfer. One reason for this omission is that this component is difficult to quantify accurately, but it may also be because it is assumed that such material does not usually reach the ocean in this state and therefore does not contribute to the global land-ocean POC flux. For example, Sparkes (2012) has documented the paucity of woody debris in foreland basins. Short, steep transport paths are required for such material to escape the fluvial system, so it is possible that this may be important in flexural basins surrounding high source areas. Even if this does occur—for example in extreme cases such as Typhoon Morakot in Taiwan (West *et al.* , 2011)—buoyant plant matter does not easily sink and may require particularly unusual conditions to be buried. However, little quantitative work has been done on coarse woody debris mobilisation, transport and burial, and even less that connects these three processes.

7.4.2 Oxidation of fossil organic carbon

As discussed in Section 1.3.4.2 (page 13), erosion and riverine transport of organic carbon can be a source as well as a sink for atmospheric CO_2, if fossil organic carbon is mobilised and subsequently oxidised before reburial (Bouchez *et al.* , 2010; Hedges, 1992; Yue *et al.* , 2012). Such sources must be quantified if a full carbon budget for the process of riverine erosion is to be developed, as has been done by Hilton *et al.* (2011a) for Taiwan, where <15% is lost due to weathering between erosion and re-deposition in the ocean.

With regard to the catchments in this study, most of the Oregon catchments are on volcanic substrate and so fossil POC is not a consideration. In the Alptal, Raman spectroscopy has shown that some fossil organic material has undergone several orogenic cycles and is now recalcitrant and highly likely to be reburied again. Such material is more prevalent in turbidites elsewhere in Alpine systems (Sparkes, 2012), suggesting that fossil POC oxidation as a result of fluvial erosion may not be widespread at least in small mountain river systems where there is no protracted floodplain transport before reaching the ocean.

Oxidative loss during exhumation but before erosion—as observed in the Alsea bedrock cores—is another issue of interest, but not one that bears on the fate of POC in the suspended load as measured in this project.

7.4.3 Response to climate and environmental change, and potential feedbacks

This thesis has shown that in both Switzerland and Oregon, precipitation is key to mobilising POC, and non-fossil POC in particular. Shifts in regional rainfall patterns as a consequence of climate change are therefore very likely to affect the POC harvesting mechanisms and export fluxes of particular areas, and thus the global contribution of runoff-driven POC erosion to CO_2 drawdown. Conversely, as climate patterns and biome distribution have changed over Earth history, global POC export has likely also fluctuated, potentially feeding back into the Earth's climate. While this section focuses on future change, the links between climate and environment that it explores could conceivably also be applied to the historical and geological past.

In Europe, annual precipitation is generally predicted to increase by 15–30% by the latter half of the twenty-first century for much of western, northern and central parts (Field *et al.* , 2007). Figure 7.8 shows the predicted change in annual runoff over Europe in the 2020s and 2070s for two models: there is minimal change or a slight

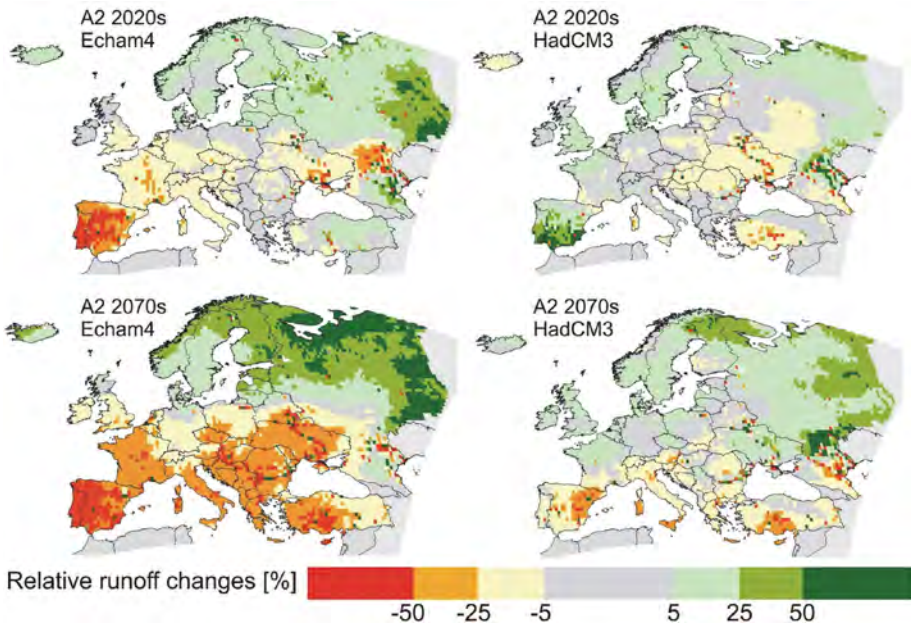

Figure 7.8: Change in annual river runoff between the 1961–1990 baseline period and two future time slices (2020s and 2070s) for the A2 scenarios (Alcamo *et al.* , 2007), from Field *et al.* (2007), page 549.

decrease for Switzerland, an increase in the north-east, and a decrease in the south. However, it is not enough to consider bulk shifts; only changes in the magnitude and frequency of events in which POC is mobilised are relevant. For many of these areas summer precipitation will decrease, while there may be increased frequency and magnitude of winter floods (Field *et al.* , 2007). Lower summer rainfall may act to reduce both the tPOC yield from the Alptal and its F_{nf}, leading to reduced burial of biogenic material by this pathway, higher levels of atmospheric CO_2 and a positive feedback loop. However, if less rainfall is concentrated in fewer but more intense events—higher maximum temperatures on warm days are predicted (Field *et al.* , 2007), and thus more numerous and more intense thunderstorms—then the opposite effect may occur, creating a negative feedback loop. The effect of increased winter precipitation, concentrated into storm events, cannot be predicted because it is unclear whether relationships between discharge and suspended sediment and POC are the same in summer and winter conditions. If hillslopes remain snow-covered during winter storms then such events are unlikely to have a large impact on POC export.

In the Pacific Northwest, all models predict increased precipitation; in Canada, increases of up to 20% for the annual mean and up to 30% for winter are expected (Field *et al.* , 2007). A higher proportion of this is likely to fall as rain than currently, since annual mean temperature increases of up to 3°C are predicted (Field *et al.* ,

2007). Widespread increases in extreme precipitation events are also likely (Field *et al.* , 2007). If the trends shown in Figure 6.17(a) (page 171) are valid under conditions of intense rainfall and high flow, and there is no supply limitation, then these shifts will result in more biogenic POC being exported than currently. This will increase the potential for CO_2 sequestration and form a negative feedback loop.

In addition to the direct link between precipitation and POC, climate, environmental and land use changes are likely to have indirect effects on ecosystem biology and soil development, factors that have been shown to be important controls on POC export style. In particular, the dramatic contrast between Flynn Creek and Deer Creek is a warning of the potential effects of intensive forest management and other land use changes not only on sediment production, a topic already receiving attention (e.g. Nadeu *et al.* , 2012; Walling, 2006), and water quality, but on carbon dynamics and the ability of the organic pathway to sequester significant amounts of CO_2.

7.5 Chapter summary

Although runoff-driven POC mobilisation and export operates in both locations, the natural headwaters of the Alptal and Oregon exhibit fundamentally contrasting behaviour. Alptal suspended load shows binary mixing between fossil organic carbon from bedrock and non-fossil organic carbon from soil, while Oregon suspended load contains no fossil organic carbon, even where it is present in the substrate. Instead, POC results from mixing between soil and the foliage and wood of many individual plants. Beyond this fundamental division the studied catchments form a continuum of POC export styles, with variations in SSC, C_{org} and F_{nf} leading to differing yields of total, fossil and non-fossil POC. The Erlenbach is at one end of the natural spectrum and H.J. Andrews at the other. Deer Creek, with high SSC and tPOC yield but F_{nf} <0.5, is a radical departure from this continuum and, when contrasted with its twin catchment Flynn Creek, illustrates the effect of severe forest management on carbon dynamics.

Natural differences in POC export styles are directly explained by geomorphological contrasts. The presence or absence of active channel incision, thickly vegetated riparian zones, and soil porosity control the degree of channel-hillslope coupling; that is, the extent to which hillslope material can be washed into the channel during rain. This is high in the Erlenbach and low in natural Oregon catchments. The principal underlying control on these geomorphological factors is ecosystem biology, which explains both the inherent difference between Switzerland and Oregon, and the deviant behaviour of Deer Creek. Lithology, which can also affect soil structure, is a secondary

control and accounts for the difference between the Erlenbach and the Vogelbach.

To a first approximation and with a number of assumptions, the global significance of runoff-driven erosion of soil-derived POC may be speculatively assessed. The fluxes of nfPOC from the studied catchments are of the same order of magnitude as those from active mountain belts, yet unlike the latter, the potential area available for this runoff-driven POC export extends to large parts of the Earth's continents. Biomes with the potential to host such processes make up over 60% of global land area. There must also be a hillslope angle threshold for the onset of these processes, which is at present unconstrained; hence, the actual area where they operate under natural conditions is probably somewhat less than 60%. Taking the tPOC yield and F_{nf} midway between the two end member catchments in this study as global means (15 t km^{-2} yr^{-1} and 0.8 respectively), the global flux of nfPOC would be 180x10^6 t km^{-2} yr^{-1} if runoff-driven POC erosion operates over 10% of global land area, and 720x10^6 t km^{-2} yr^{-1} if 40%. The equivalent figures for tPOC are 225x10^6 t km^{-2} yr^{-1} and 900x10^6 t km^{-2} yr^{-1}. Comparing these to extant global flux estimates of 98x10^6 t km^{-2} yr^{-1} for nfPOC (Meybeck, 1993) and ~200x10^6 t km^{-2} yr^{-1} for tPOC (Schlünz & Schneider, 2000; Seitzinger *et al.* , 2005) suggests that the contribution of temperate forested areas to riverine POC erosion, and hence the global fluxes themselves, may have been underestimated.

Because runoff-driven POC export depends heavily on precipitation, it is sensitive to shifts in regional rainfall that may result from climate change. If catchments become wetter (particularly if the additional precipitation is concentrated in storm events) as a result of CO_2-induced warming, then more biogenic carbon may be sequestered via the organic pathway and a negative feedback loop created. If catchments become drier and rainfall events less extreme, then the opposite will occur. Other environmental changes, related to either climate or land use, may also affect the landscape's ability to draw down CO_2 in this way. Knowledge of the factors controlling POC export—principally rainfall and ecosystem biology—could ultimately be used to model carbon cycle dynamics in the geological past. However, to progress this discussion, more constraints are needed regarding the fate of POC exported from temperate headwaters, in particular the burial efficiency of biogenic material and the in-transit oxidation of petrogenic organic carbon.

Chapter 8

Conclusions and future work

The first section of this chapter covers nothing new, but provides a summary of the general conclusions of the thesis. Much more detailed conclusions have already been given in the synthesis, Chapter 7. The second part identifies areas of investigation where further research and more constraints would lead to a better understanding of carbon dioxide drawdown via the organic pathway, of which this thesis has probed only a small part.

8.1 Overall conclusions

Temperate forested uplands under natural conditions, such as those in Switzerland and Oregon studied in this project, can be an important source of fluvial particulate organic carbon (POC). Their contribution is particularly significant when only non-fossil POC is considered. The mechanisms by which POC is mobilised in such settings are not the same as those primarily operating in active mountain belts.

On decadal timescales, there is no extreme mass-wasting in these temperate settings as there is in many active mountain belts: deep-seated landslides and debris flows capable of eroding bedrock—and with it entire soil profiles and overlying vegetation—do not occur. Instead, POC is mobilised by rain alone, which must be of a duration and intensity great enough to raise discharge above background flow, but generally occurs several times per year as a result of either winter frontal systems or convective summer storms.

In systems where there is a high degree of channel–hillslope coupling and soil exposure sustained by stream incision, such rain activates hillslopes by initiating overland flow. Soil-derived modern organic carbon is thus eroded and transferred to the channel, where it is immediately exported. Plant matter does not contribute directly; only via the homogenising "soil window". Clastic material—including fossil organic carbon

if present in the substrate—is also mobilised, but at a slower rate than hillslope soil, and hence the fraction of organic carbon in the suspended load derived from non-fossil sources (F_{nf}) increases with rising discharge.

In systems where thick plant growth halts incision and allows riparian buffer zones to develop, or where the soil is porous enough to preclude overland flow, soil and plant matter builds up in and next to the channel by slower accumulation processes between mobilisation events, and is eroded and exported when stream flow rises. Clastic yield is very low, and little fossil organic carbon enters the suspended load even when it is present in the bedrock.

These two systems likely represent close to end member states. The first, represented by the Erlenbach catchment in Switzerland, exports around three times as much total POC and around twice as much non-fossil POC per unit area as the second, represented by H.J. Andrews Forest in the Oregon Cascades. Other catchments in the study fall between these end members in terms of both processes and fluxes, and it is clear that a graduated continuum of POC export styles bounded by them is possible. The precise style is controlled principally by ecosystem biology and secondarily by lithology, but the only common requirement is rain on vegetated, soil-mantled hillslopes. Although the proportions of each style operating worldwide are not yet known, a first approximation of the average total POC export flux from temperate forested uplands globally might be given by the midpoint between the two end member catchments in this study. The result is $\sim$15 t km^{-2} yr^{-1} for total POC, and F_{nf} of 0.8, giving $\sim$12 t km^{-2} yr^{-1} for non-fossil POC.

It is likely that many active mountain belts also host this runoff-driven, high F_{nf} mode of POC export, but the process may be less efficient there than in temperate uplands because soil is generally less well-developed. In many cases, it may be masked by deep-seated landslide-driven POC erosion. Non-fossil POC fluxes reported from active mountain belts are of the same order of magnitude as the average flux from temperate forested uplands derived above. Yet they are insignificant in terms of global land cover, while the potential area available for runoff-driven POC export extends to large parts of the Earth's continents. Considering these findings in the context of current global estimates of riverine POC discharge, it seems likely that the collective contribution of catchments where rain mobilises soil and vegetation may be more important than previously thought. Consequently, the global fluxes themselves, particularly that of non-fossil POC, may also have been underestimated.

If the non-fossil POC exported from these settings is ultimately buried in the ocean, this mechanism could significantly contribute to CO_2 drawdown on geological timescales. Because of its dependence on rain, the nature and occurrence of runoff-

driven POC export processes, and hence the global discharge of non-fossil POC to the ocean, is sensitive to climate and environmental change. This mechanism could, therefore, play an important role in controlling the Earth's thermostat via feedback loops.

8.2 Future work

There are currently two major areas where further investigation would greatly aid the calculation of robust global headwater export fluxes of total and non-fossil POC. Firstly, confirmation should be made that runoff-driven POC erosion does occur wherever rain falls on soil-covered slopes, by studying catchments in biomes other than temperate forests, such as tropical forests and temperate grasslands. Relationships between discharge and total, non-fossil and fossil POC concentration should be established in representative catchments in these biomes, and export of these (and hence also F_{nf}) determined. Comparison with the behaviour shown by the catchments in this study will indicate whether they fit into the continuum already identified, or whether there are further system end members to consider. Secondly, the slope thresholds below and above which runoff-driven POC erosion does not occur must be identified. This knowledge should enable the global land area where such processes operate—i.e. where both slope and biome requirements are met—to be accurately determined. Mean global fluxes of total and non-fossil POC and mean global F_{nf}, weighted according to the operating area and POC export parameters of each biome or end member, are the ultimate goal.

The amounts of total and non-fossil POC exported from headwaters are not equal to the amounts eventually buried in oceanic or terrestrial basins, and it is only the latter quantity that finally determines the effect of the organic pathway on the long-term carbon cycle. More detailed and targeted research is needed into the downstream fate of eroded organic material in temperate settings; in particular, studies which measure POC concentrations and characteristics at intervals from headwaters to ocean outflow in the same river system, and using the same methods, would be welcome. The concurrent oxidation of fossil organic carbon in these systems, which counteracts the sequestration of CO_2 via biomass burial, must also be properly quantified in order for full carbon budgets to be developed. Progressive measurement of fossil organic carbon concentration between headwaters and river mouth would again be a useful tool for this, as well as direct investigation of reactions occurring in transit or temporary storage. The potential for loss of fossil organic carbon by oxidation in open-structure

rocks and soils, such as those in the Alsea watershed, might also be quantified.

If this level of understanding is achieved, there is huge potential for a comprehensive assessment of the links and feedbacks between continental biomass erosion and climate on scales from the very localised to global, which could then be incorporated into increasingly sophisticated models of climate and environmental change in the past and future. In the long term, it is likely that POC-mobilising conditions other than those sampled in this study, such as higher-discharge events in Oregon, or winter storms in Switzerland, will become common, and further sampling will be required to maintain accurate characterisation of carbon dynamics even in these presently well-understood systems. The effects of forest management and land use change in these systems and elsewhere must also be monitored to this end.

Two aspects of POC dynamics that have received little attention are the export of floating coarse woody debris, and the export of both fossil and non-fossil organic material in bedload—largely because they are difficult to quantify accurately. While these components are unlikely to contribute a great amount to the land-ocean POC flux in temperate environments unaffected by cyclonic storms and lacking short, steep transport paths, the mobility, behaviour and fate of organic material in bedload and coarse woody debris throughout the fluvial system nevertheless has a bearing on both local carbon budgets and the global carbon cycle. It is therefore an unexplored area of considerable interest.

References

Ader, M., Cartigny, P., Boudou, J.-P., Oh, J.-H., Petit, E., & Javoy, M. 2006. Nitrogen isotopic evolution of carbonaceous matter during metamorphism: Methodology and preliminary results. *Chemical Geology*, **232**, 152–169. 8

Alcamo, J., Flörke, M., & Märker, M. 2007. Future long-term changes in global water resources driven by socio-economic and climatic changes. *Hydrological Sciences Journal*, **52**, 247–275. 197

Aller, R.C. 1998. Mobile deltaic and continental shelf muds as suboxic, fluidized bed reactors. *Marine Chemistry*, **61**, 143–155. 12

Amundson, R., Austin, A.T., Schuur, E.A.G., Yoo, K., Matzek, V., Kendall, C., Uebersax, A., Brenner, D., & Baisden, W.T. 2003. Global patterns of the isotopic composition of soil and plant nitrogen. *Global Biogeochemical Cycles*, **17**, 1031. 8

Anderson, S.P., & Dietrich, W.E. 2001. Chemical weathering and runoff chemistry in a steep headwater catchment. *Hydrological Processes*, **15**, 1791–1815. 41

Andrews, E.D. 1980. Effective and bankfull discharges of streams in the Yampa River basin, Colorado and Wyoming. *Journal of Hydrology*, **46**, 311–330. 102, 172

Atkinson, J. 2005. Soil Mechanics. *Pages 184–193 of:* Selley, R.C., Cocks, L.R.M., & Plimer, I.R. (eds), *Encyclopedia of Geology, Vol. 5.* Elsevier. 65

Atwater, T. 1970. Implications of plate tectonics for the Cenozoic tectonic evolution of western North America. *Geological Society of America Bulletin*, **81**, 3513–3536. 32

Aufdenkampe, A.K., Mayorga, E., Raymond, P.A., Melack, J.M., Doney, S.C., Alin, S.R., Aalto, R.E., & Yoo, K. 2011. Riverine coupling of biogeochemical cycles between land, oceans, and atmosphere. *Frontiers in Ecology and the Environment*, **9**, 53–60. 13, 195

Balesdent, J., Girardin, C., & Mariotti, A. 1993. Site-related δ^{13}C of tree leaves and soil organic matter in a temperate forest. *Ecology*, **74**, 1713–1721. 141

Benda, L., & Dunne, T. 1997. Stochastic forcing of sediment supply to channel networks from landsliding and debris flow. *Water Resources Research*, **33**, 2849–2863. 146, 172

Berner, R.A. 1982. Burial of organic carbon and pyrite sulfur in the modern ocean; its geochemical and environmental significance. *American Journal of Science*, **282**, 451–473. 7, 12, 101

Berner, R.A. 1999. A new look at the long-term carbon cycle. *GSA Today*, **9**, 1–6. 2, 4

Bernet, M., Zattin, M., Garver, J.I., Brandon, M.T., & Vance, J.A. 2001. Steady-state exhumation of the European Alps. *Geology*, **29**, 35–38. 21

Beschta, R.L. 1978. Long-term patterns of sediment production following road construction and logging in the Oregon Coast Range. *Water Resources Research*, **14**, 1011–1016. 33

Beschta, R.L., & Jackson, W.L. 2008. Forest practices and sediment production in the Alsea Watershed Study. *Pages 55–66 of:* Stednick, J.D. (ed), *Hydrological and Biological Responses to Forest Practices*. New York, USA: Springer. 32, 36, 40, 41, 43, 45, 169

Beyssac, O., Goffé, B., Petitet, J.-P., Froigneux, E., Moreau, M., & Rouzaud, J.-N. 2003. On the characterization of disordered and heterogeneous carbonaceous materials by Raman spectroscopy. *Spectrochimica Acta Part A: Molecular and Biomolecular Spectroscopy*, **59**, 2267–2276. 76

Bianchi, T.S. 2011. The role of terrestrially derived organic carbon in the coastal ocean: A changing paradigm and the priming effect. *Proceedings of the National Academy of Sciences*, **108**, 19473 –19481. 4

Bianchi, T.S., Wysocki, L.A., Stewart, M., Filley, T.R., & McKee, B.A. 2007. Temporal variability in terrestrially-derived sources of particulate organic carbon in the lower Mississippi River and its upper tributaries. *Geochimica et Cosmochimica Acta*, **71**, 4425–4437. 10

Bird, M., Santrùcková, H., Lloyd, J., & Lawson, E. 2002. The isotopic composition of soil organic carbon on a north-south transect in western Canada. *European Journal of Soil Science*, **53**, 393–403. 8

Bird, M.I., Haberle, S.G., & Chivas, A.R. 1994. Effect of altitude on the carbon-isotope composition of forest and grassland soils from Papua New Guinea. *Global Biogeochemical Cycles*, **8**, 13–22. 8

Bird, M.I., Chivas, A.R., & Brunskill, G.J. 1995. Carbon-isotope composition of sediments from the Gulf of Papua. *Geo-Marine Letters*, **15**, 153–159. 11

Blair, N.E., & Aller, R.C. 2012. The fate of terrestrial organic carbon in the marine environment. *Annual Review of Marine Science*, **4**, 401–423. 12, 101

Blair, N.E., Leithold, E.L., Ford, S.T., Peeler, K.A., Holmes, J.C., & Perkey, D.W. 2003. The persistence of memory: the fate of ancient sedimentary organic carbon in a modern sedimentary system. *Geochimica et Cosmochimica Acta*, **67**, 63–73. 3, 9

Bonin, H.L., Griffiths, R.P., & Caldwell, B.A. 1999. Effects of storage on measurements of potential microbial activities in stream fine benthic organic matter. *Journal of Microbiological Methods*, **38**, 91–99. 114

Bouchez, J., Beyssac, O., Galy, V., Gaillardet, J., France-Lanord, C., Maurice, L., & Moreira-Turcq, P. 2010. Oxidation of petrogenic organic carbon in the Amazon floodplain as a source of atmospheric CO_2. *Geology*, **38**, 255–258. 3, 13, 103, 196

Bowen, G.J. 2010. Isoscapes: spatial pattern in isotopic biogeochemistry. *Annual Review of Earth and Planetary Sciences*, **38**, 161–187. 7, 8

Bowman, D.M.J.S., Balch, J.K., Artaxo, P., Bond, W. J., Carlson, J.M., Cochrane, M.A., DAntonio, C.M., DeFries, R.S., Doyle, J.C., Harrison, S.P., Johnston, F.H., Keeley, J.E., Krawchuk, M.A., Kull, C.A., Marston, J.B., Moritz, M.A., Prentice, I.C., Roos, C.I., Scott, A.C., Swetnam, T.W., van der Werf, G.R., & Pyne, S.J. 2009. Fire in the Earth System. *Science*, **324**, 481–484. 42, 45

Brodie, C.R., Casford, J.S.L., Lloyd, J.M., Leng, M.J., Heaton, T.H.E., Kendrick, C.P., & Yongqiang, Z. 2011. Evidence for bias in C/N, δ^{13}C and δ^{15}N values of bulk organic matter, and on environmental interpretation, from a lake sedimentary sequence by pre-analysis acid treatment methods. *Quaternary Science Reviews*, **30**, 3076–3087. 66

Bunte, K. 2001. *Field testing the sampling efficiency of bedload traps at East St. Louis Creek, CO.* Report submitted to the Stream Systems Technology Center, USDA Forest Service, Rocky Mountain Research Station. Fort Collins, Colorado, USA. 173

Bunte, K., & Swingle, K. 2003. *Results from testing the bedload traps at Little Granite Creek, 2002.* Report submitted to the Stream Systems Technology Center, USDA Forest Service, Rocky Mountain Research Station. Fort Collins, Colorado, USA. 173

Burbank, D.W., Leland, J., Fielding, E., Anderson, R.S., Brozovic, N., Reid, M.R., & Duncan, C. 1996. Bedrock incision, rock uplift and threshold hillslopes in the northwestern Himalayas. *Nature*, **379**, 505–510. 13

Burdige, D.J. 2005. Burial of terrestrial organic matter in marine sediments: A re-assessment. *Global Biogeochemical Cycles*, **19**, GB4011. 3, 12, 194

Carcaillet, C. 2001. Are Holocene wood-charcoal fragments stratified in alpine and subalpine soils? Evidence from the Alps based on AMS ^{14}C dates. *The Holocene*, **11**, 231–242. 89

Carey, A.E., Gardner, C.B., Goldsmith, S.T., Lyons, W.B., & Hicks, D.M. 2005. Organic carbon yields from small, mountainous rivers, New Zealand. *Geophysical Research Letters*, **32**, L15404. 13

Cenciani, K., Freitas, S.D.S., Critter, S.A.M., & Airoldi, C. 2008. Microbial enzymatic activity and thermal effect in a tropical soil treated with organic materials. *Scientia Agricola*, **65**, 674–680. 8

Cleveland, C.C., & Liptzin, D. 2007. C:N:P stoichiometry in soil: Is there a "Redfield ratio" for the microbial biomass? *Biogeochemistry*, **85**, 235–252. 8

Cloern, J.E., Canuel, E.A., & Harris, D. 2002. Stable carbon and nitrogen isotope composition of aquatic and terrestrial plants of the San Francisco Bay estuarine system. *Limnology and Oceanography*, **47**, 713–729. 145

Cole, J., Prairie, Y., Caraco, N., McDowell, W., Tranvik, L., Striegl, R., Duarte, C., Kortelainen, P., Downing, J., Middelburg, J., & Melack, J. 2007. Plumbing the global carbon cycle: integrating inland waters into the terrestrial carbon budget. *Ecosystems*, **10**, 172–185. 13

Copard, Y., Amiotte-Suchet, P., & Di-Giovanni, C. 2007. Storage and release of fossil organic carbon related to weathering of sedimentary rocks. *Earth and Planetary Science Letters*, **258**, 345–357. 3, 8

Coplen, T.B. 1994. Reporting of stable hydrogen, carbon and oxygen isotopic abundances (Technical Report). *Pure And Applied Chemistry*, **66**, 273–276. 7

Coyle, J.S., Dijkstra, P., Doucett, R.R., Schwartz, E., Hart, S.C., & Hungate, B.A. 2009. Relationships between C and N availability, substrate age, and natural abundance ^{13}C and ^{15}N signatures of soil microbial biomass in a semi-arid climate. *Soil Biology and Biochemistry*, **41**, 1605–1611. 8, 57, 154

Creel, C., & Henshaw, D. 2005. *Stage measurement and recording instrumentation - H.J. Andrews Experimental Forest gaged watersheds.* Blue River, Oregon, USA: Andrews Experimental Forest. 63

Creel, C., & Henshaw, D. 2007. *Description of new proportional water sampling system.* Blue River, Oregon, USA: Andrews Experimental Forest. 54

Dadson, S.J., Hovius, N., Chen, H., Dade, W.B., Hsieh, M.-L., Willett, S.D., Hu, J.-C., Horng, M.-J., Chen, M.-C., Stark, C.P., Lague, D., & Lin, J.-C. 2003. Links between erosion, runoff variability and seismicity in the Taiwan orogen. *Nature*, **426**, 648–651. 34

Daly, C., & McKee, W. 2012. *Meteorological data from benchmark stations at the Andrews Experimental Forest (Dataset).* Corvallis, Oregon, USA: Long-Term Ecological Research; Forest Science Data Bank. http://andrewsforest.oregonstate.edu/data/abstract.cfm?dbcode=MS001. 35, 163

Dean, W.E., & Gorham, E. 1998. Magnitude and significance of carbon burial in lakes, reservoirs, and peatlands. *Geology*, **26**, 535–538. 6, 9, 13

Denman, K.L., Brasseur, G., Chidthaisong, A., Ciais, P., Cox, P.M., Dickinson, R.E., Hauglustaine, D., Heinze, C., Holland, E., Jacob, D., Lohmann, U., Ramachandran, S., da Silva Dias, P.L., Wofsy, S., & Zhang, X. 2007. Couplings between changes in the climate system and biogeochemistry. *In:* Solomon, S., Qin, D., Manning, M., Chen, Z., Marquis, M., Averyt, K.B., Tignor, M., & Miller, H.L. (eds), *Climate Change 2007: The Physical Science Basis. Contribution of Working Group I to the Fourth Assessment Report of the Intergovernmental Panel on Climate Change.* Cambridge, United Kingdom and New York, NY, USA: Cambridge University Press. 4, 5

Dijkstra, P., Ishizu, A., Doucett, R., Hart, S.C., Schwartz, E., Menyailo, O.V., & Hungate, B.A. 2006. ^{13}C and ^{15}N natural abundance of the soil microbial biomass. *Soil Biology and Biochemistry*, **38**, 3257–3266. 8, 114, 154

Dijkstra, P., Laviolette, C.M., Coyle, J.S., Doucett, R.R., Schwartz, E., Hart, S.C., & Hungate, B.A. 2008. ^{15}N enrichment as an integrator of the effects of C and N on microbial metabolism and ecosystem function. *Ecology Letters*, **11**, 389–397. 57

Dixon, J.L., & von Blanckenburg, F. 2012. Soils as pacemakers and limiters of global silicate weathering. *Comptes Rendus Geoscience*, **344**, 597–609. 193

Dixon, R.K., Brown, S., Houghton, R.A., Solomon, A.M., Trexler, M.C., & Wisniewski, J. 1994. Carbon pools and flux of global forest ecosystems. *Science*, **263**, 185–190. 24, 190

Drenzek, N.J., Hughen, K.A., Montlucecon, D.B., Southon, J.R., dos Santos, G.M., Druffel, E.R.M., Giosan, L., & Eglinton, T.I. 2009. A new look at old carbon in active margin sediments. *Geology*, **37**, 239–242. 13

Dyrness, C.T. 1967. *Mass soil movements in the H.J. Andrews Experimental Forest. Research Paper PNW-42*. Portland, Oregon, USA: U.S. Department of Agriculture, Forest Service, Pacific Northwest and Range Experiment Station. 36

Dyrness, C.T., Norgren, J., & Lienkaemper, G. 2005. *Soil survey (1964, revised in 1994), Andrews Experimental Forest (Spatial dataset)*. Corvallis, Oregon, USA: Long-Term Ecological Research; Forest Science Data Bank. http://andrewsforest.oregonstate.edu/data/abstract.cfm?dbcode=SP026. 42

Eglinton, T.I., & Eglinton, G. 2008. Molecular proxies for paleoclimatology. *Earth and Planetary Science Letters*, **275**, 1–16. 10

Fetherston, K.L., Naiman, R.J., & Bilby, R.E. 1995. Large woody debris, physical process, and riparian forest development in montane river networks of the Pacific Northwest. *Geomorphology*, **13**, 133–144. 41, 173

Field, C.B., Mortsch, L.D., Brklacich, M., Forbes, D.L., Kovacs, P., Patz, J.A., Running, S.W., & Scott, M.J. 2007. *Impacts, adaptation and vulnerability. Contribution of Working Group II to the Fourth Assessment Report of the Intergovernmental Panel on Climate Change*. Cambridge, United Kingdom: Cambridge University Press. 196, 197, 198

Finlay, J.C. 2001. Stable-carbon-isotope ratios of river biota: implications for energy flow in lotic food webs. *Ecology*, **82**, 1052–1064. 138, 145, 154

Finlay, J.C., Power, M.E., & Cabana, G. 1999. Effects of water velocity on algal carbon isotope ratios: implications for river food web studies. *Limnology and Oceanography*, **44**, 1198–1203. 6, 9, 145

Finlay, J.C., Hood, J.M., Limm, M.P., Power, M.E., Schade, J.D., & Welter, J.R. 2011. Light-mediated thresholds in stream-water nutrient composition in a river network. *Ecology*, **92**, 140–150. 145

France-Lanord, C., & Derry, L.A. 1994. δ^{13}C of organic carbon in the Bengal Fan: Source evolution and transport of C3 and C4 plant carbon to marine sediments. *Geochimica et Cosmochimica Acta*, **58**, 4809–4814. 66

France-Lanord, C., & Derry, L.A. 1997. Organic carbon burial forcing of the carbon cycle from Himalayan erosion. *Nature*, **390**, 65–67. 7, 194

Franklin, J.F., & Dyrness, C.T. 1973. *Natural vegetation of Oregon and Washington.* Portland, Oregon, USA: U.S. Department of Agriculture, Forest Service, Pacific Northwest Research Station. 43

Freer, J., McDonnell, J.J., Beven, K.J., Peters, N.E., Burns, D.A., Hooper, R.P., Aulenbach, B., & Kendall, C. 2002. The role of bedrock topography on subsurface storm flow. *Water Resources Research*, **38**, 1269. 48

Frentress, J., & McDonnell, J.J. 2011. Personal communication regarding the observation of diatoms in the streams at H.J. Andrews. 145

Frisch, W. 1979. Tectonic progradation and plate tectonic evolution of the Alps. *Tectonophysics*, **60**, 121–139. 21

Gabet, E.J. 2003. Sediment transport by dry ravel. *Journal of Geophysical Research: Solid Earth*, **108**, 2049. 45

Gaillardet, J., Dupré, B., Louvat, P., & Allègre, C.J. 1999. Global silicate weathering and CO_2 consumption rates deduced from the chemistry of large rivers. *Chemical Geology*, **159**, 3–30. 4, 5

Galy, A. 2013. Personal communication regarding the use of peak area and amplitude for determining mass spectrometer internal blank. 71

Galy, V., & Eglinton, T. 2011. Protracted storage of biospheric carbon in the Ganges-Brahmaputra basin. *Nature Geoscience*, **4**, 843–847. 13

Galy, V., Bouchez, J., & France-Lanord, C. 2007a. Determination of total organic carbon content and δ^{13}C in carbonate-rich detrital sediments. *Geostandards and Geoanalytical Research*, **31**, 199–207. 66, 68

Galy, V., France-Lanord, C., Beyssac, O., Faure, P., Kudrass, H., & Palhol, F. 2007b. Efficient organic carbon burial in the Bengal fan sustained by the Himalayan erosional system. *Nature*, **450**, 407–410. 3, 12, 189, 194

Galy, V., Beyssac, O., France-Lanord, C., & Eglinton, T. 2008. Recycling of Graphite During Himalayan Erosion: A Geological Stabilization of Carbon in the Crust. *Science*, **322**, 943–945. 97, 121, 124

Gearing, J.N, Gearing, P.J, Rudnick, D.T, Requejo, A.G, & Hutchins, M.J. 1984. Isotopic variability of organic carbon in a phytoplankton-based, temperate estuary. *Geochimica et Cosmochimica Acta*, **48**, 1089–1098. 145

Gimmi, U., Wolf, A., Bürgi, M., Scherstjanoi, M., & Bugmann, H. 2008. Quantifying disturbance effects on vegetation carbon pools in mountain forests based on historical data. *Regional Environmental Change*, **9**, 121–130. 25

Goñi, M.A., & Montgomery, S. 2000. Alkaline CuO oxidation with a microwave digestion system: Lignin analyses of geochemical samples. *Analytical Chemistry*, **72**, 3116–3121. 75, 84

Goñi, M.A., Monacci, N., Gisewhite, R., Crockett, J., Nittrouer, C., Ogston, A., Alin, S.R., & Aalto, R. 2008. Terrigenous organic matter in sediments from the Fly River delta-clinoform system (Papua New Guinea). *Journal of Geophysical Research*, **113**, F01S10. 12

Goñi, M.A., Hatten, J.A., Wheatcroft, R.A., & Borgeld, J.C. 2013. Particulate organic matter export by two contrasting small mountainous rivers from the Pacific Northwest, U.S.A. *Journal of Geophysical Research: Biogeosciences*, **118**, 1–23. 15, 42, 146, 168, 187, 195

Goldsmith, S.T., Carey, A.E., Lyons, W.B., Kao, S.-J., Lee, T.-Y, & Chen, J. 2008. Extreme storm events, landscape denudation, and carbon sequestration: Typhoon Mindulle, Choshui River, Taiwan. *Geology*, **36**, 483–486. 14

Gomez, B., Baisden, W.T., & Rogers, K.M. 2010. Variable composition of particle-bound organic carbon in steepland river systems. *Journal of Geophysical Research*, **115**, F04006. 14, 91, 100

Gordon, E.S., & Goñi, M.A. 2003. Sources and distribution of terrigenous organic matter delivered by the Atchafalaya River to sediments in the northern Gulf of Mexico. *Geochimica et Cosmochimica Acta*, **67**, 2359–2375. 10, 12, 15

Grant, G.E., & Wolff, A.L. 1991. Long-term patterns of sediment transport after timber harvest, western Cascade Mountains, Oregon, USA. *Pages 31–40 of: Sediment and stream water quality in a changing environment: trends and explanation, Proceedings of the Vienna IAHS symposium, Vienna, Austria. IAHS Publication No. 203.* Oxfordshire, United Kingdom: International Association of Hydrological Sciences. 43, 172

Grant, G.E., Swanson, F.J., & Wolman, M.G. 1990. Pattern and origin of stepped-bed morphology in high-gradient streams, Western Cascades, Oregon. *Geological Society of America Bulletin*, **102**, 340–352. 40

Graz, Y., Di-Giovanni, C., Copard, Y., Elie, M., Faure, P., Laggoun Defarge, F., Lévèque, J., Michels, R., & Olivier, J.E. 2011. Occurrence of fossil organic matter in modern environments: Optical, geochemical and isotopic evidence. *Applied Geochemistry*, **26**, 1302–1314. 103

Gudasz, C., Bastviken, D., Steger, K., Premke, K., Sobek, S., & Tranvik, L.J. 2010. Temperature-controlled organic carbon mineralization in lake sediments. *Nature*, **466**, 478–481. 13

Guehl, J.M., Domenach, A.M., Bereau, M., Barigah, T.S., Casabianca, H., Ferhi, A., & Garbaye, J. 1998. Functional diversity in an Amazonian rainforest of French Guyana: A dual isotope approach (δ^{15}N and δ^{13}C). *Oecologia*, **116**, 316–330. 7, 8, 89

Guzzetti, F., Peruccacci, S., Rossi, M., & Stark, C.P. 2007. Rainfall thresholds for the initiation of landslides in central and southern Europe. *Meteorology and Atmospheric Physics*, **98**, 239–267. 101

Hagedorn, F., Schleppi, P., Waldner, P.A., & Flühler, H. 2000. Export of dissolved organic carbon and nitrogen from Gleysol dominated catchments - The significance of water flow paths. *Biogeochemistry*, **50**, 137–161. 24, 91, 100, 190

Hagedorn, F., Bucher, J.B., & Schleppi, P. 2001. Contrasting dynamics of dissolved inorganic and organic nitrogen in soil and surface waters of forested catchments with Gleysols. *Geoderma*, **100**, 173–192. 21

Harr, R.D. 1981. Some characteristics and consequences of snowmelt during rainfall in western Oregon. *Journal of Hydrology*, **53**, 277–304. 36, 46

Hastings, R.H., Goñi, M.A., Wheatcroft, R.A., & Borgeld, J.C. 2012. A terrestrial organic matter depocenter on a high-energy margin: The Umpqua River system, Oregon. *Continental Shelf Research*, **39–40**, 78–91. 10, 15, 82, 195

Hatten, J.A., Goñi, M.A., Wheatcroft, R.A., Borgeld, J.C., Padgett, J.S., Pasternack, G.B., Gray, A.B., Watson, E.B., & Warrick, J.A. 2010. Watershed fire regime effects on particulate organic carbon composition in Oregon and California Coast Range rivers. *In: AGU Fall Meeting Abstracts, abstract number B33E-0434*. American Geophysical Union. 45

Hatten, J.A., Goñi, M.A., & Wheatcroft, R.A. 2012. Chemical characteristics of particulate organic matter from a small, mountainous river system in the Oregon Coast Range, USA. *Biogeochemistry*, **107**, 43–66. 15, 42, 91, 145, 146, 169, 195

Hayes, J.M. 1993. Factors controlling ^{13}C contents of sedimentary organic compounds: Principles and evidence. *Marine Geology*, **113**, 111–125. 7

Hayes, J.M., Strauss, H., & Kaufman, A.J. 1999. The abundance of ^{13}C in marine organic matter and isotopic fractionation in the global biogeochemical cycle of carbon during the past 800 Ma. *Chemical Geology*, **161**, 103–125. 3

Hedges, J.I. 1992. Global biogeochemical cycles: progress and problems. *Marine Chemistry*, **39**, 67–93. 3, 196

Hedges, J.I., & Ertel, J.R. 1982. Characterization of lignin by gas capillary chromatography of cupric oxide oxidation products. *Analytical Chemistry*, **54**, 174–178. 75

Hedges, J.I., & Keil, R.G. 1995. Sedimentary organic matter preservation: an assessment and speculative synthesis. *Marine Chemistry*, **49**, 81–115. 3, 12, 194

Hedges, J.I., & Mann, D.C. 1979a. The characterization of plant tissues by their lignin oxidation products. *Geochimica et Cosmochimica Acta*, **43**, 1803–1807. 10, 76, 84

Hedges, J.I., & Mann, D.C. 1979b. The lignin geochemistry of marine sediments from the southern Washington coast. *Geochimica et Cosmochimica Acta*, **43**, 1809–1818. 10, 76

Hedges, J.I., Cowie, G.L., Ertel, J.R., Barbour, R.J., & Hatcher, P.G. 1985. Degradation of carbohydrates and lignins in buried woods. *Geochimica et Cosmochimica Acta*, **49**, 701–711. 84

Hedges, J.I., Keil, R.G., & Benner, R. 1997. What happens to terrestrial organic matter in the ocean? *Organic Geochemistry*, **27**, 195–212. 6, 194

Hegg, C., McArdell, B.W., & Badoux, A. 2006. One hundred years of mountain hydrology in Switzerland by the WSL. *Hydrological Processes*, **20**, 371–376. 25

Heimsath, A.M., Dietrich, W.E., Nishiizumi, K., & Finkel, R.C. 2001. Stochastic processes of soil production and transport: erosion rates, topographic variation and cosmogenic nuclides in the Oregon Coast Range. *Earth Surface Processes and Landforms*, **26**, 531–552. 33, 41

Heller, P.L., & Ryberg, P.T. 1983. Sedimentary record of subduction to forearc transition in the rotated Eocene basin of western Oregon. *Geology*, **11**, 380–383. 32

Henshaw, D. 2002. *HJA flume calibration summary—rating curve equations by set and version.* Blue River, Oregon, USA: Andrews Experimental Forest. 64

Henshaw, D., & Creel, C. 2005. *Meteorological station locations, Andrews Experimental Forest (Spatial dataset).* Corvallis, Oregon, USA: Long-Term Ecological Research; Forest Science Data Bank. http://andrewsforest.oregonstate.edu/data/abstract.cfm?dbcode=MS026. 61

Hilton, R.G. 2008. *Erosion of Organic Carbon from Active Mountain Belts.* PhD thesis, University of Cambridge, Cambridge, United Kingdom. 2, 4, 5, 8, 9, 194

Hilton, R.G., Galy, A., & Hovius, N. 2008a. Riverine particulate organic carbon from an active mountain belt: Importance of landslides. *Global Biogeochemical Cycles*, **22**, GB1017. 8, 9, 13, 14, 66, 189, 194

Hilton, R.G., Galy, A., Hovius, N., Chen, M.-C., Horng, M.-J., & Chen, H. 2008b. Tropical-cyclone-driven erosion of the terrestrial biosphere from mountains. *Nature Geoscience*, **1**, 759–762. 3, 9, 12, 13, 14, 189, 194

Hilton, R.G., Galy, A., Hovius, N., Horng, M.-J., & Chen, H. 2010. The isotopic composition of particulate organic carbon in mountain rivers of Taiwan. *Geochimica et Cosmochimica Acta*, **74**, 3164–3181. 8, 9, 71, 91, 96, 98

Hilton, R.G., Galy, A., Hovius, N., Horng, M.-J., & Chen, H. 2011a. Efficient transport of fossil organic carbon to the ocean by steep mountain rivers: An orogenic carbon sequestration mechanism. *Geology*, **39**, 71–74. 3, 196

Hilton, R.G., Meunier, P., Hovius, N., Bellingham, P.J., & Galy, A. 2011b. Landslide impact on organic carbon cycling in a temperate montane forest. *Earth Surface Processes and Landforms*, **36**, 1670–1679. 14, 189

Hilton, R.G., Galy, A., Hovius, N., Kao, S.-J., Horng, M.-J., & Chen, H. 2012a. Climatic and geomorphic controls on the erosion of terrestrial biomass from subtropical mountain forest. *Global Biogeochemical Cycles*, **26**, GB3014. 188, 189

Hilton, R.G., Galy, A., West, A.J., Hovius, N., & Roberts, G.G. 2012b. Geomorphic control on the δ^{15}N of mountain forest. *Biogeosciences Discuss.*, **9**, 12593–12626. 71, 155

Holtvoeth, J., Kolonic, S., & Wagner, T. 2005. Soil organic matter as an important contributor to late Quaternary sediments of the tropical West African continental margin. *Geochimica et Cosmochimica Acta*, **69**, 2031–2041. 7

Horton, R.E. 1945. Erosional development of streams and their drainage basins; hydrophysical approach to quantitative morphology. *Geological Society of America Bulletin*, **56**, 275–370. 14, 99

Hren, M.T., Hilley, G.E., & Chamberlain, C.P. 2007. The relationship between tectonic uplift and chemical weathering rates in the Washington Cascades: Field measurements and model predictions. *American Journal of Science*, **307**, 1041–1063. 33, 42

Hurrell, E.R., Barker, P.A., Leng, M.J., Vane, C.H., Wynn, P., Kendrick, C.P., Verschuren, D., & StreetPerrott, F.A. 2011. Developing a methodology for carbon isotope analysis of lacustrine diatoms. *Rapid Communications in Mass Spectrometry*, **25**, 1567–1574. 145

Ice, G.G., Hale, C., Schoenholtz, S., Light, J., Johnson, S.L., Bousquet, T., & Stednick, J.D. 2005. The New Alsea Watershed Study. *In: Proceedings of the 2005 Society of American Foresters National Convention, Fort Worth, TX*. 30, 45

Ittekkot, V. 1988. Global trends in the nature of organic matter in river suspensions. *Nature*, **332**, 436–438. 10

Jackson, M., & Roering, J.J. 2009. Post-fire geomorphic response in steep, forested landscapes: Oregon Coast Range, USA. *Quaternary Science Reviews*, **28**, 1131–1146. 45

Johnson, S.L. 2012. Personal communication regarding bias in suspended sediment sampling methods at H.J. Andrews. 147

Johnson, S.L., & Frederiksen, R.L. 2012. *Long-term stream chemistry concentrations and fluxes: Small watershed proportional samples in the Andrews Experimental Forest (Dataset)*. Corvallis, Oregon, USA: Long-Term Ecological Research; Forest Science Data Bank. http://andrewsforest.oregonstate.edu/data/abstract.cfm?dbcode=CF002. 48

Johnson, S.L., & Lienkaemper, G. 2005a. *Experimental watershed boundaries and gaging station locations, Andrews Experimental Forest (Spatial dataset)*. Corvallis, Oregon, USA: Long-Term Ecological Research; Forest Science Data Bank. http://andrewsforest.oregonstate.edu/data/abstract.cfm?dbcode=HF014. 61

Johnson, S.L., & Lienkaemper, G. 2005b. *Stream network (1976 survey), Andrews Experimental Forest (Spatial dataset)*. Corvallis, Oregon, USA: Long-Term Ecological Research; Forest Science Data Bank. http://andrewsforest.oregonstate.edu/lter/data/abstract.cfm?dbcode=HF013. 61

Johnson, S.L., & Rothacher, J. 2012. *Stream discharge in gaged watersheds at the Andrews Experimental Forest (Dataset).* Corvallis, Oregon, USA: Long-Term Ecological Research; Forest Science Data Bank. http://andrewsforest.oregonstate.edu/data/abstract.cfm?dbcode=HF004. 46, 47, 48, 64, 171

Johnson, S.L., Swanson, F.J., Grant, G.E., & Wondzell, S.M. 2000. Riparian forest disturbances by a mountain flood—The influence of floated wood. *Hydrological Processes*, **14**, 3031–3050. 41, 173

Jones, J.A. 2000. Hydrologic processes and peak discharge response to forest removal, regrowth, and roads in 10 small experimental basins, western Cascades, Oregon. *Water Resources Research*, **36**, 2621–2642. 43

Kao, S.-J., & Liu, K.-K. 1996. Particulate organic carbon export from a subtropical mountainous river (Lanyang Hsi) in Taiwan. *Limnology and Oceanography*, **41**, 1749–1757. 101

Karlsson, E.S., Charkin, A., Dudarev, O., Semiletov, I., Vonk, J.E., Sánchez-García, L., Andersson, A., & Gustafsson, Ö. 2011. Carbon isotopes and lipid biomarker investigation of sources, transport and degradation of terrestrial organic matter in the Buor-Khaya Bay, SE Laptev Sea. *Biogeosciences*, **8**, 1865–1879. 10

Keller, H.M., Weibel, P., Peters, N.E., & Walling, D.E. 1991. Suspended sediments in streamwater - indicators of erosion and bed load transport in mountainous basins. *Pages 53–61 of: Sediment and stream water quality in a changing environment: Trends and explanation. Proc. Symposium, Vienna, 1991.* Oxfordshire, United Kingdom: International Association of Hydrological Sciences. 28

Kelsey, H.M., Ticknor, R.L., Bockheim, J.G., & Mitchell, E. 1996. Quaternary upper plate deformation in coastal Oregon. *Geological Society of America Bulletin*, **108**, 843–860. 33

Kirsch, J., Burlando, P., Molnar, P., & Hinz, E. 2007. Modeling the effects of land cover changes on sediment transport in the Vogelbach Basin, Switzerland. *Pages 171–216 of:* Westrich, B., & Förstner, U. (eds), *Sediment Dynamics and Pollutant Mobility in Rivers.* Berlin & Heidelberg, Germany; New York, USA: Springer. 21, 22, 24

Kögel, I., & Bochter, R. 1985. Characterization of lignin in forest humus layers by high-performance liquid chromatography of cupric oxide oxidation products. *Soil Biology and Biochemistry*, **17**, 637–640. 75

Komada, T., Druffel, E.R.M., & Trumbore, S.E. 2004. Oceanic export of relict carbon by small mountainous rivers. *Geophysical Research Letters*, **31**, L07504. 9

Komada, T., Druffel, E.R.M., & Hwang, J. 2005. Sedimentary rocks as sources of ancient organic carbon to the ocean: An investigation through $\Delta^{14}C$ and $\delta^{13}C$ signatures of organic compound classes. *Global Biogeochemical Cycles*, **19**, GB2017. 8, 9

Körner, Ch., Farquhar, G.D., & Roksandic, Z. 1988. A global survey of carbon isotope discrimination in plants from high altitude. *Oecologia*, **74**, 623–632. 8

Körner, Ch., Farquhar, G.D., & Wong, S.C. 1991. Carbon isotope discrimination by plants follows latitudinal and altitudinal trends. *Oecologia*, **88**, 30–40. 8

Krause, K. 2010. Personal communication regarding the natural isotopic composition of Erlenbach norway spruce. 88

Leithold, E.L., Blair, N.E., & Perkey, D.W. 2006. Geomorphologic controls on the age of particulate organic carbon from small mountainous and upland rivers. *Global Biogeochemical Cycles*, **20**, GB3022. 9, 182

Levin, I., & Hesshaimer, V. 2006. Radiocarbon; a unique tracer of global carbon cycle dynamics. *Radiocarbon*, **42**, 69–80. 9, 99

Litherland, A.E. 1984. Accelerator mass spectrometry. *Nuclear Instruments and Methods in Physics Research Section B: Beam Interactions with Materials and Atoms*, **5**, 100–108. 75

Lorenzoni, L., Benitez-Nelson, C.R., Thunell, R.C., Hollander, D., Varela, R., Astor, Y., Audemard, F.A., & Muller-Karger, F.E. 2012. Potential role of event-driven sediment transport on sediment accumulation in the Cariaco Basin, Venezuela. *Marine Geology*, **307–310**, 105–110. 12

Ludwig, W., Probst, J.-L., & Kempe, S. 1996. Predicting the oceanic input of organic carbon by continental erosion. *Global Biogeochemical Cycles*, **10**, 23–41. 6, 11

Lupker, M., France-Lanord, C., Lavé, J., Bouchez, J., Galy, V., Métivier, F., Gaillardet, J., Lartiges, B., & Mugnier, J.-L. 2011. A Rouse-based method to integrate the chemical composition of river sediments: Application to the Ganga basin. *Journal of Geophysical Research: Earth Surface*, **116**. 194

Lyons, W.B., Nezat, C.A., Carey, A.E., & Hicks, D.M. 2002. Organic carbon fluxes to the ocean from high-standing islands. *Geology*, **30**, 443–446. 13

Mace, G., Masundire, H., & Baillie, J. 2005. Chapter 4—Biodiversity. *Pages 77–122 of:* Hassan, R., Scholes, R., & Ash, N. (eds), *Ecosystems and Human Well-being: Current State and Trends, Volume 1 (Millennium Ecosystem Assessment Report)*. USA: Island Press. 190

Macko, S.A., & Estep, M.L.F. 1984. Microbial alteration of stable nitrogen and carbon isotopic compositions of organic matter. *Organic Geochemistry*, **6**, 787–790. 8

Mariotti, A., Pierre, D., Vedy, J.C., Bruckert, S., & Guillemot, J. 1980. The abundance of natural nitrogen 15 in the organic matter of soils along an altitudinal gradient (Chablais, Haute Savoie, France). *Catena*, **7**, 293–300. 84

Martinelli, L.A., Piccolo, M.C., Townsend, A.R., Vitousek, P.M., Cuevas, E., McDowell, W., Robertson, G.P., Santos, O.C., & Treseder, K. 1999. Nitrogen stable isotopic composition of leaves and soil: Tropical versus temperate forests. *Biogeochemistry*, **46**, 45–65. 8

Masiello, C.A., & Druffel, E.R.M. 2001. Carbon isotope geochemistry of the Santa Clara River. *Global Biogeochemical Cycles*, **15**, 407–416. 101

Masson, D.G., Huvenne, V.A.I., Stigter, H.C. de, Wolff, G.A., Kiriakoulakis, K., Arzola, R.G., & Blackbird, S. 2010. Efficient burial of carbon in a submarine canyon. *Geology*, **38**, 831–834. 12

McCabe, G.J., Hay, L.E., & Clark, M.P. 2007. Rain-on-snow events in the Western United States. *Bulletin of the American Meteorological Society*, **88**, 319–328. 36

McCaffrey, R., Qamar, A.I., King, R.W., Wells, R., Khazaradze, G., Williams, C.A., Stevens, C.W., Vollick, J.J., & Zwick, P.C. 2007. Fault locking, block rotation and crustal deformation in the Pacific Northwest. *Geophysical Journal International*, **169**, 1315–1340. 32, 33

McDonnell, J.J. 2003. Where does the water go when it rains? Moving beyond the variable source area concept of rainfall-runoff response. *Hydrological Processes*, **17**, 1869–1875. 48, 166

McGuire, K.J., McDonnell, J.J., Weiler, M., Kendall, C., McGlynn, B.L., Welker, J.M., & Seibert, J. 2005. The role of topography on catchment-scale water residence time. *Water Resources Research*, **41**, W05002. 47

McGuire, K.J., Weiler, M., & McDonnell, J.J. 2007. Integrating tracer experiments with modeling to assess runoff processes and water transit times. *Advances in Water Resources*, **30**, 824–837. 48

Meckler, A.N., Schubert, C.J., Hochuli, P.A., Plessen, B., Birgel, D., Flower, B.P., Hinrichs, K.-U., & Haug, G.H. 2008. Glacial to Holocene terrigenous organic matter input to sediments from Orca Basin, Gulf of Mexico - A combined optical and biomarker approach. *Earth and Planetary Science Letters*, **272**, 251–263. 12

Medeiros, P.M., & Simoneit, B.R.T. 2008. Multi-biomarker characterization of sedimentary organic carbon in small rivers draining the Northwestern United States. *Organic Geochemistry*, **39**, 52–74. 10

Meigs, G.W., Donato, D.C., Campbell, J.L., Martin, J.G., & Law, B.E. 2009. Forest fire impacts on carbon uptake, storage, and emission: The role of burn severity in the eastern Cascades, Oregon. *Ecosystems*, **12**, 1246–1267. 45

Melillo, J., Aber, J., Linkins, A., Ricca, A., Fry, B., & Nadelhoffer, K. 1989. Carbon and nitrogen dynamics along the decay continuum: Plant litter to soil organic matter. *Plant and Soil*, **115**, 189–198. 8, 114, 154, 155

Meybeck, M. 1993. Riverine transport of atmospheric carbon: Sources, global typology and budget. *Water, Air, & Soil Pollution*, **70**, 443–463. 6, 10, 11, 190, 199

Meyers, P.A. 1997. Organic geochemical proxies of paleoceanographic, paleolimnologic, and paleoclimatic processes. *Organic Geochemistry*, **27**, 213–250. 10

Middelburg, J.J., & Nieuwenhuize, J. 1998. Carbon and nitrogen stable isotopes in suspended matter and sediments from the Schelde Estuary. *Marine Chemistry*, **60**, 217–225. 8

Milliman, J.D., & Syvitski, J.P.M. 1992. Geomorphic/tectonic control of sediment discharge to the ocean: the importance of small mountainous rivers. *Journal of Geology*, **100**, 525–544. 13

Milzow, C., Molnar, P., McArdell, B.W., & Burlando, P. 2006. Spatial organization in the step-pool structure of a steep mountain stream (Vogelbach, Switzerland). *Water Resources Research*, **42**, W04418. 21, 22, 24, 26, 190

Molnar, P., & England, P. 1990. Late Cenozoic uplift of mountain ranges and global climate change: chicken or egg? *Nature*, **346**, 29–34. 194

Montgomery, D.R., & Buffington, J.M. 1997. Channel-reach morphology in mountain drainage basins. *Geological Society of America Bulletin*, **109**, 596–611. 40

Montgomery, D.R., Dietrich, W.E., Torres, R., Anderson, S.P., Heffner, J.T., & Loague, K. 1997. Hydrologic response of a steep, unchanneled valley to natural and applied rainfall. *Water Resources Research*, **33**, 91–109. 49, 166

Motter, K., & Jones, C. 2010. *Standard operating procedure for the determination of suspended sediments. CCAL 12A.1.* Corvallis, Oregon, USA: Cooperative Chamical Analytical Laboratory, College of Forestry, Oregon State University. 54

Muller, N. 1997. *Short-term response of the ground vegetation in a montane forest ecosystem under increased nitrogen deposition—influence of light and competition.* PhD thesis, ETHZ, Zurich, Switzerland. 25

Nadeu, E., Berhe, A.A., de Vente, J., & Boix-Fayos, C. 2012. Erosion, deposition and replacement of soil organic carbon in Mediterranean catchments: a geomorphological, isotopic and land use change approach. *Biogeosciences*, **9**, 1099–1111. 198

Nash, D.B. 1994. Effective sediment-transporting discharge from magnitude–frequency analysis. *The Journal of Geology*, **102**, 79–95. 102, 172

Natelhoffer, K.J., & Fry, B. 1988. Controls on natural nitrogen-15 and carbon-13 abundances in forest soil organic matter. *Soil Science of America Journal*, **52**, 1633–1640. 8

Oak Ridge National Laboratory Distributed Active Archive Center, ORNL DAAC. 2011. *MODIS subsetted land products, Collection 5.* Oak Ridge, Tennessee, USA: ORNL DAAC. http://daac.ornl.gov/MODIS/modis.html. 24

O'Leary, M.H. 1981. Carbon isotope fractionation in plants. *Phytochemistry*, **20**, 553–567. 8, 89

Olson, D.M., Dinerstein, E., Wikramanayake, E.D., Burgess, N.D., Powell, G.V.N., Underwood, E.C., D'amico, J.A., Itoua, I., Strand, H.E., Morrison, J.C., Loucks, C.J., Allnutt, T.F., Ricketts, T.H., Kura, Y., Lamoreux, J.F., Wettengel, W.W., Hedao, P., & Kassem, K.R. 2001. Terrestrial ecoregions of the world: a new map of life on Earth. *BioScience*, **51**, 933–938. 191

Ometto, J.P.H.B., Ehleringer, J.R., Domingues, T.F., Berry, J.A., Ishida, F.Y., Mazzi, E., Higuchi, N., Flanagan, L.B., Nardoto, G.B., & Martinelli, L.A. 2006. The stable carbon and nitrogen isotopic composition of vegetation in tropical forests of the Amazon Basin, Brazil. *Biogeochemistry*, **79**, 251–274. 8, 89

Peck, D.L. 1961. *Geologic map of Oregon west of the 121st meridian 1:500 000.* USGS, Department of the Interior, in collaboration with Oregon Department of Geology and Mineral Industries. 31, 32

Pelletier, J.D. 2012. Fluvial and slopewash erosion of soil-mantled landscapes: detachment- or transport-limited? *Earth Surface Processes and Landforms*, **37**, 37–51. 47

Personius, S.F. 1995. Late Quaternary stream incision and uplift in the forearc of the Cascadia subduction zone, western Oregon. *Journal of Geophysical Research*, **100**, 20193–20210. 33

Peterson, B.J., & Fry, B. 1987. Stable isotopes in ecosystem studies. *Annual Review of Ecology and Systematics*, **18**, 293–320. 8

Petsch, S.T., Berner, R.A., & Eglinton, T.I. 2000. A field study of the chemical weathering of ancient sedimentary organic matter. *Organic Geochemistry*, **31**, 475–487. 3

Post, D.A., & Jones, J.A. 2001. Hydrologic regimes of forested, mountainous, headwater basins in New Hampshire, North Carolina, Oregon, and Puerto Rico. *Advances in Water Resources*, **24**, 1195–1210. 47, 48

Post, W.M., Emanuel, W.R., Zinke, P.J., & Stangenberger, A.G. 1982. Soil carbon pools and world life zones. *Nature*, **298**, 156–159. 4

Prahl, F.G, Ertel, J.R, Goñi, M.A, Sparrow, M.A, & Eversmeyer, B. 1994. Terrestrial organic carbon contributions to sediments on the Washington margin. *Geochimica et Cosmochimica Acta*, **58**, 3035–3048. 10, 12, 15

Prentice, I.C., Farquhar, G.D., Fasham, M.J.R., Goulden, M.L., Heimann, M., Jaramillo, V.J., Kheshgi, H.S., Le Quéré, C., Scholes, R.J., & Wallace, D.W.R. 2001. The carbon cycle and atmospheric carbon dioxide. *Pages 183–237 of: Climate Change 2000: the science of climate change. Contribution of Working Group I to the Third Assessment Report of the Intergovernmental Panel on Climate Change*. Cambridge, United Kingdom: Cambridge University Press. 4, 5, 6

Ramos Scharrón, C.E., Castellanos, E.J., & Restrepo, C. 2012. The transfer of modern organic carbon by landslide activity in tropical montane ecosystems. *Journal of Geophysical Research*, **117**, G03016. 13

Raymo, M.E., & Ruddiman, W.F. 1992. Tectonic forcing of late Cenozoic climate. *Nature*, **359**, 117–122. 6, 194

Raymo, M.E., Ruddiman, W.F., & Froelich, P.N. 1988. Influence of late Cenozoic mountain building on ocean geochemical cycles. *Geology*, **16**, 649–653. 194

Reiners, P.W., Ehlers, T.A., Mitchell, S.G., & Montgomery, D.R. 2003. Coupled spatial variations in precipitation and long-term erosion rates across the Washington Cascades. *Nature*, **426**, 645–647. 33

Renée Brooks, J., Barnard, H.R., Coulombe, R., & McDonnell, J.J. 2010. Ecohydrologic separation of water between trees and streams in a Mediterranean climate. *Nature Geoscience*, **3**, 100–104. 48

Rickenmann, D. 1997. Sediment transport in Swiss torrents. *Earth Surface Processes and Landforms*, **22**, 937–951. 21

Rickenmann, D., & McArdell, B.W. 2007. Continuous measurement of sediment transport in the Erlenbach stream using piezoelectric bedload impact sensors. *Earth Surface Processes and Landforms*, **32**, 1362–1378. 28, 107

Rickenmann, D., Turowski, J.M., Fritschi, B., Klaiber, A., & Ludwig, A. 2012. Bedload transport measurements at the Erlenbach stream with geophones and automated basket samplers. *Earth Surface Processes and Landforms*, **37**, 1000–1011. 28, 107

Rochelle, J., O'Neil, T., Langhoff, C., & O'Neil, E. 2005. *A Guide to Oregon's Forest Wildlife*. Portland, Oregon, USA: Oregon Forest Resources Institute. 43

Roering, J.J., Schmidt, K.M., Stock, J.D., Dietrich, W.E., & Montgomery, D.R. 2003. Shallow landsliding, root reinforcement, and the spatial distribution of trees in the Oregon Coast Range. *Canadian Geotechnical Journal*, **40**, 237–253. 39, 187

Roering, J.J., Kirchner, J.W., & Dietrich, W.E. 2004. Characterizing structural and lithologic controls on deep-seated landsliding: Implications for topographic relief and landscape evolution in the Oregon Coast Range, USA. *Geological Society of America Bulletin*, **117**, 654 –668. 33, 39, 41

Rolfe, J.E. 2012. Personal communication regarding the precision of the Godwin Lab's two mass spectrometers. 69

Rosentrater, L.D. 1997. *The thermal climate of the H.J. Andrews Experimental Forest, Oregon*. M.S. thesis, University of Oregon, Eugene, Oregon, USA. 34

Sarmiento, J.L., & Sundquist, E.T. 1992. Revised budget for the oceanic uptake of anthropogenic carbon dioxide. *Nature*, **356**, 589–593. 5, 10

Schleppi, P. 2013. Personal communication regarding net primary productivity in the Alptal. 24

Schleppi, P., Muller, N., Feyen, H., Papritz, A., Bucher, J.B., & Flhler, H. 1998. Nitrogen budgets of two small experimental forested catchments at Alptal, Switzerland. *Forest Ecology and Management*, **101**, 177–185. 28

Schleppi, P., Muller, N., Edwards, P.J., & Bucher, J.B. 1999. Three years of increased nitrogen deposition do not affect the vegetation of a montane forest ecosystem. *Phyton*, **39**, 197–204. 24, 25

Schleppi, P., Waldner, P.A., & Fritschi, B. 2006. Accuracy and precision of different sampling strategies and flux integration methods for runoff water: Comparisons based on measurements of the electrical conductivity. *Hydrological Processes*, **20**, 395–410. 25, 52, 110

Schlesinger, W.H. 1984. Soil organic matter: a source of atmospheric CO_2. *In:* Woodwell, G.M. (ed), *SCOPE 23—The role of terrestrial vegetation in the global carbon cycle: Measurement by remote sensing*. John Wiley & Sons Ltd. 4

Schlesinger, W.H. 1995. Soil respiration and changes in soil carbon stocks. *In:* Woodwell, G.M., & Mackenzie, F.T. (eds), *Biotic Feedbacks in the Global Climatic System: Will the Warming Feed the Warming?* Oxford, United Kingdom: Oxford University Press. 3

Schlesinger, W.H., & Melack, J.M. 1981. Transport of organic carbon in the world's rivers. *Tellus*, **33**, 172–187. 10

Schlunegger, F., & Hinderer, M. 2003. Pleistocene/Holocene climate change, re-establishment of fluvial drainage network and increase in relief in the Swiss Alps. *Terra Nova*, **15**, 88–95. 21

Schlünz, B., & Schneider, R.R. 2000. Transport of terrestrial organic carbon to the oceans by rivers: re-estimating flux- and burial rates. *International Journal of Earth Sciences*, **88**, 599–606. 3, 5, 6, 11, 12, 193, 194, 199

Schuerch, P., Densmore, A.L., McArdell, B.W., & Molnar, P. 2006. The influence of landsliding on sediment supply and channel change in a steep mountain catchment. *Geomorphology*, **78**, 222–235. 20, 23, 24, 100

Schulze, M. 2005. *Vegetation classification, Andrews Experimental Forest and vicinity (1988, 1993, 1996, 1997, 2002) (Spatial dataset).* Corvallis, Oregon, USA: Long-Term Ecological Research; Forest Science Data Bank. http://andrewsforest.oregonstate.edu/lter/data/abstract.cfm?dbcode=TV061. 44

Schulze, M. 2011. Personal communication regarding overland flow at H.J. Andrews. 166

Seitzinger, S.P., Harrison, J.A., Dumont, E., Beusen, A.H.W., & Bouwman, A.F. 2005. Sources and delivery of carbon, nitrogen, and phosphorus to the coastal zone: An overview of Global Nutrient Export from Watersheds (NEWS) models and their application. *Global Biogeochemical Cycles*, **19**, GB4S01. 11, 193, 199

Siegenthaler, U., & Sarmiento, J.L. 1993. Atmospheric carbon dioxide and the ocean. *Nature*, **365**, 119–125. 4

Sigman, D.M., & Boyle, E.A. 2000. Glacial/interglacial variations in atmospheric carbon dioxide. *Nature*, **407**, 859–869. 4, 5, 6

Sikes, E.L., Uhle, M.E., Nodder, S.D., & Howard, M.E. 2009. Sources of organic matter in a coastal marine environment: Evidence from n-alkanes and their δ^{13}C distributions in the Hauraki Gulf, New Zealand. *Marine Chemistry*, **113**, 149–163. 12

Skaugset, A.E., Li, J., Cromack, K., Gresswell, R.E., & Adams, M. 2004. *Cumulative environmental effects of contemporat forest management activities in headwater basins of Western Oregon: The Hinkle Creek Paired Watershed Study.* Tech. rept. Watersheds Research Cooperative, Corvallis, Oregon, USA. 30, 31, 35, 42, 43, 44, 54

Smith, S.V., Renwick, W.H., Buddemeier, R.W., & Crossland, C.J. 2001. Budgets of soil erosion and deposition for sediments and sedimentary organic carbon across the conterminous United States. *Global Biogeochemical Cycles*, **15**, 697–707. 3, 13

Snyder, K.U. 2000. *Debris flows and flood disturbance in small, mountain watersheds.* M.S. thesis, Oregon State University, Corvallis, Oregon. 39, 165

Sparkes, R.B. 2012. *Marine sequestration of particulate organic carbon from mountain belts.* PhD thesis, University of Cambridge, Cambridge, United Kingdom. 3, 8, 9, 13, 66, 76, 79, 122, 194, 195, 196

Spies, T. 2011. *LiDAR data (August 2008) for the Andrews Experimental Forest and Willamette National Forest study areas (Spatial dataset).* Corvallis, Oregon, USA: H.J. Andrews Experimental Forest; Forest Science Data Bank. http://andrewsforest.oregonstate.edu/data/abstract.cfm?dbcode=GI010. 166

Stallard, R.F. 1998. Terrestrial sedimentation and the carbon cycle: Coupling weathering and erosion to carbon burial. *Global Biogeochemical Cycles*, **12**, 231–257. 6, 13

Stednick, J.D. 2008. Effects of timber harvesting on streamflow in the Alsea watershed study. *Pages 19–36 of:* Stednick, J.D. (ed), *Hydrological and Biological Responses to Forest Practices.* New York, USA: Springer. 35

Stock, J.D., & Dietrich, W.E. 2006. Erosion of steepland valleys by debris flows. *Geological Society of America Bulletin*, **118**, 1125–1148. 36

Stoffel, M., & Wilford, D.J. 2012. Hydrogeomorphic processes and vegetation: disturbance, process histories, dependencies and interactions. *Earth Surface Processes and Landforms*, **37**, 9–22. 43, 146, 187

Stott, T., Leeks, G., Marks, S., & Sawyer, A. 2001. Environmentally sensitive plot-scale timber harvesting: impacts on suspended sediment, bedload and bank erosion dynamics. *Journal of Environmental Management*, **63**, 3–25. 43

Sundquist, E.T. 1993. The global carbon dioxide budget. *Science*, **259**, 934–941. 4, 5

Sundquist, E.T., & Visser, K. 2003. The geologic history of the carbon cycle. *Pages 425–472 of:* Holland, H.D., & Turekian, K.K. (eds), *Treatise on Geochemistry—Volume 8: Biogeochemistry.* Oxford, United Kingdom: Elsevier-Pergamon. 4, 5

Swanson, F.J. 2012. Personal communication regarding industrial broadcast burning at Hinkle. 162

Swanson, F.J., & James, M.E. 1975. *Geology and geomorphology of the H.J. Andrews Experimental Forest, Western Cascades, Oregon.* Portland, OR: USDA Forest Service and Pacific Northwest Forest and Range Experiment Station. 31, 36, 39, 40

Swanson, F.J., & Jones, J.A. 2002. Geomorphology and hydrology of the H.J. Andrews Experimental Forest, Blue River, Oregon. *Pages 288–314 of:* Moore, G.W. (ed), *Field guide to geologic processes in Cascadia: field trips to accompany the 98th annual meeting of the Cordilleran section of the Geological Society of America (Special paper 36).* Portland, Oregon, USA: Oregon Department of Geology and Mineral Industries. 34, 36, 39, 43, 46

Swanson, F.J., & Lienkaemper, G. 2005. *Road construction history (1952-1990), Andrews Experimental Forest (Spatial dataset).* Corvallis, Oregon, USA: Long-Term Ecological Research; Forest Science Data Bank. http://andrewsforest.oregonstate.edu/data/abstract.cfm?dbcode=DH001. 61

Swanson, F.J., & Swanston, D.N. 1977. Complex mass-movement terrains in the western Cascade Range, Oregon. *Reviews in Engineering Geology*, **3**, 113–124. 39

Thornton, S.F., & McManus, J. 1994. Application of organic carbon and nitrogen stable isotope and C/N ratios as source indicators of organic matter provenance in estuarine systems: evidence from the Tay Estuary, Scotland. *Estuarine, Coastal and Shelf Science*, **38**, 219–233. 8

Tippett, J.M., & Kamp, P.J.J. 1993. Fission track analysis of the Late Cenozoic vertical kinematics of continental pacific crust, South Island, New Zealand. *Journal of Geophysical Research*, **98**, 16119–16148. 34

Tipping, E. 2002. *Cation Binding by Humic Substances.* Cambridge, United Kingdom: Cambridge University Press. 68

Townsend-Small, A., McClain, M.E., & Brandes, J.A. 2005. Contributions of carbon and nitrogen from the Andes Mountains to the Amazon River: Evidence from an elevational gradient of soils, plants, and river material. *Limnology and Oceanography*, **50**, 672–685. 8

Turowski, J.M. 2012a. Personal communication regarding coarse woody debris in the Erlenbach. 98, 107

Turowski, J.M. 2012b. Personal communication regarding the size distribution of material in the Erlenbach sediment retention basin. 107

Turowski, J.M., Yager, E.M., Badoux, A., Rickenmann, D., & Molnar, P. 2009. The impact of exceptional events on erosion, bedload transport and channel stability in a step-pool channel. *Earth Surface Processes and Landforms*, **34**, 1661–1673. 21, 22, 24, 28

Turowski, J.M., Rickenmann, D., & Dadson, S.J. 2010. The partitioning of the total sediment load of a river into suspended load and bedload: a review of empirical data. *Sedimentology*, **57**, 1126–1146. 107

Turowski, J.M., Badoux, A., & Rickenmann, D. 2011. Start and end of bedload transport in gravel-bed streams. *Geophysical Research Letters*, **38**, L04401. 27

Tyson, R.V., & Follows, B. 2000. Palynofacies prediction of distance from sediment source: A case study from the Upper Cretaceous of the Pyrenees. *Geology*, **28**, 569–571. 13

Uhlenbrook, S., Didszun, J., Tilch, N., McDonnell, J., & McGuire, K. 2007. Breaking up is always difficult—landscape discretization as a process-transfer approach for prediction in ungauged basins. *Pages 102–109 of: Predictions in Ungauged Basins: PUB Kick-off (Proceedings of the PUB Kick-off meeting held in Brasilia, 20-22 November 2002). IAHS Publ. 309*, vol. 309. IAHS. 36, 190

Valentine, T., & Lienkaemper, G. 2005. *10 meter digital elevation model (DEM) clipped to the Andrews Experimental Forest (Spatial dataset).* Corvallis, Oregon, USA: Long-Term Ecological Research; Forest Science Data Bank. http://andrewsforest.oregonstate.edu/data/abstract.cfm?dbcode=GI003. 30, 39, 61

Van Tuyl, S., Law, B.E., Turner, D.P., & Gitelman, A.I. 2005. Variability in net primary production and carbon storage in biomass across Oregon forests - an assessment integrating data from forest inventories, intensive sites and remote sensing. *Forest Ecology and Management*, **209**, 273–291. 42

Vane, C.H. 2012a. *Assessment of lignin in soils and sediments from Switzerland using alkaline CuO oxidation with gas-chromatography mass spectrometry.* Tech. rept. British Geological Survey, Keyworth, Nottingham, United Kingdom. 84

Vane, C.H. 2012b. Personal communication regarding the expected (Ad/Al)v values of fresh plant matter. 89

Vane, C.H., Martin, S.C., Snape, C.E., & Abbott, G.D. 2001a. Degradation of lignin in wheat straw during growth of the oyster mushroom (*Pleurotus ostreatus*) using off-line thermochemolysis with tetramethylammonium hydroxide and solid-state ^{13}C NMR. *Journal of Agricultural and Food Chemistry*, **49**, 2709–2716. 76, 84

Vane, C.H., Abbott, G.D., & Head, I.M. 2001b. The effect of fungal decay (*Agaricus bisporus*) on wheat straw lignin using pyrolysisGCMS in the presence of tetramethylammonium hydroxide (TMAH). *Journal of Analytical and Applied Pyrolysis*, **60**, 69–78. 76

von Wühlisch, C. 2008. *EUFORGEN Technical Guidelines for genetic conservation of European beech (Fagus sylvatica)*. Rome, Italy: Bioversity International. 25, 125

Wakeham, S.G., Canuel, E.A., Lerberg, E.J., Mason, P., Sampere, T.P., & Bianchi, T.S. 2009. Partitioning of organic matter in continental margin sediments among density fractions. *Marine Chemistry*, **115**, 211–225. 12, 15

Walker, G.W., & King, P.B. 1969. *Geologic map of Oregon 1:2 000 000*. USGS, Department of the Interior, in collaboration with Oregon Department of Geology and Mineral Industries. 31, 32, 132

Walling, D.E. 2006. Human impact on land–ocean sediment transfer by the world's rivers. *Geomorphology*, **79**, 192–216. 198

Wand, J.O., Gillespie, R., & Hedges, R.E.M. 1984. Sample preparation for accelerator-based radiocarbon dating. *Journal of Archaeological Science*, **11**, 159–163. 74

Waring, R.H., Landsberg, J.J., & Williams, M. 1998. Net primary production of forests: a constant fraction of gross primary production? *Tree Physiology*, **18**, 129–134. 42

Watersheds Research Cooperative, Oregon State University. 2008. *Trask River Contextual Analysis*. Tech. rept. 30, 32, 35, 40, 41, 42, 44, 49

Wemple, B.C., Swanson, F.J., & Jones, J.A. 2001. Forest roads and geomorphic process interactions, Cascade Range, Oregon. *Earth Surface Processes and Landforms*, **26**, 191–204. 39

West, A.J., Lin, C.-W., Lin, T.-C., Hilton, R.G., Liu, S.-H., Chang, C.-T., Lin, K.-C., Galy, A., Sparkes, R.B., & Hovius, N. 2011. Mobilization and transport of coarse woody debris to the oceans triggered by an extreme tropical storm. *Limnology and Oceanography*, **56**, 77–85. 12, 14, 98, 195

Wheatcroft, R.A., & Sommerfield, C.K. 2005. River sediment flux and shelf sediment accumulation rates on the Pacific Northwest margin. *Continental Shelf Research*, **25**, 311–332. 50

Wheatcroft, R.A., Goñi, M.A., Hatten, J.A., Pasternack, G.B., & Warrick, J.A. 2010. The role of effective discharge in the ocean delivery of particulate organic carbon by small, mountainous river systems. *Limnology and Oceanography*, **55**, 161–171. 14, 25, 101, 102, 103, 171, 172

Winkler, W., Wildi, W., van Stuijvenberg, J., & Caron, C. 1985. Wägital-Flysch et autres flyschs penniques en Suisse Centrale: Stratigraphie, sédimentologie et comparaisons. *Eclogae Geologicae Helvetiae*, **78**, 1–22. 20, 21

Wittmann, Hella, von Blanckenburg, F., Kruesmann, T., Norton, K.P., & Kubik, P.W. 2007. Relation between rock uplift and denudation from cosmogenic nuclides in river sediment in the Central Alps of Switzerland. *Journal of Geophysical Research: Earth Surface*, **112**, F04010. 21

Wohl, E. 2011. Threshold-induced complex behavior of wood in mountain streams. *Geology*, **39**, 587–590. 41

Wondzell, S. 2012. Personal communication regarding the likelihood of fires reaching stream riparian zones in Oregon. 162

Wright, R.F., & Rasmussen, L. 1998. Introduction to the NITREX and EXMAN projects. *Forest Ecology and Management*, **101**, 1–7. 28

Wynn, J.G., Bird, M.I., & Wong, V.N.L. 2005. Rayleigh distillation and the depth profile of $^{13}C/^{12}C$ ratios of soil organic carbon from soils of disparate texture in Iron Range National Park, Far North Queensland, Australia. *Geochimica et Cosmochimica Acta*, **69**, 1961–1973. 141

Wynn, J.G., Harden, J.W., & Fries, T.L. 2006. Stable carbon isotope depth profiles and soil organic carbon dynamics in the lower Mississippi Basin. *Geoderma*, **131**, 89–109. 141

Xu, G.-L., Schleppi, P., Li, M.-H., & Fu, S.-L. 2009. Negative responses of Collembola in a forest soil (Alptal, Switzerland) under experimentally increased N deposition. *Environmental Pollution*, **157**, 2030–2036. 24

Yue, Y., Ni, J., Borthwick, A.G.L., & Miao, C. 2012. Diagnosis of river basins as CO_2 sources or sinks subject to sediment movement. *Earth Surface Processes and Landforms*, **37**, 1398–1406. 13, 196

Zimmerman, S., Luster, J., Blaser, P., Walthert, L., & Luscher, P. 2006. *Waldböden der Schweiz 3: Regionen Mittelland und Voralpen*. Birmensdorf and Bern, Germany: Eidgenossische Forschungsanstalt WSL and Hep Verlag. 24

Data tables

The following tables, comprising a total 25 pages, provide sample details and results for all individual analyses used in this project and not already given in the main body of the text.

Table 1

Samples from organic carbon stores of all catchments. Columns are: 1) the catchment from which the sample was collected; 2) the unique sample identifier; 3) date of collection; 4) location at which sample was collected; 5) type of sample; 6) depth at which sample was collected (in cm) for profiles and cores only; 7) species for foliage and standing wood samples only; 8) organic carbon concentration in weight percent; 9) nitrogen concentration in weight percent; 10) stable isotopic composition of organic carbon in parts per thousand; 11) stable isotopic composition of nitrogen in parts per thousand. For Alsea bedrock core samples, date given is the date of sub-sampling from the cores; date of core collection is unknown. Location is given as a grid reference where known, and otherwise as a description (refer to Figures 2.1, 2.10, 3.2, 3.3 and 3.4). Grid references are in the Swiss Reference System CH1903 for the Erlenbach and Vogelbach, and in the United States National Grid USNG for the remaining catchments. Sample types are as described in Section 3.2.2. Depth is depth below ground surface for soil samples and depth below soil base for bedrock core samples.

Table 2

Suspended sediment samples from all catchments. Columns are: 1) the catchment from which the sample was collected; 2) the type of sample—whether river, forest hillslope runoff (runoff-F) or meadow hillslope runoff (runoff-M); 3) the sampling method—whether instantaneous (inst), discharge-proportional compound (comp), or turbidity threshold (TTS); 4) the unique sample identifier; 5) date of collection; 6) time of collection for instantaneous samples only; 7) discharge in litres per second;

8) suspended sediment concentration in milligrams per litre; 9) organic carbon concentration in weight percent; 10) nitrogen concentration in weight percent; 11) stable isotopic composition of organic carbon in parts per thousand; 12) stable isotopic composition of nitrogen in parts per thousand. Times are given in local time, i.e. UTC+2 for Switzerland and UTC–8 for Oregon. See Section 3.2.1 for a description of the different sampling methods, and Section 3.2.3 for details of how discharge values were assigned to compound samples. SSC is calculated from sample weight. Note that samples from Hinkle, Trask and the Alsea catchments were collected at more than one gauge in each watershed.

Table 3

Untreated and acid-treated vegetation samples. Columns are: 1) the unique sample identifier; 2) the type of vegetation in question. These are followed by the organic carbon concentration in weight percent, nitrogen concentration in weight percent, stable isotopic composition of organic carbon in parts per thousand and stable isotopic composition of nitrogen in parts per thousand for aliquots that had not undergone the carbonate removal process described in Section 3.3.2 (A) and those that had (B).

Table 4

Analyses replicated a year apart. Columns are: 1) the unique sample identifier; 2) the type of material in question. These are followed by the organic carbon concentration in weight percent, nitrogen concentration in weight percent, stable isotopic composition of organic carbon in parts per thousand and stable isotopic composition of nitrogen in parts per thousand for replicates analysed in October 2010 (A) and those analysed in September 2011 (B).

Table 5

Multiple replicates analysed consecutively. Columns are: 1) the unique sample identifier; 2) the type of material in question; 3) the replicate number; 4) organic carbon concentration in weight percent; 5) nitrogen concentration in weight percent; 6) stable isotopic composition of organic carbon in parts per thousand; 7) stable isotopic composition of nitrogen in parts per thousand.